ISTANBUL TECHNICAL UNIVERSITY ★ INSTITUTE OF SCIENCE AND TECHNOLOGY

THE SYNTHESIS OF MACROMOLECULES VIA CLICK REACTIONS

Ph. D. Thesis by
Aydan DAĞ

Department : Polymer Science and Technology

Programme : Polymer Science and Technology

SEPTEMBER 2011

ISTANBUL TECHNICAL UNIVERSITY ★ INSTITUTE OF SCIENCE AND TECHNOLOGY

THE SYNTHESIS OF MACROMOLECULES VIA CLICK REACTIONS

Ph.D. Thesis by
Aydan DAĞ
(515052002)

Date of submission : **18 July 2011**
Date of defence examination : **19 September 2011**

Supervisor (Chairman) : **Prof. Dr. Gürkan HIZAL (ITU)**
Members of the Examining Committee : **Prof. Dr. Ümit TUNCA (ITU)**
Assoc. Prof. Dr. A. Ersin ACAR (BU)
Prof. Dr. Niyazi BIÇAK (ITU)
Assoc. Prof. Dr. Amitav SANYAL (BU)

SEPTEMBER 2011

İSTANBUL TEKNİK ÜNİVERSİTESİ ★ FEN BİLİMLERİ ENSTİTÜSÜ

CLICK REAKSİYONLARI İLE MAKROMOLEKÜLLERİN SENTEZİ

DOKTORA TEZİ

Aydan DAĞ
(515052002)

Tezin Enstitüye Verildiği Tarih : **18 Temmuz 2011**
Tezin Savunulduğu Tarih : **19 Eylül 2011**

Tez Danışmanı : **Prof. Dr. Gürkan HIZAL (İTÜ)**
Diğer Jüri Üyeleri : **Prof. Dr. Ümit TUNCA (İTÜ)**
Doç. Dr. A. Ersin ACAR (BÜ)
Prof. Dr. Niyazi BIÇAK (İTÜ)
Doç. Dr. Amitav SANYAL (BÜ)

EYLÜL 2011

FOREWORD

I would like to extend my thanks to my supervisor, Prof. Dr. Gürkan Hızal, who has been a tireless guide and advisor throughout this thesis. I would also like to thank Prof. Dr. Ümit Tunca, for his inspiring comments and recommendations throughout this thesis.

I would also like to thank the member of my thesis committee Assoc. Prof. Dr. A. Ersin Acar for their time and valuable instruction during my thesis.

Also, many thanks to Prof. Dr. Levent Demirel (Koç University) for his help in AFM measurements.

I feel very privilege and fortunate to be able to work with Res. Assist. Dr. Hakan Durmaz whose help, suggestions and encouragement never are going to be forgotten.

I would like to thank Dr. Eda Güngör.

I would also like to give special thanks to the Prof. Dr. Turan Öztürk group, especially İpek Ösken who made the times inside and outside the lab enjoyable.

I would like to thank my friends for all their help. In particular, Res. Assist. Dr. Şebnem İnceoğlu, Dr. Yasemin Yüksel Durmaz, Res. Assist. Dr. Bünyamin Karagöz, Assist. Prof. Dr. Mehmet Atilla Taşdelen, Dr. Binnur Aydoğan, Muhammet U. Kahveci, Aslı Çapan and Res. Assist. Dr. Abdullah Aydoğan. It has been really a wonderful experience for me to know with so many highly talented and motivated people, and they have helped me in numerous ways along these years. In addition, many thanks go to all of the former and current members in the Hizal and Tunca group laboratory who also made my experience here memorable.

Finally, I would like to dedicate this thesis to my family who always supported me throughout this thesis and never complained about my overtime work. Without their patience, understanding and morale support, it would have been impossible to take on such major challenges in life.

This work is supported by ITU Institute of Science and Technology.

Temmuz 2011 Aydan DAĞ

TABLE OF CONTENTS

Page

ABBREVIATIONS

AFM : Atomic Force Microscopy
ATRP : Atom Transfer Radical Polymerization
ε-CL : ε-caprolactone
CMS : 4-Chloro methyl styrene
CuAAC : Copper catalyzed azide-alkyne cycloaddition
$CDCl_3$: Deuterated chloroform
CH_2Cl_2 : Dichloromethane
DSC : Differential Scanning Calorimetry
DMF : *N*,*N*-Dimehthylformamide
DVB : Divinyl benzene
DLS : Dynamic Light Scattering
EtOAc : Ethyl acetate
FT-IR : Fourier Transform Infrared Spectrophotometer
GC : Gas Chromatography
GPC : Gel Permeation Chromatography
^{1}H NMR : Hydrogen Nuclear Magnetic Resonance Spectroscopy
MeOH : Methanol
MMA : Methyl Methacrylate
MWD : Molecular Weight Distribution
NMP : Nitroxide Mediated Polymerization
PMDETA : *N, N, N',N'', N''*-Pentamethyldiethylenetriamine
PCL : Poly(ε-caprolactone)
PDI : Polydispersity Index
PEG : Poly(ethylene glycol)
PMMA : Poly(methyl metacrylate)
PS : Poly(styrene)
P*t*BA : Poly(*tert*-butyl acrylate)
RAFT : Reversible Addition Fragmentation Chain Transfer
St : Styrene
***t*BA** : *tert*-Butylacrylate
THF : Tetrahydrofuran
TEMPO : 2,2,6,6-Tetramethylpiperidine-*N*-oxyl
TEA : Triethylamine
TD-GPC : Triple Detector-Gel Permeation Chromatography
UV : Ultra Violet

LIST OF SYMBOLS

A	**:** Absorbance
k_{act}	**:** Activation rate constant
C	**:** Concentration
g′	**:** Contraction factor
k_{deact}	**:** Deactivation rate constant
***R*h**	**:** Hydrodynamic radius
[η]	**:** Intrinsic viscosity
K	**:** Mark-Houwink-Sakurada constant
Mp	**:** Melting point
ε	**:** Molar extinction coefficient
M	**:** Molarity
nm	**:** Nanometer
f	**:** Number of arm
R$^{\cdot}$	**:** Radical
R_p	**:** Rate of polymerization
d*n*/dc	**:** Refractive index increment
M_w/M_n	**:** Polydispersity index
M_n	**:** The number average molecular weight
M_w	**:** The weight average molecular weight
λ	**:** Wavelength
w	**:** Weight fractions

LIST OF TABLES

Page

LIST OF FIGURES

Page

THE SYNTHESIS OF MACROMOLECULES VIA CLICK REACTIONS

SUMMARY

The synthesis of well-defined macromolecules with controlled compositions and architectures had been the ultimate challenge of polymer chemists until the development of ionic polymerization methods opened a new field of polymer science. However, the development of ionic polymerization research meets some serious obstacles associated with stringent process conditions with regards to high purity and incompatibility with a variety of functional monomers. Although, free radical polymerization is more tolerant to impurities and is capable of polymerizing a vast variety of vinyl monomers, the main drawback of radical polymerizations is that they have not been able to offer the same degree of control over the polymer structure and functionality as do ionic polymerizations. Therefore, considerable efforts have been devoted to implement the free radical polymerization in controlled fashion. Eventually, the revolution of free radical polymerization has led to development of controlled/‘‘living” radical polymerization (C/LRP) methods that have been facilitated the access to the construction of well-defined macromolecules without stringent requirements on the experimental conditions. Currently, three methods appear to be most efficient and can be successfully applied: stable free radical polymerization (SFRP), best represented by nitroxide mediated radical polymerization (NMP), atom transfer radical polymerization (ATRP), and reversible addition-fragmentation chain transfer (RAFT). Ultimately, their widespread acceptance and exploitation in polymer synthesis is justified by their seemingly unlimited potential to create a wide range of well-defined macromolecules with precise control over composition, architecture and functionality.

The term “click” refers to versatile, efficient, specific and energetically-favored chemical reactions, which could become universal tools first in synthetic chemistry lately extremely popular in polymer and materials science. Click reactions, in particular Cu(I)-catalyzed azide-alkyne cycloaddition (CuAAC) reaction and Diels-Alder reaction, have recently shown to be extremely powerful tools for advanced macromolecular design.

In this thesis, functional polymeric materials with novel macromolecular architectures such as graft and star copolymers were envisaged and synthesized, combining the merits of both C/LRP techniques and “click” chemistry.

In the first study, a combination of C/LRP methods (NMP and ATRP) to produce polymers with well-defined chain length and functionality at spesific positions and double “click” reactions (CuAAC and Diels-Alder) to quantitatively couple these polymer chains together were applied *in situ* to form hetero graft copolymers in *N*,*N*-dimehthylformamide (DMF) for 48 h at 120 ^{o}C (Figure 1).

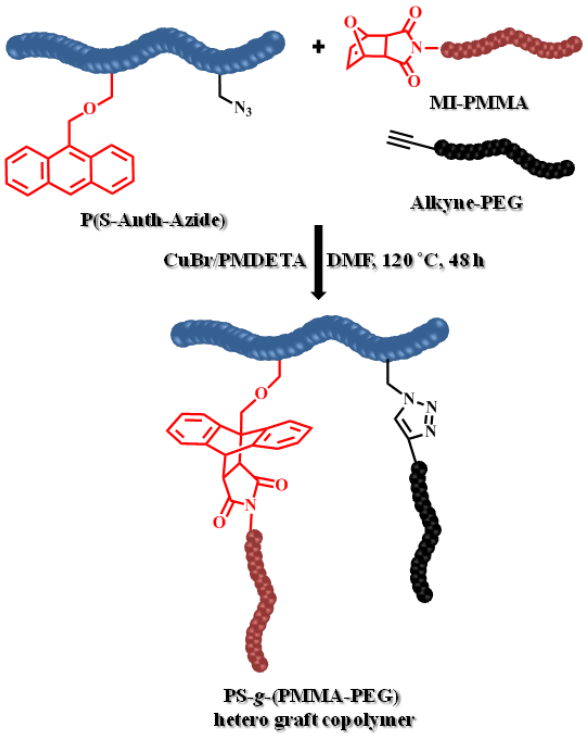

Figure 1 : Synthesis of heterograft copolymers via one-pot CuAAC and Diels–Alder click reactions.

Second, two types of 3-arm star-block copolymers: (PS-*b*-PMMA)$_3$, and (PS-*b*-PEG)$_3$, were prepared using *in situ* double click reactions: CuAAC and Diels–Alder reactions (Figure 2).

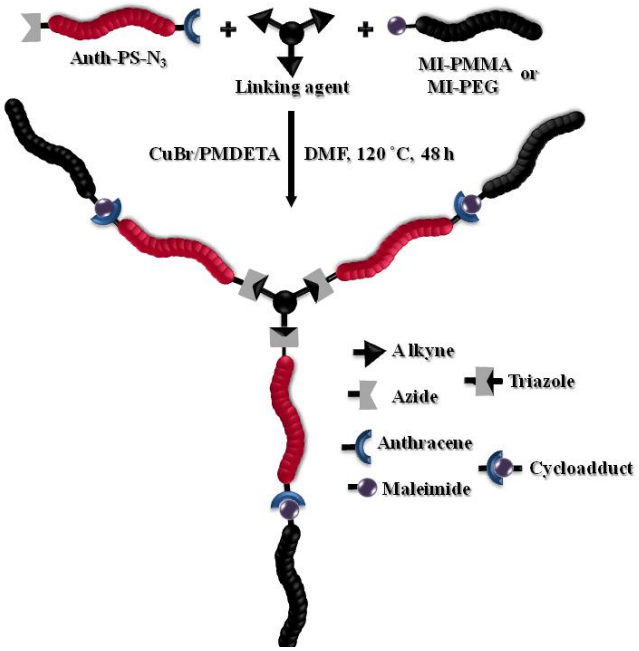

Figure 2 : Synthesis of 3-arm star block copolymers via one-pot CuAAC and Diels–Alder click reactions.

In the third study, multiarm star block (and mixed-block) copolymers: (P*t*BA)$_m$-(PS)$_n$-poly(divinylbenzene) (polyDVB) and (PEG)$_k$-(PS)$_n$-polyDVB and (PEG)$_k$-(P*t*BA)$_m$-(PS)$_n$-polyDVB were efficiently prepared via a combination of cross-linking and CuAAC click reaction (Figure 3).

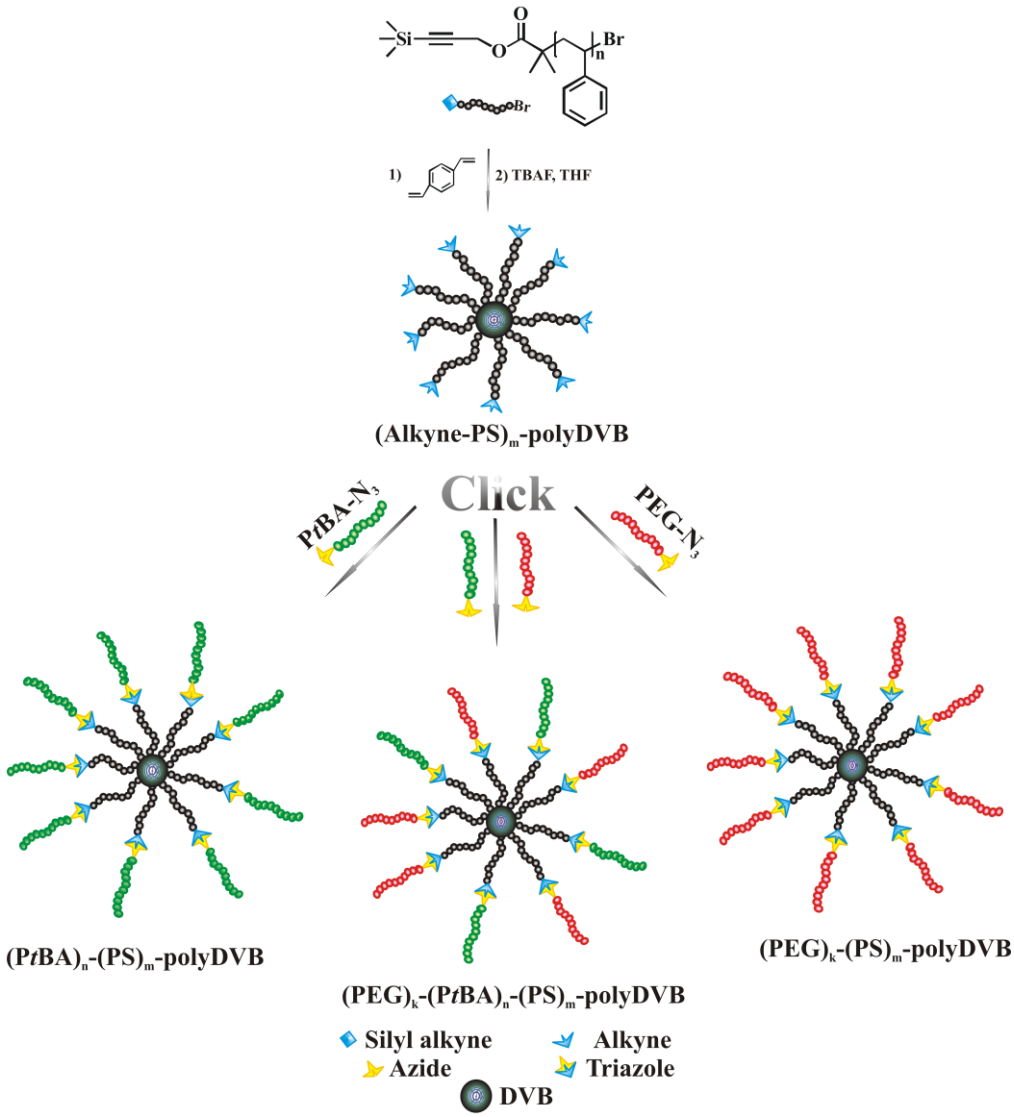

Figure 3 : Synthesis of multiarm star block (and mixed-block) copolymers via CuAAC click reaction.

Finally, a new efficient route to prepare well-defined multi-miktoarm star block copolymers, (P*t*BA)$_n$-(PS)$_m$-polyDVB-(PS-Anth)$_m$ and (P*t*BA)$_n$-(PS)$_m$-polyDVB-(PS)$_m$-(PMMA)$_k$, were shown via a combination of cross-linking and sequential double click reactions including CuAAC and Diels–Alder (Figure 4).

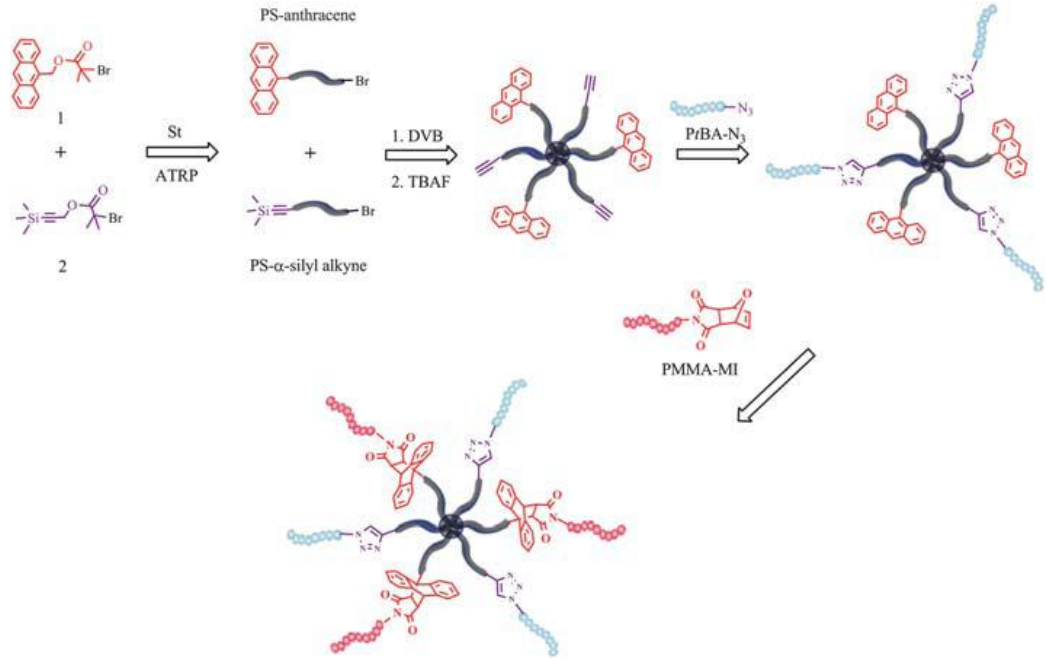

Figure 4 : Synthesis of multi-miktoarm star block copolymers via sequential CuAAC and Diels–Alder click reactions.

CLICK REAKSİYONLARI İLE MAKROMOLEKÜLLERİN SENTEZİ

ÖZET

Kontrollü kompozisyon ve yapılarda iyi tanımlanmış makromoleküllerin sentezi polimer biliminde yeni bir alan açan iyonik polimerizasyon yöntemlerinin gelişimine kadar kimyagerler için sorun olmuştu. Ancak, iyonik polimerizasyon araştırmalarının gelişimi zorlu işlem koşulları; yüksek saflık ve çeşitli fonksiyonel monomerlerle uyumsuzluk söz konusu olduğundan bazı ciddi engeller ile karşılaşmaktadır. Serbest radikal polimerizasyonu safsızlıklara daha toleranslıdır ve çok çeşitli vinil monomerlerinin polimerleştirilmesi yeteneğine sahiptir fakat en büyük dezavantajı iyonik polimerizasyondaki gibi polimer yapı ve fonksiyonalite kontrolünün aynı derecede mümkün olmamasıdır. Bu nedenle, kaydadeğer çabalar serbest radikal polimerizasyonunu kontrollü bir şekilde gerçekleştirmek için harcanmıştır. Neyse ki, serbest radikal polimerizasyonunundaki devrim herhangi bir zorlu deneysel koşul gereksinimleri olmayan, iyi tanımlanmış makromoleküllerin inşasına erişim kolaylığı sağlayan kontrollü/"yaşayan" radikal polimerizasyon (C/LRP) yöntemlerinin gelişimlerine yol açmıştır. Günümüzde, en etkili ve en sık kullanılan üç C/LRP yöntemi: kararlı serbest radikal polimerleşmesi (SFRP) veya en sık kullanılan ifadesi ile nitroksit ortamlı radikal polimerleşmesi (NMP), atom transfer radikal polimerleşmesi (ATRP), ve tersinir eklenme-ayrılma zincir transfer polimerleşmesidir. Sonuç olarak, bu yöntemlerin polimer sentezinde geniş bir yelpazede yaygın olarak kabulu ve yararlanılması iyi tanımlanmış makromoleküllerin kontrollü kompozisyon, yapı ve fonksiyonalitede yapılmasındaki sınırsız potansiyellerine dayanır.

Çok yönlü, verimli, özel ve enerji olarak tercih edilen kimyasal reaksiyonlar anlamına gelen "click" terimi ilk sentetik kimyada daha sonraları polimer ve malzeme biliminde son derece popüler evrensel araçlar haline gelmiştir. Son zamanlarda, "click" reaksiyonları, özellikle Cu (I)-katalizli azit-alkin siklokatılma (CuAAC) reaksiyonu ve Diels-Alder reaksiyonu ileri makromoleküler tasarım için son derece güçlü araçlar olarak gösterilmiştir.

Bu tezde, aşı ve yıldız kopolimerleri gibi yeni makromoleküler yapılarda fonksiyonel polimerik malzemeler hem C/LRP teknikleri hem de "click" kimyasının yararlarının birleştirilmesiyle tasarlandı ve sentezlendi.

İlk çalışmada, iyi tanımlanmış zincir uzunluğu ve spesifik pozisyonlarda fonksiyonalitelere sahip polimerlerin sentezinde kullanılan C/LRP (NMP ve ATRP) yöntemlerinin, bu polimerleri etkin bir biçimde birleştirmede başvurulan çift "click" (CuAAC and DA) reaksiyonlarıyla bir arada uygulanması ile farklı kollu aşı kopolimerlerin sentezleri gerçekleştirilmiştir (Şekil 1).

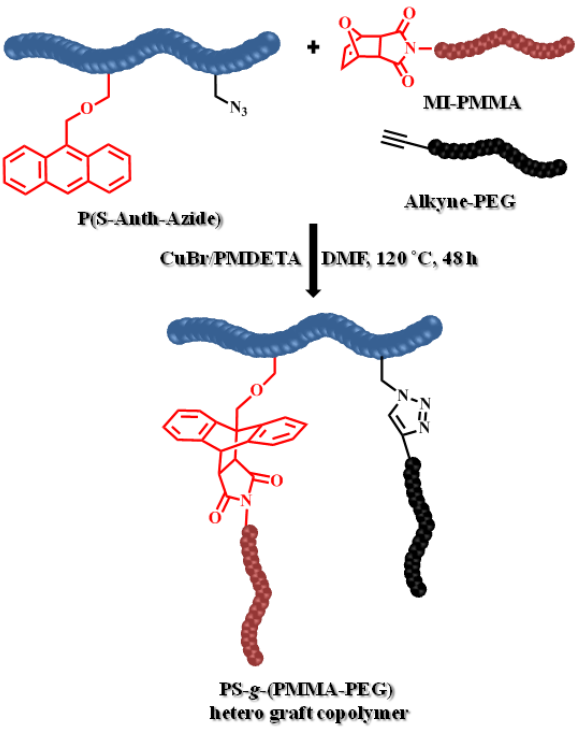

Şekil 1 : CuAAC ve Diels–Alder click reaksiyonları ile tek aşamada farklı kollu aşı kopolimerlerin sentezi.

İkinci çalışmada, iki farklı (PS-*b*-PMMA)$_3$ ve (PS-*b*-PEG)$_3$ 3-kollu yıldız blok kopolimerleri CuAAC ve Diels–Alder reaksiyonlarının birlikte kullanılamasıyla tek aşamada sentezlenmişlerdir (Şekil 2).

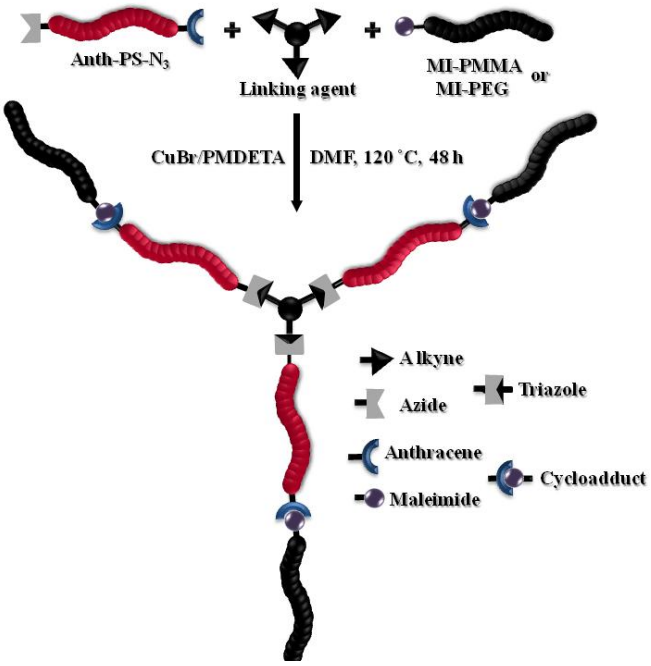

Şekil 2 : CuAAC ve Diels–Alder click reaksiyonları ile tek aşamada 3-kollu yıldız blok kopolimerlerin sentezi.

Üçüncü çalışmada, (P*t*BA)$_m$-(PS)$_n$-poli(divinilbenzen) (poliDVB), (PEG)$_k$-(PS)$_n$-poliDVB ve (PEG)$_k$-(P*t*BA)$_m$-(PS)$_n$-poliDVB çok kollu yıldız blok ve farklı kollu yıldız blok kopolimerleri çapraz-bağlanma ve CuAAC click reaksiyonlarının birlikte kullanılması ile sentezlenmişlerdir (Şekil 3).

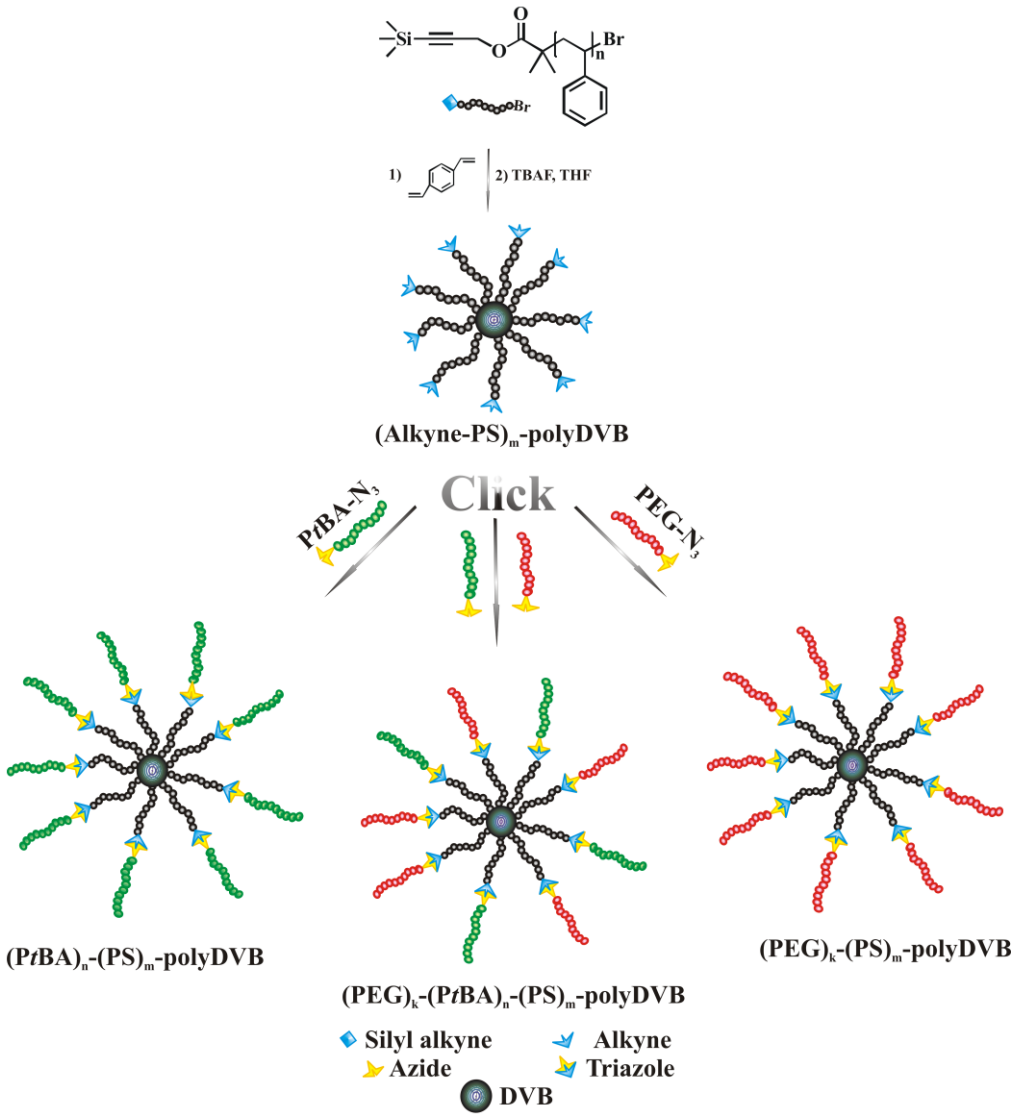

Şekil 3 : CuAAC click reaksiyonu ile çok kollu yıldız blok ve farklı kollu yıldız blok kopolimerlerin sentezi.

Son olarak, iyi tanımlanmış çok ve farklı kollu yıldız blok kopolimerlerin; (P*t*BA)$_n$-(PS)$_m$-polyDVB-(PS-Anth)$_m$ ve (P*t*BA)$_n$-(PS)$_m$-polyDVB-(PS)$_m$-(PMMA)$_k$ hazırlanmasında çapraz bağlanma ile CuAAC ve Diels-Alder reaksiyonlarını içeren ard arda uygulanan çift "click" reaksiyonlarının kombinasyonu yeni etkili bir yol olarak gösterilmiştir (Şekil 4).

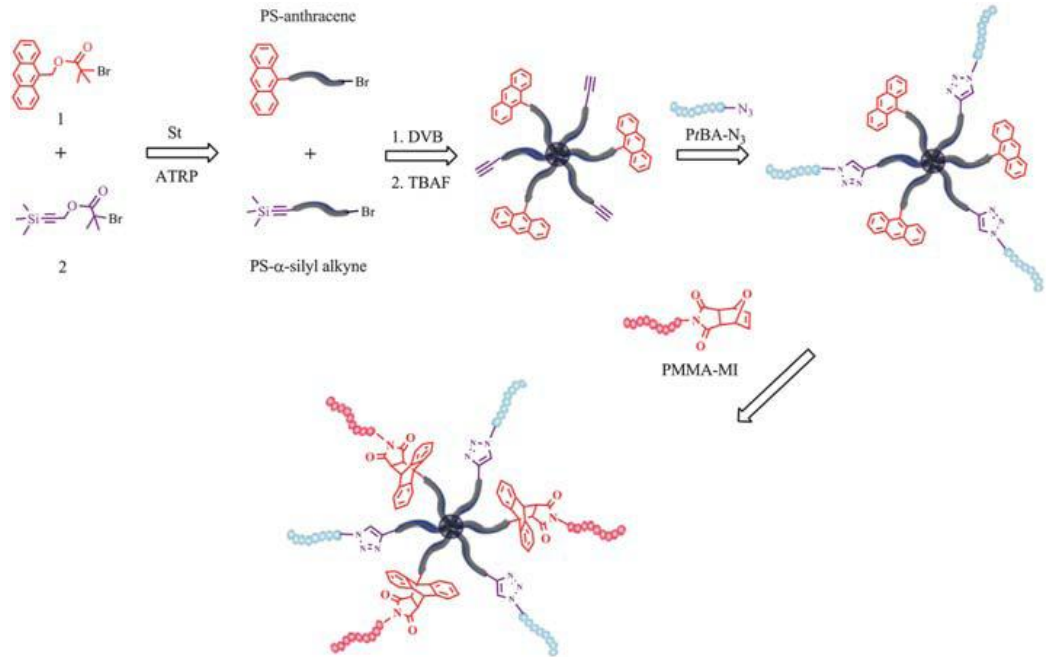

Şekil 4 : Ard arda gerçekleştirilen CuAAC ve Diels–Alder click reaksiyonları ile çok ve farklı kollu yıldız blok kopolimerlerin sentezi.

1. INTRODUCTION

The research to design novel macromolecular architectures with unusual properties has led to the synthesis of block, graft, star polymers with well-defined end functional groups, controlled molecular weights, and narrow molecular weight distributions. Traditionally, control of polymerization processes has been achieved with "living" polymerization techniques such as ionic (anionic or cationic), group transfer and transition-metal-catalyzed processes [1-6]. However, these methods suffer from rigorous process conditions imposed by the high purity required and incompatibility with a variety of functional monomers. Therefore, much interest has recently been focused toward free radical chemistry to achieve control over polymerization process due to their tremendous commercial significance [7]. Even though free radical initiated polymerizations are synthetically less rigorous and are compatible with a wide range of monomers, they, in general, lack the ability to accurately control molecular weight distribution and end functional groups. The main drawback of radical polymerizations is that they have not been able to offer the same degree of control over the polymer structure and functionality as do ionic polymerizations. In this connection, there is increasing interest in methods based on radical chemistry that allow for the preparation of polymers in controlled fashion. Eventually, the concept of controlled/''living" radical polymerization (C/LRP) has been introduced in which the control and precision of living polymerization and the robustness of radical polymerization are put together in a single process [8-10]. Several methods have been developed over the years to attain control of radical polymerizations. Particularly, the three most well-known C/LRP techniques are nitroxide mediated radical polymerization (NMP) [11, 12], atom transfer radical polymerization (ATRP) [13-17], and reversible addition-fragmentation chain transfer (RAFT) polymerization [18-20].

The concept of click chemistry, introduced by Sharpless and co-workers has attracted widespread attention in polymer science due to its high specificity, quantitative yields, and fidelity in the presence of a wide variety of solvents and functionalities

[21]. The Cu(I)-catalyzed azide-alkyne cycloaddition (CuAAC) and Diels-Alder click reactions are the most frequently employed click reactions, which are capable of selectively combining two components in terms of covalent bonds in excellent yields. In order to expand the applicability of this concept, other click chemistry-type reactions, such as thiol-ene reaction, nucleophilic substitution and radical reactions have also been developed.

The great potential of click reactions combination with their compatible partner of C/LRP processes for the construction of novel macromolecular architectures such as graft and star polymers has been pursued by synthetic polymer chemists in recent years, and is now the subject of intensive research in polymer science.

Since graft copolymers have many structural variables (composition, backbone length, branch length, branch spacing, etc.), they have great potential to realize new properties. Three different approaches have been applied to the synthesis of graft copolymers. Firstly the ‘‘*grafting onto*’’ strategy, where end-functionalized preformed polymer grafts are linked in a chemical reaction with reactive side chains of a polymer backbone. Secondly, the ‘‘*grafting from*’’ strategy, consists in a polymerization of the grafts from a polymer backbone bearing initiating sites. The last approach is the ‘‘*grafting through*’’ strategy which relies on polymerization of appropriate macromonomers.

Additionally, it is well-known that star polymers have a fascinating macromolecular architecture due to their unique properties that differentiate them from their linear counterparts, such as a smaller hydrodynamic volume and lower viscosity at a given molecular weight as a consequence of their compact structure and globular shape. To date, known synthetic strategies for the formation of star polymers can be generalized into three main categories: (1) “core-first”; (2) “arm-first”; and (3) “coupling onto”. The core-first technique involves the use of a multifunctional initiator. The arm-first technique involves the synthesis of preformed arms followed by reaction with a cross-linking agents usually by using a divinyl cross-linker. The third method is a slight variation of the arm-first technique, which involves the synthesis of preformed arms followed by reaction with a multifunctional coupling agent.

The aim of this thesis is to use a combination of C/LRP to produce polymers with well-defined chain length and end group functionality at specific locations and "click" reactions to quantitatively couple these polymer chains together to form novel macromolecular architectures such as graft and star copolymers. The first study concerns the synthesis of hetero graft copolymers in terms of using double click reactions (CuAAC and Diels–Alder reactions) in one-pot technique. Subsequently, double click reactions were applied to the synthesis of 3-arm star-block polymers (A_3B_3) using trialkyne functional linking agent in one-pot technique. In addition, multiarm star block and mixed-block copolymers were prepared via a combination of cross-linking and CuAAC reaction based on "arm-first" and "coupling-onto" methodologies. Finally, a new efficient route to prepare well-defined multi-miktoarm star block copolymers were prepared via a combination of cross-linking and sequential double click reactions including CuAAC and Diels–Alder.

2. THEORETICAL PART

2.1 Living Polymerizations

The considerable attention to the field of living polymerization techniques is due to the increasing demand for well-defined functional polymers with fully controllable molecular characteristics. Living polymerization, the concept of which was first introduced by Szwarc in 1956, is one of the most promising ways for the synthesis of well-defined polymers [1, 2]. A living polymerization is defined as a chain polymerization that proceeds in the absence of chain transfer and chain termination as indicated by Szwarc. His pioneering work on the anionic polymerization of St initiated with sodium naphthalenide opened the field of living polymers with controlling the molecular weight and molecular weight distributions as well as the structure of the end-groups.

After the discovery of living anionic polymerization, critical research on cationic polymerization was performed in the "living" era**.** An equimolar mixture of HI/I_2 was the first system used for the initiation of such polymerizations of vinyl ethers [3]**.** In this system, the initially formed adduct of HI to a vinyl ether is activated by iodine. The fast initiation realized ideal living cationic polymerization of alkyl vinyl ethers. Thus, homopolymers and block copolymers with narrow molecular weight distributions were first synthesized in cationic polymerization.

Since then, much progress has been made in these living ionic polymerization techniques and polymerization of various monomers have been examined, for which numerous types of initiators have been developed. While these techniques are undoubtedly successful, they do suffer from rigorous synthetic requirements including the use of very pure reagents and the total exclusion of water and oxygen and incompatibility with a variety of functional monomers. Definitely, with so many parameters to control, such requirements represent a grand challenge to synthetic polymer chemists and somewhat delay their practical use. Aware of the intrinsic limitations of ionic polymerizations, many efforts have been made to find new routes which could address the development of a free radical polymerization. This process

is tolerant to impurities, very versatile with respect to compatibility with broad range of functional monomers, and relatively easy to implement in an industrial plant.

2.2 Controlled/‘‘Living” Radical Polymerizations (C/LRP)

Conventional free radical polymerization (FRP) remains the most convenient method to synthesize high molecular weights polymers since it provides high versatility, commercial productivity, and tolerance to many functionalities and impurities. Moreover, free radical polymerization has been shown to be applicable to the polymerization of a wide range of monomers under mild reaction conditions over a large temperature range (-100 to 250 ^{o}C) [22]. However, the major drawback of free radical polymerization is its poor-control in molecular weight and well-defined chain end structure as well as its inability to synthesize block copolymers and complex polymeric architectures.

Conventional free radical polymerization consists of four elementry steps: initiation, propagation, termination, and chain-transfer reactions. Once the initiating radical is formed by various stimuli, e.g., thermolysis, photolysis, and redox processes, reacts rapidly with vinyl monomers to grow the polymer chains (propagation). In contrast to ionic polymerizations, the propagating radical species undergo bimolecular termination reactions by recombination or disproportionation to give dead polymers. The propagating radical also undergoes a chain-transfer reaction to generate a new propagating radical and a dead polymer chain. However, because of slow initiation and fast radical-radical termination reactions, the resulting materials are polydisperse (M_w/M_n>1.5), and the control over molecular weight and functionality is very difficult.

As a result of the in effectiveness to accurately control molecular weight distribution and end functional groups, great progress has been made toward free radical polymerization achieving better control over polymer structure and possessing the characteristics of a living process. Thus, the concept of controlled/‘‘living” radical polymerization (C/LRP) has been introduced in which the control and precision of living polymerization and the robustness of radical polymerization are put together in a single process [8-10, 23, 24]. C/LRP is a powerful process, which allows the preparation of polymers with well-defined features such as control molecular

weights, narrow molecular weight distributions (M_w/M_n<1.1), high degrees of functionality and compositional variation under relatively facile conditions.

Even though FRP and C/LRP proceed via the same radical mechanism, the difference between conventional free radical polymerization and C/LRP is that the radical end does not deactivate during the polymerization. Therefore, all of the C/LRPs based on the reversible generation of carbon-centered radicals from a so-called dormant species, which possesses appropriate functional groups at the polymer end for radical generation (Scheme 2.1). This "pseudo" deactivation of the growing radical species to the dormant species decreases the concentration of radical species in reaction intermediates and reduces the probability of undesirable side reactions making the reaction proceed almost like a "living" process [25].

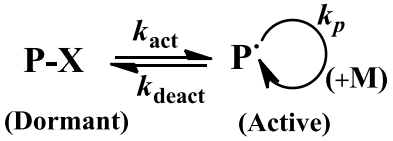

(2.1)

Consequently, the key to molecular weight control mainly lies in the predominant formation of the dormant species from the growing radical species, as well as the establishment of an extremely fast activation-deactivation process relative to the fast propagation.

The origin of controlling molecular weight and end functional groups by free radical chemistry can be traced back to the "*iniferter*" system developed by Otsu in 1982 using thiurams and dithiocarbamates as chain transfer agents [26]. In this case, the photoinitiator (**1**) decomposes homolytically to generate two unsymmetrical free radicals, one of which acts as the initiator (**2**) while the other behaves as the molecular weight controlling agent (**3**) (Scheme 2.2). In this way, the overall concentration of the reactive radicals can be controlled, and the termination can be restricted to a primary radical termination process. However, this approach is inefficient in many respects, particularly because, the polymers obtained by the "*iniferter*" approach were found to have higher molecular weight distributions.

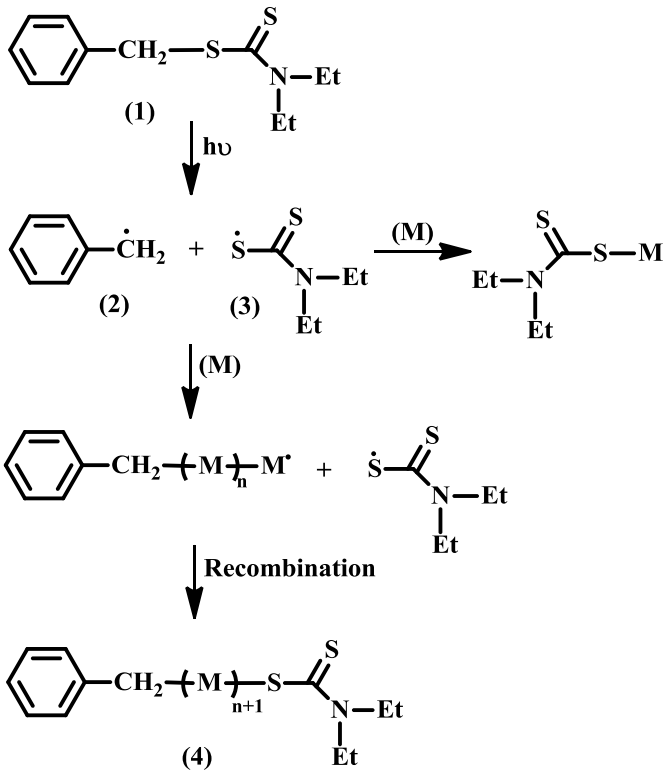

(2.2)

Although not truly ‘‘living”, this was the starting point for a C/LRP process. Nowadays, among the most efficient C/LRP systems are nitroxide-mediated radical polymerization (NMP) [11, 12], atom transfer radical polymerization (ATRP) [13, 14, 16, 17], and reversible addition-fragmentation chain transfer (RAFT) [18-20, 27]. These methods will be discussed in the context of the following sections.

2.2.1 Nitroxide mediated radical polymerization (NMP)

Nitroxide mediated radical polymerization (NMP) is a member of the family of C/LRP systems that gained attention after the seminal paper by Georges [11] and was initially reported in 1985 by Solomon and Rizzardo [28]. The NMP process has a similar mechanism to the use of iniferters and it has now emerged as one of the most versatile for conferring living characteristics on a radical polymerization. The principle of NMP is summarized in Scheme 2.3.

The key to the success of this approach is that the concentration of the reactive chain ends is reduced by reversible termination of the growing polymeric chain end. The low overall concentration of the propagating chain end will minimize undesired side reactions, such as irreversible termination reactions through combination or disproportionation. Thus control over the entire polymerization process is achieved

since all the chains should be initiated only from the desired initiating species and propagation should proceed in a controlled fashion.

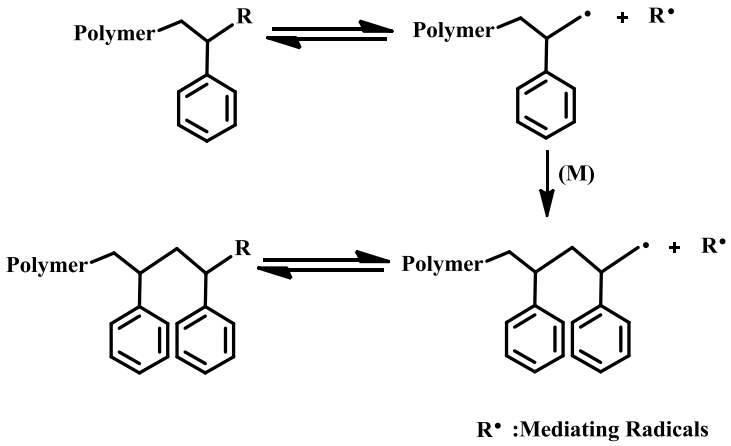

(2.3)

R• :Mediating Radicals

The identity of the mediating radical, R·, is critical to the success of living free radical procedures and a variety of different persistent, or stabilized radicals have been employed. These range from (arylazo)oxy [29], substituted triphenyls,[30] verdazyl [31], triazolinyl [32], nitroxides [33] etc. with the most widely studied and certainly most successful class of compounds being the nitroxides, especially 2,2,6,6-tetramethylpiperidinoxy (TEMPO), and their associated alkylated derivatives, alkoxyamines.

In general, two procedures have been applied to initiate NMP. On the one hand, the alkoxyamine is formed *in situ* from the nitroxide and radicals generated using a conventional initiator for a bimolecular system. On the other hand, the initiation can occur by using an alkoxyamine acting as an initiator and a control agent for a unimolecular system. Basically, during the NMP, the initiation step occurs under thermal conditions.

Moad, Solomon and Rizzardo first introduced the use of TEMPO for controlled radical polymerization [28]. The goal of synthesizing narrowly dispersed polymer using the nitroxide remained elusive until a procedure reported by Georges et al. [11]. This group synthesized PS with a relatively narrow molecular weight distribution (< 1.3) using a bimolecular mixture of benzoyl peroxide and TEMPO.

While successful in yielding low polydispersity products of predictable molecular weight, the poorly defined structure and unknown concentration of the initiating species in this process resulted in less than ideal control of the polymerizations (Scheme 2.4).

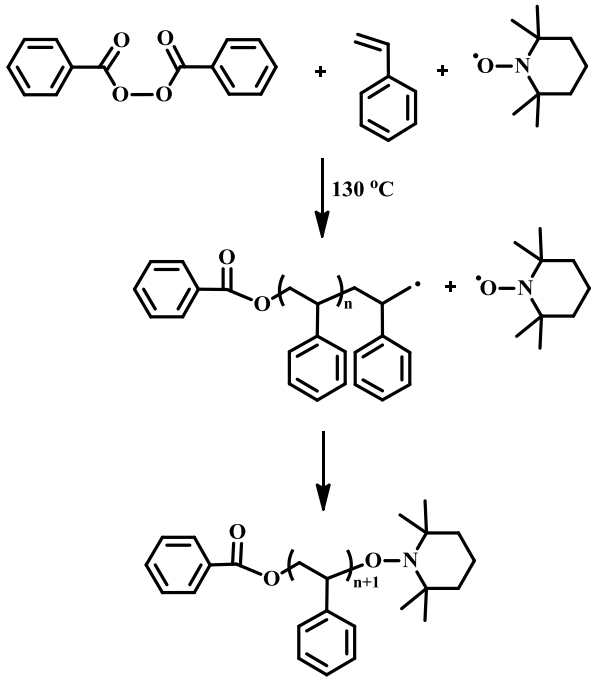

(2.4)

In contrast, thermolysis of a well-defined unimolecular initiator, typically an alkoxyamine, releases both the initiating radical and the nitroxide in a 1/1 molar ratio. Therefore, the initiator efficiency is close to unity, and the structure of the chain ends is well defined with the initiating fragment of the alkoxyamine being attached at the α-chain end and the nitroxide at the *ω*-chain end of the chains (Scheme 2.5).

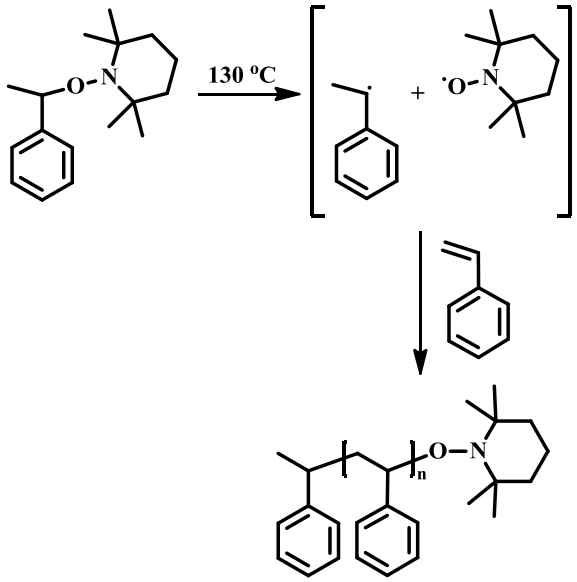

(2.5)

The importance of this is great, as each polymer chain initiated will be capped by nitroxide leading to controlled living polymerization and ultimately polymers with low MWD. The amount of initiator added to the polymerization can be accurately weighted, and consequently, the resulting polymer chain length can be determined by

the monomer to initiator ratio. The structure of the typically used original unimolecular initiators for NMP can be seen in scheme 2.6.

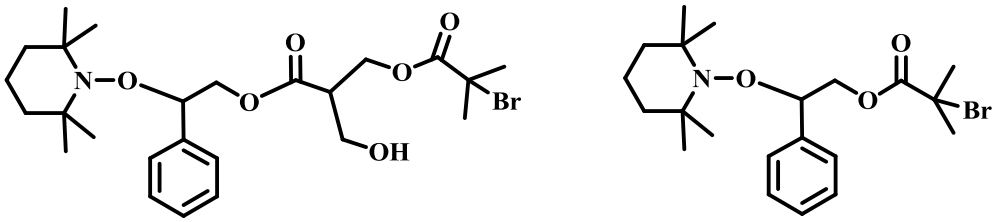

(2.6)

Although NMP is one of the simplest methods of living free radical polymerization, it has many disadvantages. The major disadvantage of NMP results from the limited scope of monomers mainly St and its derivates in its early versions. Notable advances have been accomplished with the appearances of novel nitroxides [34-37]. Another limitation can be the requirement of a high temperature of polymerization (110 ºC).

The structure of the nitroxides strongly affects their ability to efficiently mediate C/LRPs of various monomers. Different nitroxides have been developed and used for NMP, many of which have proved to be far superior to the TEMPO type, giving better molecular weight distributions in addition to faster polymerizations. Polymerization of non-styrenic monomers by NMP was made possible with the development of second generation acyclic nitroxides such as 2,2,5-trimethyl-4-phenyl-3-azahexane nitroxide (TIPNO) (Scheme 2.7, (b)) and *N*-*tert*-butyl-1-diethylphosphono- 2,2-dimethylpropyl nitroxide (DEPN) also called SG1 (Scheme 2.7, (c)). Gnanou was the first to show this significance, demonstrating that the *α*-hydrogen enabled extensive control over the polymerization process of *n*-butyl acrylate by using DEPN molecule [35].

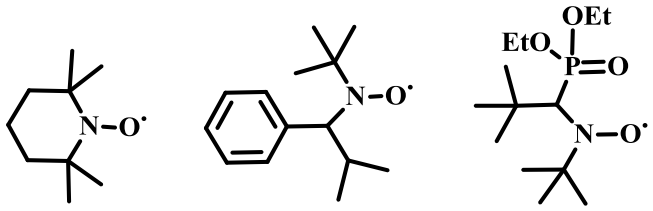

(2.7)

TEMPO **TIPNO** **SG1**

(a) **(b)** **(c)**

Compared with other reversible-deactivation radical polymerization methods, NMP possesses several advantages, such as easier product purification and an excellent functional group tolerance since no metal complex is used [38-40].

2.2.2 Atom transfer radical polymerization (ATRP)

Transition-metal mediated controlled/‘‘living” radical polymerization, reported independently by Matyjaszewski [41], Sawamoto [14] and Percec [42] in 1995, is one of the most powerful techniques to obtain polymers with high control over compositions, architectures, and functionalities. The polymerization, which is mechanistically similar to atom transfer radical addition (ATRA), therefore, is often termed as atom transfer radical polymerization (ATRP).

A general mechanism for ATRP is shown in Scheme 2.8. ATRP is based on the reversible homolytic cleavage of carbon-halogen bond by a redox reaction. Homolytic cleavage of the alkyl (pseudo)halogen bond (RX) by a transition metal complex (activator, M_t^n –Y / ligand, where Y may be another ligand or a counterion) in the lower oxidation state generates an alkyl radical ($R^{\bullet}$) and a transition metal complex (deactivator, $X–M_t^{n+1}$ / ligand) in the higher oxidation state. The formed radicals can initiate the polymerization by adding across the double bond of a vinyl monomer, propagate, terminate by either coupling or disproportionation, or be reversibly deactivated by the transition metal complex in the higher oxidation state to reform the dormant species and the activator.

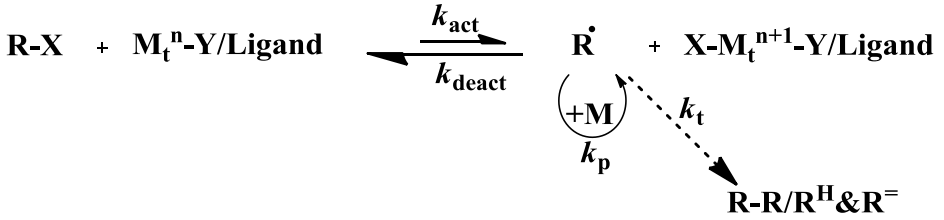

(2.8)

This process occurs with a rate constant of activation, k_{act}, and deactivation k_{deact}, respectively. Polymer chains grow by the addition of the free radicals to monomers in a manner similar to a conventional radical polymerization, with the rate constant of propagation, k_p. Termination reactions (k_t) also occur in ATRP, mainly through radical coupling and disproportionation; however, in a well-controlled ATRP, no more than a few percent of the polymer chains undergo termination. Typically, no more than 5% of the total growing polymer chains terminate during the initial, short, nonstationary stage of the polymerization. Other side reactions may additionally limit the achievable molecular weights.

This process generates oxidized metal complexes, the deactivators, which behave as persistent radicals to reduce the stationary concentration of growing radicals and thereby minimize the contribution of termination at later stages. A successful ATRP

will have not only small contribution of terminated chains but also uniform growth of all the chains; this is accomplished through fast initiation and rapid reversible deactivation.

The ATRP equilibrium (K_{eq}= k_{act}/k_{deact}) essentially mediates the rate of polymerization (R_p), defined by eq 2.1, by ensuring steady and concurrent growth of all polymer chains, resulting in well-defined polymers with narrow molecular weight distributions. K_{eq} must be low to maintain a low stationary concentration of radicals; thus, the termination reaction is suppressed.

$$\mathbf{R_p = k_p.K_{eq}\frac{[R\text{-}X][M_t^n]}{[M_t^{n+1}]}.[M]} \qquad \textbf{(Eq. 2.1)}$$

$$\frac{M_w}{M_n} = 1 + \left(\frac{k_p[R\text{-}X]}{k_{deact}[M_t^{n+1}]}\right)\left(\frac{2}{p} - 1\right) = 1 + \frac{2}{k_{act}[M_t^n]t} \qquad \textbf{(Eq. 2.2)}$$

The rate of ATRP, R_p, has been shown to be the first order with respect to the monomer [M] and initiator [R-X]. The rate of polymerization is also influenced by the ratio of concentrations of the activator to the deactivator, although this may change during polymerization.

Equation 2.2, which shows how the polydispersity index in ATRP (in the absence of chain termination and transfer) relates to the concentrations of initiator (RX) and deactivator (M_t^{n+1}), the rate constants of propagation (k_p), deactivation (k_{deact}), and monomer conversion (p). Lower polydispersities are obtained at higher conversion, higher k_{deact} relative to k_p, higher concentration of deactivator, and higher monomer to initiator ratio, $[M]_0/[I]_0$ [17, 43, 44].

An ATRP system consists of the monomer, an initiator, and a catalyst composed of a transition metal species complexed with any suitable ligand. A detailed discussion of the basic components of ATRP is elucidated extensively in the following sections.

2.2.2.1 Basic components of ATRP

Monomers

Most vinyl monomers used in free radical polymerizations have been successfully polymerized via ATRP, e.g. St derivates, (meth)acrylates, (meth)acrylamides, dienes, and acrylonitrile which contain substituents that are capable of stabilizing the propagating radicals [45]. ATRP is tolerant to many functional polar groups in monomers, however, a few monomers can not be polymerized with currently

available ATRP catalysts. Some groups react rapidly with the catalyst system (such as acids; (meth)acrylic acid) creating metal carboxylates which are ineffective catalysts for ATRP. Some other monomers may be difficult to polymerize since they exhibit side reactions. An example of such a monomer is 4-vinyl pyridine (4-VP), which can undergo quaternization by the (alkyl halide) initiator [46]. Monomers often have a major effect on the ATRP, several variables can account for the influence of the used monomer. For each monomer the rates of activation and deactivation (k_{act} and k_{deact}) are unique, and these in combination with the rate of propagation k_p determine the polymerization rate. The most common monomers in the order of their decreasing ATRP reactivity are methacrylates, acrylonitrile, styrenes, acrylates, (meth)acrylamides [47].

Initiators

Generally, initiators used in ATRP are alkyl halides (RX) (or pseudohalides,) with α-phenyl, vinyl, carbonyl, cyano groups and multiple halogen atoms as well as any compound with a weak halogen-heteroatom bond, such as sulfonyl halides. The primary role of the initiator is to determine the number of dormant chains and to provide the end groups of the polymer chains.

To obtain well-defined polymers with narrow molecular weight distributions, the (pseudo)halide group, X, must rapidly and selectively migrate between the growing chain and the transition metal complex. Thus far, bromine and chlorine are the halogens that afford the best molecular weight control. Iodine works well for acrylate polymerizations; however, in styrene polymerizations the heterolytic elimination of hydrogen iodide is too fast at high temperatures. Fluorine is not used because the carbon–fluorine bond is too strong to undergo homolytic cleavage. As for other X groups, some pseudohalogens, specifically thiocyanates, have been used successfully in polymerization of acrylates and styrenes [48-50].

Initiator efficiency is of prime importance for succesful ATRP. Generally, alkyl halides RX with resonance stabilizing substituents are efficient initiators for ATRP. Often, the structure of the initiator is analogous to the structure of the halogenated polymer chain end to obtain similar reactivity of the carbon-halogen bond. For example, styrene polymerizations often incorporate 1-phenylethyl chlorides or bromides as the initiators [13]. However, this guideline does not always hold as demonstrated in the polymerization. The use of sulfonyl chlorides as universal initiator in ATRP of styrene and methacrylates was reported [51].

The initiator can not only be a small molecule, but also a polyfunctional small molecule, or a macromolecule, which would produce end-functional polymers, star polymers, and graft copolymers, respectively.

Catalysts

Catalyst is the most important component of ATRP. It is the key to ATRP since it determines the position of the atom transfer equilibrium and the dynamics of exchange between the dormant and active species. There are several prerequisites for an efficient transition metal catalyst. An efficient catalyst should be able to expand its coordination sphere and oxidation number upon halogen abstraction from an initiator (alkyl halide) or dormant polymer chains. The metal center should have reasonable affinity toward a halogen. Additionally, the catalyst should not participate in any side reactions which would lower its activity or change the radical nature of the ATRP process.

Various transition metals, such Re [52], Ru [53, 54], Rh [55], Fe [56-61], Ni [62, 63], Pd [64] and Cu [13, 17] has been successfully used as catalysts for ATRP. Among them, Cu seems to be the most efficient metal as determined by the successful application of its complexes as catalysts in the ATRP of a broad range of monomers in diverse media. A recent work from Sawamoto and co-workers shows that the Ru-based complexes can compete with the Cu-based systems on many fronts. A specific Fe-based catalyst has also been reported to polymerize vinyl acetate via an ATRP mechanism. The transition metal complex is very often a metal halide, but pseudohalides, carboxylates, and compounds with noncoordinating triflate and hexafluorophosphate anions were also used successfully [65].

Ligands

Ligand plays a critical role in the activation/deactivation equilibrium in ATRP. The type of a ligand including electronic, steric and solubility characters, greatly affects the reactivity of the catalyst complex and control over the polymerization [13, 66]. The main role of a ligand in ATRP is to solubilize the transition metal salt in the organic media and to adjust the redox potential and halogenophilicity of the metal center forming a complex with an appropriate reactivity and dynamics for the atom transfer. The ligand should complex strongly with the transition metal, and should also allow expansion of the coordination sphere, and should allow selective atom transfer without promoting other reactions.

Ligands for ATRP systems include multidentate alkyl amines, pyridines, pyridineimines, phosphines, ethers or half-metallocene species. Copper complexes with various multidentate *N*-containing ligands are most often used as ATRP catalysts such as PMDETA, and tris[2-(dimethylamino) ethyl]amine (Me_6-TREN)**.** [67] The ATRP catalytic activity of Cu(I) complexes increases in the order bipyridine (bpy)< 1, 1, 4, 7, 10, 10- hexamethyltriethylene tetramine (HMTETA)< PMDETA< tris(2-pyridylmethyl)amine (TPMA)< Me_6-TREN< dimethyl cross-bridge cyclam (DMCBCy). The most active complex known to date is derived from the cross-bridged cyclam ligand DMCBCy [17].

While nitrogen ligands are typically used for copper-based ATRP, phosphorus-based ligands are used for most other transition metals in ATRP.

Solvents

ATRP can be performed in bulk, in solution and in heterogeneous systems (e.g. emulsion and suspension). Generally used solvents are nonpolar, such as toluene, xylene, benzene but some polar aprotic solvents, such as anisole, p-dimethoxybenzene, diphenyl ether, *N*,*N*-dimethylformamide, ethylene carbonate, acetonitrile, and polar protic solvents such as alcohols and water have been successfully used in ATRP. The solvent can have a large influence on the polymerization reaction, both on the polymerization rate and the final properties of the prepared polymer. The influence of solvents on the polymerization rate is attributed to a change in the the structure of the catalyst and/or a change in the solubility of the catalyst complex. For example, when the ATRP of *n*-butyl acrylate was carried out with CuBr/bipyridine complex as catalayst in different sonvents also in bulk, the polymerization rate was found to decrease in the order: ethylene carbonate> bulk> anisole> *p*-dimethoxybenzene> diphenyl ether> propylene carbonate [68]. A solvent is sometimes necessary, especially when the polymer is insoluble in its monomer (e.g., polyacrylonitrile). Several factors affect the solvent choice. Chain transfer to solvent should be minimal. In addition, specific interactions between solvent and the catalytic system should be considered. Catalyst poisoning by the solvent (e.g., carboxylic acids or phosphine in copper-based ATRP) [69]and solvent-assisted side reactions, such as elimination of HX from polystyryl halides, which is more pronounced in a polar solvent [70], should be minimized.

Among the various methods of C/LRP, facile experimental setup and commercial availability of most reagents required for ATRP has resulted in a majority of the

literature reports concerning the synthesis of polymeric materials with well defined compositions, architectures and functionalities.

However, ATRP has some limitations. ATRP is especially sensitive to oxygen, since oxygen can inhibit polymerization not only by the formation of unreactive peroxy radicals but also by the irreversible oxidation of transition metal catalysts. To overcome this problem using air stable catalysts in their higher oxidation states was successfully developed and used as a tool in preparing well-defined polymers [71]. Additionally, reducing the concentrations of catalyst would be beneficial from both industrial and environmental standpoints. Several modified ATRP techniques have been developed that require significantly reduced the amount of catalyst used in ATRP systems [72-74]. These techniques include initiators for continuous activator regeneration (ICAR) ATRP [75], activator regenerated by electron transfer (ARGET) ATRP [76, 77], activators generated by electron transfer (AGET) ATRP [78-80] and single electron transfer living radical polymerization (SET-LRP) [81-85]. In these systems, oxidatively stable Cu(II) complexes were reduced to the Cu(I) complexes at the beginning of the reaction with radicals formed by decomposition of radical initiators or various reducing agents, such as tin(II) 2-ethylhexanoate [76, 78, 80], ascorbic acid [80, 86, 87], phenol [88] or thiophenol and derivatives [89] or sugars [90]. SET-LRP is distinct in that it uses metallic copper as the catalyst.

2.2.3 Reversible addition–fragmentation chain transfer process (RAFT)

A subclass of C/LRP systems, reversible addition-fragmentation chain transfer (RAFT) polymerization, is one of the most extensively studied C/LRP methods [19]. RAFT polymerization is arguably the most adaptable of all the C/LRP techniques due to the ability of polymerizations to be conducted under a variety of conditions [91]. It is the most flexible technique with respect to monomer choice and functional group tolerance and allows for the construction of well-defined polymeric materials with complex architectures. Moreover, a distinct advantage of RAFT polymerization is its relative simplicity and versatility, since conventional free radical polymerizations can be readily converted into a RAFT process by adding an appropriate RAFT agent while other reaction parameters can be kept constant.

The selection of an appropriate RAFT agent for any particular monomer is probably the most crucial step in performing a successful RAFT polymerization. RAFT agent have in common to contain a thiocarbonylthio function, and their structure can be

schemed as [Z-(C=S)S-R] (Figure 2.1), where the R and Z groups both play vital roles in a controlled/living fashion. The R group must be a better leaving group and efficiently reinitiate polymerization and the Z group should first activate the C=S bond toward radical addition and then stabilize the intermediate radical formed. RAFT agents can be categorized into four classes depending on the different substituent group next to the C=S functionality: dithioesters (Z = alkyl or aryl), trithiocarbonates (Z = SR), xanthates (dithiocarbonates) (Z = O-alkyl) and dithiocarbamates ($Z = NR_2$) (R = alkyl or H) (Figure 2.1) [92, 93].

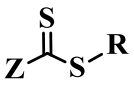

R	Z	Class of RAFT agent
$-CH_2CN$, $-CH_2Ph$	$-Ph$	Dithioseter
$-C(CH_3)_2(COOEt)$	$-C_nH_{2n+1}$	
$-C(CH_3)_2CN$	$-NEt_2$	Dithiocarbamate
$-C(CH_3)_2Ph$	$-OEt$	Xanthate (MADIX agent)
$-C(CH_3)_2CN$	$-SCH_3$	Trithiocarbonate

Figure 2.1: Main classes of RAFT agents.

Unlike ATRP and NMP, where the equilibrium between the dormant and active, propagating chains is based on reversible termination, RAFT polymerization is based on reversible or degenerate chain transfer.

The generally accepted mechanism for a RAFT polymerization is depicted in Figure 2.2 [94]. The first step of polymerization is the initiation step, where a radical is created and reacts with the monomer (step I). This growing polymer chain rapidly adds to the reactive [S=C(Z)SR] bond of the RAFT agent to form a radical intermediate (the radical initiator may add directly onto the RAFT agent, before reacting with any monomer). Step II shows the fragmentation of the intermediate occurring reversibly either toward the initial growing chain or to free the re-initiating group ($R^{\bullet}$) and a polymeric RAFT agent. The radical $R^{\bullet}$ can then re-initiate polymerization by reacting with the monomers or react back on the polymeric RAFT agent (step III). Once the initial RAFT agent has been entirely consumed, the polymeric RAFT agent is solely present in the reaction medium and enters equilibrium (IV). This equilibrium is considered the main equilibrium, and a rapid exchange between active and dormant (thiocarbonyl- thio capped) chains ensures equal probability for all chains to grow, therefore leading to the production of narrow

polydispersity polymers. Although limited, termination reactions still occur v*ia* combination or disproportionation mechanisms (step IV). When the polymerization is complete, the great majority of the chains contain the thiocarbonylthio moiety as the end group which has been identified by ^{1}H NMR and UV–vis spectroscopy [20]. Additional evidence for the proposed mechanism was provided by the identification of the intermediate thioketal radical by electron spin resonance (ESR) spectroscopy [95].

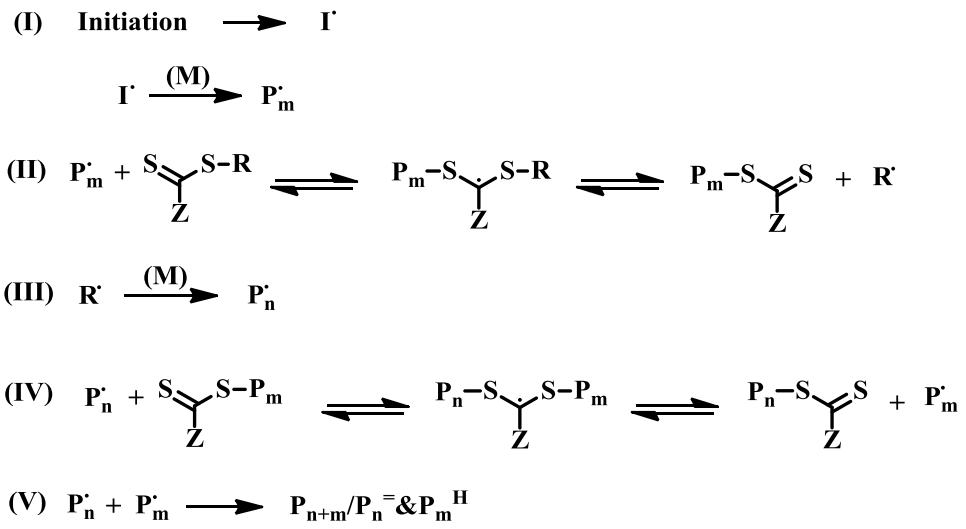

Figure 2.2: Proposed general mechanism of RAFT polymerization.

Many different sources of initiation have been reported for a RAFT polymerization, such as the thermal initiation, direct photochemical stimulation of the RAFT agent by ultraviolet light or γ radiation and by decomposition of organic initiators. The thermal decomposition of radical initiators is, however, the most widely adopted method of initiation, due to the commercial availability of such compounds. Polymerization temperature is usually in the range of 60–80 ^{o}C, which corresponds to the optimum decomposition temperature interval of the well-known initiator azobis(isobutyronitrile) (AIBN). However, even room temperature and high temperature conditions can also be applied [96, 97]. Generally, a RAFT agent/free-radical ratio of 1:1 to 10:1 yields polymers with narrow molecular weight distributions.

Photo- and γ-ray-induced reactions, which use light energy to generate radicals in RAFT polymerization, offer a number of advantages compared with thermally initiated ones. The major advantage is to allow the polymerization to be conducted at room temperature with relatively shorter reaction times. In photoinduced reactions,

however, the RAFT agent should carefully be selected, as in some cases control over the molecular weight cannot be attained, particularly at high conversions because it may also decompose under UV light [98]. γ-Ray-induced RAFT polymerization appeared to be more penetrating compared with the corresponding UV-induced processes [99, 100].

2.3. Click Chemistry

The term 'click chemistry', or 'click reaction', was coined by Sharpless and co-workers in 2001 to describe an approach to building complex molecules from a few, straightforward, thermodynamically favorable reactions, commonly involving the construction of carbon atom–heteroatom linkages [21]. To be classified as click reaction Sharpless et al. outlined a set of certain criteria that a reaction obey. For example, the reaction must be modular, wide in scope, give (near) quantitative yields, generate inoffensive byproducts, be stereospecific and involve simple experimental procedure. They should also make use of readily available starting materials, enviromentally frendly conditions (water as solvent or solvent-free conditions), and should avoid chromatographic isolations. In that sense, click chemistry is not limited to a specific type of reaction but rather defines a synthetic concept that comprises a range of reactions, with different reaction mechanisms, but common reaction criteria. Examples of reactions that fulfill this criteria include the Cu(I) catalyzed reaction between an alkyne and an azide, Diels–Alder reactions in general, C=C bond additions, non-Aldol carbonyl chemistry, and nucleophilic ring opening reactions, especially involving epoxides.

In this section, the most well-known of click reactions, the copper(I)-catalyzed azide/alkyne cycloaddition (CuAAC) reaction and Diels-Alder reaction will be discussed along with another increasingly popular click reaction, such as thiol-ene radical addition reaction.

2.3.1 Copper(I) catalyzed azide-alkyne cycloaddition (CuAAC) reaction

The copper(I) catalyzed azide-alkyne cycloaddition (CuAAC) reaction is derived from the original 1,3-dipolar cycloaddition of organic azides to terminal alkynes discovered by Huisgen et al. [101] and later enhanced and popularized by Sharpless [21], is a very efficient coupling reaction. This methodology was also independently

discovered by Meldal et al. [102] at about the same time that provides diverse applications ranging from small organic molecule synthesis, drug discovery to polymer and materials science.

The critical invention of this process is the transformation of a purely thermal 1,3-dipolar cycloaddition process to a 1,3-dipolar cycloaddition process catalyzed by metal salts (mostly Cu(I) salts, but recently also Ru, Ni, Pd, Pt and Fe salts) which runs at ambient temperature, is nearly solvent insensitive, and with an extremely high tolerance of numerous functional groups. In the absence of an appropriate catalyst, in most cases, this reaction is generally slow and not regioselective [103], but in the presence of Cu(I), which binds to terminal alkynes to form intermediate copper acetylides, this cycloaddition reaction is dramatically accelerated, regioselective and highly efficient. Cu(I) catalysis directs the reaction to form the 1,4-regioisomer exclusively (Scheme 2.9) and increases the reaction rate up to 10^7 times [104], eliminating the need for elevated temperatures.

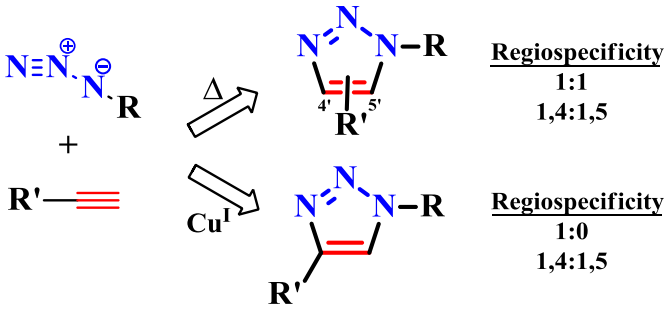

(2.9)

The mechanism of the reaction is different from that of a purely thermal 1,3-dipolar cycloaddition. According to Sharpless *et al*. [105] , modified by Finn *et al*. [106, 107] by computational methods [108, 109] , and finally revised by Bock *et al*. [110] , the metal-catalyzed reaction involves: (a) an up to 10^5 times rate acceleration and an absolute 1,4-regioselectivity of the Cu(I)-catalyzed process; (b) a kinetic feature of the reaction indicating at least second-order kinetics with respect to the concentration of the copper species, [107] thus involving at least two copper centers within the catalytic cycle, presumably linking two acetylenes via a μ-bridge [111]; (c) a significant autoacceleration if multiple triazoles are formed [112] , revealing intermolecular ligands effects; and (d) a significant rate-reduction with strongly increasing amount of copper. Another report supported by DFT calculations described rate enhancement is due to a stepwise process lowering the transition state energy compared to the uncatalyzed concerted cycloaddition [109].

Although CuAAC click reacton was initially postulated as a general concept for organic synthesis, this strategy also has an enormous potential in polymer science. The important application of CuAAC in polymer chemistry is not only the synthesis of functionalized polymers (either end-functionalized or side-functionalized) but also the construction of polymers with well-defined architectures. Since the first report of click chemistry in polymer science by Hawker, Sharpless and coworkers, the construction of well-defined and complex macromolecular architectures via click chemistry has been fully exploited [113]. Afterwards, the number of publications in this field has increased dramatically within the years.

2.3.2 Diels-Alder reaction

The Diels-Alder reaction is defined as the cycloaddition reaction between a conjugated diene and a second component, called dienophile to construct a six membered ring in a regio- and stereo controlled way. The Diels-Alder reaction was discovered in 1928 by Otto Diels and his student Kurt Alder awarded the Nobel Prize in 1950 bearing their names [114]. The discovery of this reaction, has had a significant impact on mechanistic and synthetic organic chemistry.

The reaction is classified as a [4π + 2π] cycloadditon; 4 and 2 identify both the number of π electrons involved in the electronic rearrangement and the number of atoms originating unsaturated six-membered ring. The reorganization of the π electrons and the formation of two new sigma bonds and one new π bond all take place in a concerted manner as illustrated in Scheme 2.10.

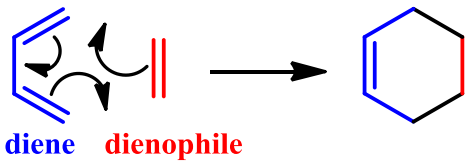

(2.10)

A great variety of conjugated dienes and dienophiles can be used for constructing simple and complex molecules. In the typical Diels-Alder reaction the diene is substituted with electron donating functional groups (like -OR, -NR_2, etc) and the dienophile is substituted with electron-withdrawing functional groups (like -CN, -CO, -COOR, -NO_2, etc).

The basic requirement is that the conjugated dienes must have *cisoid* conformation in order to participate in the Diels-Alder reaction Scheme 2.11. Even though rigid transoid structures of dienes that are more stable due to steric reasons are unreactive

in the Diels-Alder reactions [115]. Additionally, cyclic conjugated dienes, which are locked into the rigid *cisoid* form, are particularly more reactive.

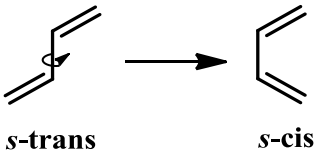

(2.11)

With the potential of forming carbon-carbon, the reaction has remained as one of the best powerful organic transformations in chemical synthesis. When diene and/or dienophile have a heteroatom, the cycloaddition is called a hetero-Diels Alder reaction. The Diels-Alder reaction can be intermolecular or intramolecular and can be carried out under a variety of experimental conditions. Many factors have contributed to the popularity of the Diels-Alder reaction in organic synthesis. One of the considerable advantage of this reaction is the readiness of many adducts to undergo the reverse reaction which is also known as the retro Diels–Alder reaction when heated to an appropriate temperature, thus regenerating the starting reactants.

2.3.2.1 Stereochemistry of Diels-Alder reaction

The regio- and stereoselectivities of the Diels-Alder cycloaddition depends on the number and the nature of the substutients on the diene and dienophile as well as on the reaction conditions (catalyst, temperature, pressure, solvent, etc.) explained in terms of the frontier molecular orbitals (FMO) of dienes and dienophiles. Frontier orbitals are the highest occupied molecular orbital (HOMO) and lowest unoccupied molecular orbital (LUMO). FMO theory give a better explanation matching of the complementary rectivity surfaces of the diene and dienophile. Woodward and Hoffmann pointed out that if the cycloaddition is concerted (bonds are being formed and broken at the same time), during the Diels-Alder reaction the HOMO of the diene interacts in phase (constructive overlap) with LUMO of the dienophile (Scheme 2.12):

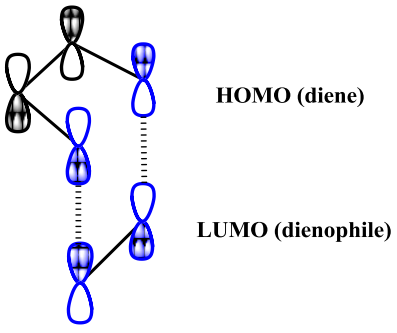

(2.12)

Since the Diels-Alder reaction is suprafacial reaction (sigma bonds are formed or broken on the same face of the π system) relative stereochemistry of the substituents in the 1,4-position of the diene and 1,2-positions of the dienophile is retained in the product. Thus, a *cis* dienophile gives cis substutients in the product, and a *trans* dienophile gives *trans* substutients in the product [116]. Similarly, *trans,trans*-1,4 disubstituted dienes give rise to adducts in which the 1,4-substituents are *cis* relative to each other. The *cis, trans* isomer of the dienes give products in which the 1,4-substituents are *trans* (Figure 2.3) [117-119].

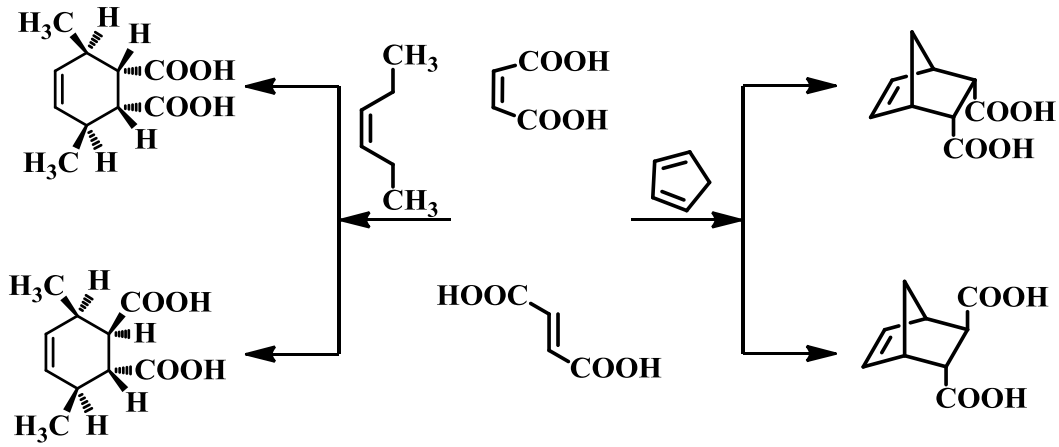

Figure 2.3: Illustration of the '*cis*' rule in Diels-Alder reaction.

When an unsymmetrical diene reacts with an unsymetrical dienophile, the mixture of regioisomers can be formed depending on the orientation of the substituents of the diene and dienophile in the transition state. In most cases of the regioselectivity of Diels-Alder reactions, ortho and para orientations in products are usually favored over meta orientation in unsymmetrically substituted diene and dienophile [120]. The regioselectivity in Diels-Alder reactions is exemplified in Scheme 2.13.

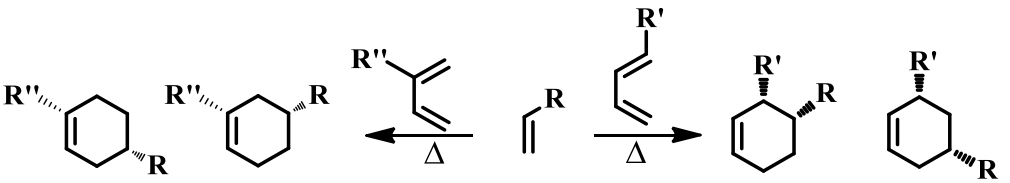

(2.13)

para		meta	R''	R	R'	ortho		meta
80	:	20	$-CH_3$	$-COOCH_3$	$-CH_3$	89	:	11
80	:	20	-Ph	$-COOCH_3$	$-N(C_2H_5)_2$	100	:	0

If the diene is cyclic, the substituent on the dienophile can be either endo or exo in the product, based on the orientation of the diene and dienophile with respect to each other in the transition state. However, Diels-Alder reaction is known as highly

selective reaction and quite often gives the *endo* product. This is the "*endo* rule", first proposed by Alder [116]. According to the endo mode of attack the substituent on the dienophile is underneath the diene framework (*endo* approach), while in the exo mode of addition the substituent on the dienophile is away from the diene framework (*exo* approach) (Scheme 2.14).

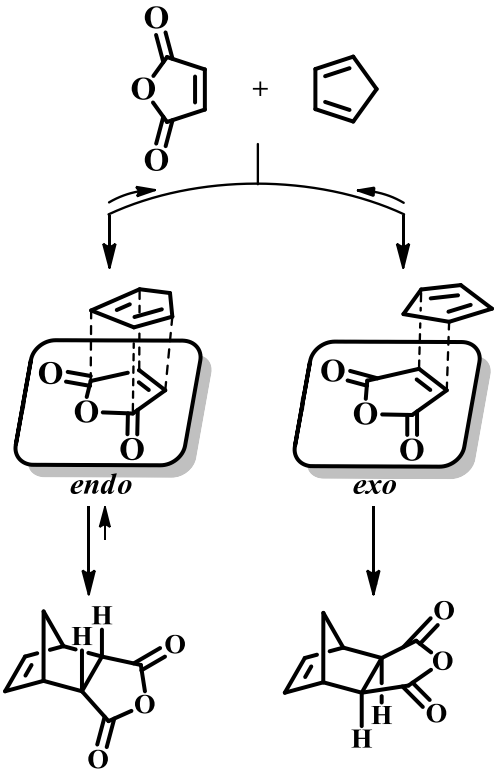

(2.14)

The "*endo* rule" is usually rationalized as a result of the principle of maximum spatial overlap of the unsaturated centers of the diene and the dienophile. However, the *endo* isomer is less stable (because of steric repulsions) thermodynamically than the exo isomer and is said to be formed under kinetic control. In spite of this, the *endo* tends to be major product because of stabilizing secondary orbital interactions in the transition state. Woodward, Hoffman, and Fukui showed that favorable interaction between the substituent π system and that of the diene during cyclization overcomes the steric hindrance and thus favors the *endo* isomer over the *exo* (Scheme 2.15) [121, 122].

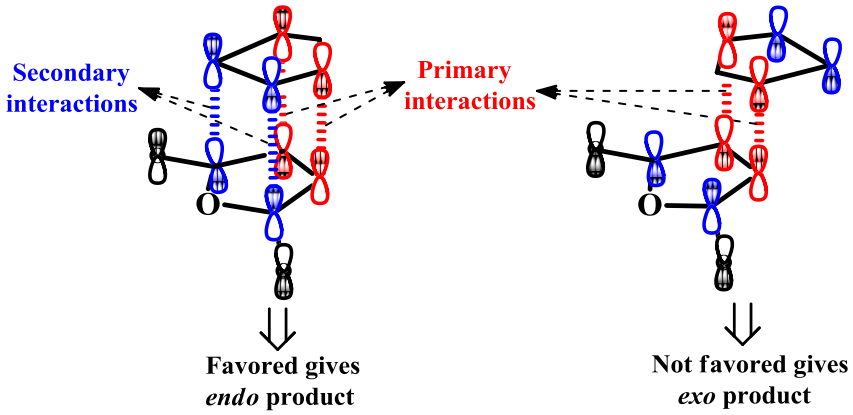

(2.15)

Considering that the Diels-Alder reaction is reversible at elevated temperatures, the *endo*/*exo* ratio depends on the reaction temperature. Therefore use of high temperature and extended periods of time can results in the formation of the thermodynamically more favorable exo product at the expence of the *endo* product.

2.3.2.2 Catalyst

The presence of a Lewis acid catalyst in Diels-alder reaction often allows for a dramatic increase in the rate of cycloaddition; this has been attributed to changes in energy of molecular orbitals when complexed so that there is a lower activation energy.

Because the Lewis acid coordinates at the Lewis base side of the dienophile (Scheme 2.16), it makes the reactions possible with low reactive dienes with dienophiles more electron-withdrawing and, therefore, more reactive [123].

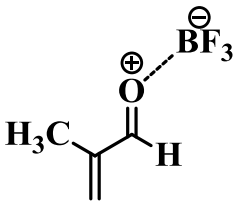

(2.16)

A large number of Lewis acids have been advocated for the catalysis of the Diels-Alder reaction like $AlCl_3$, Et_2AlCl, BF_3, $B(OAc)_3$, $ZnCl_2$, $SnCl_4$ and $TiCl_4$ [124]. In addition to Lewis acids, proteins, antibodies, enzymes and radicals have been found to catalyze the Diels-Alder cycloaddition [125].

The use of a catalyst allows the cycloaddition to be carried out under mild conditions shorter reaction time at lower temperatures and, thus, allows for greater differentiation of the regio- and stereoselectivity. The addition of a Lewis acid appears to be essential to maximize selectivity for the vast majority of Diels-Alder

reactions [126-128]. Two examples of the effects of Lewis acids on selectivities are given in Scheme 2 17 [129, 130]. The reaction catalyst by anhdrous $AlCl_3$ showed much higher *endo* selectivity than the uncatalyst reaction.

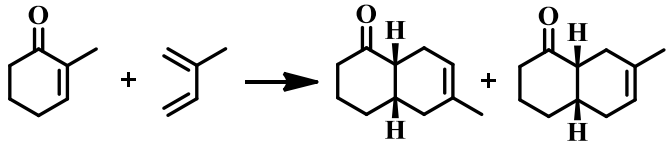

Reaction Conditions	para/meta
150 °C, 142 h	65:35
$AlCl_3$, 25 °C, 17 h	97:3

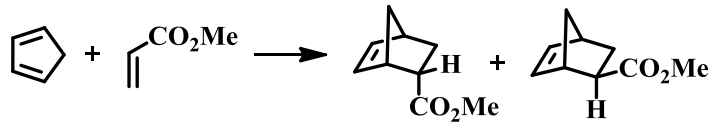

(2.17)

Reaction Conditions	*endo/exo*
CH_2Cl_2, 0 °C, 67 h	92:8
CH_2Cl_2, $AlCl_3$, 0 °C, 1 h	98:2

2.3.2.3 Solvent

It is known that the Diels-Alder reaction is moderately sensitive to solvent effects; [125, 131, 132] however, water was shown to have a positive effect on both the reaction rate and stereoselectivity. The positive effects of water are due to the hydrophobic packing and the enforced hydrophobic hydration in addition to the hydrogen-bonding effects [133].

The Diels-Alder reaction is a valuable, competitive, and alternative to CuAAC "click" chemistry. Many factors have contributed to the popularity of this reaction in polymer science. Major interest has risen within the past few years as research groups have started to acknowledge all the benefits this reaction can offer in designing novel macromolecules. So far, the use of Diels-Alder ''click'' reaction in combination with C/LRP techniques have been facilitated access to the construction of various architectures (e.g. block copolymers [134, 135], star polymers [136], dendronized polymers [137-140] and graft copolymers [141-143]).

2.3.3 Thiol-ene reaction

The thiol-ene reaction is an emerging synthetic tool that is considered to be a "click" reaction because the reaction has many of the attributes of the click reaction, for example, quantitative yields, rapid reaction rates, mild reaction conditions, and tolerant of various solvents and functional groups.

The thiol-ene chemistry, which involves the hydrothiolation of a C=C bond, can be induced photochemically or thermally at ambient temperature to mainly give an anti-Markownik-type product. Generally, the thiol-ene reaction follows a radical-mediated process, with initiation, propagation and termination steps. Initiation involves the treatment of a thiol with an initiator, under irradiation or heat, subsequently generating a thiyl radical, $RS^{\cdot}$, via hydrogen abstraction, plus other byproducts (Scheme 2.18). Propagation then occurs in two step which involves first the direct addition of the thiyl radical to the C=C bond producing an intermediate thioether carbon radical followed by chain transfer to a second molecule of thiol to give the thiol-ene addition product with the concomitant generation of a new thiyl radical. Termination is believed to ocur through the radical-radical recombination of the thioether carbon and/or thiyl radicals.

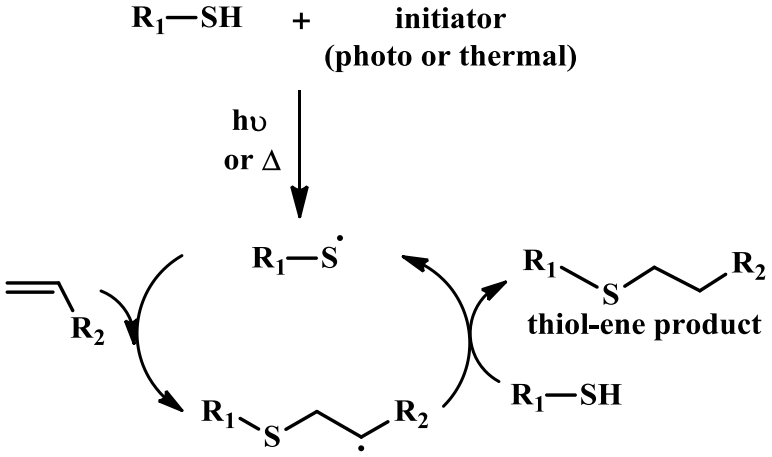

(2.18)

Although thiol–ene click reaction has mainly been focused on a radical-mediated version to non-activated alkenes, this reaction can also proceed via Michael addition, especially when the vinyl group is alpha to an electron withdrawing moiety. The Michael addition applies to α, β- unsaturated carbonyl compounds such as acrylate, maleimido, etc., and an intermediate thioanion is usually generated owing to the usage of a base or nucleophilic catalysis such as NEt_3, primary/secondary amines or certain phosphines for the reaction.

The thiol-ene ‘‘click’’ reactions, through either a radical or nucleophilic mechanism, provide efficient hydrothiolation routes across virtually any double bond. [144-148]

Over the years, the thiol-ene ‘‘click’’ reaction has been extensively exploited in polymer chemistry since it can be conducted under various conditions without any metal catalyst. The UV-induced crosslinking of unsaturated polymers (photocuring) by reaction with multifunctional thiols is currently employed in surface coating

owing to a number of advantages over other curing methods. Biomaterials for application in medicine, especially dentistry, have been prepared by using this process. Only recently, however, has the click aspect of the thiol-ene ‘‘click’’ reaction been fully appreciated in the field of polymer science. The use of thio-Michael addition as a click reaction was recently reported by Lowe et al. for the synthesis of star polymers [149]. The great potential of thiol–ene chemistry was exploited by Hawker and co-workers in the synthesis of poly(thioether) dendrimers [150]. Consequently, numerous examples are available in the literature for polymer end group and backbone modification [151-153], many of which are covered in various excellent reviews [145, 154, 155].

2.4 Polymer Topology

The need to synthesize polymers with new and/or improved properties properties has driven the effort to design polymers with novel macromolecular architectures. The properties of polymers depend strongly on their topologies, and finding facile and feasible synthetic methods for polymers with different topological structures remains a goal for polymer chemists. Polymer topology can be generally defined as the fabrication of complex macromolecular structures with defined composition, functionality, and architecture (e.g. telechelic polymers, block copolymers, macromolecular brushes, stars, and networks) as depicted in Figure 2.4.

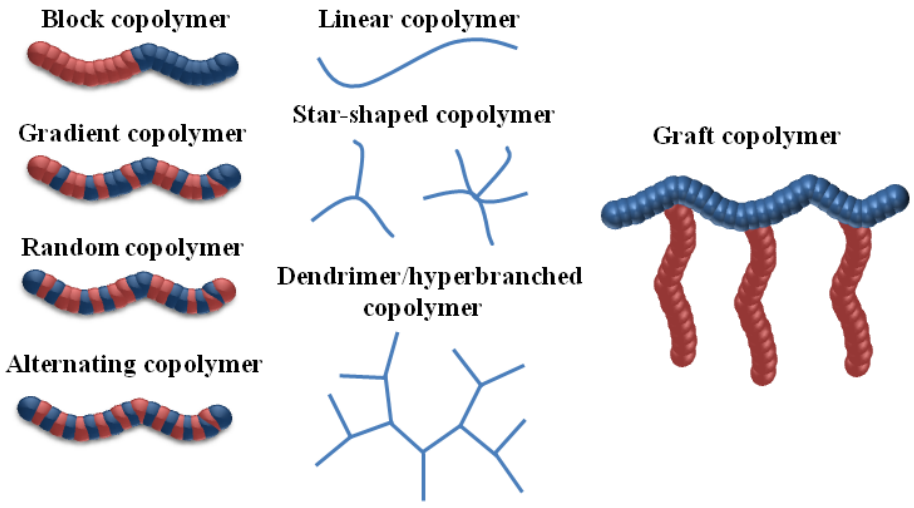

Figure 2.4: Schematic represantation of selected (co)polymer architectures.

C/LRP techniques are well suited for preparation of polymers with precisely controlled architectures, including graft and star polymers as well as branched,

dendritic, network, and cyclic type structures. In addition to versatile polymerization chemistry, the synthesis of such complex macromolecules often requires the use of efficient and specific postpolymerization modification techniques to incorporate functionality potentially incompatible with the polymerization conditions and to build novel structures by coupling preformed polymers. In this respect, click reactions are especially well conformed for such advanced macromolecular design. Indeed, click strategies have served as a complementary tools for most of the major synthetic polymerization techniques, such as ring opening polymerization (ROP), ring opening metathesis polymerization (ROMP), polycondensation, conventional free-radical polymerization, and C/LRPs.

2.4.1 Graft copolymers

Graft polymers refer to the special type of branched polymers in which branched chains are structurally distinct from the main chain. The main chain is commonly called as the backbone and the branches as the side chains which are distributed along the backbones either randomly or uniformly.

When graft polymers characterized by a high density of grafted chains they were named ‘‘macromolecular brushes’’. In terms of chemical composition, macromolecular brushes can be categorized into homopolymer brushes and copolymer brushes. The latter typically consist of two or more types of polymer side chains. When only two types of polymer grafts are involved, they can be arranged in a random, alternating, block, and “centipede” manner.

Graft copolymers have been the subject of continuously increasing interest due to their unique specific properties (morphology, phase behaviour, etc.). In general, graft copolymers can be prepared following three main strategies: (a) the “*grafting onto*”, (b) the “*grafting from*”, and (c) *the* “*grafting through*” strategies which differentiate from each other based on the formation principle. The different pathways are schematically depicted in Figure 2.5 and will be discussed in the context of the ensuing sections.

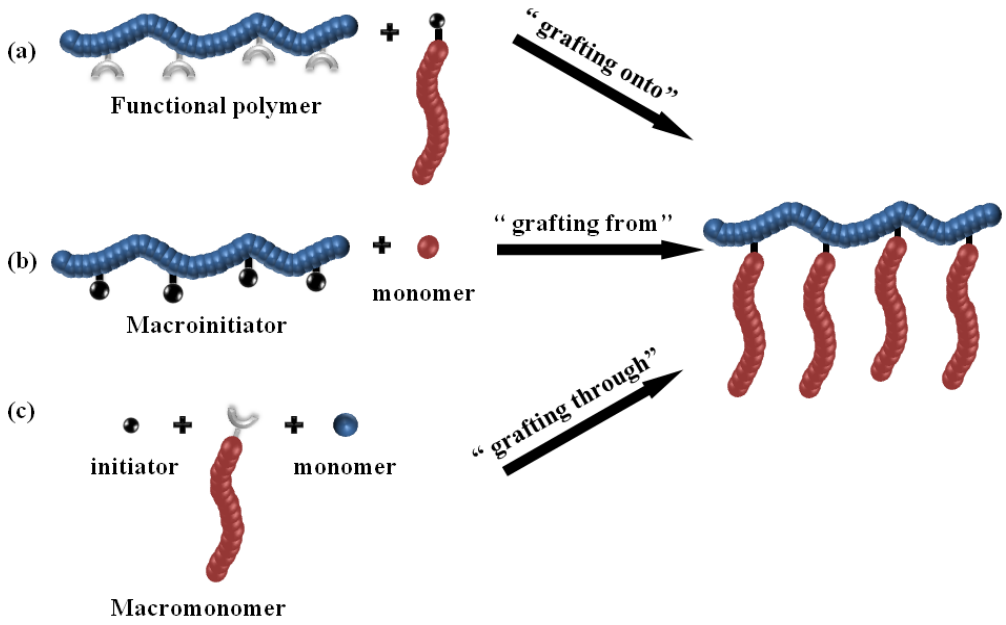

Figure 2.5: Strategies for the synthesis of graft copolymer: (a) ‘‘grafting onto’’, (b) ‘‘grafting from’’, and (c) ‘‘grafting through’’.

The ‘‘*grafting onto*’’ strategy involves the attachment of preformed polymer chains via chemical reaction with reactive side chains of a polymer backbone. Secondly, the ‘‘*grafting from*’’ strategy, consists in a polymerization of the grafts from a polymer backbone bearing initiating sites. The last approach is the ‘‘grafting through’’ strategy which relies on polymerization of appropriate macromonomers.

Each of these strategies controls different structural parameters, including chemical composition, grafting density, degree of polymerization (DP) of side chains, and DP of the backbone. Even though each strategy demonstrates distinct advantages with respect to the molecular design, there are also limitations from a synthetic perspective. There are several strategies that have been employed to synthesize graft polymers thus, increasing interest in their various possible applications. Graft copolymers can be synthesized using any of the various polymerization techniques available including: anionic polymerization, ROMP, conventional radical polymerization, C/LRPs, and various coupling reactions (‘‘click chemistry’’).

2.4.1.1 General synthetic routes

The ‘‘*grafting onto*’’ strategy

The ‘‘*grafting onto*’’ method (a) relying on grafting of preformed side chains onto a backbone is carried out via a coupling reaction between the pendant functional

groups distributed randomly on the backbone and the complementary end-functional groups of side chains.

The primary advantage of this method is that both backbone and side chains are prepared separately via different living polymerization techniques allowing the more accurate characterization of the resulting polymer with respect to their backbone and side chains. On the other hand, the number of grafted polymer chains is limited due to the steric hindrance and low reactivity of functional groups of the polymer chains resulting in insufficient grafting efficiency.

Usually, ‘‘g*rafting onto*’’ reactions involve the preparation of well-defined side chains by living anionic polymerization and their subsequent reaction with a backbone of monomer units that are susceptible to nucleophilic attack. Examples of such functional groups include esters, anhydrides, benzylic halides, nitriles, chlorosilanes, and epoxides. So far, polymers bearing highly reactive benzylic halides, particularly poly(chloromethylstyrene)s, have been largely used as backbones subsequent reaction with the living polymers [156-159]. A number of different ways have been tried to improve the grafting density by reducing the contribution of side reactions resulting from the halogen–metal exchange. In this respect, the chloromethyl groups were transformed to the chlorosilyl groups before reaction with the living polymers. A representative example is the preparation of poly(Bd-*g*-St) copolymers, where the polybutadiene (PBd) backbone is synthesized by anionic polymerization, followed by introduction of chlorosilane groups, via postpolymerization hydrosilylation, and, finally, linking with living PS anions [160-162].

Beside the above mentioned anionic polymerization techniques, so far, extensive attempts for the preparation of graft copolymers using ‘‘click’’ chemistry and combined with some of the other C/LRP techniques that have been used to construct a graft architecture applying a ‘‘*grafting onto*” concept. Click reactions are expected to efficiently attach side chains to a backbone in ‘‘*grafting onto*’’ method. Obviously, this technique offering unique opportunities to improve the grafting efficiency have been explored. However, the problems for controlling the grafting density remain a challenge especially when clicking long or ‘‘thick’’ chains to the backbone.

By means of the high coupling efficiency between bromine and TEMPO groups poly(4-glycidyloxy-2,2,6,6-tetramethylpiperidine-1-oxyl-*co*-ethylene oxide)-*g*-PS

and P*t*BA have been constructed via the Atom Transfer Nitroxide Radical Coupling (ATNRC) method (Scheme 2.19) [163].

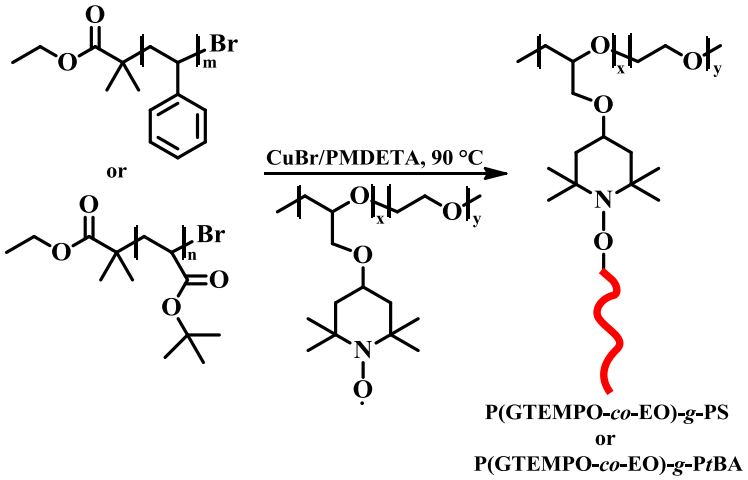

(2.19)

Where the ‘‘click’’ chemistry is concerned, Matyjaszewski and co-workers reported on the poly(hydroxyethyl methacrylate) (PHEMA) modification with 4-pentynoic acid in order to incorporate alkyne functionality along the backbone, followed by reaction with azido-terminated polymers via enabled synthesis of well-defined graft copolymers in an efficient manner (Scheme 2.20) [164]. For the bulkier side chains such as PS, PBA, and PBA-*b*-PS, grafting densities were lower than 50% because the steric hindrance of attached side chains; while the relatively ‘‘thinner’’ PEO side chains were grafted onto the backbone, the grafting density reached up to 88.4%.

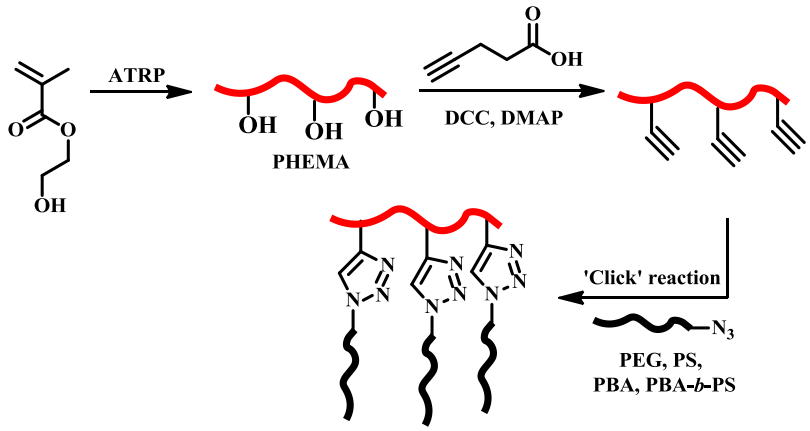

(2.20)

The same authors exploited a similar click concept to prepare graft copolymer [165]. Poly(glycidyl methacrylate-*co*-methyl methacrylate) P(GMA-*co*-MMA) copolymer were synthesized by ATRP. The epoxide ring in copolymer was efficiently opened with sodium azide in the presence of ammonium chloride. Then, poly(ethylene oxide) methyl ether pentynoate was added azide functional P(GMA-*co*-MMA)

copolymer through CuAAC reaction to form respective loosely grafted polymeric brushes with hydrophilic poly(ethylene oxide) side chains.

In an effort to further expand the versatility of click reaction toward the synthesis of graft copolymer, Stenzel and coworkers [166] reported a ‘‘*grafting onto*” approach of combining RAFT polymerization and CuAAC reactions. In this case, propargyl methacrylate (PgMA) with its acetylene function protected with a silyl group was polymerized via the RAFT process. Subsequent deprotection of the representative acetylene species followed by reaction with azide functionalized poly(vinyl acetate) (PVAc) via cycloaddition process to afford the graft copolymer (Scheme 2.21).

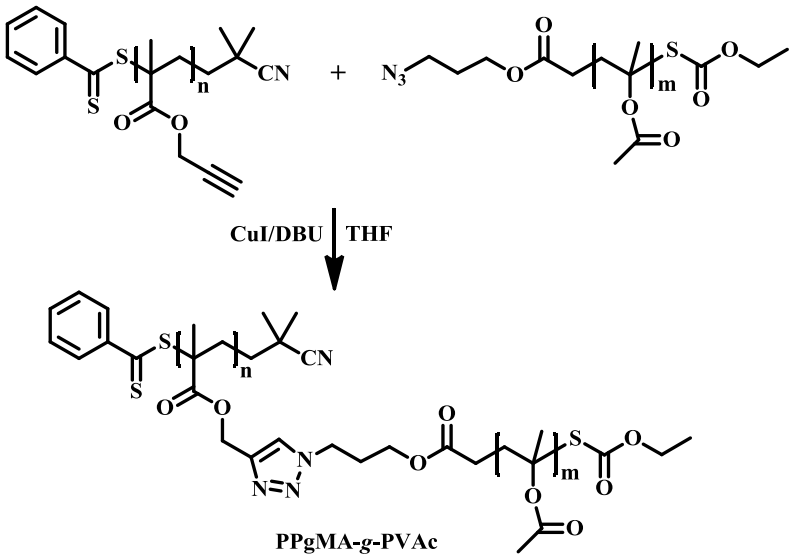

(2.21)

In a similar fashion, a Diels-Alder click reaction has been used to prepare graft copolymers. Gacal et al. also applied the “*grafting onto*” approach to the synthesis of graft copolymers containing PS backbone and side chains with either PEG or PMMA units using Diels-Alder click reaction (Scheme 2.22) [141].

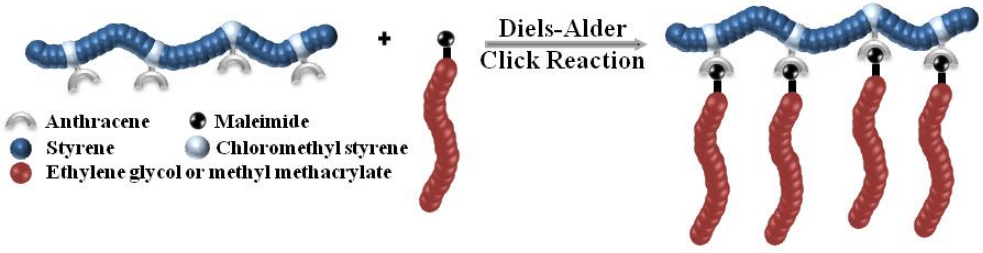

(2.22)

The thiol-ene ‘‘click’’ reaction is one of the most favorable chemical approaches for polymer synthesis. Nuyken et al. firstly synthesized poly[2-(4-methoxybenzylsulfanyl) ethyl-2-oxazoline]-co-poly- (ethyl-2-oxazoline) biocompatible copolymers bearing potential thiol groups with different molecular weights and functional group densities [167]. After quantitative deprotection of thiol

groups and thiol-ene coupling reaction of those SH groups of the copolymer with acrylamide or maleimide in the end of poly(2-methyl-2-oxazoline)s, a series of graft copolymers containing poly(2-oxazoline)s as both backbone and side chains with different lengths of side chains were prepared with a quantitative conversion.

In addition to chemical strategies, physical interactions such as hydrogen bonding [168-170], ionic interactions [171, 172], and coordination bonding [173, 174], have also been used to construct a graft copolymer.

The ‘‘*grafting from*’’ strategy

In the “*grafting from*” (b) method, a polymer backbone (macroinitiator) with a predetermined number of initiation sites is generated, followed by grafting the side chains from the macroinitiator. The number of grafted chains can be controlled by the number of initiation sites generated along the backbone assuming that each one participates in the formation of one branch.

The “*grafting from*” approach has been extensively used in the synthesis of well-defined macromolecular grafts and brushes. For instance, PI-*g*-PS and PBd-*g*-PS well-defined copolymers were synthesized several years ago employing anionic polymerization [175, 176].

C/LRP techniques are suitable for polymer brush synthesis via grafting from method since low concentration of instantaneous propagating species limit the coupling and termination reactions and the gradual growth of side chains can effectively decrease the steric effect which is inevitable for either ‘‘*grafting-onto*’’ or ‘‘*grafting-through*’’ strategies.

ATRP is a particularly attractive and has been proved to be a highly versatile method to synthesize the graft polymers with well-defined structure including the controllable molecular weight and narrow molecular weight distribution. Matyjaszewski and co-workers have previously described the controlled synthesis of molecular brush copolymers by “*grafting from*” a macroinitiator using ATRP [177]. The macroinitiator was obtained by polymerization of 2-(trimethylsilyloxy)ethyl methacrylate (HEMA-TMS), followed by cleavage of the TMS protective groups and esterification with 2-bromopropionyl bromide to produce poly(2-(2-bromopropionyloxy)- ethyl methacrylate) (pBPEM) (Scheme 2.23). This was used as macroinitiators for ATRP of St and butyl acrylate (BA). In order to suppress the coupling and termination reactions, the polymerizations of monomers were

conducted in bulk but under dilute conditions and low conversions (<20%) were maintained.

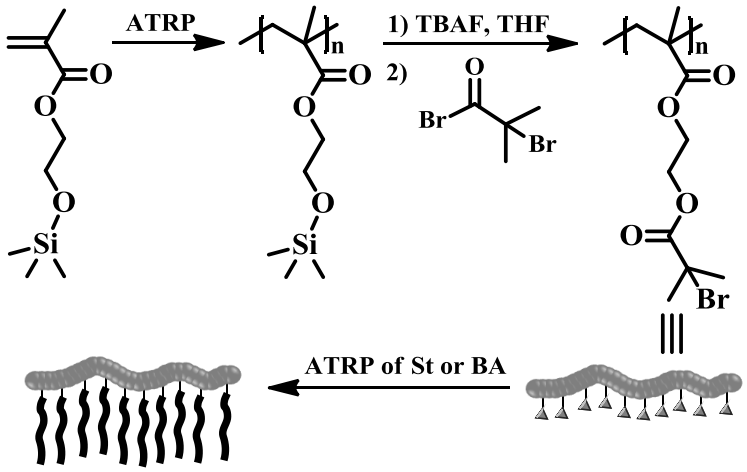

(2.23)

Grubbs et al. reported the preparation of graft and dentritic graft copolymers by successive NMP and ATRP [178]. The backbone was produced by copolymerization of St and p-(4-chloromethylbenzyloxymethyl) styrene via NMP. Through ATRP of St, MMA, and *n*-butyl methacrylate (BMA) initiated by PS backbone containing chloromethyl groups, a series of graft copolymers containing PS backbone and PS, PMMA, or PBMA side chains were prepared.

Inceoglu et al. prepared well-defined graft and block-graft copolymers via the ATRP-NMP combination [179]. First, using ATRP process, MMA and 2-phenyl-2-[(2,2,6,6-tetramethylpiperidino)oxy] ethyl methacrylate as comonomer were polymerized in the presence of CuCl/PMDETA as a catalyst and ethyl-2-bromoisobutyrate or 2-phenyl-2-[(2,2,6,6-tetramethylpiperidino)oxy] ethyl 2-bromopropanoate as an initiator. Second, the corresponding copolymers with TEMPO functionality were then used as polyfunctional macroinitiator in NMP of St to yield the resulting graft and block-graft copolymers (Scheme 2.24).

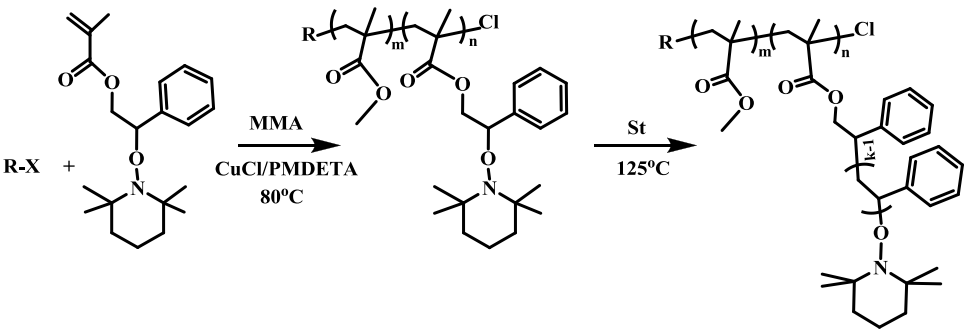

(2.24)

Synthesis of graft copolymer containing PBA-*b*-PS side chains through successive ATRP [180] and PCL-*b*-PBA side chains via the combination of ROP and ATRP

[181] were also reported. Using this similar strategy, Muller et al. synthesized more complex amphiphilic graft copolymers containing PS-*b*-PAA or PAA-*b*-PS side chains [182]. Matyjaszewski et al. also employed AGET ATRP to prepare PBA side chains using poly(2-(2-bromopropionyloxy)ethyl methacrylate) (PPEM) as macroinitiator in mini-emulsion system with relatively high monomer conversion and short reaction time [183].

The ‘‘g*rafting through*’’ strategy

The ‘‘g*rafting through*’’ approach (c) is based on the synthesis of a terminally functional polymer chain followed by a polymerization of this macromonomer.

The attractive feature of this method is that the length of side chains and the grafting density can be controlled by adjusting the degree of polymerization of side chains and backbone, respectively. Also, because the macromonomers are prepared separately, the side chains can be characterized prior to polymerization. This method allows preparation of macromolecular brushes with well-defined grafting density and side-chain length. However, the ‘‘g*rafting through*’’ method suffers from the degree of polymerization of the backbone being dependent on the macromonomer length and type. Additionally, due to the necessarily low concentration of polymerizable end groups and high steric hindrance of the propagating chain end, polymerizations can be slow and not proceed to high conversion [184].

The combination of different polymerization approaches such as ROP, ROMP, C/LRP, and living anionic polymerization, “*grafting through*” led to graft copolymers with precisely controlled M_w/M_n, functionality, copolymer composition, backbone length, branch length, and branch spacing.

There have been several reports on anionic polymerizations of various macromonomers including polyisoprene (PI), PBd, and PS with terminal styrenic and methacrylic functionalities. Hadjichristidis et al. reported that the reaction of polyisoprenyllithium (PI–Li) and polystyrene-*b*-polyisoprenyllithium (PS-*b*-PI–Li) prepared by living anionic polymerization with 4-chlorodimethylsilylstyrene led to the successful preparation of styryl-terminated PI and PS-*b*-PI macromonomers due to the faster reaction of the living polymers with the chlorosilane group than with the styryl-tipped double bond [185]. Thereafter, a series of triblock-graft copolymers of PS-*b*-(PI-*g*-PI)-*b*-PS, PS-*b*-[PI-*g*-(PI-*b*-PS)]-*b*-PS, and (PS-*g*-PS)-*b*-(PI-*g*-PI)-*b*-(PS-*g*-PS) were synthesized by utilizing the macromonomer as a key building block.

ROMP has been considered to be an efficient way to synthesize polymacromonomer with complete conversion as well as with a uniform molecular weight distribution since the ring strain and a larger space of ring functional group provide a favorable environment for polymerization. Grubbs et al. firstly prepared a variety of polymers including PS, PMMA, and P*t*BA, via ATRP [186]. The bromide end groups in these polymers were subsequently converted to azides. (Scheme 2.25) Regardless of the type of polymers, the azido-terminated polymers were reacted with a norbornene monomer containing an alkynyl group through CuAAC reaction. Next, a series of graft copolymers were prepared by ROMP.

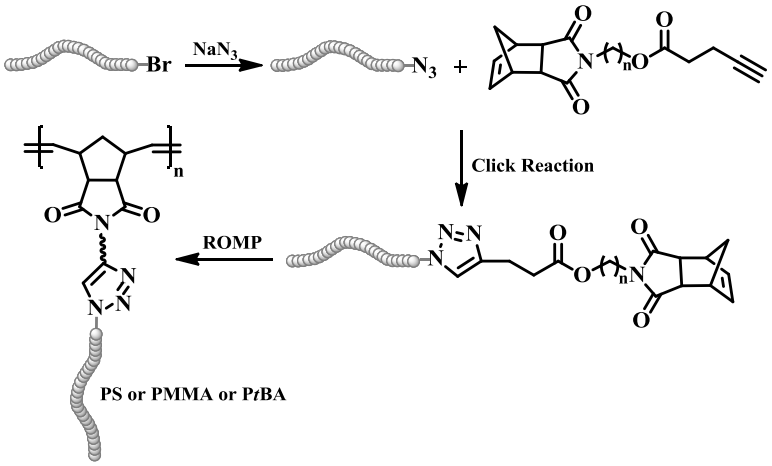

(2.25)

Recently, Durmaz et al. has reported the synthesis of graft copolymers via combination of ROMP with Diels-Alder click reaction [142]. In this case, anthracene-functionalized oxanorbornene monomer and oxanorbornenyl PS with ω-anthracene end-functionalized macromonomer were first polymerized via ROMP then coupled with maleimide end-functionalized polymers, including PEG, PMMA, and P*t*BA via Diels-Alder click reaction to create corresponding graft copolymers, as shown in Scheme 2.26.

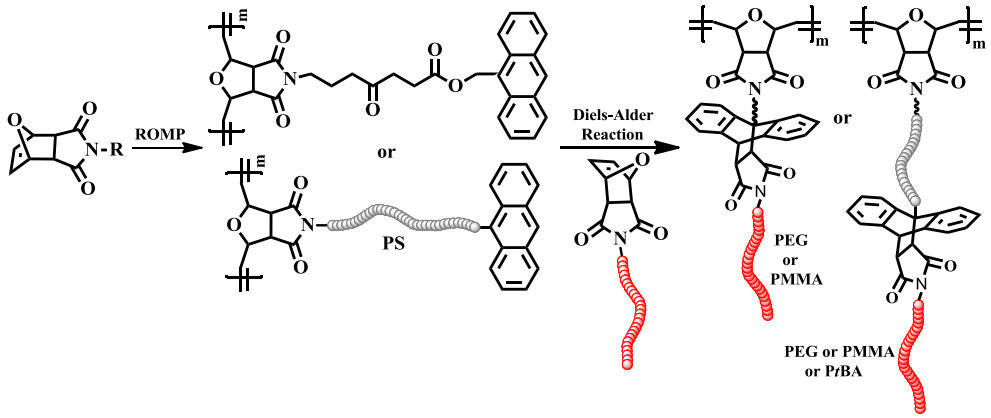

(2.26)

2.4.2 Star polymers

A star polymer consists of several linear polymer chains connected at one central core is one of the simplest form of branched topologies. The presence of a central core in these macromolecules has lead to new, often improved characteristics, compared with their linear polymer analogs. The main feature of star polymers differing them from the linear analogues of identical molar masses, is their compact structure (smaller hydrodynamic volume and radius of gyration, and therefore lower viscosity) and the multiple functionality. This generates several potential applications for star polymers, including drug delivery, cosmetics, coatings, membrane, or lithography.

Depending on their chain composition, star polymers can be classified into two structural categories; homoarm and miktoarm (or heteroarm) star types. In the former case, all arms have the same chemical structure, while in the latter case, two or more than two different types of arms build the star molecule. Thus, miktoarm star polymers are comprised of chemically different arms linked to the branch point. Asymmetry is introduced when arms of different molecular weights, chemical compositions or topologies are incorporated into the same macromolecule. From the viewpoint of asymmetry their structures are shown in Figure 2.6.

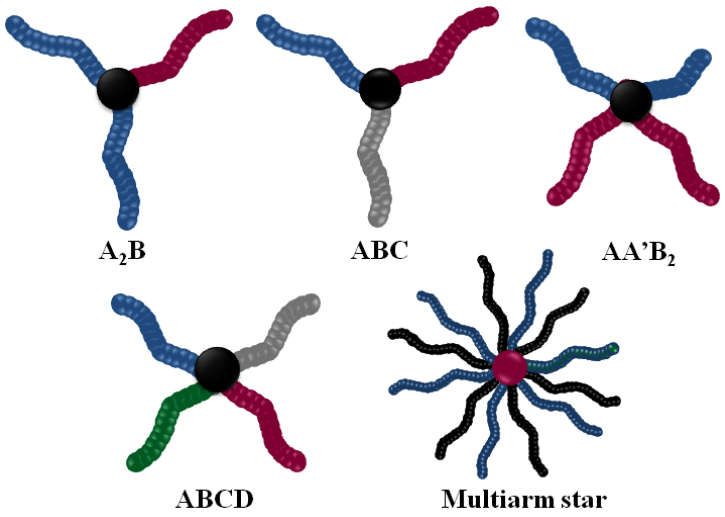

Figure 2.6: Schematic represantation of the some different types of miktoarm star polymers.

Star polymers can be obtained using different polymerization methods, namely anionic polymerization, cationic polymerization, ring-opening polymerization (ROP) and a variety of C/LRP techniques including ATRP, NMP, and RAFT

polymerization. Synthetic strategies for the construction of star polymers can be divided into three main categories according to their formation sequence of core and arms; (i) "core-first"; (ii) "arm-first"; and (iii) "coupling onto". Each of these approaches has associated advantages and disadvantages. The synthetic aspects of all approaches will be discussed in detail below.

2.4.2.1 "Core-first" strategy

In the "core-first" strategy, the polymerization of monomer from the initiating functions present on the preformed multifunctional initiator (core) generates a star molecule with preserved initiating functions at the chain end of each arm, which can be further used for chain extension with a second monomer to form star block copolymers (Figure 2.7).

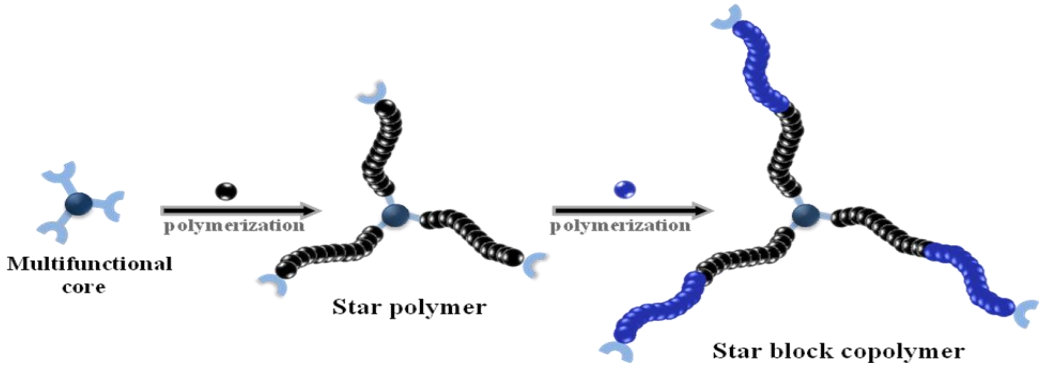

Figure 2.7: Schematic representation of the synthesis of star and star block copolymers by "core-first" method.

In the ''core-first'' method, there are several requirements that a multifunctional initiator has to fulfill in order to produce star polymers with uniform arms, low molecular weight distribution, and controllable molecular weights. All the initiation sites must be equally reactive and have the same rate of initiation [187]. Aditionaly, broad molecular weight distribution was observed because of the large amounts of initiating sites and high probability of radical-radical recombination. Therefore, the polymerization is usually limited to low monomer conversion (<20%) to avoid the star-star coupling reaction [188].

The first successful synthesis of an entire array of homoarm star polymers by "core-first" method was reported by using anionic polymerization [189, 190]. For instance, Quirk et al. achieved the synthesis of well-defined three arm PS using a trifunctional initiator 1,3,5-tris(1 phenylethenyl)-benzene (tri-DPE), was prepared by the reaction

of 3 moles of s-BuLi [191]. In addition, Sawamoto et al. managed to carried out the synthesis of well-defined tri arm PIBVE star polymer using living cationic polymerization [192].

The first example of the synthesis of stars with six arms via ATRP process was reported in 1995; hexakis(chloromethyl)benzene was used as the initiator for St polymerization [193]. Subsequently, star polymers with 3, 4, 6 and 8 arms were prepared using various initiators based on inorganic cores, and various organic structures including core-functional initiators based on natural products [188, 194-199].

NMP was tested for the synthesis of three arm PS [200]. In this study, a trifunctional unimolecular initiator with hydrolysible core was prepared and utilized for the polymerization of St at higher temperature. Analysis of the product revealed a molecular weight comparable to that expected from the initiator to monomer ratio and a narrow polydispersity. These results demonstrated that each of the initiating units in the tris-alkoxyamine was active and the individual PS arms grow at approximately the same rate with little or no cross-linking due to radical coupling reactions.

It is convenient to introduce a wide variety of monomers into the final polymeric structure by means of the combination of different polymerization methods. Because of the variety of polymerization methods and their accompanying choice of monomers, it is easy to see why the ‘‘core-first’’ technique is a versatile and efficient synthetic strategy in the formation of miktoarm star polymers, and it has received great attention.

Using the ‘‘core-first’’ method, Tunca and coworkers was synthesized well-characterized AB_2 miktoarm star polymers, in which the first step was the synthesis of a multifunctional initiator designed for sequential ROP and ATRP [201]. In this study, they used a novel miktofunctional intiator possessing one initiating site for ROP and two initiating sites for ATRP. The successive ROP and ATRP processes yielded the desired AB_2 miktoarm star polymer. The described core-first approach provides another level of control to the synthesis of miktoarm star polymers by employing different miktofunctional initiators (Scheme 2.27).

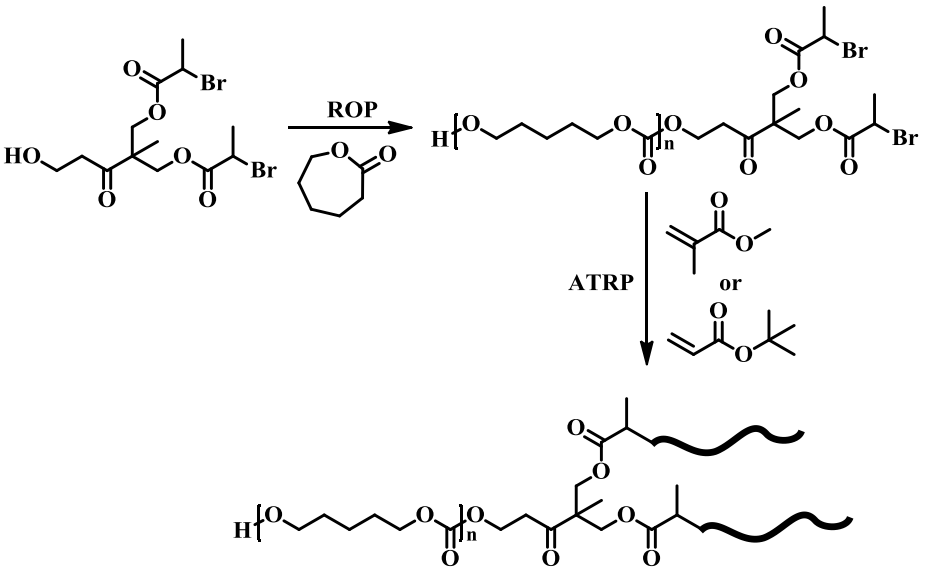

(2.27)

Hizal and coworkers reported a new method to synthesize ABC miktoarm star terpolymers by combining three different controlled/"living" polymerization techniques: ring-opening polymerization ROP, ATRP, and NMP [202]. A trifunctional initiator bearing a hydroxy group, an ATRP initiator, and a NMP initiator was synthesized to create an ABC miktoarm star polymer where each polymerization step does not require end-group modification for subsequent polymerization reactions (Scheme 2.28). This polymer was composed of polycaprolactone (PCL), PS, and P*t*BA.

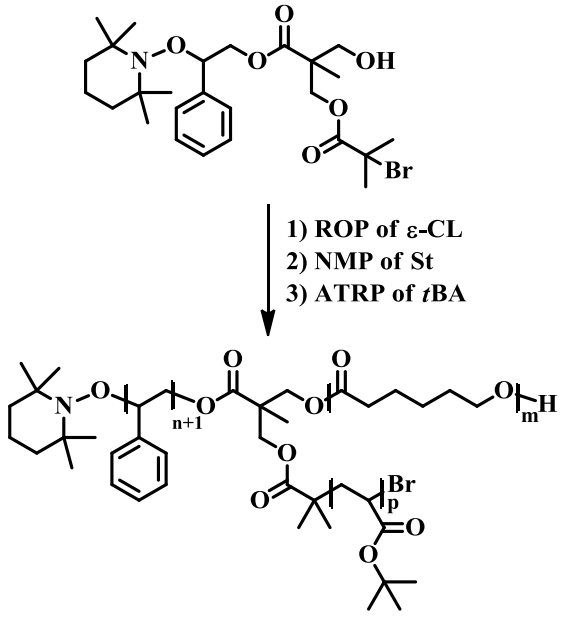

(2.28)

Additionally, Tunca and co-workers synthesized AB_2C_2 type miktoarm star polymer consisting of PS (A), P*t*BA (B) and PMMA (C) with a combination of NMP and ATRP techniques [203]. In this case, they prepared a trifunctional initiator bearing a

NMP initiator and dual ATRP initiators. First NMP of St subsequently ATRP of *t*BA were carried out to create (PS)(P*t*BA)$_2$ miktoarm star polymer. Then, the initiating sites preserved on the AB$_2$ type star polymers was further used for chain extension with a second monomer (MMA) to form (PS)(P*t*BA)$_2$(PMMA)$_2$ miktoarm star polymer.

While variations in either polymer arms or core can lead to an array of new morphologies, the use of responsive core can lead to changes within a single miktoarm star, and therefore can offer potential in applications of these polymers. For instance, in a ‘‘core-first’’ fashion with multifunctional initiator with two bromide (for ATRP) and two TEMPO (for NMP) functionalities, the same group synthesized photoresponsive A$_2$B$_2$ miktoarm stars with an azobenzene unit at core by combination of ATRP and NMP routes (Scheme 2. 29) [204].

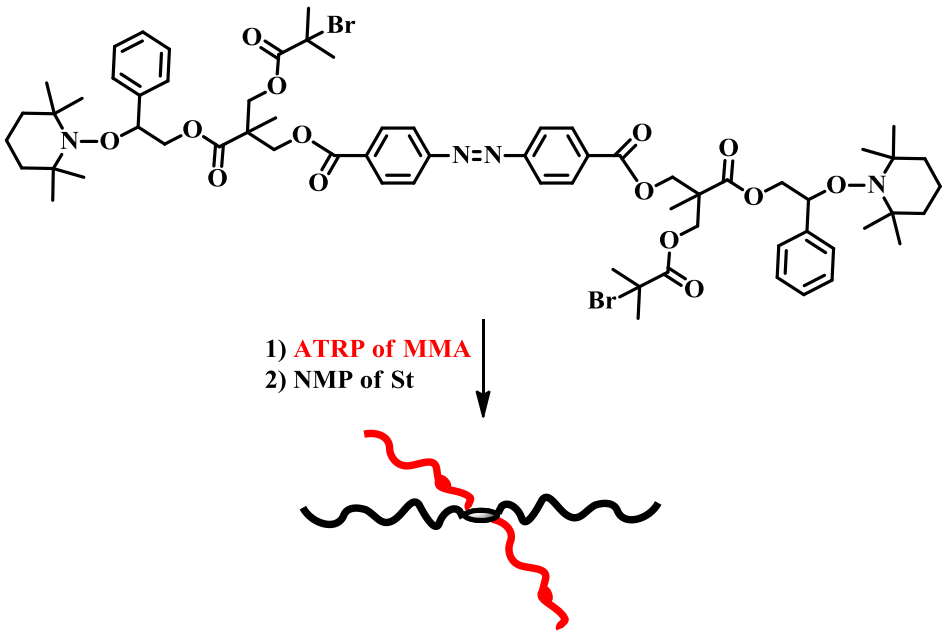

(2.29)

2.4.2.2 “Arm-first” strategy

In the “arm-first method”, a star polymer is synthesized by crosslinking of linear arm precursors to form the core with cross-linking agents usually by using a divinyl cross-linker (Figure 2.8).

While the “core-first” and “coupling onto” methods based on multifunctional initiators or cores with an accurate number of functional groups can afford star polymers with the desired number of arms, the arm-first with divinyl compounds of linear polymers results in statistically distributed numbers of arms due to occurring cross-linking reactions. However, the “arm-first” method can produce star polymers

with a large number of arms (10-100) and consists of relatively simple procedures. This method is more practical than the "core-first" and "coupling onto" methods which require the complicated synthesis of the multifunctional agents.

The star polymer synthesis based on the "arm-first" aproach was first developed in a living anionic polymerization. Zilliox et al. first employed anionic polymerization to prepare star polymers in high yield via the cross-linking of living PS with divinylbenzene (DVB) [205]. On the other hand, the "arm-first" aproach has been studied in living cationic polymerization. The successful preparation of star polymers was first reported by Kanaoka et al. and involved the cationic polymerization of poly(isobutyl vinyl ether) with divinyl ether cross-linkers [206].

With the development of the C/LRP methods have superseded both living anionic and cationic polymerisation methods mainly due to the less stringent reaction conditions and wide range of monomers. So far, ATRP has been extensively used to prepare star polymers via the arm-first method. Matyjaszewski and coworkers first reported the synthesis of star polymers with a coss-linked core by ATRP. In this case, they established that cross-linker (DVB)/ macroinitiator molar ratios of between 5 and 15 were optimal for the formation of core cross-linked star polymers from PS [207] and P*t*BA macroinitiators [208]. Following the preliminary study of Matyjaszewski and coworkers several research groups have conducted detailed examinations into the preparation of core cross-linked star polymers via ATRP [209-212].

Regardless of the linear arm precursors, the preparation of core cross linked star polymers by "arm-first" technique can be categorized into two broad strategies: macroinitiator and macromonomer (Figure 2.8). In the macroinitiator strategy, the star macromolecules formed by crosslinking linear macroinitiator, where both the initiating sites and the arms of the star molecule originate from the macroinitiator. A major drawback to star synthesis using linear macroinitiator as the arm precursor is that the star polymer usually have a broad polydispersity due to the significant level of star-star coupling reactions. When a linear macromonomer is employed to copolymerize with divinyl cross-linker by using a low-molar-mass initiator, the number of arms (derived from macromonomer) per star molecule is independently controlled. Thus, a low molar ratio of initiator to macromonomer decreases the number of initiating sites in the star core, which effectively limits the extent of star-star coupling reactions and results in star polymers with low polydispersity.

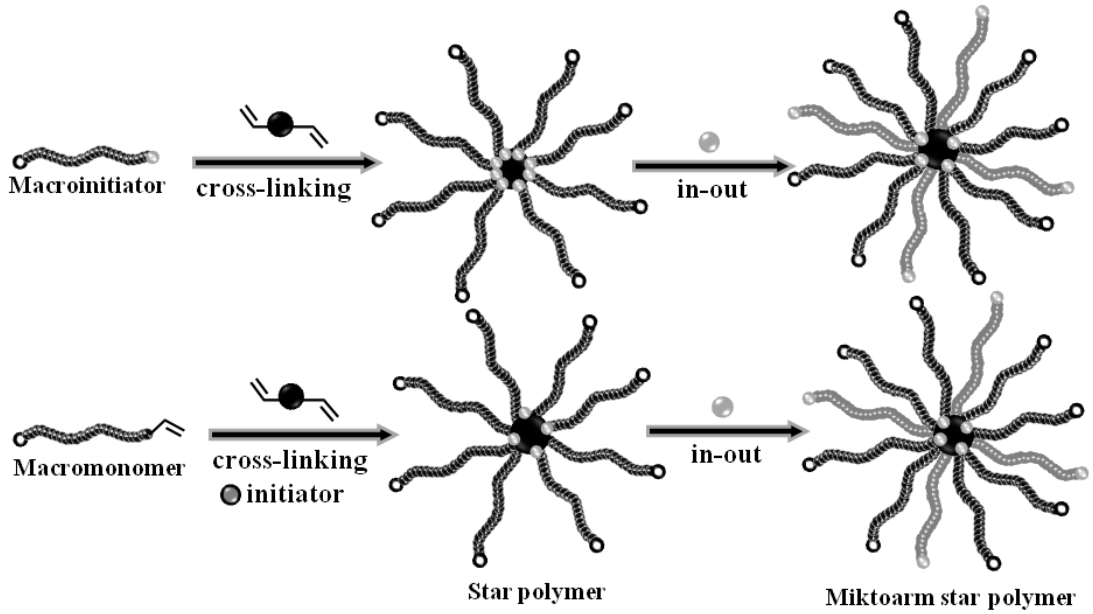

Figure 2.8: Schematic representation of the "arm-first" method for star polymer synthesis.

In addition, the further chain extension of the preserved initiating sites from the core to initiate the polymerization of another monomer will induce formation of miktoarm star polymer by the ''in-out'' method (Figure 2.8).

There are several parameters in an ATRP that should be controlled carefully in order to maximize the yield of stars and prevent star–star coupling reactions. The effects of type of cross-linker, cross-linker/macroinitiator molar ratio, macroinitiator DP, macroinitiator concentration, catalyst concentration, solvent nature, reaction temperature, and reaction time on the structure and yield of core cross-linked star polymers prepared via ATRP were investigated in several reports.

It is important to note that the "arm-first" process leads to preparation of multifunctional star polymers when functional initiators are used for the synthesis of the arms. Indeed, this method provides an efficient route to prepare multiarm star homo and block copolymers.

In that sence, a particularly well-suited example comes from Tunca and coworkers who have prepared multiarm star block copolymers based on the combination of ''arm first'' method with Diels-Alder click reaction to conjugate building blocks [213]. In this case, an α-anthracene and α-maleimide end functionalized polymers : Anth-PS, MI-PMMA and MI-P*t*BA were prepared by ATRP. Then, multiarm star polymer with anthracene functionality as reactive periphery group was synthesized

by a cross-linking reaction of DVB using Anth-PS as a macroinitiator. Subsequently, the formation of multiarm star block copolymers were achieved via Diels–Alder click reaction between the reactive core and maleimide-end functionalized polymers (Scheme 2.30).

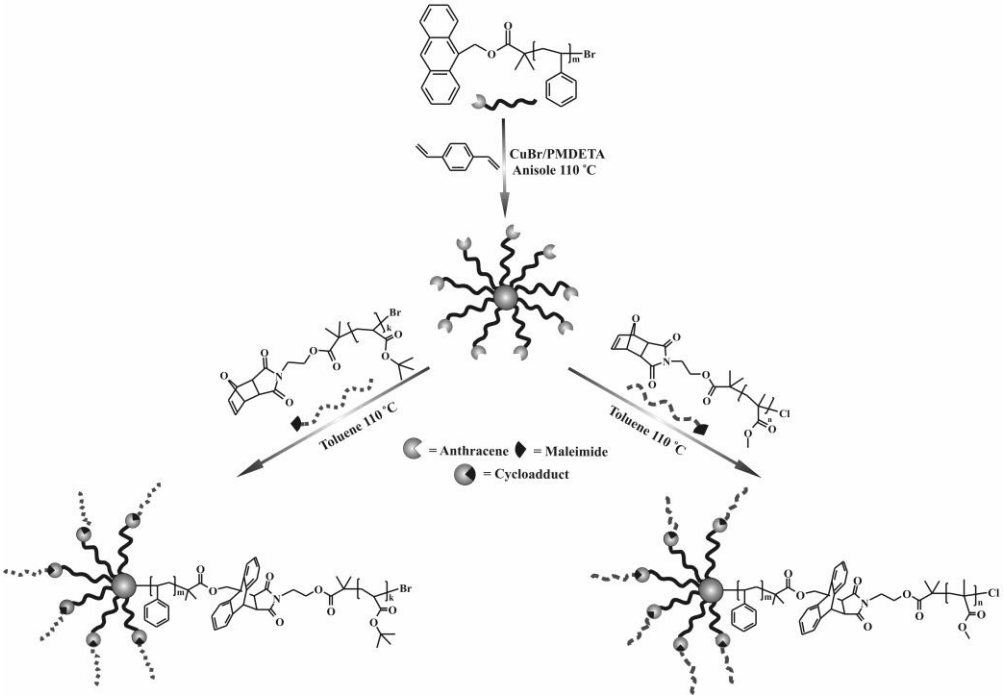

(2.30)

This successful approach was further expand to prepare multiarm star triblock terpolymers using double click reactions sequentialy [214].

In order to synthesize miktoarm star polymers with potentially any desired molar ratio and composition of the arms, Gao et al. reported a new strategy for the synthesis of miktoarm star copolymers using a simple and general ‘‘arm-first’’ method, i.e. one-pot ATRP cross-linking a mixture of different linear macroinitiators and/or macromonomers with a divinyl cross-linker [215]. When linear macromonomers were partially or completely used as arm precursors instead of macroinitiators, miktoarm star copolymers with a high star yield and a low polydispersity were successfully synthesized (Scheme 2.31).

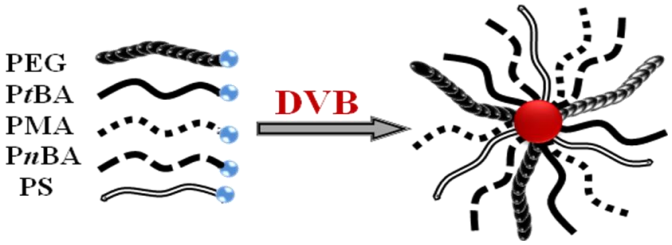

(2.31)

Alternatively, NMP has been applied to the design of core cross-linked star polymers. Solomon and co-workers first prepared poly(4- *tert*-butylstyrene) via

NMP followed by synthesizing the $(PS)_n$-polyDVB star polymers via ‘‘arm-first’’ aproach using DVB as cross-linker [216]. In order to increase the high star, different molar ratios of DVB to macroinitiators were examined to get optimum conditions in several reports [217-219]. The desire to prepare star polymers with high star yield and narrow polydispersities has provided a progressive impetus to the development of new strategies for their creation. The NMP approach has since been refined by the introduction of improved alkoxyamine functionalised initiators, which have permitted the use of a wide range of monomer families and enabled the production of narrow polydispersity core cross-linked star polymers, in high yield, using a variety of alkoxyamine terminated macroinitiators and functional monomers [220, 221].

Compared to the broad applications of ATRP and NMP for the synthesis of functional star polymers using the “arm-first” method, only limited success has been obtained with RAFT polymerizations. Moad first proposed the possibility of using the “arm-first” method in RAFT polymerization for the synthesis of star polymers with a cross-linked core [222]. The first experimental proof of the synthesis of star polymers with a cross-linked core by RAFT was reported by Davis and coworkers although the synthesized $(PS)_n$-polyDVB star polymers were poorly controlled with low star yield and high polydispersity [223].

2.4.2.3 ‘‘Coupling-onto’’ strategy

In the third ‘‘coupling onto’’ method, the linear arms of the star polymers are synthesized first followed by the coupling reactions between arms containing a reactive chain end group and a multifunctional coupling agent (core).

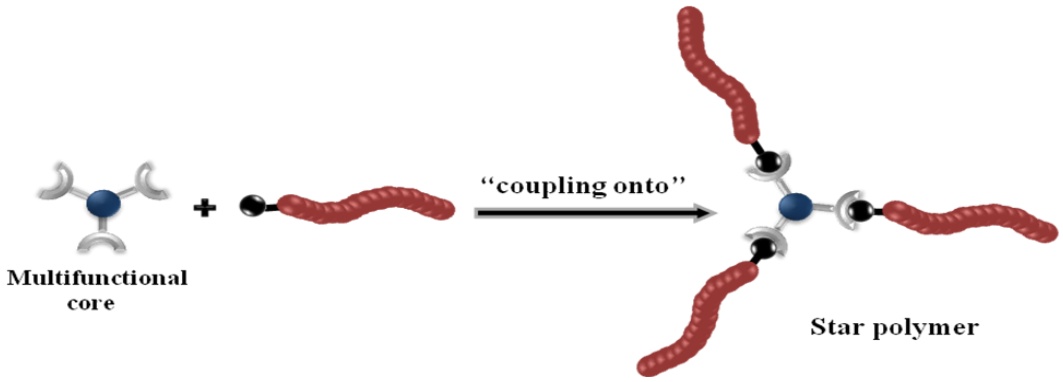

Figure 2.9: Schematic representation of the synthesis of star polymers by “coupling onto” method.

The most general and accurate way to prepare star homopolymers and block copolymers by anionic polymerization was the coupling of living polymers with multifunctional linking compounds. Several linking agents which are the chlorosilanes [224] and the chloromethyl or bromomethyl benzene derivatives [225, 226] have been used for the synthesis of star polymers. By using this method, star polymers with different arm numbers have been prepared [227, 228]. These model homopolymer and block copolymer stars are playing a critical role in the study of the relation between the architecture, the chain conformation, and the properties of the polymers. Pennisi and Fetters employed that approach to prepare narrow molecular weight distribution three-arm PS and PBd stars, where one of the three arms differs in molecular weight from the remaining two [229]. By using this strategy, Mays prepared 3-arm star copolymer of the A_2B type, where A was polyisoprene (PI) and B was PS [230]. The chlorosilane approach has been extended to prepare a new type of model polymer: the 3-miktoarm star terpolymer, an ABC type where A is PI, B is PS, and C is PBd [231].

Recently, the combination of C/LRP methods with highly efficient and orthogonal post-polymerization coupling reactions widened the possibilities to access complex macromolecular architectures from individual building blocks. Such click approaches, including CuAAC, Diels–Alder, and thiol-ene conjugations, allowed for the synthesis of well-defined star polymers, star block copolymers, and miktoarm star copolymers.

Matyjaszewski and coworkers reported the first synthesis of star polymers with different arm numbers by "coupling-onto" method using a combination of ATRP and click chemistry. In this case, the click coupling reactions between azido-terminated PS ($PS\text{-}N_3$) and alkyne-containing multifunctional compounds (bis-, tris- or tetra-alkyne) were fast and highly efficient [232]. The effect of several parameters, such as the molecular weight of the initial $PS\text{-}N_3$ samples, the presence of Cu(0) as reducing agent, and the stoichiometry between the azido and alkynyl groups, on the final yield of coupling product was investigated. It was found that the fraction of coupling products decreased when the molecular weight of $PS\text{-}N_3$ chains increased. The yield of coupling product was higher in the presence of Cu(0). The stoichiometry between azido and alkynyl groups also influenced the ratio of species in the final product. The

highest yield of the coupling product was obtained when the molar ratio of azido/alkynyl groups was 1.

On the basis of similar principle, Tunca and coworkers prepared 3-arm star polymers (A_3) via Diels-Alder click reaction of furan protected maleimide end-functionalized linear precursors with trianthracene functional linking agent (Scheme 2.32) [136].

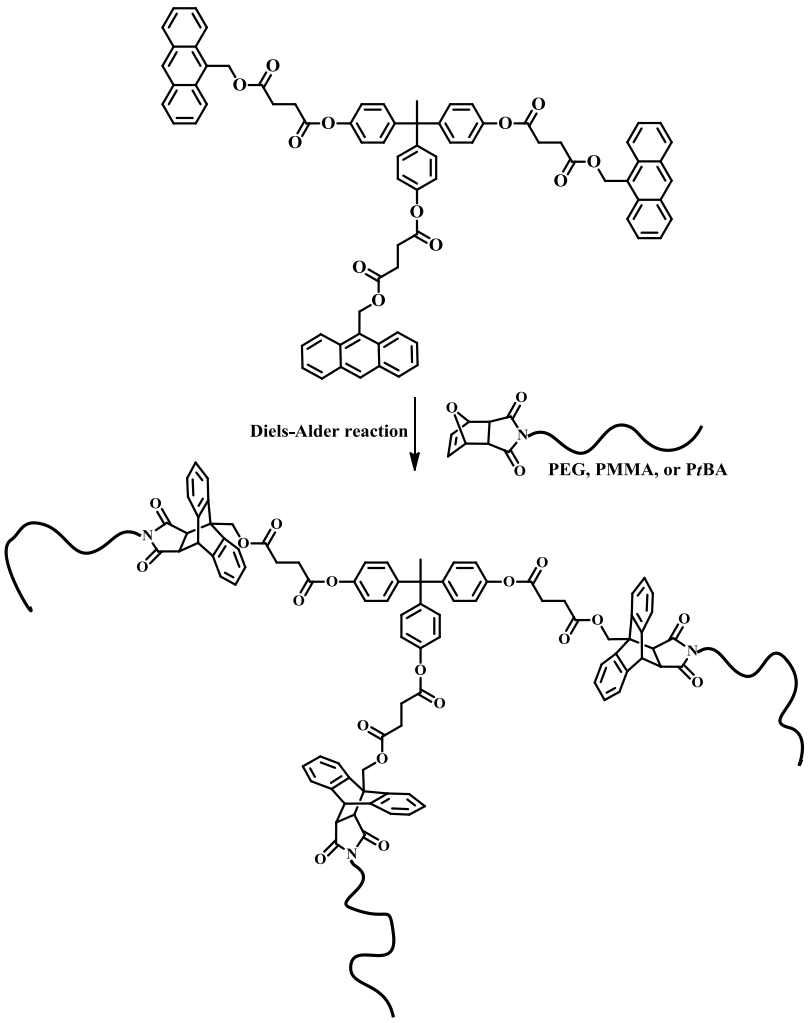

(2.32)

Tunca and coworkers demostrated one of the most standard examples of the coupling onto technique to prepare ABC-type miktoarm star polymer [233]. In this study, ATRP and NMP were used to polymerize PMMA and PS respectively from a trifunctional core, giving a block copolymer with an alkyne which is located at the junction. Subsequent ‘‘click’’ reaction with either azide-terminated PEG or P*t*BA yielded PMMA-PS-P*t*BA and PMMA-PS-PEG miktoarm star polymers .

Similarly, Tunca and coworkers combined the CuACC click reaction with ROP and NMP to synthesize ABC type miktoarm polymers composed of PS, PCL and either

P*t*BA, PMMA or PEG in two different one-pot techniques: one-pot/onestep and one-pot/two-step (Scheme 2.33) [234].

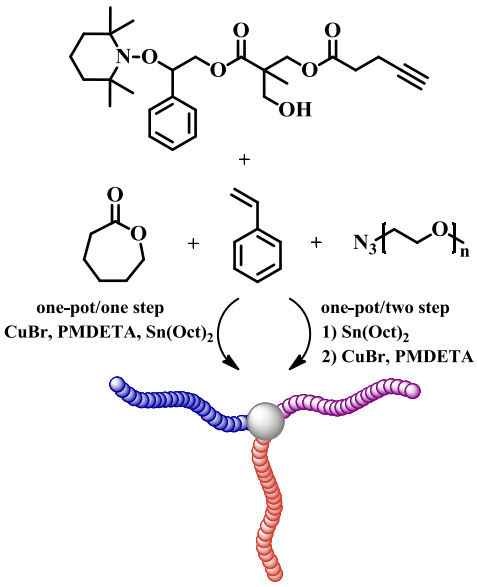

(2.33)

Additionally, the group of Tunca has created an ABC type miktoarm polymer utilizing ‘‘core-in’’and ‘‘core-out’’ methods by combining of Diels–Alder reaction, NMP, and ATRP. First, in DA reaction, MI-PEG precursor was reacted with trifunctional core bearing anthracene moiety to give macroinitiator, which has appropriate functional groups for NMP and ATRP. Then, NMP was used to grow PS and ATRP for *t*BA was employed to yield the final ABC type miktoarm star terpolymer (PEG-PS-P*t*BA) with controlled molecular weight and low polydispersity (M_w/M_n < 1.27). (Scheme 2.34) [235].

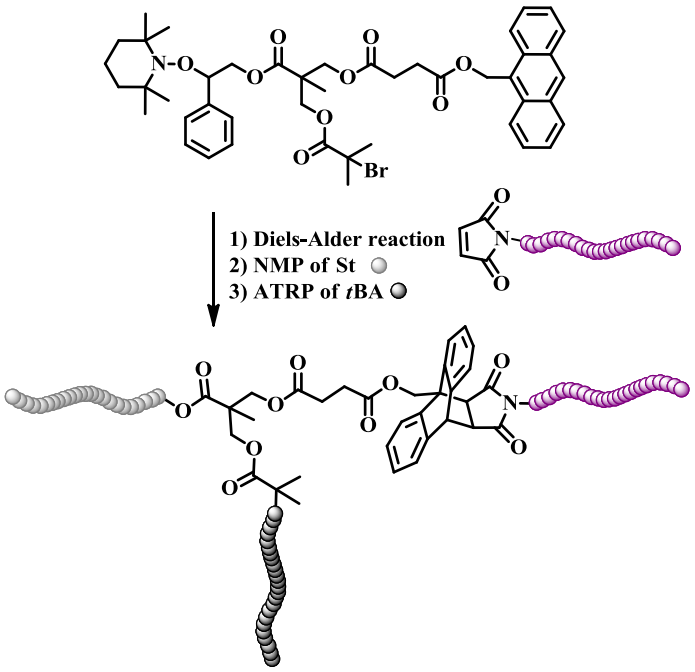

(2.34)

Moreover, our group first time used a combination of ROMP and click chemistry in the preparation of A_3 type homoarm star polymer [236] and ABC-type miktoarm star polymer [237]. In the synthesis of ABC-type miktoarm star polymer, the bromide end-functionality of monotelechelic poly(N-butyl oxanorbornene imide) (PNBONI) obtained from ROMP of NBONI was first transformed to azide and then reacted with PS-*b*-PMMA copolymer having alkyne at the junction point via click chemistry, producing PS-PMMA-PNBONI.

The click reaction has also been used to make ABCD type miktoarm star polymers by coupling between two diblock copolymers [238] The same strategy of coupling two block copolymers together through ‘‘click chemistry’’ to create the final miktoarm star was employed to yield unique H-shaped polymers composed of either five different arms (ABCDE) [239, 240] or three different arms (ABCAB) [241] in moderately high yield.

3. EXPERIMENTAL WORK

3.1. Materials and Chemicals

Styrene (St, 99%, Merck), methyl metacrylate (MMA, 99%, Aldrich) and *tert*-butylacrylate (*t*BA, 99%, Aldrich) were passed through basic alumina column to remove inhibitor and then distilled from CaH_2 in vacuum prior to use. 4-Chloromethylstyrene (CMS; ca. 60/40 meta/para isomer mixture; 97%, Aldrich) was distilled under reduced pressure. Furan (99%, Aldrich), maleic anhydride (99%, Aldrich), ethanolamine (99.5%, Aldrich), succinic anhydride (97%, Aldrich), 9-anthracene methanol (97%, Aldrich), α-bromoisobutryl bromide (98%, Aldrich), triethylamine (Et_3N, 99.5%, Aldrich), propargyl alcohol (99%, Aldrich), *N,N'*-dicyclohexylcarbodiimide (DCC, 99%, Aldrich), 4-dimethylaminopyridine (DMAP, 99%, Aldrich), 4-pentynoic acid (98%, Aldrich), 1,1,1-tris(4-hydroxyphenyl)ethane (99%, Aldrich), 3-trimethylsilyl-2-propyn-1-ol (99%, Aldrich), tin(II)-2-ethylhexanoate (Aldrich, 98%), tributyltinhydride (97%, Aldrich), divinylbenzene (DVB, 80%, Aldrich), CuBr (99.9%, Aldrich), and CuCl (99.9%, Aldrich) were used as received. *N*, *N*, *N*', *N*", *N*"'-pentamethyldiethylenetriamine (PMDETA, 99%, Aldrich) was distilled over NaOH prior to use. Poly(ethylene glycol) monomethylether (PEG-OH, M_n = 550, Acros, and M_n = 2000, Fluka) were dried by azeotropic distillation with anhydrous toluene. Tetrahydrofuran (THF, 99.8%, J.T. Baker) was dried and distilled from benzophenone-Na. *N*,*N*-dimethylformamide (DMF, 99.8%, Aldrich) was dried and distilled under vacuum over CaH_2. Dichloromethane (CH_2Cl_2, 99%, J. T. Baker) was dried and distilled over and P_2O_5. Diethyl ether (99.7%, Aldrich), 1.4-dioxane (99.8%, Aldrich), toluene (99.8%, Aldrich), methanol (99.8%, Aldrich) were used without further purification. Ethyl acetate (EtOAc) and hexane were in technical grade and distilled prior to use.

3.2 Equipments

Nuclear magnetic resonance spectroscopy (NMR)

^{1}H NMR measurements were recorded in $CDCl_3$ with $Si(CH_3)_4$ as internal standard, using a Bruker AC250 (250 MHz) instrument.

Infrared spectrophotometer (FT-IR)

FT-IR spectra were recorded on a Thermo Nicolet 6700 FT-IR spectrometer.

UV-visible spectrophotometer (UV-vis)

UV-visible spectra were recorded on a Shimadzu UV-1601 UV-visible spectrophotometer.

Gel permeation chromatography (GPC)

(a) The conventional Gel Permeation Chromatography (GPC) measurements were conducted in THF at 30 °C using an Agilent instrument (Model 1100) consisting of a pump (0.3 mL/min) and four Waters Styragel columns (guard, HR 5E, HR 4E, HR 3, HR 2), (4.6 mm internal diameter, 300 mm length, packed with 5 μm particles) in series with two detection systems: a refractive index and UV detectors). Toluene was used as an internal standard. The determination of apparent molecular weights for the polymers was based on linear PS standards (Polymer Laboratories), whereas linear PMMA standards (Polymer Laboratories) were only used for the molecular weight determination of the PMMA homopolymer using PL Caliber Software from Polymer Laboratories.

(b) The second GPC system (TD-GPC) is equipped with an Agilent model isocratic pump, four Waters Styragel columns (guard, HR 5E, HR 4, HR 3, and HR 2), and a Viscotek TDA 302 triple detector (RI, dual laser light scattering (LS) (λ = 670 nm, 90° and 7°) and a differential pressure viscometer). TD-GPC was conducted to measure the absolute molecular weights in THF with a flow rate of 0.5 mL/min at 35 °C. All three detectors were calibrated with a PS standard having narrow molecular weight distribution (M_n = 115,000 g/mol, M_w/M_n = 1.02, [η] = 0.519 dL/g at 35 °C in THF, dn/dc = 0.185 mL/g) provided by Viscotek company. Typical sample concentrations for GPC-analysis were in the range of 1–10 mg/mL depending on molecular weight of analyzed polymers. Data analyses were performed with OmniSec 4.5 software from Viscotek Company.

Gas chromatography (GC)

DVB conversion was determined using the Agilent 6890N gas chromatograph, equipped with an FID detector using a wide-bore capillary column (HP5, 30 m x 0.32 mm x 0.25μm, J&W Scientific). Injector and detector were kept constant at 280 and 285 ºC, respectively. The chromatographic conditions: Injector and detector were kept constant at 280 °C and 285 ºC, respectively. Initial column temperature is 40 ºC, finally reaching up to 120 ºC at a heating rate of 40 ºC/min.

Mass spectroscopy (MS)

Mass spectroscopy was performed on Thermo LCQ-Deca ion trap mass instrument.

Differential scanning calorimeter (DSC)

Differential scanning calorimeter (DSC) was performed on a Perkin Elmer Diamond DSC with a heating rate of 10 ^{o}C min^{-1} under nitrogen.

Dynamic Light Scattering (DLS)

Dynamic Light Scattering (DLS) measurements were done at 25 ^{o}C using Malvern Nano-S particle size analyzer. For DLS measurements, multiarm star polymers were dissolved in CH_2Cl_2 at a concentration of 10^{-1}-10^{-3} mg/mL. Up to 500 measurements each having 10 s correlation times were recorded for each sample. The average hydrodynamic diameter was determined by fitting a Gaussian curve to the histogram of the measured data.

Atomic force microscopy (AFM)

Atomic Force Microscopy (AFM) images were taken by NT-MDT Solver P47 in tapping mode. Ultra sharp Si cantilevers having force constant of 48 N/m were used.

3.3 Synthetic Procedures

4,10-Dioxatricyclo[5.2.1.0^{2,6}]dec-8-ene-3,5-dione (**1**) [242], 4-(2-hydroxyethyl)-10-oxa-4-azatricyclo[5.2.1.0^{2,6}]dec-8-ene-3,5-dione (**2**) [242], 2-bromo-2-methyl propionic acid 2-(3,5-dioxo-10-oxa-4-azatricyclo[5.2.1.02,6]dec-8-en-4-yl) ethyl ester (**3**) [242], 1,1,1-tris [4-(2-propynyloxy)phenyl]-ethane (**4**) [243], succinic acid mono-anthracen-9-ylmethyl-ester (**5**) [244], 3-azidopropanol (**6**) [245], 9-anthyrylmethyl 2-bromo-2-methyl propanoate (**9**) [246], 3-(trimethylsilyl)prop-2-

ynyl 2-bromo-2-methylpropanoate (**11**) [247] and 2-azidoethanol (**12**) [245] were prepared according to literature procedures.

3.3.1 Synthesis of 4,10-Dioxatricyclo[5.2.1.$0^{2,6}$]dec-8-ene-3,5-dione (1)

Maleic anhydride (30 g, 0.30 mol) was suspended in 150 mL of toluene and the mixture warmed to 80 °C. Furan (33.4 mL, 0.45 mol) was added via syringe and the turbid solution stirred for 6 h. The mixture was then cooled to ambient temperature white solids formed during standing were collected by filtration and washed with 2 × 30 mL of petroleum ether and once with diethyl ether (50 mL) yielding **1** as white needless. (Yield= 44.4 g, 87%). Mp: 114-115 ^{o}C (DSC). ^{1}H NMR ($CDCl_3$, δ) 6.57 (s, 2H, C*H*=C*H*, bridge protons), 5.45 (s, 2H, -C*H*O, bridge-head protons), 3.17 (s, 2H, C*H*-C*H*, bridge protons). ^{13}C NMR ($CDCl_3$, δ) 170.18, 137.29, 82.46, 48.88. Mass spectrometry (+EI) *m*/*z* (%): 167 [MH+] (50), 144 (35), 130 (20).

3.3.2 Synthesis of 4-(2-hydroxyethyl)-10-oxa-4-azatricyclo[5.2.1.$0^{2,6}$]dec-8-ene-3,5- dione (2)

The adduct **1** (10 g, 60 mmol) was suspended in methanol (150 mL) and the mixture was cooled to 0 °C. A solution of ethanolamine (3.6 mL, 60 mmol) in 30 mL of methanol was added dropwise (10 min) to the reaction mixture, and the resulting solution was stirred for 5 min at 0 °C, then 30 min at ambient temperature, and finally refluxed for 8 h. After cooling the mixture to ambient temperature, solvent was removed under reduced pressure, and residue was dissolved in 150 mL of CH_2Cl_2 and washed with 3 × 100 mL of water. The organic layer was separated, dried over Na_2SO_4 and filtered. Removal of the solvent under reduced pressure gave white-off solid which was further purified by flash chromatography eluting with ethylacetate (EtOAc) to give the product as a white solid. (Yield= 4.9 g, 40%). Mp = 138-139 °C (DSC). ^{1}H NMR ($CDCl_3$, δ) 6.51 (s, 2H, C*H*=C*H*, bridge protons), 5.26 (s, 2H, -C*H*O, bridge-head protons), 3.74-3.68 (m, 4H, NCH_2CH_2OH), 2.88 (s, 2H, C*H*-C*H*, bridge protons). ^{13}C NMR ($CDCl_3$, δ) 177.03, 136.60, 81.09, 60.53, 47.74, 42.03. Mass spectrometry (+EI) *m*/*z* (%): 210 [MH+] (50), 145 (22), 142 (100), 124 (17).

3.3.3 Synthesis of 2-bromo-2-methyl propionic acid 2-(3,5-dioxo-10-oxa-4-azatricyclo [5.2.1.$0^{2,6}$] dec-8-en-4-yl) ethyl ester (3)

In a 250 mL of round bottom flask were added **2** (2.0 g, 9.55 mmol) and Et_3N (1.44 mL, 10.54 mmol) in 100 mL of THF. The mixture was cooled to 0 °C, and a solution of 2-bromo isobutyryl bromide (2.34 g, 10.0 mmol) in 25 mL of THF was added dropwise (30 min) to the reaction mixture. The white suspension was stirred for 3 h at 0 °C and subsequently at ambient temperature for overnight. The ammonium salt was filtered off and the solvent was removed under reduced pressure to give a pale-yellow residue that was further purified by column chromatography over silica gel eluting with EtOAc /hexane (1:4) to give **3** as a white solid. (Yield= 1.86 g, 55%). Mp = 81-82 °C (DSC). ^{1}H NMR ($CDCl_3$, δ) 6.49 (s, 2H, C*H*=C*H*, bridge protons), 5.24 (s, 2H, -C*H*O, bridge-head protons), 4.31 (t, *J* = 5.2 Hz, 2H, NCH_2CH_2OC=O), 3.79 (t, *J* =5.2 Hz, 2H, NCH_2CH_2OC=O), 2.85 (s, 2H, C*H*-C*H*, bridge protons), 1.87 (s, 6H, $C(CH_3)_2$-Br). ^{13}C NMR ($CDCl_3$, δ) 176.12, 171.55, 136.83, 81.09, 62.36, 55.96, 47.74, 37.69, 30.83. Mass spectrometry (+EI) *m*/*z* (%): 360 [MH+] (100).

3.3.4 General procedure for the preparation of furan protected maleimide end-functionalized PMMA (MI-PMMA)

The MI-PMMA was prepared by ATRP of MMA. In a 50 mL of Schlenk tube, MMA (5 mL, 46.7 mmol), toluene (5 mL), PMDETA (0.196 mL, 0.940 mmol), CuCl (0.093 g, 0.940 mmol), and **3** (0.336 g, 0.940 mmol) were added and the reaction mixture was degassed by three freeze-pump-thaw (FPT) cycles and left in argon. The tube was then placed in an oil bath thermostated at 40 ^{o}C for predetermined times. Tributyltinhydride (2.73 g, 9.40 mmol) was added to the reaction mixture and stirred further 30 min. The polymerization mixture was then diluted with THF, passed through a basic alumina column to remove the catalyst, and precipitated in hexane. The polymer was dried for 24 h in a vacuum oven at 30 ºC. ^{1}H NMR ($CDCl_3$, δ) 6.5 (s, 2H, C*H*=C*H*, bridge protons), 5.3 (s, 2H, -C*H*O, bridge-head protons), 4.1 (m, 2H, NCH_2CH_2OC=O), 4.0-3.2 (br, OCH_3 of PMMA and NCH_2CH_2OC=O), 2.9 (s, 2H, C*H*-C*H*, bridge protons), 2.5-0.5 (br, aliphatic protons of PMMA).

3.3.5 Preparation of alkyne end-functionalized PEG (Alkyne-PEG)

PEG-OH (M_n = 550) (3 g, 5.4 mmol) was dissolved in 25 mL of CH_2Cl_2. 4-Pentynoic acid (0.8 g, 8.2 mmol) and DMAP (0.67 g, 5.4 mmol) were successively added to the reaction mixture. After stirring 5 min at room temperature, a solution of DCC (1.69 g, 8.2 mmol) in 15 mL of CH_2Cl_2 was added to the reaction mixture and stirred overnight at room temperature. After filtration off the salt, the solution was concentrated and viscous brown product was purified by column chromatography over silica gel eluting with CH_2Cl_2/ethyl acetate mixture (1:10) and then with CH_2Cl_2/methanol (10:1) to give Alkyne-PEG as a viscous yellow liquid. (Yield= 3 g, 87%). ^{1}H NMR ($CDCl_3$, δ) 4.23 (t, 2H, PEG-OCH_2CH_2OC=O), 3.89 (t, 2H, PEG-OCH_2CH_2OC=O), 3.67-3.62 (m, 4H, -OCH_2CH_2, repeating unit of PEG), 3.54 (t, 2H, CH_3O-CH_2CH_2-O), 3.34 (s, 3H, PEG-O-CH_3), 2.58–2.48 (m, 4H, CH≡CCH_2 CH_2C=O), 1.96 (t, 1H, C*H*≡CCH_2CH_2C=O).

3.3.6 Preparation of copolymers of St and 4-chloromethylstyrene, P(S-*co*-CMS)

P(S-*co*-CMS) copolymers containing two different amounts of CMS (15 and 30 mol % in the feed ratios) were prepared via NMP of St and CMS at 125 ºC.

3.3.6.1 Preparation of P(S-*co*-CMS)-1 copolymer

P(S-*co*-CMS) was prepared via NMP of styrene and CMS at 125 ºC. In a 25 mL of Schlenk tube, St (3.19 mL, 27.8 mmol), CMS (0.69 mL, 4.91 mmol), TEMPO (0.1 g, 0.6 mmol) and AIBN (0.053 g, 0.321 mmol) were added and the reaction mixture was degassed by three FPT cycles. The tube was placed in a thermostated oil bath at 125 ºC for 17 h. The polymerization mixture was precipitated in methanol and dried for 24 h in a vacuum oven at 30 ºC. (Yield= 1.3 g). ^{1}H NMR ($CDCl_3$, δ) 7.5-6.5 (Ar*H* of PS), 4.5 (Ph-CH_2Cl), 2.2-0.6 (aliphatic protons).

3.3.6.2 Preparation of P(S-*co*-CMS)-2 copolymer

P(S-*co*-CMS) was prepared via NMP of styrene and CMS at 125 ºC. In a 25 mL of Schlenk tube, St (2.63 mL, 22.93 mmol), CMS (1.39 mL, 9.83 mmol), TEMPO (0.1 g, 0.6 mmol) and AIBN (0.053 g, 0.321 mmol) were added, the reaction mixture was degassed by three FPT cycles. The tube was then placed in a thermostated oil bath at 125 ºC for 11.5 h. The polymerization mixture was precipitated in methanol and

dried for 24 h in a vacuum oven at 30 ºC. (Yield: 1.2 g). ^{1}H NMR ($CDCl_3$, δ) 7.5-6.5 (ArH of PS), 4.5 (Ph-CH_2Cl), 2.2-0.6 (aliphatic protons).

3.3.7 Preparation of PS with anthracene and azide pendant groups PS-Anth-Azide-1

Sodium hydride (60 wt % dispersion in mineral oil) (0.125 g, 3.13 mmol, 20 equiv.) was added to a solution of 9-anthracene methanol (0.097 g, 0.470 mmol, 3 equiv.) in dry 20 mL of THF and the reaction mixture was stirred at room temperature under nitrogen for 30 min. A solution of random copolymer P(S-*co*-CMS)-1 (0.680 g, 0.156 mmol, 1 equiv.) in dry THF was then added to the mixture. The solution was refluxed for 12 h in the dark, cooled to room temperature, evaporated to half of its volume and then precipitated in methanol. The light yellow product P(S-CMS-Anth)-1 with anthryl pendant groups was dried for 24 h in a vacuum oven at 30 ºC. ^{1}H NMR ($CDCl_3$, δ) 8.5-7.4 (Ar*H* of anthracene), 7.4-6.5 (Ar*H* of PS), 5.4 (CH_2-anthracene), 4.6 (Ph-CH_2O), 4.5 (Ph-CH_2Cl), 2.2-0.6 (aliphatic protons).

Previously obtained P(S-CMS-Anth)-1 (0.45 g, 0.092 mmol) was dissolved in DMF (10 mL) and NaN_3 (0.18 g, 2.75 mmol) was added to the reaction mixture. After stirring at room temperature overnight, the product was recovered by precipitation into excess amount of methanol. The polymer was dissolved in THF and precipitated in methanol. The light yellow product, PS-Anth-Azide-1 having both the anthryl and azide pendant groups was dried for 24 h in a vacuum oven at 30 ºC. ^{1}H NMR ($CDCl_3$, δ) 8.5-7.4 (Ar*H* of anthracene), 7.4-6.5 (Ar*H* of PS), 5.4 (CH_2-anthracene), 4.6 (Ph-CH_2O), 4.2-3.9 (Ph-CH_2N_3), 2.2-0.6 (aliphatic protons).

3.3.8 Preparation of PS with anthracene and azide pendant groups PS-Anth-Azide-2

Sodium hydride (60 wt % dispersion in mineral oil) (0.08 g, 2.05 mmol, 20 equiv.) was added to a solution of 9-anthracene methanol (0.1 g, 0.5 mmol, 5 equiv.) in dry 20 mL of THF. The reaction mixture was stirred at room temperature under nitrogen for 30 min. A solution of random copolymer P(S-*co*-CMS)-2 (0.45 g, 0.102 mmol, 1 equiv.) in dry THF was then added to this mixture, and the reaction mixture was refluxed for 12 h in the dark. It was then cooled to room temperature, evaporated to half of its volume and then precipitated in methanol. The light yellow product, P(S-CMS-Anth)-2 with anthryl pendant groups was dried for 24 h in a vacuum oven at 30

ºC. ^{1}H NMR ($CDCl_3$, δ) 8.5-7.4 (Ar*H* of anthracene), 7.4-6.5 (Ar*H* of PS), 5.4 (CH_2-anthracene), 4.6 (Ph-CH_2O), 4.5 (Ph-CH_2Cl), 2.2-0.6 (aliphatic protons).

Previously obtained P(S-CMS-Anth)-2 copolymer with anthryl pendant groups (0.47 g, 0.092 mmol) was dissolved in DMF (20 mL) and NaN_3 (0.18 g, 2.78 mmol) was added to the reaction mixture. After stirring at room temperature for overnight, the product was recovered by precipitation into excess amount of methanol. The polymer then dissolved in THF and precipitated in methanol. The light yellow product, PS-Anth-Azide-2 with anthryl and azide pendants was dried for 24 h in a vacuum oven at 30 ºC. ^{1}H NMR ($CDCl_3$, δ) 8.5-7.4 (Ar*H* of anthracene), 7.4-6.5 (Ar*H* of PS), 5.4 (CH_2-anthracene), 4.6 (Ph-CH_2O), 4.2-3.9 (Ph-CH_2N_3), 2.2-0.6 (aliphatic protons).

3.3.9 One-pot preparation of PS-*g*-(PMMA-PEG) hetero graft copolymer from PS-Anth-Azide-1

MI-PMMA (0.30 g, 0.097 mmol, $M_{n,NMR}$= 3100 g/mol), Alkyne-PEG (0.10 g, 0.15 mmol, $M_{n,NMR}$= 685 g/mol) and PS-Anth-Azide-1 (0.15 g, 0.03 mmol, $M_{n,GPC}$= 5150 g/mol) were dissolved in nitrogen purged DMF (5 mL) in a Schlenk tube. CuBr (0.021 g, 0.15 mmol), PMDETA (0.03 mL, 0.15 mmol), and a catalytic amount of butylated hydroxyl toluene (BHT) as a radical inhibitor were added to the reaction mixture. The solution was degassed by three FPT cycles and left in argon and stirred in the dark at 120 ^{o}C for 48 h. Polymer solution was passed through alumina column to remove copper salt and precipitated in methanol, repeatedly two times. Finally, the polymer was dried in a vacuum oven at 30 ºC (Yield = 0.32 g). ^{1}H NMR ($CDCl_3$, δ) 7.65 (C=CH of triazole) 6.3-7.5 (Ar*H* of PS), 5.2-4.9 (cycloadduct-CH_2OC=O and Ph-CH_2-triazole), 4.7 (C*H*, bridge-head proton), 4.2 (C=OOCH_2CH_2O, end group of PEG), 3.9 (C=OOCH_2CH_2N), 3.7-3.6 (OCH_2CH_2O, repeating unit of PEG), 3.6-3.5 (OCH_3 of PMMA), 3.4 (OCH_3 end group of PEG), 3.3 (C*H*-C*H*, bridge protons of cycloadduct and CH_2-N), 2.6 (triazole-CH_2CH_2C=O), 2.2-0.6 (aliphatic protons).

3.3.10 One-pot preparation of PS-*g*-(PMMA-PEG) hetero graft copolymer from PS-Anth-Azide-2

MI-PMMA (0.5 g, 0.16 mmol, $M_{n,NMR}$= 3100 g/mol), Alkyne-PEG (0.18 g, 0.27 mmol, $M_{n,NMR}$= 685 g/mol), and PS-Anth-Azide-2 (0.15 g, 0.03 mmol, $M_{n,GPC}$= 5150 g/mol) were dissolved in nitrogen purged DMF (5 mL) in a Schlenk tube. CuBr (0.038 g, 0.27 mmol) PMDETA (0.055 mL, 0.27 mmol), and a catalytic amount of

BHT as a radical inhibitor were added to the solution. The reaction mixture was degassed by three FPT cycles and left in argon and stirred in the dark at 120 ^{o}C for 48 h. Polymer solution was passed through alumina column to remove copper salt, precipitated in methanol, repeatedly two times. Finally, the polymer dried in vacuum oven at 30 ºC (Yield = 0.46 g). ^{1}H NMR ($CDCl_3$, δ) 7.65 (C=CH of triazole) 6.3-7.5 (Ar*H* of PS), 5.2-4.9 (cycloadduct-CH_2OC=O and Ph-CH_2-triazole), 4.7 (C*H*, bridge-head proton), 4.2 (C=OOCH_2CH$_2$O, end group of PEG), 3.9 (C=OOCH_2CH$_2$N), 3.7-3.6 (OCH_2CH_2O, repeating unit of PEG), 3.6-3.5 (OCH_3 of PMMA), 3.4 (OCH_3 end group of PEG), 3.3 (C*H*-C*H*, bridge protons of cycloadduct and CH_2-N), 2.6 (triazole-CH_2CH_2C=O), 2.2-0.6 (aliphatic protons).

3.3.11 Synthesis of 1,1,1-tris[4-(2-propynyloxy)phenyl]-ethane (4)

1,1,1-Tris(4-hydroxyphenyl)ethane (0.75 g, 2.45 mmol) was dissolved in dimethylformamide (DMF; 10 mL), and propargyl bromide (80% in toluene; 1 mL, 9 mmol) and K_2CO_3 (2.4 g, 17 mmol) were added to the mixture. The reaction mixture was stirred for 24 h at 110 ºC. After the reaction was completed, the mixture was filtered and evaporated in vacuo to remove DMF. CH_2Cl_2 (200 mL) was added, and the reaction mixture was washed three times with distilled water (100 mL x 3). The combined organic phase was dried over Na_2SO_4, filtered, and evaporated. The remaining product was further purified by column chromatography over silica gel eluting with ethyl acetate/hexane (1:9) to obtain pure **4** as a yellow-green liquid. Yield: 0.684 g, (67%). ^{1}H NMR ($CDCl_3$): 7.01–6.96 (m, 6H, ArH), 6.88–6.82 (m, 6H, ArH), 4.66 (d, J = 2.4 Hz, 6H, HCC-CH_2) 2.50 (t, J = 2.4 Hz, 3H, *H*CC-CH$_2$), 2.09 (s, 3H, CH_3).

3.3.12 Synthesis of succinic acid mono-anthracen-9-ylmethyl-ester (5)

9-Anthryl methanol (4.16 g, 20 mmol) was dissolved in 150 mL of CH_2Cl_2. To the reaction mixture were added Et_3N (14 ml, 100 mmol) and DMAP (2.44 g, 20 mmol), and succinic anhydride (8 g, 80 mmol) in that order. The mixture was stirred for overnight at room temperature. The reaction solution was poured into ice-cold water (150 ml) and stirred for 30 min. at room temperature. The organic phase was extracted with 1M HCl (150 ml). The aqueous phase extracted with CH_2Cl_2. Combined organic phase were dried over Na_2SO_4 and concentrated to give **5** as a green solid. Yield: 5.85 g (95%). Mp = 130-131 ºC (DSC). ^{1}H NMR **(**$CDCl_3$, δ**)** 8.51

(s, 1H, Ar*H* of anthracene), 8.31 (d, *J* = 8.8 Hz, 2H, Ar*H* of anthracene), 8.03 (d, *J* = 8.3 Hz, 2H, Ar*H* of anthracene), 7.60-7.45 (m, 4H, Ar*H* of anthracene), 6.16 (s, 2H, CH_2-anthracene), 2.69-2.62 (s, 4H, C=OCH_2CH_2C=OOH). ^{13}C NMR ($CDCl_3$, δ) 177.72, 172.46, 131.57, 131.35, 129.29, 129.07, 127.01, 126.05, 125.41, 124.04, 59.39, 29.01. Mass spectrometry (+EI) *m*/*z* (%): 308 [MH+] (65), 307 (92), 290 (30), 277 (47), 207 (58), 191 (100), 179 (25).

3.3.13 Synthesis of 3-azidopropanol (6)

To a 100 mL of round bottom flask was added 3-bromo propanol (5 g, 0.036 mol) in 50 mL of water/acetone (1:4, v/v). NaN_3 (2.8 g, 0.043 mol) was added in one portion to the reaction and the mixture was sitirred at 70 ºC for overnight. After acetone was removed, remaining liquid dissolved in CH_2Cl_2 and extracted with water. The aqueous layer was extracted with CH_2Cl_2 (50 mL) and combined organic layers were dried over Na_2SO_4. Solvent was removed under vacuum and 3-azido propanol was obtained as a pale yellow oil. Yield: 3.4 g (94%). ^{1}H NMR ($CDCl_3$, δ) 3.74 (t, 2H, CH_2-O), 3.44 (t, 2H, CH_2-N_3), 1.84-1.70 (m, 2H, CH_2C$H_2$$CH_2$).

3.3.14 Synthesis of anthracen-9-yl methyl 3-azidopropyl succinate (7)

Succinic acid mono-athracen-9-yl methyl ester (**5**) (1.52 g, 4.93 mmol) was dissolved in 25 mL of dry CH_2Cl_2. 3-Azido propanol (**6**) (0.60 g, 5.92 mmol) and DMAP (0.60 g, 4.9 mmol) were then added to the reaction mixture. After stirring for 5 min, a solution of DCC (1.22 g, 5.92 mmol) in 5 mL of CH_2Cl_2 was added to the reaction medium and stirred overnight at room temperature. After filtration, the solution was evaporated and the crude product was extracted with CH_2Cl_2 and water. The organic phase was separated and aqueous phase was again extracted with CH_2Cl_2 and combined organic phases were dried with Na_2SO_4. The crude product was finally purified by column chromatography over silica gel eluting with ethyl acetate/ hexane (1/4) gradually increased to ethyl acetate to give the product 7 as yellow oil. Yield = 1.4 g, (73%). ^{1}H NMR (δ, $CDCl_3$) 8.51 (s, 1H, Ar*H*), 8.32 (d, J = 8.6 Hz, 2H, Ar*H*), 8.02 (d, J = 8.1 Hz, 2H, Ar*H*), 7.61–7.46 (m, 4H, Ar*H*), 6.17 (s, 2H, ArCH_2O), 4.07 (t, 2H, J = 6.1 Hz, C= OOCH_2CH_2), 3.26 (t, 2H, J = 6.6 Hz, C$H_2$$N_3$), 2.67–2.59 (m, 4H, C=OCH_2CH_2C=O), 1.76 (q, 2H, J = 6.3 Hz, C=OOC$H_2$$CH_2$). ^{13}C NMR (δ, $CDCl_3$) 172.3 (C=O), 171.9 (C=O), 131,4 (Ar-C), 131.1 (Ar-C), 129.2 (Ar-C), 129.1

(Ar-C), 126.7 (Ar-C), 126.1 (Ar-C), 125.1 (Ar-C), 123.9 (Ar-C), 61.5 ($ArCH_2O$), 59.1 (CH_2O), 48.1 (CH_2N_3), 29.2 (CH_2), 29.1 (CH_2), 28.05 (CH_2).

3.3.15 Model reaction of 4-(2-hydroxyethyl)-10-oxa-4- azatricyclo[5.2.1.$0^{2,6}$]dec-8-ene-3,5-dione, 2, and 1,1,1-tris[4-(2-propynyloxy)phenyl]-ethane, 4, with anthracen-9-yl methyl 3-azidopropyl Succinate, 7 (8)

Compounds **2** (0.295 g, 1.41 mmol) and **7** (0.18 g, 0.43 mmol) were added to a stirred solution of **4** (0.55 g, 1.11 mmol) in 5 mL of DMF in a Schlenk tube. The mixture was stirred for 10 min at room temperature, CuBr (0.018 g, 0.130 mmol) and PMDETA (0.045 mL, 0.21 mmol) were then added to the reaction mixture and immediately subjected to three FPT, left in argon and stirred at 120 ºC for 48 h. The mixture was diluted with THF, passed through a basic alumina column to remove the catalyst, and precipitated in diethyl ether. This procedure was repeated two times to obtain pure model compound **8** as a white solid Yield: 0.55 g, (64%). ($M_{n,\,theo}$ = 2000; $M_{n,\,GPC}$ = 1830). Mp = 119 ºC (DSC). ^{1}H NMR (δ, $CDCl_3$) 7.75 (s, 3H, C*H* of triazole ring), 7.38–7.18 (m, 24H, Ar*H*), 6.96–6.83 (m, 12H, Ar*H*), 5.49 (dd, 6H, J = 11.8 Hz, CH_2 linked to cycloadduct), 5.18 (s, 6H, OCH_2-triazole), 4.77 (s, 6H, C*H*CH=CHC*H*, bridge-head protons), 4.45 (bs, 6H, CH_2-triazole ring), 4.11 (bs, 6H, CH_2OC=O), 3.74 (bs, 3H, OH), 3.30–3.26 (m, 12H, NCH_2CH_2OH), 3.07 and 3.05 (bs, 6H, C=OC*HCHC*=O bridge protons), 2.77 and 2.70 (bs, 12H, OC=OCH_2CH_2C=OO), 2.24 (bs, 6H, triazole-CH_2C$H_2$$CH_2$O), 2.06 (bs, 3H, C$H_3$); ^{13}C NMR (δ, $CDCl_3$) 176.7, 175.8, 172.0, 156.4, 144.3, 142.3, 141.7, 140.9, 139.0, 138.4, 129.7, 127.1, 126.9, 126.8, 125.4, 124.2, 123.1, 122.2, 114.0, 62.1, 61.3, 59.9, 50.7, 47.7, 47.2, 46.2, 45.8, 41.3, 30.7, 29.2, 29.1, 25.6.

3.3.16 Synthesis of 9-anthyrylmethyl 2-bromo-2-methyl propanoate (9)

9-Anthryl methanol (1.50 g, 7.18 mmol) and DMAP (0.18 g, 1.44 mmol) were dissolved in 10 mL of THF, and Et_3N (1.2 mL, 8.6 mmol) was added. The reaction mixture was then cooled to 0 ºC. 2-Bromo isobutryl bromide (1.82 g, 7.89 mmol) was added dropwise within 30 minutes. The reaction mixture was stirred for 15 min. at 0 ºC then over night at room tempeature. The reaction was filtered off, solvent evaporated then extracted with CH_2Cl_2, and saturated aqueous $NaHCO_3$. The water phase again extracted with CH_2Cl_2, and combined organic phase dried with Na_2SO_4. The solution was concantrated, and the crude product was purified by column

chromatography over silica gel eluting with hexane/ethylacetate (10:1) to give the **9** as a yellow solid. Yield: 1.78 g (70%). Mp = 83-84 ºC (DSC). ^{1}H NMR ($CDCl_3$, δ) 8.51 (s, 1H, Ar*H* of anthracene), 8.33 (d, *J* = 8.7 Hz, 2H, Ar*H* of anthracene), 8.03 (d, *J* = 8.2 Hz, 2H, Ar*H* of anthracene), 7.60-7.45 (m, 4H, Ar*H* of anthracene), 6.21 (s, 2H, CH_2-anthracene), 1.86 (s, 6H, C(CH_3)$_2$-Br). ^{13}C NMR ($CDCl_3$, δ) 172.01, 131.57, 131.11, 129.29, 129.07, 127.01, 126.05, 125.41, 124.04, 60.99, 56.19, 30.83. Mass spectrometry (+EI) *m*/*z* (%): 358 [MH+] (20), 207 (27), 191 (100).

3.3.17 Preparation of with α-anthracene and ω-azide end-functional PS (Anth-PS-N_3)

α-Anthracene-ω-bromide terminated PS (Anth-PS-Br) was prepared by ATRP of St at 110 ºC. St (15.0 mL, 130 mmol), PMDETA (0.136 mL, 0.655 mmol), CuBr (0.0939 g, 0.655 mmol), and **9** (0.234 g, 0.655 mmol) were added in a 50 mL of Schlenk tube, and the reaction mixture was degassed by three FPT cycles and left in vacuum. The tube was then placed in a thermostated oil bath at 110 ºC for 40 min. The dark-green polymerization mixture was diluted with THF, passed through a basic alumina column to remove the catalyst, and precipitated in methanol. The polymer was dried for 24 h in a vacuum oven at 30 ºC. ^{1}H NMR ($CDCl_3$, δ) 8.45-7.96 (br, 5H, Ar*H* of anthracene), 7.5-6.2 (br, Ar*H* of anthracene and Ar*H* of PS), 5.8 (br, 2H, CH_2-anthracene), 4.4 (br, 1H, C*H*(Ph)-Br), 0.6-2.2 (br, aliphatic protons of PS).

Previously obtained Anth-PS-Br (2.4 g, 0.46 mmol, $M_{n,GPC}$= 5200 g/mol) was dissolved in DMF (20 mL), and NaN_3 (0.65 g, 10 mmol) was added to the reaction mixture. After stirring the reaction mixture for overnight at room temperature, the product was precipitated in an excess amount of methanol. Anth-PS-N_3 was dried for 24 h in a vacuum oven at 30 ºC (Yield= 2.35 g, 98%). ^{1}H NMR ($CDCl_3$, δ) 8.45-7.96 (br, 5H, Ar*H* of anthracene), 7.5-6.2 (br, Ar*H* of anthracene and Ar*H* of PS), 5.8 (br, 2H, CH_2-anthracene), 3.9 (br, 1H, C*H*(Ph)-N_3), 0.6-2.2 (br, aliphatic protons of PS).

3.3.18 Synthesis of 4-(2-[(3-acetyl-7-oxabicyclo[2.2.1]heptyl) carbonyl] amino ethoxy)-4-oxobutanoic acid (10)

2 (5 g, 24 mmol) was dissolved in 150 mL of 1,4-dioxane. To the reaction mixture were added Et_3N (16.58 mL, 119.6 mmol), DMAP (4.38 g, 35.8 mmol), and succinic anhydride (9.56 g, 95.6 mmol) in that order. The reaction mixture was stirred

overnight at 50 ºC, then poured into ice-cold water and extracted with CH_2Cl_2. The organic phase was washed with 1 M HCl, dried over Na_2SO_4 and concentrated. The crude product was crystallized from ethanol to give **10** as white crystal. Yield: 5.9 g (80%). Mp = 122-123 ºC (DSC). ^{1}H NMR ($CDCl_3$, δ) 6.50 (s, 2H, C*H*=C*H*, bridge protons), 5.25 (s, 2H, -C*H*O, bridge-head protons), 4.25 (t, *J* = 5.2 Hz, 2H, NCH_2CH_2OC=O), 3.74 (t, *J* =5.2 Hz, 2H, NCH_2CH_2OC=O), 2.87 (s, 2H, C*H*-C*H*, bridge protons), 2.66-2.53 (m, 4H, C=OCH_2CH_2C=OOH). ^{13}C NMR ($CDCl_3$, δ) 177.26, 176.35, 172.01, 136.83, 81.09, 61.22, 47.74, 37.92, 29.24. Mass spectrometry (+EI) *m*/*z* (%): 310 [MH+] (100), 242 (100), 142 (18), 124 (13).

3.3.19 Preparation of furan-protected maleimide-end-functionalized PEG (MI-PEG)

PEG-OH (M_n = 2000) (2.0 g, 1 mmol) was dissolved in 80 mL of CH_2Cl_2. To the reaction mixture were added DMAP (0.13 g, 1.0 mmol) and **10** (0.62 g, 2 mmol) in that order. After stirring 5 min at room temperature, a solution of DCC (0.41 g, 2.0 mmol) in 10 mL of CH_2Cl_2 was added. Reaction mixture was stirred overnight at room temperature. After filtration off the urea byproduct, the mixture was precipitated into diethyl ether for three times to obtain pure MI-PEG as a pale white solid. Yield: 1.9 g (83%). ^{1}H NMR ($CDCl_3$, δ) 6.50 (s, 2H, C*H*=C*H* as bridge protons), 5.25 (s, 2H, -C*H*O, bridge-head protons), 4.23 (m, 4H, CH_2OC=O), 3.75-3.51 (m, OCH_2CH_2 repeating unit of PEG, C=ONCH_2, and CH_2-PEG repeating unit), 3.36 (s, 3H, PEG-OCH_3), 2.87 (s, 2H, C*H*-C*H*, bridge protons) 2.61-2.56 (m, 4H, C=OCH_2CH_2C=O).

3.3.20 One-pot preparation of 3-arm star-block copolymer (PS-*b*-PMMA)$_3$ via double-click reactions

Anth-PS-N_3 (0.3 g, 0.05 mmol, $M_{n,NMR}$= 6000 g/mol), MI-PMMA (0.156 g, 0.06 mmol, $M_{n,NMR}$= 2600 g/mol), and trialkynefunctional linking agent **4** (0.007 g, 0.016 mmol) were dissolved in nitrogen-purged DMF (5 mL) in a Schlenk tube. CuBr (0.012 g, 0.080 mmol) and PMDETA (0.017 mL, 0.080 mmol) were added, and the reaction mixture was degassed by three FPT cycles and left in argon then stirred at 120 ºC for 48 h. Polymer solution was passed through neutral alumina column to remove copper salt, precipitated in methanol, and dried in a vacuum oven at 30 ºC (Yield= 0.35 g, 81%).

^{1}H NMR ($CDCl_3$, δ) 7.5-6.3 (m, Ar*H* of **4**, Ar*H* of PS and Ar*H* of cyclo adduct), 5.2-4.9 (br, 15H, PhOC*H*$_2$-triazole, cycloadduct-C*H*$_2$OC=O, and C*H*(Ph)-triazole), 4.7 (s, 3H, C*H*, bridge-head protons), 3.58 (br, OC*H*$_3$ of PMMA and NCH$_2$C*H*$_2$OC=O), 3.28 (br, 12H, NC*H*$_2$CH$_2$OC=O and C*H*-C*H* of bridge protons), 2.2-0.7 (m, aliphatic protons of PS and PMMA).

3.3.21 One-pot preparation of 3-arm star-block copolymer (PS-*b*-PEG)$_3$ via double-click reactions

Anth-PS-N_3 (0.3 g, 0.05 mmol, $M_{n,NMR}$= 6000), MI-PEG (0.17 g, 0.06 mmol, $M_{n,NMR}$= 2800 g/mol), and trialkyne-functional linking agent **4** (0.007 g, 0.016 mmol) were dissolved in nitrogen-purged DMF (5 mL) in a Schlenk tube. PMDETA (0.017 mL, 0.080 mmol) and CuBr (0.012 g, 0.080 mmol) were added, and the reaction mixture was degassed by three FPT cycles and left in argon then stirred at 120 ºC for 48 h. Polymer solution was passed through neutral alumina column to remove copper salt, precipitated into methanol, and dried in a vacuum oven at 30 ºC (Yield= 0.33 g, 75%). ^{1}H NMR ($CDCl_3$, δ) 7.5-6.3 (Ar*H* of **4**, Ar*H* of PS and Ar*H* of cyclo adduct), 5.2-4.9 (br, 15H, PhOC*H*$_2$-triazole, cycloadduct-C*H*$_2$OC=O, and C*H*(Ph)-triazole), 4.73 (s, 3H, C*H*, bridge-head protons), 4.2 (t, 6H, PEG-OCH$_2$C*H*$_2$OC=O), 4.0-3.5 (br, -OC*H*$_2$C*H*$_2$, repeating unit of PEG, and NCH$_2$C*H*$_2$OC=O), 3.4 (s, 9H, PEG-OC*H*$_3$), 3.28 (br, 12H, NC*H*$_2$CH$_2$OC=O and C*H*-C*H* of bridge protons), 2.6-2.5 (m, 12H, C=OC*H*$_2$C*H*$_2$C=O), 2.2-0.6 (aliphatic protons of PS).

3.3.22 Sythesis of 3-(1,1,1-trimethylsilyl)-2-propynyl 2-bromo-2-methylpropanoate (11)

A solution of 2-bromo isobutyryl bromide (2.15 g, 9.37 mmol) in CH_2Cl_2 (20 mL) was added dropwise to a solution of 3-trimethylsilyl-2-propyn-1-ol (1 g, 7.8 mmol) and triethylamine (1.14 mL, 9.37 mmol) in CH_2Cl_2 (40 mL) at 0 ^{o}C. After complete addition, the reaction mixture was allowed to stir for 1 h at 0 ^{o}C and overnight at room temperature. The formed triethylammonium bromide was filtered off and the solvent was removed in vacuum. The crude product was dissolved in CH_2Cl_2 and washed two times with a saturated aqueous $NaHCO_3$ and two times with distilled water (100 mL). The organic layer was dried with magnesium sulfate and solvent was removed in vacuum, afforded a yellow oil which was further purified by flash chromatography over silica gel eluting with hexane/EtOAc (9:1, v/v). The product

was isolated as colorless oil. Yield: 1.65 g, (76%). ^{1}H NMR ($CDCl_3$, δ) 4.75 (s, 2H, $Si(CH_3)_3C{\equiv}C\mathit{H}_2$-O), 1.96 (s, 6H, $C(C\mathit{H}_3)_2$-Br), 0.17 (s, 9H, $Si(C\mathit{H}_3)_3C{\equiv}CH_2$-O). ^{13}C NMR ($CDCl_3$, δ) 171.09, 98.45, 92.97, 56.15, 55.28, 30.83. Mass spectrometry (+EI) *m*/*z* (%): 279 [MH+] (45), 256 (15).

3.3.23 Synthesis of α–silyl protected alkyne PS (α-silyl-alkyne-PS)

St (40.0 mL, 349 mmol), PMDETA (0.36 mL, 1.74 mmol), CuBr (0.25 g, 1.74 mmol), and **11** (0.485 g, 1.74 mmol) were added to a 50 mL of Schlenk tube and the reaction mixture was degassed by three FPT cycles and left in vacuum and placed in a thermostated oil bath at 110 ^{o}C for 45 min. After the specified time, the polymerization mixture was diluted with THF, passed through a column of neutral alumina to remove catalyst and precipitated into methanol. The polymer was dried in a vacuum oven at 40 °C ^{1}H NMR 7.5-6.5 (Ar*H*), 4.4 (C*H*Br), 4.1 (C≡CCH_2O), 2.0-0.9 (CH_2 and C*H*), 0.19 ((CH_3)$_3$Si-).

3.3.24 General procedure for the preparation of azide-end functionalized P*t*BA (P*t*BA-N_3)

P*t*BA-N_3 was prepared in two steps. As a first step, bromo end-functionalized P*t*BA (P*t*BA-Br) was prepared by ATRP of *t*BA. To a 25 mL Schlenk tube, *t*BA (12 mL, 82 mmol), PMDETA (0.17 mL, 0.82 mmol), CuBr (0.12 g, 0.82 mmol), ethylene carbonate (1.05 g, 0.102 mmol), and ethyl 2-bromoisobutyrate (EiBr) **(**0.16 g**,** 0.82 mmol) were added, and the reaction mixture was degassed by three FPT cycles and left in vacuo. The tube was then placed in a thermostated oil bath at 80 ^{o}C for predetermined times. The polymerization mixture was diluted with THF, passed through a neutral alumina column to remove the catalyst, and precipitated into the solution of water and methanol (1:4 v/v). After decantation, the polymer was dissolved in CH_2Cl_2, extracted with water and the water phase was again extracted with CH_2Cl_2 and combined organic phase was dried over Na_2SO_4 and evaporated. The polymer was dried in a vacuum oven at 40 °C. ^{1}H NMR ($CDCl_3$, δ) 4.1 (m, C=OOCH_2 and C*H*Br end group of P*t*BA), 2.2 (br, C*H* of P*t*BA), 2.0-1.0 (br, aliphatic protons of P*t*BA).

Secondly, previously obtained P*t*BA-Br (1g, 0.22 mmol, $M_{n,NMR}$= 4500 g/mol) was dissolved in 10 mL of DMF and NaN_3 (0.43 g, 6.67 mmol) was added. The reaction mixture was stirred at 50 ºC for overnight, after which time it was cooled to room

temperature and diluted with CH_2Cl_2, and extracted 2 times with water. The organics were dried over Na_2SO_4 and evaporated. The polymer was dried in a vacuum oven at 40 °C. Yield = 0.8 g, (80 %). ^{1}H NMR ($CDCl_3$, δ) 4.1 (m, C=OOC*H*$_2$), 3.7 (bs, C*H*N_3 end group of P*t*BA), 2.2 (br, C*H* of P*t*BA), 2.0-1.0 (br, aliphatic protons of P*t*BA).

3.3.25 Synthesis of 2-azidoethanol (12)

To a 100 mL of round bottom flask was added 2-bromo ethanol (5 g, 0.04 mol) in 50 mL of water/acetone (1:4, v/v). NaN_3 (4 g, 0.06 mol) was added in one portion to the reaction and the mixture was sitirred at 60 ^{o}C for overnight. After acetone was removed, remaining liquid was dissolved in CH_2Cl_2 and extracted with water. The aqueous layer was extracted with CH_2Cl_2 (50 mL) and combined organic layers were dried over Na_2SO_4. Solvent was removed under vacuum and 2-azido ethanol was obtained as a pale yellow oil. Yield= 3.3 g (95%). ^{1}H NMR ($CDCl_3$, δ) 3.75 (t, 2H, C*H*$_2$-O), 3.44 (t, 2H, C*H*$_2$-N_3).

3.3.26 Preparation of azide-end functionalized PEG (PEG-N_3)

PEG-OH (5 g, 8 mmol, M_n = 550) was dissolved in 150 mL of CH_2Cl_2. Succinic anhydride (3.13 g, 32.0 mmol), triethylamine (Et_3N) (5.6 mL, 40 mmol) and DMAP (1.46 g, 12.0 mmol) were added to the reaction mixture. After stirring overnight at room temperature, solution was poured into ice-cold water (150 mL) and extracted with CH_2Cl_2. The organic layer was washed with 1 M HCl (150 mL) and then with distilled water. Finally, organic phase was dried with anhydrous Na_2SO_4 and the solvent was removed in vacuum to give mono carboxylic acid end-functionalized PEG (PEG-COOH) as colorless oil. Yield = 5 g (95%). ^{1}H NMR ($CDCl_3$, δ) 4.23 (d, 4H, C=OOC*H*$_2$), 3.52-3.65 (m, 4H, -OC*H*$_2$C*H*$_2$O-, PEG backbone), 3.35 (s, 3H, OC*H*$_3$), 2.62 (s, 4H, C=OC*H*$_2$C*H*$_2$C=O).

PEG-COOH (1.00 g, 1.53 mmol) was dissolved in 20 mL of dry CH_2Cl_2. 2-Azido ethanol (0.4 g, 4.61 mmol) and DMAP (0.19 g, 1.53 mmol) were added to the reaction mixture in that order. After stirring for 5 minutes at room temperature, DCC (0.95 g, 4.6 mmol) in 10 mL of CH_2Cl_2 was added to solution. The reaction was continued via stirring for 24 h at room temperature. Reaction solution was concentrated under reduced pressure. The crude product was purified by column over silica gel eluting first with CH_2Cl_2/ethyl acetate (1/1), then CH_2Cl_2/CH_3OH (10/1) in order to give brown oil. Yield = 1 g (91%). ^{1}H NMR ($CDCl_3$, δ) 4.23 (t, 4H,

CH_2OC=O and C=OOCH_2CH_2N$_3$), 3.70-3.45 (br, 4H, OCH_2CH_2O backbone and C=OOCH$_2$CH_2N$_3$), 3.36 (s, 3H, OCH_3), 2.67 (s, 4H, C=OCH_2CH_2C=O).

3.3.27 Preparation of (Alkyne-PS)$_n$-polyDVB multiarm star polymer

α-Silyl-alkyne-PS macroinitiator (2.00 g, 0.294 mmol, $M_{n,GPC}$= 6800 g/mol), DVB (0.633 mL, 4.44 mmol), PMDETA (0.06 mL, 0.3 mmol), CuBr (0.04 g, 0.3 mmol) and anisole (12 mL) were charged to a Schlenk tube equipped with a magnetic stirrer bar under argon atmosphere. The first sample was quickly taken from the reaction mixture for GC measurement, before the reaction mixture was degassed by using three FPT cycles. The reaction flask was back-filled with argon and immersed in oil bath at 110 ^{o}C. At time intervals, the samples were taken from the reaction mixture with argon purged-syringe under positive argon atmosphere and then diluted with THF, purified by passing through short neutral alumina column to remove the copper salt and filtered through poly(tetrafluoroethylene) (PTFE) filter (0.2 μm pore size) prior to GC and GPC analyses. After 9 h at 95 % conversion, the reaction was stopped via exposure to air. The polymerization mixture was diluted with THF, filtered through a column filled with neutral alumina to remove the copper complex and the star polymer was precipitated in methanol. The crude product was dissolved in THF, precipitated into methanol/diethyl ether (1/2; v/v) and dried under vacuum at 40 ^{o}C for 24 h. ^{1}H NMR (CDCl$_3$, δ) 7.5-6.5 (br, Ar*H* of PS), 4.05 (br, (CH_3)$_3$Si-C≡CCH_2O), 2.0-0.9 (br, aliphatic protons of PS), 0.17 (br, (CH_3)$_3$Si-).

The silyl group of (α-silyl-alkyne-PS)$_n$-polyDVB multiarm star homopolymer (1 g, 4 μmol, $M_{w,TD-GPC}$= 246100 g/mol) was deprotected by using TBAF (0.2 mL, 0.2 mmol) in THF (20 mL). The reaction mixture was stirred for 2 h at room temperature and precipitated in methanol. The recovered polymer was dried under vacuum at 40 ^{o}C for 24 h. ^{1}H NMR (CDCl$_3$, δ) 7.5-6.5 (br, Ar*H* of PS), 4.05 (br, HC≡CCH_2O), 2.0-0.9 (br, aliphatic protons of PS).

3.3.28 Preparation of (P*t*BA)$_m$-(PS)$_n$-polyDVB multiarm star block copolymer via CuAAC click reaction

P*t*BA-N$_3$ (0.157 g, 0.035 mmol, $M_{n,NMR}$= 4500 g/mol), (Alkyne-PS)$_n$-polyDVB multiarm star polymer (0.25 g, 1.0 μmol, $M_{w,TD-GPC}$= 250750 g/mol), PMDETA (10 μL, 0.050 mmol), CuBr (0.007 g, 0.05 mmol) and DMF (5 mL) were added to a 10

mL of Schlenk tube. Reaction mixture was degassed by three FPT cycles, left in vacuum and stirred for 24 h at room temperature. After the specified time, solution was diluted with THF, filtered through a column filled with neutral alumina to remove copper complex and precipitated in methanol. The dissolution-precipitation procedure was repeated two times. The recovered multiarm star block copolymer was dried in a vacuum oven at 40 ^{o}C for 24 h. ^{1}H NMR ($CDCl_3$, δ) 7.3-6.5 (br, Ar*H* of PS), 2.22 (br, C*H* of P*t*BA), 2.1-0.6 (br, aliphatic protons of PS and P*t*BA).

3.3.29 Preparation of $(PEG)_k$-$(PS)_n$-polyDVB multiarm star block copolymer via CuAAC click reaction

PEG-N_3 (0.011 g, 0.018 mmol, $M_{n,NMR}$= 620), P*t*BA-N_3 (0.085 g, 0.019 mmol, $M_{n,NMR}$= 4500 g/mol), (Alkyne-PS)$_n$-polyDVB (0.30 g 1.2 μmol, $M_{w,TD\text{-}GPC}$= 250750 g/mol) multiarm star polymer were dissolved in DMF (5 mL) in 10 mL of Schlenk tube. The mixture was stirred at room temperature for 5 min and PMDETA (10 μL, 0.05 mmol), CuBr (0.007 g, 0.05 mmol) were added immediately. Reaction mixture was degassed by three FPT cycles, left in vacuum and stirred for 24 h at room temperature. The reaction mixture was diluted with THF, filtered through a column filled with neutral alumina to remove the copper complex and precipitated into methanol. The dissolution-precipitation cycle was repeated two times. Multiarm star mixed-block copolymer was dried in a vacuum oven at 40 ^{o}C for 24 h. ^{1}H NMR ($CDCl_3$, δ) 7.3-6.5 (br, Ar*H* of PS), 3.62 (OCH_2CH_2 repeating unit of PEG), 2.5-0.5 (br, aliphatic protons and PS).

3.3.30 Preparation of $(PEG)_k$-$(P$*t*$BA)_m$-$(PS)_n$-polyDVB multiarm star mixed-block copolymer via CuAAC click reaction

PEG-N_3 (0.011 g, 0.019 mmol, $M_{n,NMR}$= 620 g/mol), P*t*BA-N_3 (0.085 g, 0.019 mmol, $M_{n,NMR}$= 4500 g/mol), (Alkyne-PS)$_n$-polyDVB (0.30 g 1.2 μmol, $M_{w,TD\text{-}GPC}$= 250750 g/mol) multiarm star polymer and were dissolved in DMF (5 mL) in 10 mL of Schlenk tube. The mixture was stirred at room temperature for 5 min and PMDETA (10 μL, 0.05 mmol), CuBr (0.007 g, 0.05 mmol) were added immediately. Reaction mixture was degassed by three FPT cycles, left in vacuum and stirred for 24 h at room temperature. The reaction mixture was diluted with THF, filtered through a column filled with neutral alumina to remove the copper complex and precipitated into methanol. The dissolution-precipitation cycle was repeated two times. Multiarm

star mixed-block copolymer was dried in a vacuum oven at 40 ^{o}C for 24 h. ^{1}H NMR ($CDCl_3$, δ) 7.3-6.5 (br, Ar*H* of PS), 3.62 (OCH_2CH_2 repeating unit of PEG), 2.22 (br, C*H* of P*t*BA), 2.0-0.6 (br, aliphatic protons of PS and P*t*BA).

3.3.31 One-pot preparation of α-silyl protected alkyne- and α-anthracene-end-functionalized PS mixture (α-silyl alkyne-PS + Anth-PS)

St (20.0 mL, 175 mmol), PMDETA (0.182 mL, 0.872 mmol), CuBr (0.125 g, 0.871 mmol), **9** (0.312 g, 0.873 mmol) and **11** (0.242 g, 0.873 mmol) were added in a 50 mL of Schlenk tube and the reaction mixture was degassed by three FPT cycles and left in vacuum. After the tube was placed in a thermostated oil bath at 110 ^{o}C for 40 min, the dark green polymerization mixture was diluted with THF, passed through a basic alumina column to remove the catalyst, precipitated in methanol and dried for 24 h in a vacuum oven at 40 ^{o}C. ^{1}H NMR ($CDCl_3$, δ) 8.4 (bs, 1H, Ar*H* of anthracene), 8.2 (bs, 2H, Ar*H* of anthracene), 7.9 (bs, 2H, Ar*H* of anthracene), 7.5 (bs, 4H, Ar*H* of anthracene), 7.2–6.5 (Ar*H* of PS), 5.8 (CH_2-anthracene), 4.4 (bs, C*H*(Ph)-Br), 4.1 (m, C≡CCH_2O), 2.3-0.8 (CH_2 and C*H*), 0.16 ((CH_3)$_3$Si-).

3.3.32 Preparation of (Alkyne-PS)$_m$-polyDVB-(PS-Anth)$_m$ multiarm star polymer bearing alkyne and anthracene functionalities at the periphery

α-Silyl alkyne-PS + Anth-PS (2.1 g, 0.39 mmol, $M_{n,GPC}$= 5400 g/mol), anisole (13.0 mL), PMDETA (0.081 mL, 0.39 mmol), DVB (0.815 mL, 5.72 mmol), and CuBr (0.056 g, 0.39 mmol) were charged to a Schlenk tube equipped with a magnetic stirrer bar under argon. The first sample was quickly taken from the reaction mixture for GC measurement, before it was degassed by using three FPT cycles. The reaction flask was back-filled with argon and immersed in a 110 ºC oil bath. At specified intervals, samples were taken from the reaction mixture with argon purged-syringe under positive argon atmosphere. The samples were diluted with THF and purified by passing through short neutral alumina column to remove the copper salt and then filtered through PTFE filter prior to GC and GPC analyses. The reaction was stopped after 12 h at 94 % conversion via exposure to air. The reaction mixture was diluted with THF, then filtered through a column filled with neutral alumina to remove the copper complex and the star polymer was precipitated in methanol. The crude product was easily purified via dissolution in THF and then precipitation in

methanol/ether (1/2; v/v) mixture to remove the linear chains. Finally, the polymer was dried under vacuum at 40 ºC for 24 h.

Subsequently, silyl groups at the periphery of the multiarm star homopolymer (1.2 g, 4.8 μmol, $M_{w,TD\text{-}GPC}$= 248000 g/mol) was deprotected by using TBAF (0.2 mL, 0.2 mmol) in THF (20 mL). The reaction mixture was stirred for 2 h at room temperature and precipitated in methanol. The recovered polymer was dried under vacuum at 40 ºC for 24 h. ^{1}H NMR ($CDCl_3$, δ) 8.4-7.9 (br, Ar*H* of anthracene), 7.5-6.5 (br, Ar*H* of PS), 5.77-5.71 (br, CH_2-anthracene), 4.05 (br, HC≡CCH_2O), 2.5-0.5 (br, aliphatic protons of PS)

3.3.33 Preparation of (P*t*BA)$_n$-(PS)$_m$-polyDVB-(PS-Anth)$_m$ multi-miktoarm star block copolymer via CuAAC click reaction

The (Alkyne-PS)$_m$-polyDVB-(PS-Anth)$_m$ multiarm star polymer (0.3 g, 1.20 μmol, $M_{w,TD\text{-}GPC}$= 250000 g/mol) and P*t*BA-N_3 (0.12 g, 0.024 mmol, $M_{n,NMR}$= 5100 g/mol) were dissolved in nitrogen purged DMF (8 mL) in a Schlenk tube. CuBr (8.5 mg, 0.06 mmol) and PMDETA (12 μL, 0.06 mmol) were added in that order, and the reaction mixture was degassed by three FPT cycles, and stirred at room temperature for 24 h. The solution was passed through a column of neutral alumina to remove the copper salt and precipitated into methanol. The crude product was purified by dissolution in THF and then precipitation in methanol/diethyl ether mixture (1/1; v/v). Finally, polymer was dried in a vacuum oven at 40 ºC for 24 h. ^{1}H NMR ($CDCl_3$, δ) 8.4-7.9 (br, Ar*H* of anthracene), 7.3-6.5 (br, Ar*H* of PS), 5.77-5.71 (br, CH_2-anthracene), 5.3 (br, triazole-CH_2OC=O), 2.22 (br, C*H* of P*t*BA), 2.1-0.6 (aliphatic protons of PS and P*t*BA).

3.3.34 Preparation of (P*t*BA)$_n$-(PS)$_m$-polyDVB-(PS)$_m$-(PMMA)$_k$ multi-miktoarm star block copolymer via Diels-Alder click reaction

A solution of MI-PMMA (0.025 g, 8.33 mmol, $M_{n,NMR}$= 3000 g/mol) in 10 mL of toluene was added to a 10 mL solution of (P*t*BA)$_n$-(PS)$_m$-polyDVB-(PS-Anth)$_m$ (0.15 g, 0.42 μmol, $M_{w,TD\text{-}GPC}$= 355000 g/mol). The reaction mixture was bubbled with nitrogen for 30 min and refluxed for 48 h under nitrogen in the dark. After a specified time toluene was evaporated under vacuum and the residual polymer was dissolved in THF, subsequently precipitated in methanol. The dissolution-precipitation was repeated two times and finally polymer was dried in a vacuum oven

at 40 ºC for 24 h. ^{1}H NMR ($CDCl_3$, δ) 7.3-6.5 (br, Ar*H* of PS), 3.59 (br,OCH_3 of PMMA), 2.22 (br, C*H* of P*t*BA), 2.0-0.6 (br, aliphatic protons of P*t*BA, PMMA and PS).

4. RESULTS AND DISCUSSION

As a general perspective, this thesis describes the design and synthesis of various macromolecular structures such as graft, star and multiarm star polymers by combination of C/LRP methods with click reactions which involve CuAAC and Diels-Alder.

In fact, it is often advantageous to employ a combination of click chemistry with C/LRP methods enabling macromolecular structures with varying composition and topology that are otherwise very difficult to prepare.

4.1. Synthesis of Heterograft Copolymers via CuAAC and Diels-Alder Click Reactions

The present study concerns with the synthesis of St copolymers bearing pendant chlorine moieties and their post modifications with suitable functional groups (anthryl and azide), including the application of double click reactions (CuAAC and Diels-Alder) in one-pot process. Thus, PS-Anth-Azide was used as a scaffold for the ligation of MI-PMMA and Alkyne-PEG to yield the corresponding heterograft copolymer.

For this purpose, the initiator with proper functionality for Diels-Alder reaction was first prepared. The synthesis of 2-bromo-2-methyl-propionic acid 2-(3,5-dioxo-10-oxa-4-azatricyclo[5.2.1.$0^{2,6}$]dec-8-en-4-yl) ethyl ester**, 3** consists mainly of three steps, as shown in Scheme 4.1. In the first step, furan and maleic anhydride were reacted in toluene at 80 ºC, and thus obtained adduct **1,** was utilized for the synthesis of **2** by adding the solution 2-amino ethanol in methanol into dispersion of **1** in methanol. Finally, **3**, was obtained via an esterification reaction between **2** and 2-bromoisobutryl bromide in THF at room temperature (Scheme 4.1).

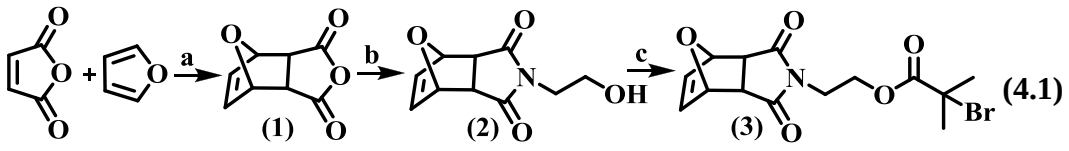

(4.1)

From overlay ^{1}H NMR spectra Figure 4.1(c), it is clearly seen that the methyl protons next to Br were detected at 1.87 ppm and the methylene protons next to the ester unit at 4.31 ppm. Moreover, the characteristic protons of the adduct were also detected at 6.49 ppm (bridge vinyl protons), 5.24 ppm (bridge-head protons) and 2.85 ppm (bridge protons) respectively. These results confirmed that the synthesis of **3** was achived.

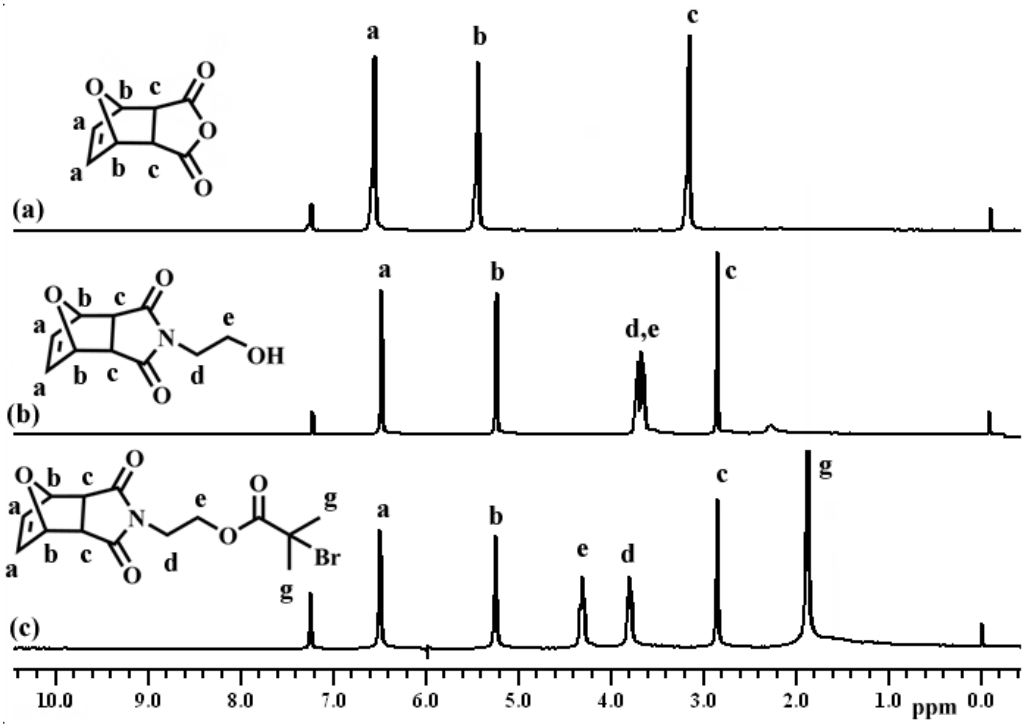

Figure 4.1 : ^{1}H NMR spectra of: a) 3-acetyl-N-(2-hydroxyethyl)-7-oxabicyclo[2.2.1]hept-5-ene-2-carboxylic acid (1); b) 3-acetyl-N-(2-hydroxyethyl)-7-oxabicyclo[2.2.1]hept-5-ene-2 carboxamide (2); c) 2-bromo-2- methyl-propionic acid 2-(3,5-dioxo-10-oxa-4-azatricyclo[5.2.1.02,6]dec-8-en-4-yl) ethyl ester (3) in CDCl3.

Then compound **3** was used as an initiator in ATRP of MMA in the presence of CuCl/PMDETA as a catalyst system at 40 ºC to obtain MI-PMMA as one of the graft chains (Scheme 4.2). The maleimide functional group of the **3** was protected with furan in order to prevent radical copolymerization of maleimide with MMA during polymerization. The polymerization temperature was deliberately kept low avoiding furan deprotection at elevated temperatures. Furthermore, the polymerization solution was *in situ* reacted with tributyltinhydride (Bu_3SnH) in order to convert chloride end group to hydrogen avoiding the probability of the radical formation caused by CuBr/PMDETA in the one-pot preparation of heterograft copolymer.

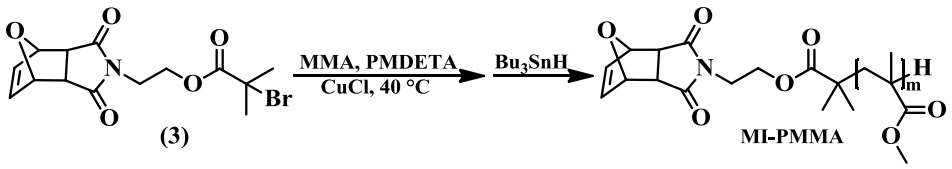

(4.2)

The NMR number-average molecular weight ($M_{n,NMR}$ = 3100 g/mol) was calculated from a ratio of the integrated values of OCH_3 of PMMA and N-CH_2 (δ 3.8 -3.4) to that of a signal at 6.5 ppm assignable to vinylic two protons, while being included the molecular weight of initiator (357 g/mol) (Figure 4.2). The number-average molecular weight obtained by GPC ($M_{n,GPC}$ = 3350 g/mol, relative to linear PMMA standarts) is an excellent agreement with $M_{n,NMR}$, thus indicating that the quantitative maleimide end-group functionalization of the PMMA was successful. Moreover, M_w/M_n = 1.22 calculated from GPC displays narrow molecular weight distribution.

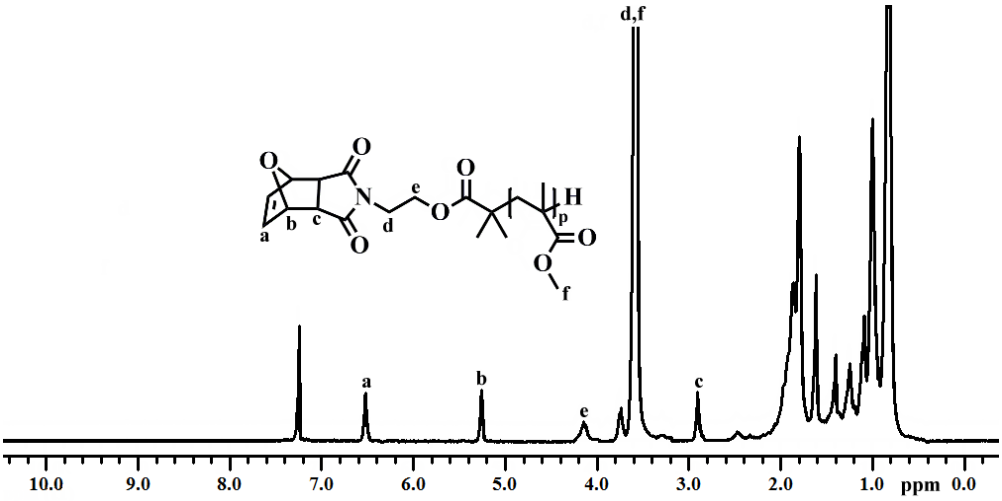

Figure 4.2 : ^{1}H NMR spectra of MI-PMMA in $CDCl_3$.

Alkyne-PEG as a second graft chain was achieved via an esterification reaction of PEG (M_n= 550) with 4-pentynoic acid (Scheme 4.3).

(4.3)

^{1}H NMR revealed the structure of Alkyne-PEG displaying characteristic peaks such as a triplet (C*H*≡C-) at 1.96 ppm and a multiplet (CH≡CCH_2CH_2C=O) at 2.5 ppm (Figure 4.3). $M_{n,NMR}$ was calculated from a ratio of the peak areas of PEG (repeating unit and -OCH_3 end group of PEG) at 3.9-3.3 and -C≡C*H* at 1.96 ppm. $M_{n,NMR}$= 685 g/mol was almost consistent with those of $M_{n,theo}$= 630 g/mol and $M_{n,GPC}$= 550 g/mol (relative to linear PS standarts).

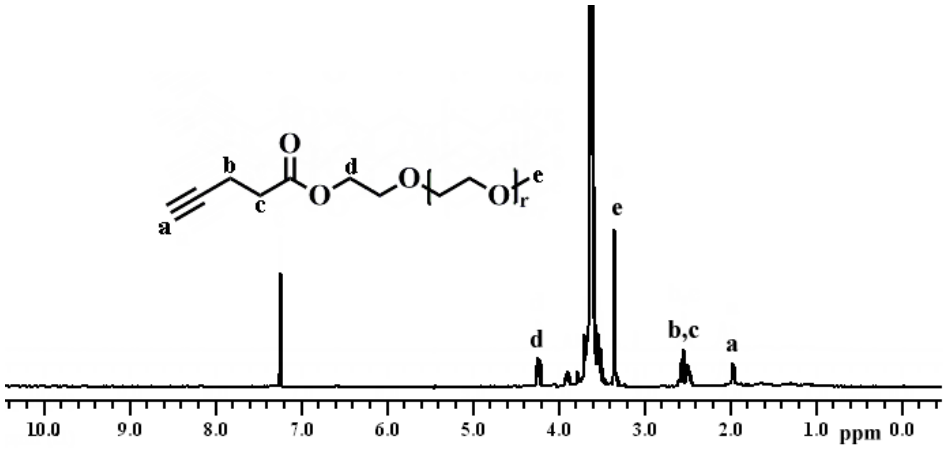

Figure 4.3 : ^{1}H NMR spectrum of Alkyne-PEG in $CDCl_3$.

To form the backbone polymers, St and CMS were polymerized via NMP at 125 ºC in order to give P(S-*co*-CMS) random copolymers using two different mol %s of CMS, 15 and 30, as the feed ratios (Scheme 4.4).

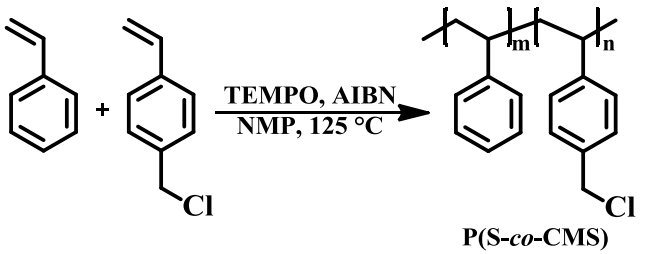

(4.4)

^{1}H NMR calculation from integrals of aromatic protons (δ 6.5-7.5) and CH_2Cl (δ 4.5) displayed 18 and 34 mol % of CMS, respectively that the incorporations of CMS into the copolymer agree well with the feed ratios (Figure 4.4, (a)). Again, exploiting the $M_{n,GPC}$ values of copolymers, DP_n of St and CMS in these copolymers (18 and 34 mol % CMS) were calculated to have 32 and 7 and 24 and 12.4, respectively.

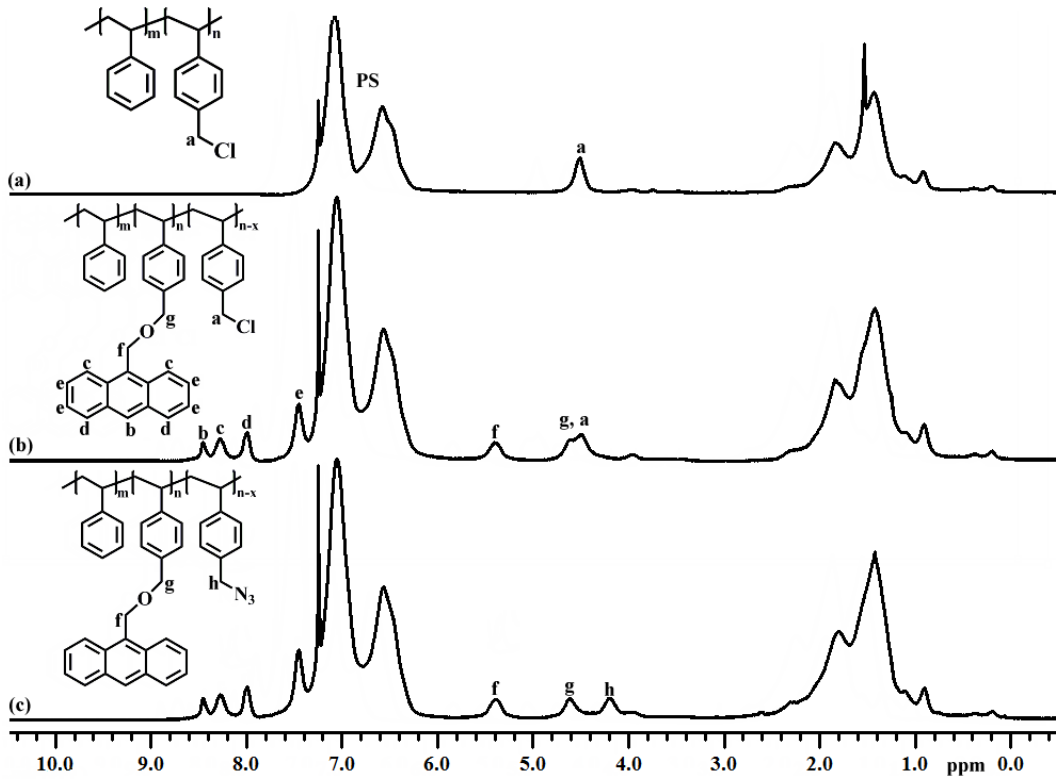

Figure 4.4 : Comparison of the ^{1}H NMR spectra of a) P(S-*co*-CMS)-1, b) P(S-CMS-Anth)-1, and c) PS-Anth-Azide-1 in $CDCl_3$.

Next, thus obtained two copolymers were reacted with 9-anthracene methanol in the presence of NaH at reflux temperature of THF for 12 h, affording PS with anthracene pendant units, P(S-CMS-Anth) (Scheme 4.5).

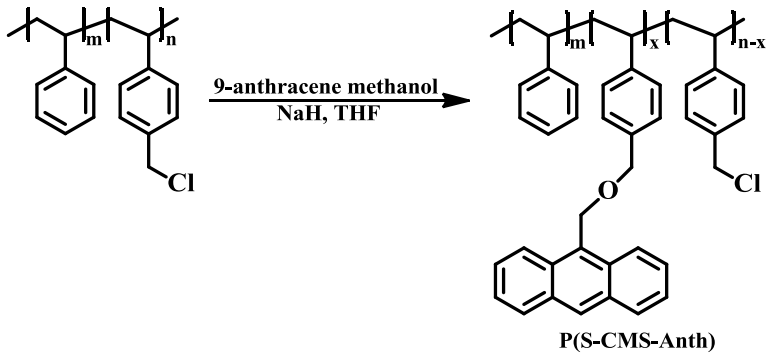

(4.5)

The structure was identified via ^{1}H NMR displaying aromatic and O*CH*$_2$ protons of anthracene at 8.5-7.4 and 5.4 ppm, respectively, along with those corresponding to St and CMS units (Figure 4.4, (b)). Anthryl functionality incorporated into the PS backbone as pendant group was calculated taking account the integrated values ratio of anthryl-C*H*$_2$O (5.4) and Ph-C*H*$_2$O and C*H*$_2$Cl (4.6 and 4.5) signals. For the copolymer P(S-CMS-Anth)-1 derived from P(S-*co*-CMS)-1, anthracene moiety was calculated to have 7.2 mol %, taking the initial DP_n of St and CMS of 32 and 7,

respectively. Similar calculation for the copolymer, PS-CMS-Anth-2 derived from P(S-*co*-CMS)-2 revealed 13 mol % of anthracene moiety in the copolymer, presuming that the initial DP_n of St and CMS were 24 and 12.4, respectively.

These two copolymers with anthryl pendant groups then were subjected to a reaction of NaN_3 in DMF overnight at room temperature, affording the corresponding copolymers with both anthryl and azide groups, PS-Anth-Azide (Scheme 4.6).

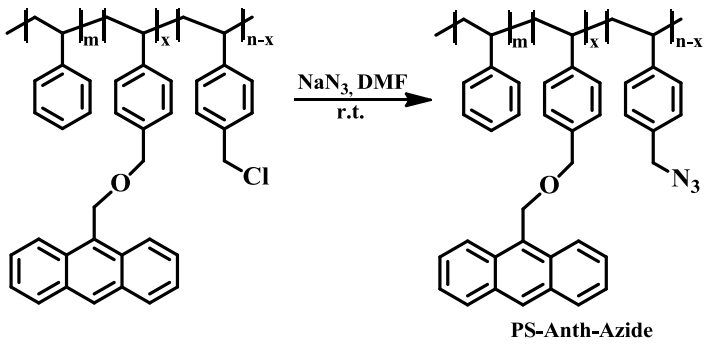

(4.6)

^{1}H NMR spectrum of the obtained copolymers showed a complete disappearance of C*H*$_2$Cl at 4.5 and an appearance of new signal related to C*H*$_2$N$_3$ at 4.2-3.9 ppm together with the characteristic signals of anthracene (Figure 4.4, (c)). A complete disappearance of CH_2Cl signal proved the quantitative azide functionalization of the remaining CMS units in the copolymer. Molecular weights and functionalities of the backbone polymers at various stages were described in Table 4.1.

Table 4.1 : Molecular weights and functionalities of the backbone polymers at various stages

Entry	Sample	Feed ratio (S/CMS)	M_n[a]	M_w/M_n[a]	Functionality[b] (mol %)		
					CMS	Anthryl	Azide
1	**P(S-*co*-CMS)-1**	85/15	4350	1.14	18	-	-
2	**P(S-CMS-Anth)-1**	-	4900	1.23	10.8	7.2	-
3	**PS-Anth-Azide-1**	-	5150	1.22	-	7.2	10.8
4	**P(S-*co*-CMS)-2**	70/30	4400	1.17	34	-	-
5	**P(S-CMS-Anth)-2**	-	5100	1.25	21	13	-
6	**PS-Anth-Azide-2**	-	5200	1.23	-	13	21

[a] Determined by GPC relative to linear PS standards.
[b] Determined by ^{1}H NMR (see text).

Previously obtained PS-Anth-Azide backbone polymers were reacted with MI-PMMA and Alkyne-PEG as grafts in one-pot process via double click reactions in the presence of CuBr/PMDETA in DMF at 120 ^{o}C for 48 h (Scheme 4.7).

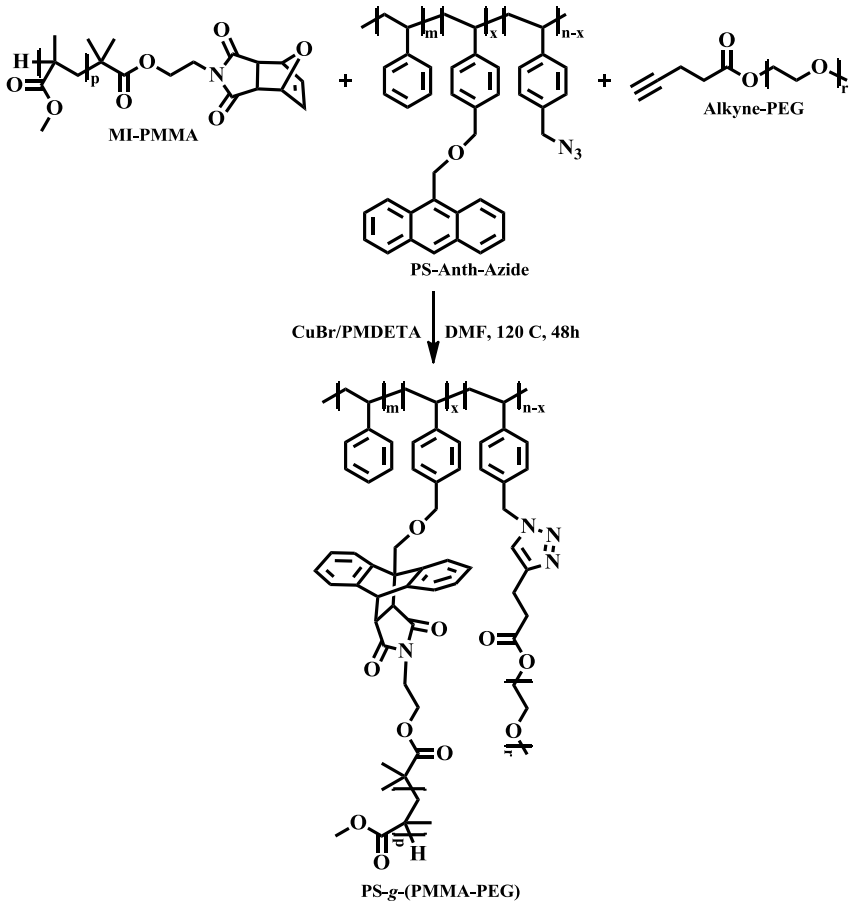

(4.7)

The ^{1}H NMR spectra of the both hetero graft copolymers displayed characteristic signals of PMMA and PEG together with those of PS, thus proving successful double click reactions (Figure 4.5).

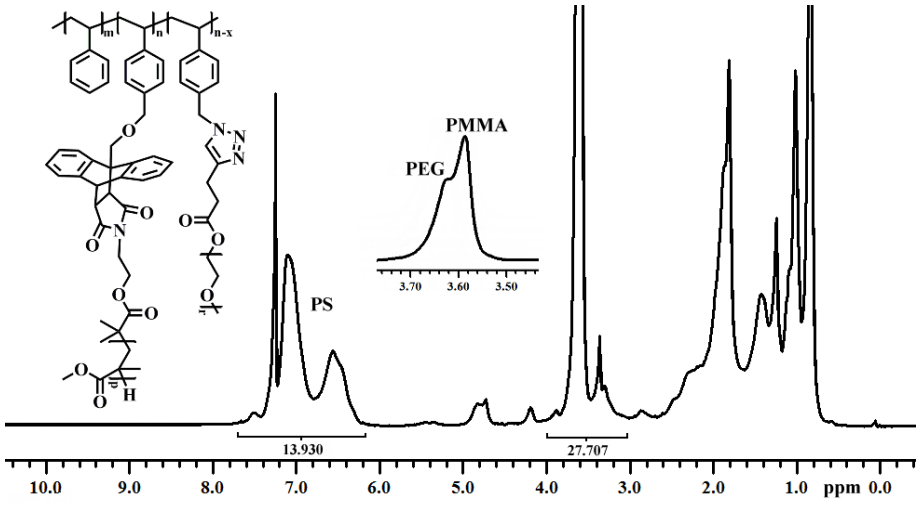

Figure 4.5 : ^{1}H NMR of PS-*g*-(PMMA-PEG) heterograft copolymer obtained from PS-Anth-Azide-1 in $CDCl_3$.

Overall click reaction efficiency (CR_{eff}) (grafting efficiency) for both heterograft copolymers was calculated by a following formula:

$$CR_{eff} = I_{aliphatic} \text{ X } (5 \text{ X } N_{St} + 12 \text{ X } N_{Anth} + 4 \text{ X } N_{Azide}) / I_{aromatic} \text{ X } [(3 \text{ X } DP_{n,PMMA} \text{ X } N_{Anth}) + (4 \text{ X } DP_{n,PEG} \text{ X } N_{Azide})]$$

where $I_{aliphatic}$ and $I_{aromatic}$ are integrated values of the sum of OCH_3 and OCH_2CH_2 protons of PMMA and PEG and the aromatic protons including phenyl and anthryl hydrogens, respectively and N_{St}, N_{Anth} and N_{Azide} are number of St, anthracene and azide groups in the backbone polymer, respectively. CR_{eff} was found to be around 94 and 90% for PS-Anth-Azide-1 and PS-Anth-Azide-2, respectively displaying the high efficiency. The $M_{n,NMR}$ values for the both graft copolymers were calculated to be 16000 and 23000, respectively using a formula:

$$M_{n,NMR} = M_{n,GPC,PS\text{-}Anth\text{-}Azide} + (N_{Anth} \text{ X } M_{n,NMR,PMMA} + N_{Azide} \text{ X } M_{n,NMR,\,PEG}) \text{ X } CR_{eff}.$$

Table 4.2 summarizes the molecular weight datas of heterograft copolymers.

Table 4.2 : Characteristic molecular weight data of heterograft copolymers

Sample	$M_{n,GPC}$[c]	M_w/M_n[c]	$M_{n,NMR}$[d]
PS-*g*-(PMMA-PEG)-1[a]	13500	1.17	16000
PS-*g*-(PMMA-PEG)-2[b]	16200	1.15	23000

[a] Obtained from PS-Anth-Azide-1. [b] Obtained from PS-Anth-Azide-2.
[c] Determined by conventional GPC (RI detection) relative to linear PS standards.
[d] Determined by ^{1}H NMR (see text).

GPC traces of PS-*g*-(PMMA-PEG) heterograft copolymers showed monomodal peak. Moreover, no additional peak was detected at lower retention time related to PS backbone polymer displaying the successful grafting of PMMA and PEG chains to the PS backbone (Figures 4.6 and 4.7). Heterograft copolymers were obtained with M_n of 13500 and 16200 respectively and low polydispersity indices of 1.17 and 1.15 respectively relative to PS standards (Table 4.2).

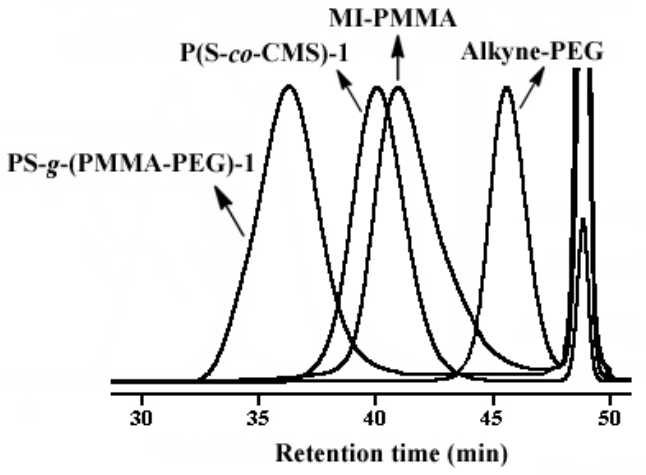

Figure 4.6 : Evolution of GPC traces of Alkyne-PEG, MI-PMMA and P(S-co-CMS)-1 precursors and target PS-*g*-(PMMA-PEG)-1 heterograft copolymer.

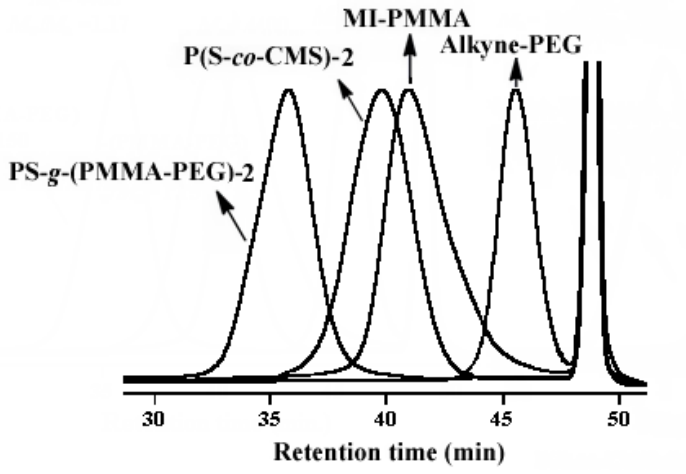

Figure 4.7 : Evolution of GPC traces of Alkyne-PEG, MI-PMMA and P(S-*co*-CMS)-2 precursors and target PS-*g*-(PMMA-PEG)-2 heterograft copolymer.

4.2. Synthesis of 3-Arm Star Block Copolymers via CuAAC and Diels-Alder Click Reactions

In this work, 3-arm star block copolymers; (PS-*b*-PMMA)$_3$ and (PS-*b*-PEG)$_3$ were successfully prepared by a coupling procedure using double "click" reactions (CuAAC and Diels-Alder) in one-pot process.

For this purpose, linear PS, PMMA and PEG polymers with well-defined chain length and end group functionalities were synthesized by ATRP of related monomers, except commercially available PEG. Thereafter, these polymers were quantitatively coupled together as pairs of PS/PMMA and PS/PEG with a trifunctional linking agent (core) using double "click" reactions (CuAAC and Diels-Alder) to construct 3-arm star block copolymers in one-pot process.

To confirm the efficiency of double click reactions in a one pot prosess, a model reaction had been studied prior to the syntheses of 3-arm star block copolymers. In this respect, first trisalkynyl-functional linking agent **4** (core) also used in the synthesis of 3-arm star block copolymers was prepared via an etherification reaction between 1,1,1-tris(4-hydroxyphenyl)ethane and propargyl bromide (Scheme 4.8).

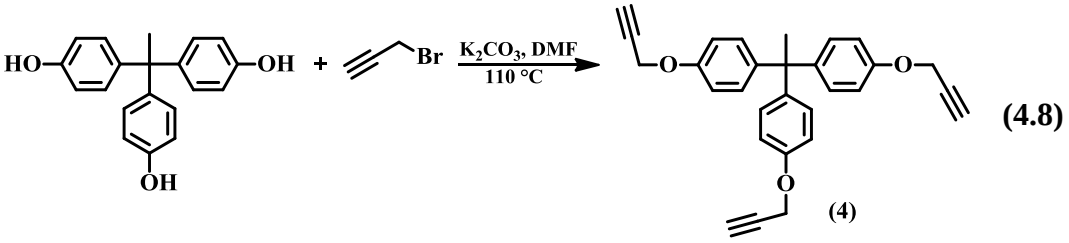

(4.8)

In the ^{1}H NMR spectrum of **4**, it was evident that CH_2 protons of propargyl bromide at 3.86 shifted to 4.66 ppm as a doublet signal of CH_2O indicating a successful etherification reaction. Alternatively, integrals of remaining protons were consistent with each other affording a successful etherification (Figure 4.8).

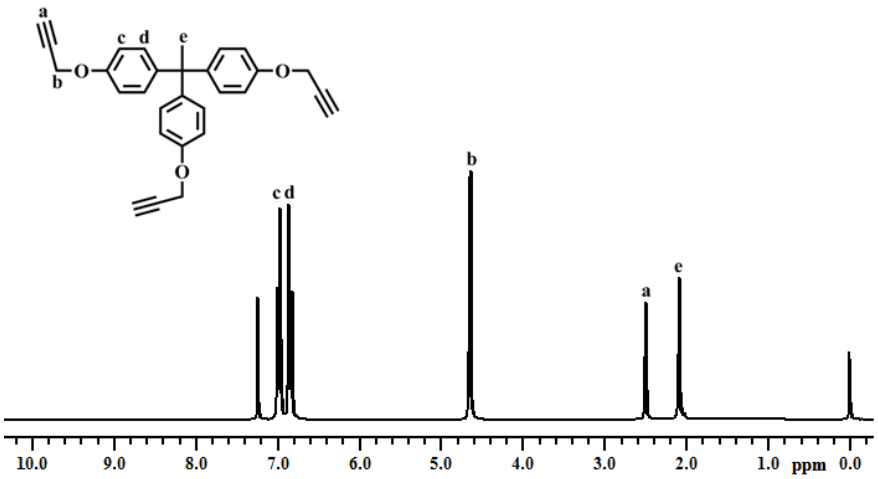

Figure 4.8 : ^{1}H NMR spectrum of **4** in $CDCl_3$.

Additionly, the second component of the model reaction was prepared in three steps. In this case, 9-anthracene methanol was used as a starting meterial. The hydoxyl functionality was converted to carboxylic acid via a reaction with succinic anhydride in the presence of Et_3N/DMAP catalyst system and CH_2Cl_2 as solvent to give **5** (Scheme 4.9).

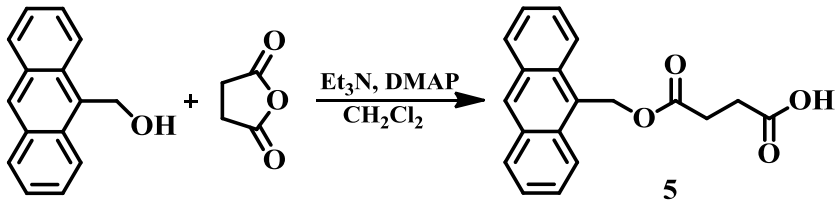

5 **(4.9)**

The structure was confirmed by ^{1}H NMR spectrum (Figure 4.9, (b)). A shift from 5.6 ppm to 6.18 ppm of methylene protons linked to anthracene ring due to esterification reaction and multiplet peaks around 2.69-2.62 ppm asigned to C=OCH_2CH_2C=O clearly indicated that **5** was achieved.

On the other hand, 3-azido propanol (**6**) was obtained quantitatively via simple substitution reaction using bromo propanol and NaN_3 in the presence of acetone/water mixture (Scheme 4.10).

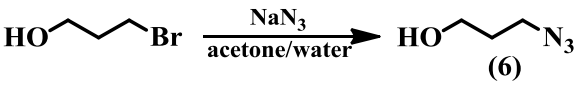

(6) **(4.10)**

It was observed from ^{1}H NMR spectrum of **6**, a signal related to methylene protons next to -Br at 4.52 ppm completely disappeared and a new signal linked to -N_3 was observed at 3.44 ppm (Figure 4.9, (a)).

The second component (**7**) of the model compound comprising both azide and anthracene unit was carried out through an esterification reaction between **5** and **6** (Scheme 4.11).

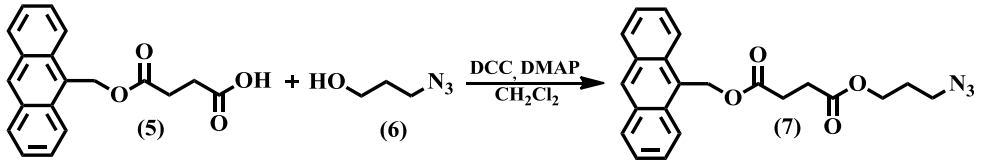

(4.11)

^{1}H NMR spectrum of **7** indicated the successful reaction (Figure 4.9, (**c**)). The methylene protons adjacent to the anthracene and ester were detected as singlet at 6.2 ppm and triplet at 4.1 ppm confirmed that the reaction was successfully carried out.

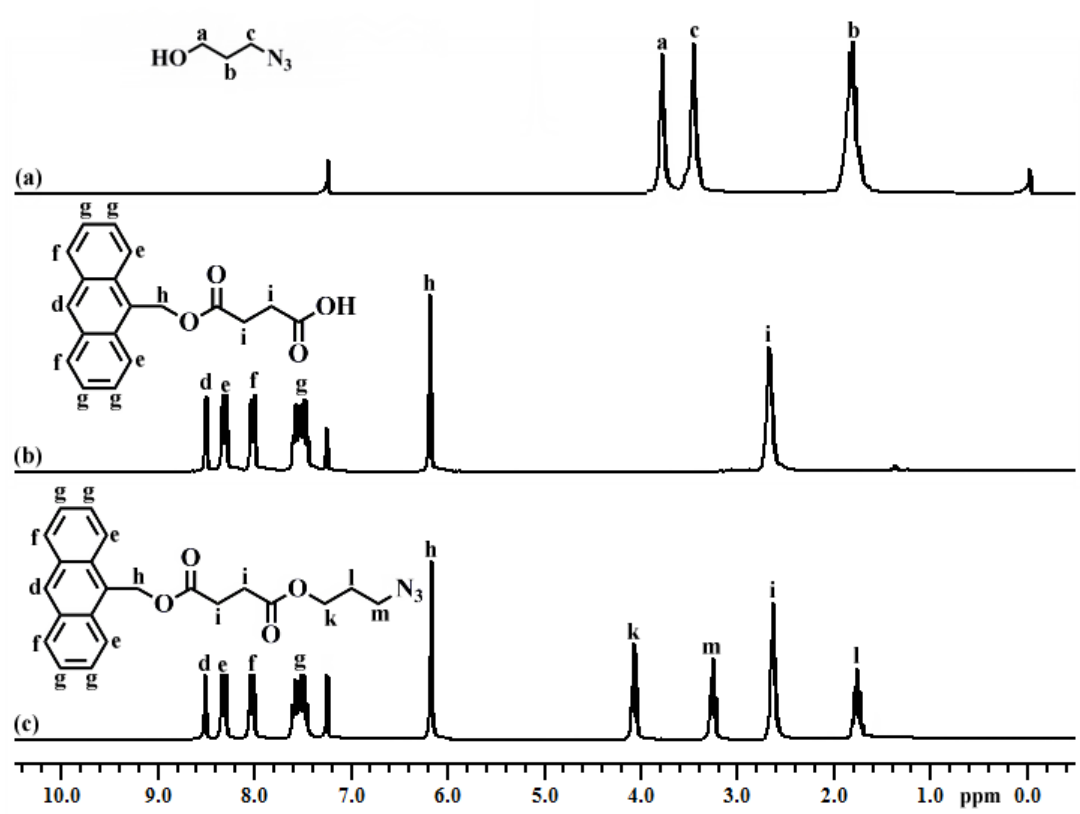

Figure 4.9 : Comparison of the ^{1}H NMR spectra of a) azido prapanol (**6**), b) succinic acid mono-anthracen-9-ylmethyl-ester (**5**), and c) anthracen-9-yl methyl 3-azidopropyl succinate (**7**) in $CDCl_3$.

Thereafter, the model reaction of **4** and **7** with **2** was carried out in the presence of CuBr/PMDETA in DMF at 120 ºC for 48 h using CuAAC and Diels-Alder click reactions in one-pot process (Scheme 4.12).

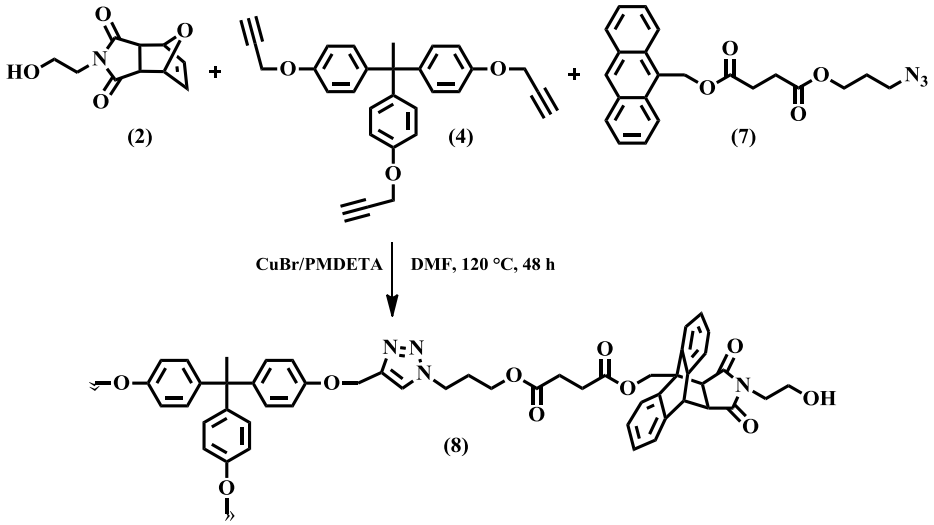

(4.12)

The model compound **8** was simply purified by precipitation in diethyl ether and its structure was identified by ^{1}H and ^{13}C NMR spectroscopy. The characteristic signals related with triazole and anthracene-maleimide cycloadducts can be detected at 7.75 (C*H* of triazole), 5.49 (CH_2-anthracene-maleimide cycloadduct), 4.77 (C*H*, bridge-head proton) and 4.45 (CH_2-triazole) (Figure 4.10). The confirmed structure of **8** proves double click reactions to have a potential in the preparation of star-block copolymers.

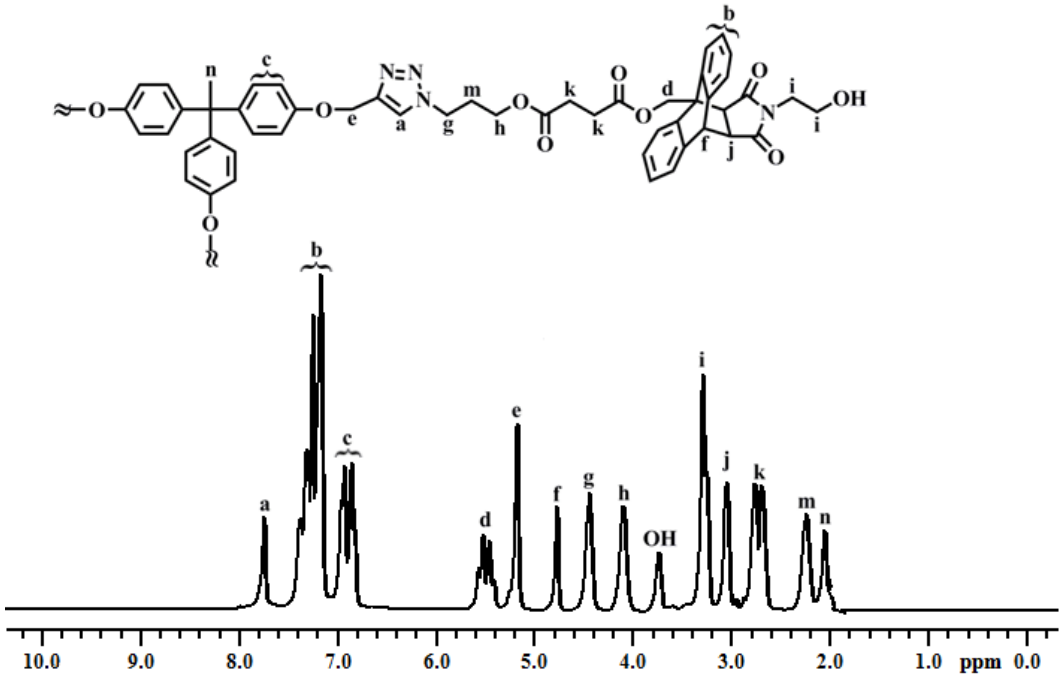

Figure 4.10 : ^{1}H NMR of the model compound (**8**) obtained from double click reactions in $CDCl_3$.

The one-pot double "click" reaction was further confirmed by FT-IR spectroscopy. From Figure 4.11, we can observe the complete disappearance of characteristic azide absorbance peak at 2100 cm^{-1} for **8**, as compared to that of **7**. Moreover, the relative intensity of the absorbance peak at 3310 cm^{-1} characteristic of terminal alkyne groups of **4** also disappeared. This further confirmed that the "click" reactions were complete.

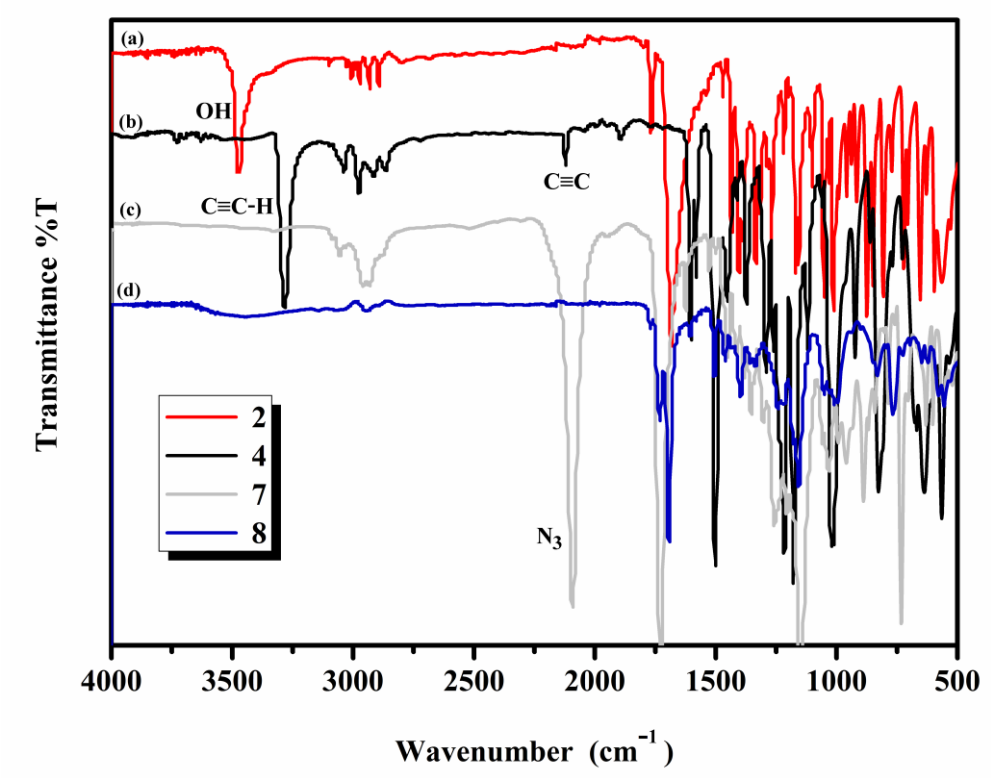

Figure 4.11 : FT-IR spectra of 2 (a), 4 (b), 7 (c) and model compound 8 (d).

After succesful preparation of this model compound via CuACC and Diels-Alder click reactions in one-pot process, the precursors of 3-arm star block copolymers were prepared.

For this purpose, 9-anthrylmethyl 2-bromo-2-methyl propanoate (**9)** was first synthesized as an ATRP initiator via an esterification reaction between 9-anthracene methanol and 2-bromoisobutryl bromide in THF at room temperature (Scheme 4.13).

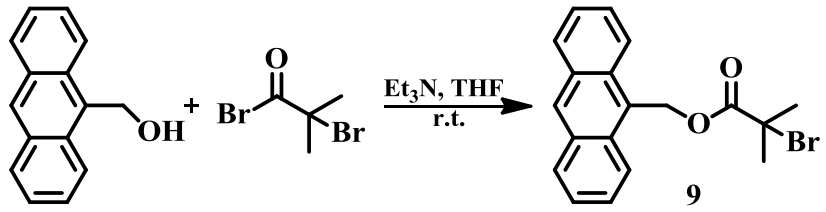

(4.13)

This compound, **9** was characterized by ^{1}H NMR. Along with anthracene protons between 8.51 and 7.45 ppm, from ^{1}H NMR spectrum (Figure 4.12), methylene protons adjacent to the anthracene and methyl protons next to Br were detected at 6.21 and 1.86 ppm, respectively. These results confirmed the structure of **9**.

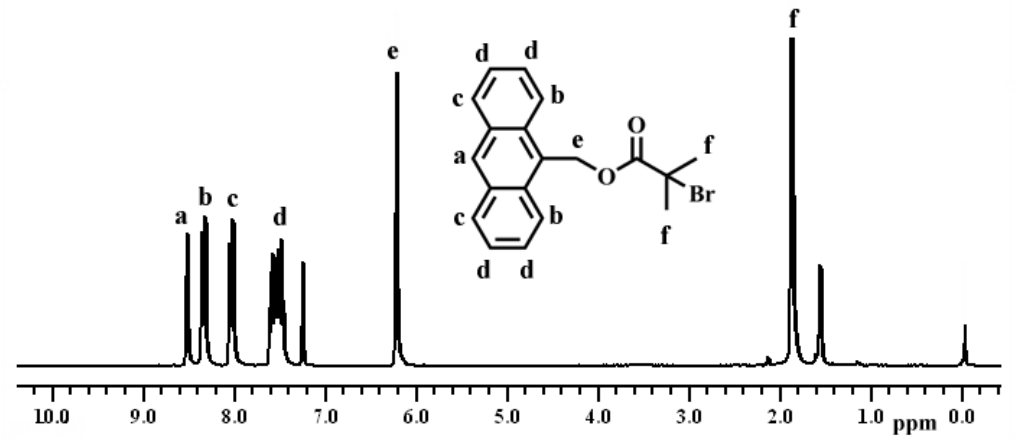

Figure 4.12 : ^{1}H NMR spectrum of 9-anthyrylmethyl 2-bromo-2-methyl propanoate (9) in $CDCl_3$.

After that, α-anthracene-ω-bromo-terminated polystyrene (Anth-PS-Br) as an inner precursor of star block copolymers was prepared by ATRP of St using **9** as initiator and CuBr/ PMDETA as catalyst at 110 °C (Scheme 4.14). The molecular weight and conditions employed for the preparation of Anth-PS-Br as well as the other linear precursors of 3-arm star block copolymers are presented in Table 4.3.

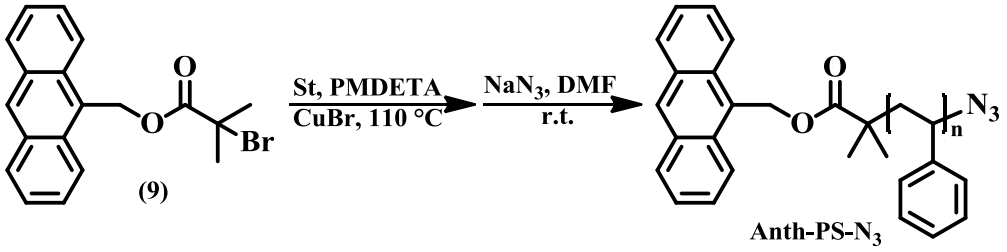

(4.14)

The $M_{n,theo}$ (4900 g/mol) value is in excellent agreement with that obtained by GPC ($M_{n,GPC}$ = 5200 g/mol relative to PS standards), and the PDI is low (M_w/M_n =1.12). Moreover, The NMR number–average molecular weight ($M_{n,NMR}$ = 6000 g/mol) of this polymer was calculated by comparing the integrations of the signals

corresponding to the aromatic protons of styrene present on each repeating unit at 6.5–7.5 ppm and that of five protons of anthracene end-group in the range of 8.4–7.9 ppm and end-group proton of PS (4.4), while being included MW of **9** (357 g/mol).

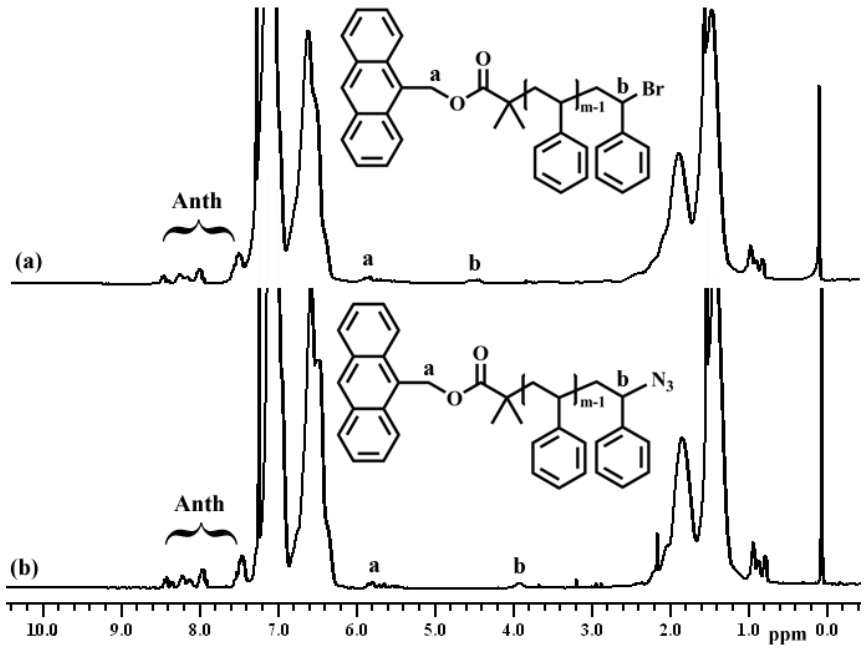

Figure 4.13 : ^{1}H NMR spectra of PS-α-anthracene-ω-bromide (Anth-PS-Br) (a) and PS-α-anthracene-ω-azide (Anth-PS-N_3) (b) in $CDCl_3$.

Furthermore, the molecular weight of Anth-PS-Br homopolymer ($M_{n,UV}$ = 5400) was calculated by employing UV-spectroscopy assuming that the molar extinction coefficient (ε=9451 L mol^{-1} cm^{-1} at 368 nm in CH_2Cl_2) of anthryl end group in the obtained polymer was the same as that of 9-anthrylmethyl 2-bromo-2-methyl propanoate, **9**, and showed good agreement with those aforementioned results.

This precursor was subsequently reacted with NaN_3 in DMF to yield the desired α-anthracene-ω-azide functional PS (Anth-PS-N_3). Qantitative transformation of ω-bromo moieties into azido moieties was detected by ^{1}H NMR in terms of observing a clear shift from 4.4 (CH-Br) to 3.9 ppm (CH-N_3) (Figure 4.13). Moreover from FT-IR spectrum the appearance of a strong absorbance at 2094 cm^{-1} was observed as a characteristic of azide streching band. Moreover, there is no change in the $M_{n,GPC}$ and polydispersity values during this transformation process (Table 4.3).

One of the outer precursors of star block copolymers, MI-PMMA, was prepared in a similar way as described in the synthesis of hetero graft copolymer (Scheme 4.2). At the end of the polymerization, chloride end-functionality of MI-PMMA was removed by similarly reacting with Bu_3SnH in order to avoid the probability of the radical

formation caused by CuBr/PMDETA in a one-pot preparation of star block copolymer. The experimental conditions and results are given in Table 4.3. $M_{n,NMR}$ was consistent with that obtained from GPC and however, higher than that from the $M_{n,theo}$. It is due to low initiation efficiency of **3** under this polymerization condition.

In order to obtain the other outer precursors of star block copolymers, MI-PEG was synthesized in two steps.

In this case, **2** was used as a starting meterial (Scheme 4.15). The hydoxyl functionality of **2** was converted to the carboxylic acid via a reaction with succinic anhydride in the presence of Et_3N/DMAP catalyst system and 1,4-dioxane as solvent in order to give **10** (Scheme 4.15).

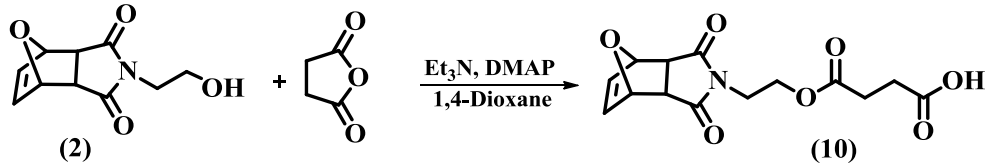

(4.15)

From ^{1}H NMR spectrum (Figure 4.14) of **10**, methylene protons next to the ester ($NCH_2CH_2OC{=}O$) and methylene protons adjacent to nitrogen ($NCH_2CH_2OC{=}O$) appeared at 4.25 ppm and 3.74 ppm respectively. Moreover, the multiplet signals around 2.66-2.53 ppm confirmed a successful conversion of the hydroxyl group to the carboxylic acid.

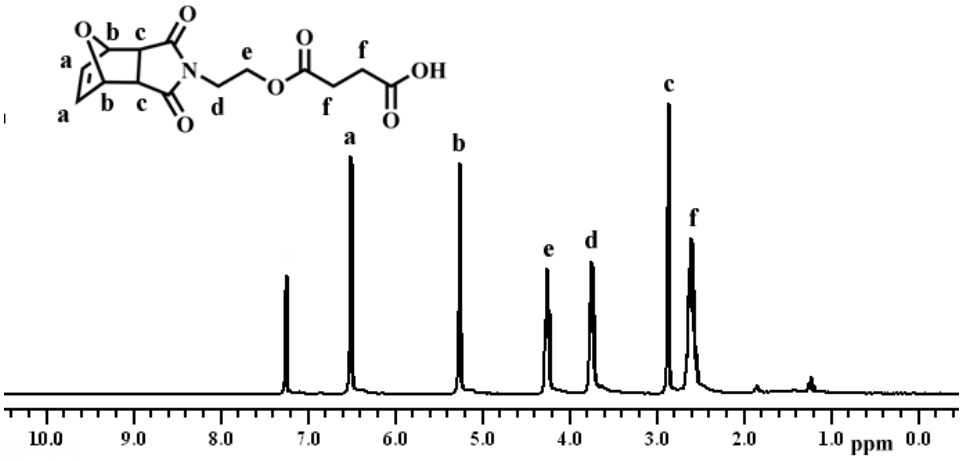

Figure 4.14 : ^{1}H NMR spectrum of 4-(2-[(3-acetyl-7-oxabicyclo[2.2.1]hept-yl)carbonyl]amino ethoxy)-4-oxobutanoic acid (**10**) in $CDCl_3$.

Then, the commercially available PEG-OH (M_n = 2000 g/mol) was reacted with **10** affording MI-PEG (Scheme 4.16).

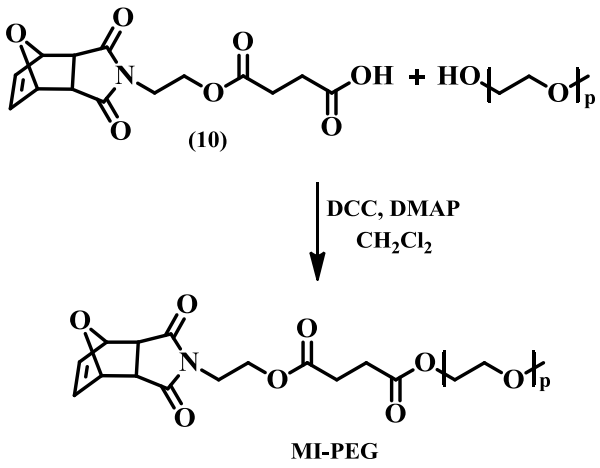

(4.16)

The structure of the desired MI-PEG could be fully identified by ^{1}H NMR (Figure 4.15). The characteristic protons of MI-PEG, such as vinyl (C*H*=C*H*), bridge-head (C*H*CH=CHC*H*), repeating unit of PEG (OCH_2CH_2) and bridge $CH_2N(C=O)CH$-*CH*) were assigned at 6.5, 5.2, 3.5-3.9 and 2.8 ppm, respectively. The $M_{n,NMR}$ was determined by comparing the integral of vinyl end group signal (δ 6.5) to those of repeating unit of PEG and N-CH_2 (δ 3.9-3.5), while including the MW of **10**. $M_{n,NMR}$ fit well with the $M_{n,theo}$ indicating a quantitative maleimide end-group functionalization (Table 4. 3).

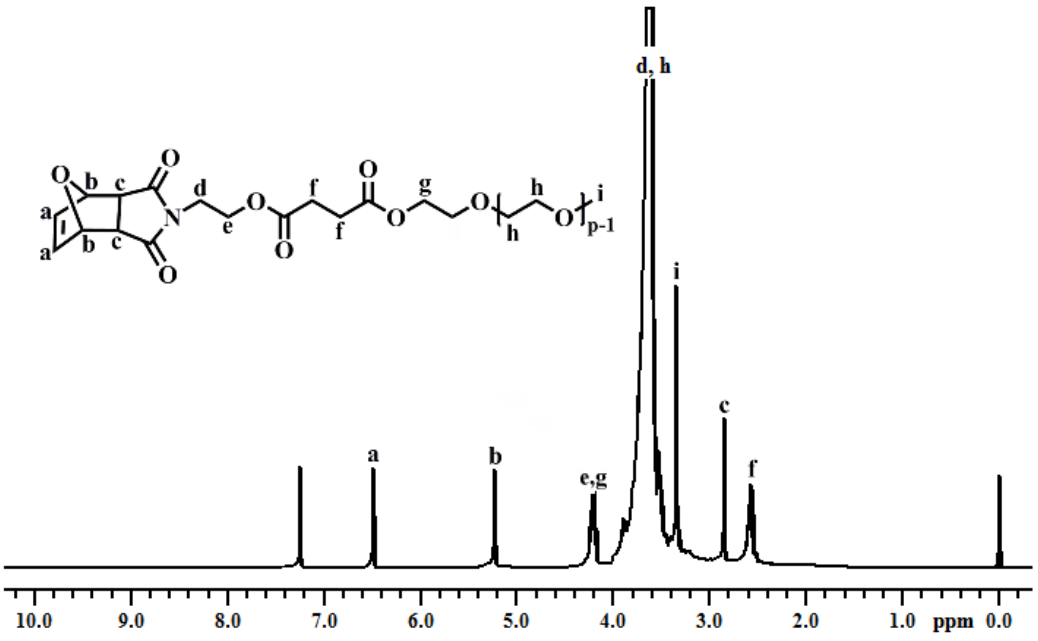

Figure 4.15 : ^{1}H NMR spectrum of the MI-PEG in $CDCl_3$.

Table 4. 3 summarizes the experimental conditions and results of the linear polymers used for the synthesis of 3-arm star block copolymers.

Table 4.3 : The conditions and results of linear polymers used in the synthesis of 3-arm star block copolymers.

Polymer	Time (min)	Conv.[d] (%)	$M_{n,GPC}$[e] (g/mol)	M_w/M_n[e]	$M_{n,theo}$ (g/mol)	$M_{n,NMR}$ (g/mol)
Anth-PS-N_3[a]	40	22	5300	1.11	4900[f]	6000
MI-PMMA[b]	210	19	2500	1.19	1350[f]	2600
MI-PEG[c]	-	-	3200	1.03	2300[g]	2800

[a] $[M]_0:[I]_0:[CuBr]:[PMDETA]$ = 200:1:1:1; polymerization was carried out at 110 °C. Then NaN_3 in DMF stirred at room temperature for overnight.
[b] $[M]_0:[I]_0:[CuCl]:[PMDETA]$ = 50:1:1:1; polymerization was carried out at 40 °C. MMA/toluene = 1/1 (v/v).
[c] Obtained by an esterification reaction between compound PEG-OH (2000) and **10**.
[d] Determined by gravimetrically.
[e] Determined by using conventional GPC (RI detection) in THF at 30 ºC relative to PS standards except MI-PMMA relative to PMMA standards.
[f] $M_{n,theo}$ = ($[M]_0/[I]_0$) X conversion % X MW of monomer + MW of initiator.
[g] $M_{n,theo}$ = M_n of PEG-OH (2000) + MW of **10**.

In the following, Anth-PS-N_3 and MI-PMMA or MI-PEG were reacted with a trialkyne-functional linking agent **4** (core) using a one-pot technique to yield two samples of 3-arm star block copolymers in the presence of CuBr/PMDETA in DMF at 120 ºC for 48 h as illustrated in Scheme 4.17.

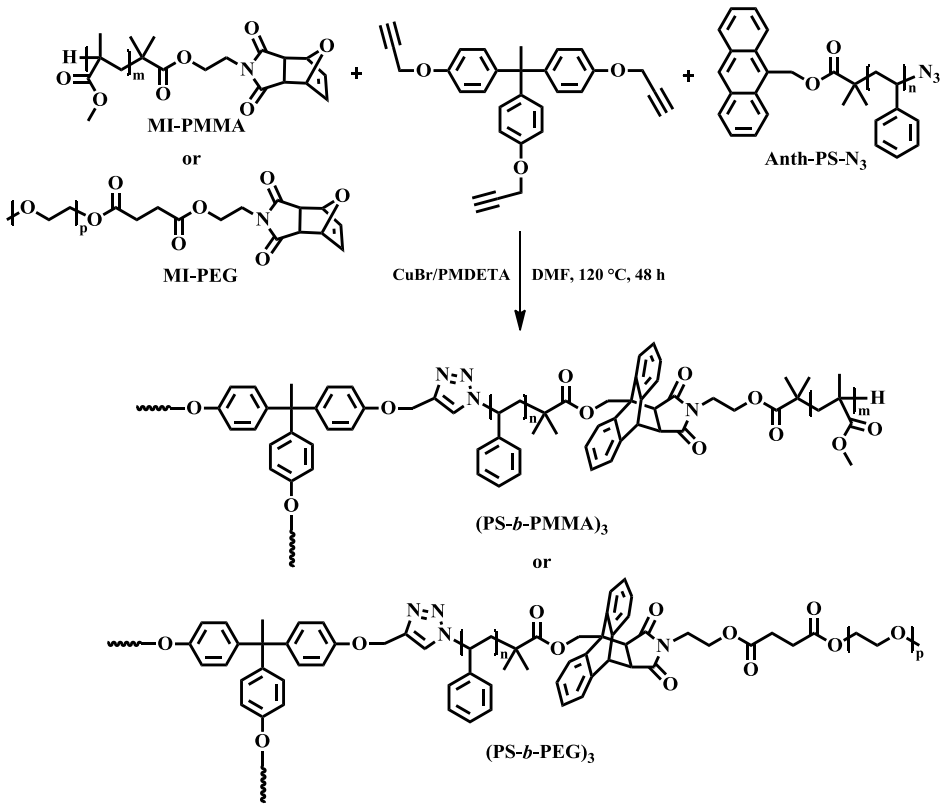

(4.17)

A molar excess of PS and PMMA or PEG was used with respect to the linking agent **4** (core). Moreover, a molar ratio of PMMA or PEG block (outer) to the PS (inner) was intentionally taken to be 1.2 due to solubility of the former in precipitation solvent methanol.

(PS-*b*-PMMA)$_3$ as a first example of star-block copolymers is simply prepared by a one-pot reaction of Anth-PS-N$_3$, MI-PMMA with a linking agent **4** exploiting the double click reactions: CuAAC and Diels-Alder.

^{1}H NMR spectrum of the obtained (PS-*b*-PMMA)$_3$ star-block copolymer clearly indicated the successful double click reactions that anthracene signals (δ 8.5-7.5) disappeared and new signals for the corresponding anthracene-maleimide cycloadduct appeared (δ 4.7 and 3.2 for a bridge-head proton and bridge protons, respectively) (Figure 4.16).

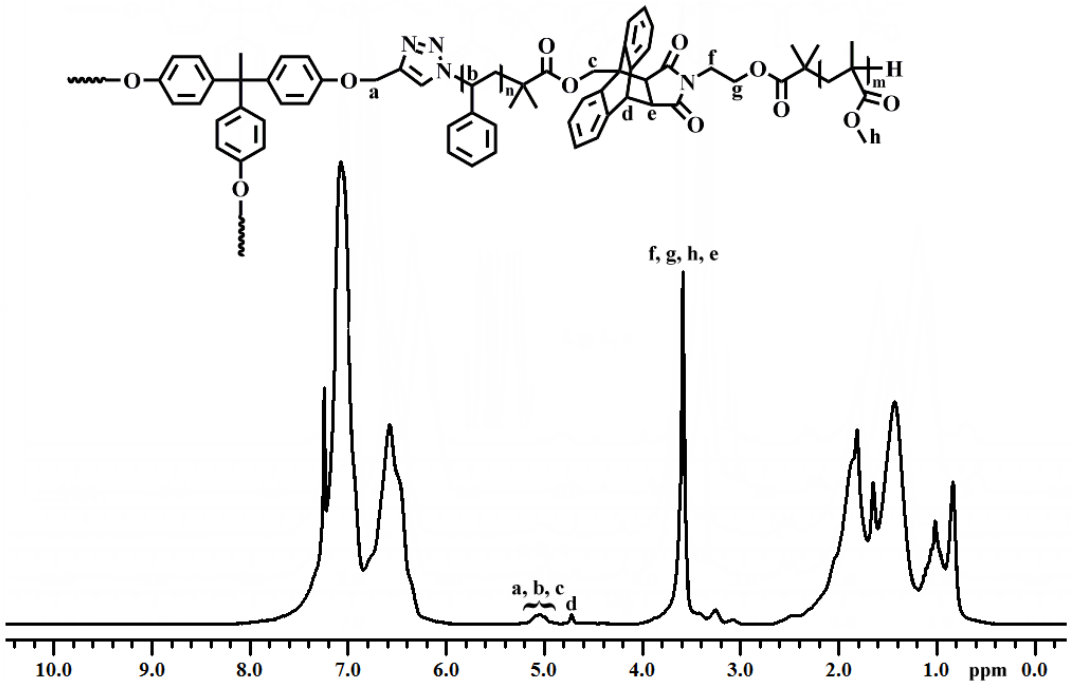

Figure 4.16 : ^{1}H NMR spectrum of the observed (PS-*b*-PMMA)$_3$ star-block copolymer in $CDCl_3$.

Figure 4.17 (a) shows the evolution of GPC traces of (PS-*b*-PMMA)$_3$ star-block copolymer, Anth-PS-N$_3$, and MI-PMMA. A shift for star block copolymer is clearly observed with respect to those of precursors.

However, since the GPC trace contains various shoulders to the higher retention time region, it is possible to deconvolute the GPC trace via peak splitting. The peak splitting technique allows the obtained GPC trace of the various reaction products to

be split into its constituent traces. For example, the obtained GPC trace for the (PS-*b*-PMMA)$_3$ represents the sum of the GPC traces of the target 3-arm star block (PS-*b*-PMMA)$_3$ and (PS-*b*-PMMA)$_2$ copolymers and linear PS-*b*-PMMA copolymer. The result of the peak splitting using a Gaussian deconvolution of the obtained GPC trace of (PS-*b*-PMMA)$_3$ displays that the area percentage ratios of 3-arm star-block (PS-*b*-PMMA)$_3$, (PS-*b*-PMMA)$_2$ and linear PS-*b*-PMMA copolymer were 88%, 8% and 4% (Figure 4.17, (b)).

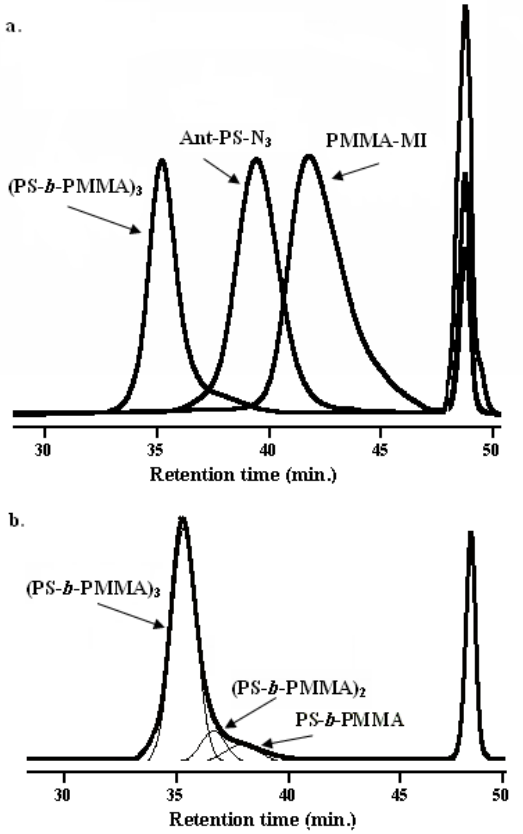

Figure 4.17 : a) Evolution of GPC traces of the obtained 3-arm star block copolymer (PS-*b*-PMMA)$_3$, Anth-PS-N$_3$ and MI-PMMA using RI detection in THF at 30 ºC; b) Deconvolution of GPC trace of the observed (PS-*b*-PMMA)$_3$ star-block copolymer via peak splitting.

(PS-*b*-PEG)$_3$ as a second sample of star-block copolymer was also characterized by conventional and triple detection ^{1}H NMR spectroscopy and GPC measurements.

Figure 4. 18 shows the ^{1}H NMR spectrum of the (PS-*b*-PEG)$_3$ star block copolymer. The disappearance of anthracene aromatic protons in the range of 8.5 to 7.5 and the appearance of bridge-head proton of anthracene-maleimide cycloadduct at 4.7 ppm are detected confirming the occurrence of double click reactions.

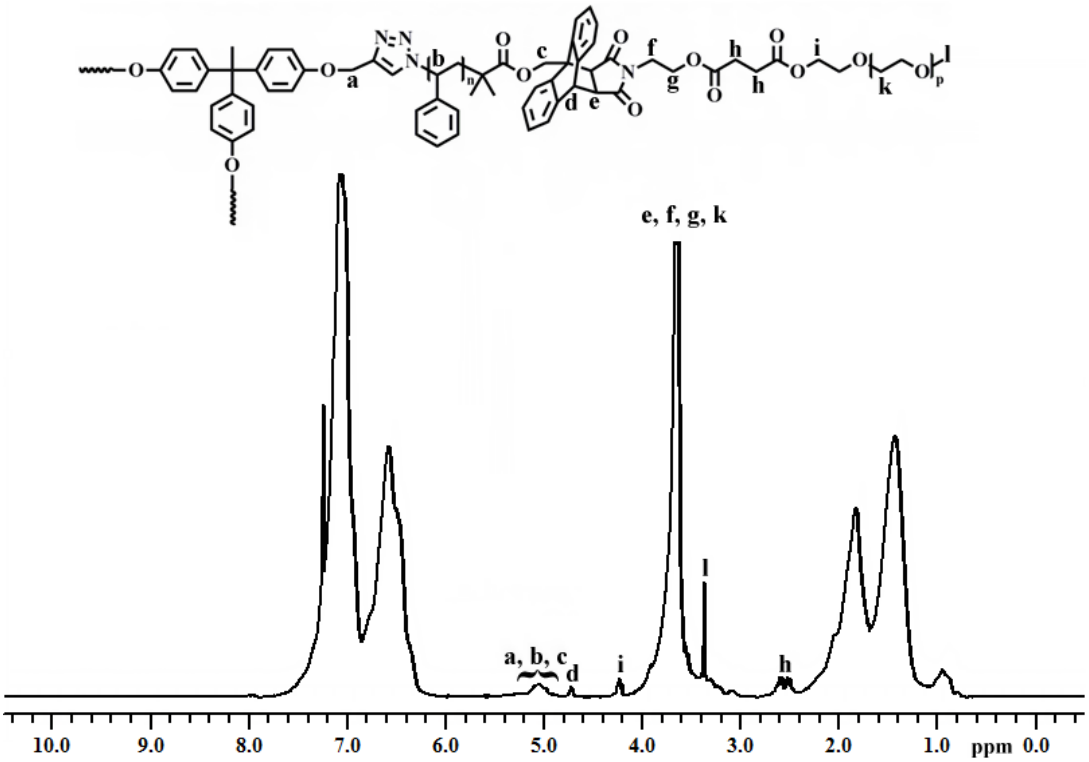

Figure 4.18 : ^{1}H NMR spectrum of the obtained (PS-*b*-PEG)$_3$ star-block copolymer in $CDCl_3$.

Figure 4.19 (a) displays the GPC traces of the obtained 3-arm star block and its precursors (Anth-PS-N_3 and MI-PEG). It is clear to detect a shift in the GPC trace of the observed 3-arm star block copolymer to lower retention times. Additionally, any GPC traces are not observed fitting the retention times of precursors.

The GPC trace of the obtained 3-arm star block copolymer is comprised of (PS-*b*-PEG)$_3$ 3-arm star-block copolymer, (PS-*b*-PEG)$_2$ copolymer and PS-*b*-PEG copolymer. Similar peak splitting analyses were performed on that GPC trace (Figure 4.19, (b)). The area percentage ratios of 3-arm star block polymer, (PS-*b*-PEG)$_2$ and PS-*b*-PEG were 82%, 9% and 9%, respectively, according to the multipeak splitting using a Gaussian function indicating that double click reactions have occurred efficiently resulting in the star-block copolymer formation.

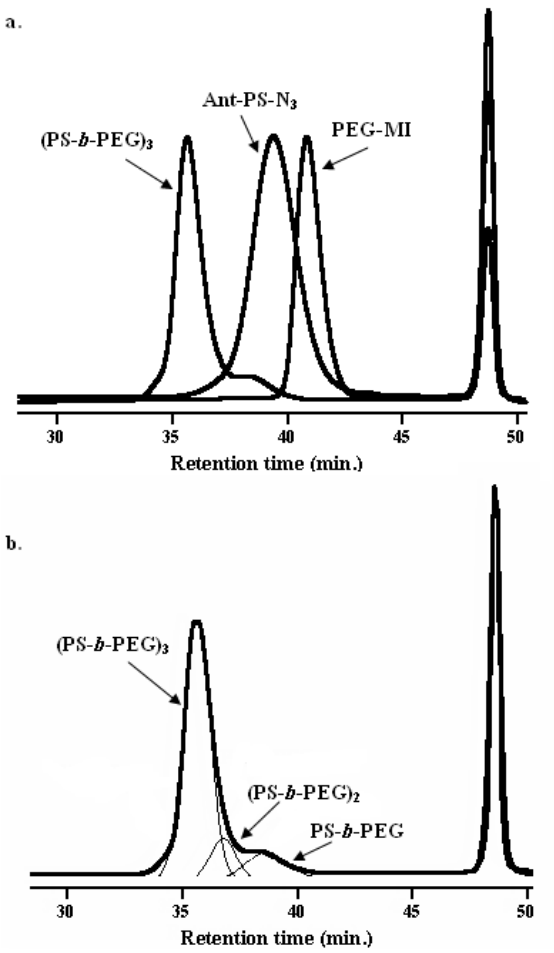

Figure 4.19 : a) Evolution of GPC traces of the obtained 3-arm star block copolymer (PS-*b*-PEG)$_3$, Anth-PS-N_3 and MI-PEG using RI detection in THF at 30 ºC; b) Deconvolution of GPC trace of the observed (PS-*b*-PEG)$_3$ star-block copolymer via peak splitting.

It is noteworthy that star polymer have more compact structure than linear polymer of equivalent molecular weight and composition resulting in smaller hydrodynamic volume, for this reason, the absolute molecular weight of the polymer was also analyzed by a second GPC (Viscotek TDA 302 triple detector) system. Essentially, refractive index (RI), light scattering (LS) and differential viscometer detectors in TD-GPC instrument provides more advanced and accurate technique to measure the absolute molecular weight of star polymer, if refractive index increment (d*n*/dc) value of the analyzed polymer is known.

In order to determine the absolute molecular weight of the 3-arm star block copolymers, firstly the d*n*/dc value of the linear precursors of PS, PMMA and PEG were measured by TD-GPC instrument and found to be 0.185 mL/g, 0.076 mL/g and 0.078 mL/g, respectively. Meanwhile, it was shown that d*n*/dc value correlates linearly with composition of block copolymer in Eq. 4.1, given in literature [215].

$(dn/dc)_{block\ copolymer} = x\ (dn/dc)_{PS} + y\ (dn/dc)_{PMMA\ /or\ PEG}$ (**Eq. 4.1**)

Where x and y are the weight fractions (*w)* of PS and PMMA /or PEG blocks from ^{1}H NMR according to the backbone protons. The weight fractions of the PS and PMMA/or PEG blocks in the (PS-*b*-PMMA)$_3$ and (PS-*b*-PEG)$_3$ star block copolymers were determined to be 0.78 and 0.22, respectively. Using Eq. 4.1, d*n*/dc values are derived to have 0.160 and 0.161 mL/g for (PS-*b*-PMMA)$_3$ and (PS-*b*-PEG)$_3$ star block copolymers respectively. Then, the absolute molecular weights of the 3-arm star block copolymers are obtained from TD-GPC instrument introducing the above d*n*/dc values into Omnisec software. Table 4.4 summarizes data obtained from both conventional GPC and TD-GPC.

Table 4.4 : GPC characterization of 3-arm star block copolymers

3-arm star block copolymer	$M_{n,theo}$ [a]	$M_{n,GPC}$ [b]	M_w/M_n [b]	$M_{n,TD\text{-}GPC}$ [c]	M_w/M_n [c]
(PS-*b*-PMMA)$_3$	26200	16500	1.11	23200	1.06
(PS-*b*-PEG)$_3$	26800	14000	1.09	24300	1.06

[a] $M_{n,theo}$ = (sum of $M_{n,NMR}$ of precursors) x 3 + MW of **4**.
[b] Calculated from conventional GPC (RI detection) using linear PS standarts in THF at 30 °C.
[c] Calculated from TD-GPC in THF at 35 °C.

A similar remark can also be given here for a comparison of $M_{n,theo}$, $M_{n,TD\text{-}GPC}$ and $M_{n,GPC}$. $M_{n,theo}$ value is close to the M_n from TD-GPC ($M_{n,TD\text{-}GPC}$), rather than that from conventional GPC ($M_{n,GPC}$), which is calculated using linear PS standards because of the differences in the hydrodynamic volume between star polymers and linear standards.

4.3. Synthesis of Multiarm Star Block and Multiarm Star Mixed-Block Copolymers via CuAAC Click Reaction

In this study, **(**P*t*BA)$_m$-(PS)$_n$-polyDVB, (P*EG*)$_k$-(PS)$_n$-polyDVB multiarm star block and (P*EG*)$_k$-(P*t*BA)$_m$-(PS)$_n$-polyDVB mixed-block copolymers were synthesized via a combination of ATRP and CuAAC reaction using the "arm first" methodology (Scheme 4.18).

In this respect, α-silyl protected alkyne PS (α-silyl-alkyne-PS) was prepared by ATRP of St and used as macroinitiator in a cross-linking reaction with DVB to yield

multiarm star homopolymer with alkyne periphery. Linear azide end-functionalized polymers including PEG-N_3 and P*t*BA-N_3 were simply clicked with the multiarm star polymer to form star block or mixed-block copolymers in DMF at room temperature for 24 h.

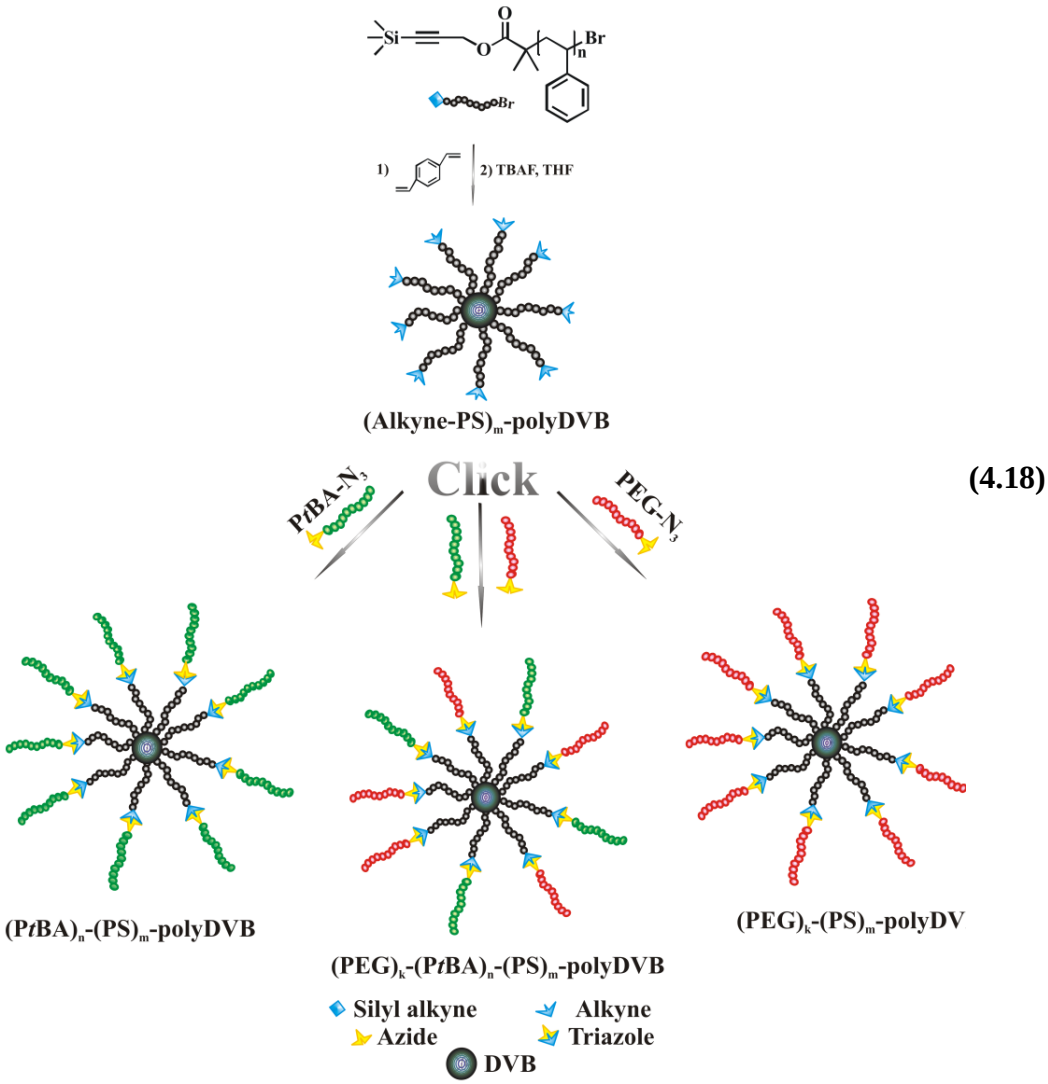

(4.18)

First, linear α-silyl protected alkyne functional initiator (**11**) was synthesized through an esterification reaction via a similar method as described before (Scheme 4.19).

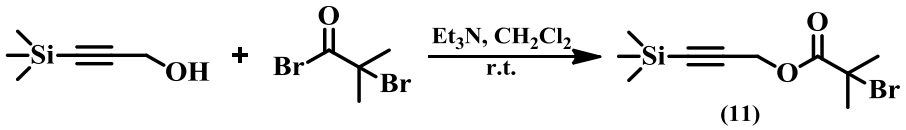

(4.19)

The ^{1}H NMR spectrum of **11** showed three singlets, methylene protons next to ester unit at 4.75 ppm, methyl protons next to Br at 1.96 ppm and methyl protons next to Si at 0.17 ppm (Figure 4.20).

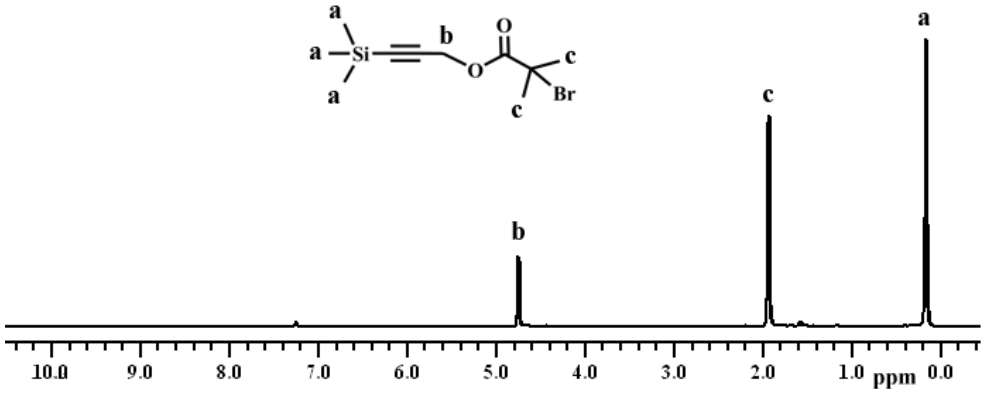

Figure 4.20 : ^{1}H NMR spectrum of 3-(1,1,1-trimethylsilyl)-2-propynyl 2-bromo-2-methylpropanoate (11) in $CDCl_3$.

Then, α-silyl protected alkyne terminated PS (α-silyl-alkyne-PS) was prepared from ATRP of St using **11** as an initiator. The silyl protection of prop-2-ynyl 2-bromo-2-methylpropanoate was carried out to prevent the radical polymerization of alkyne during ATRP of St at 110 ^{o}C (Scheme 4.20).

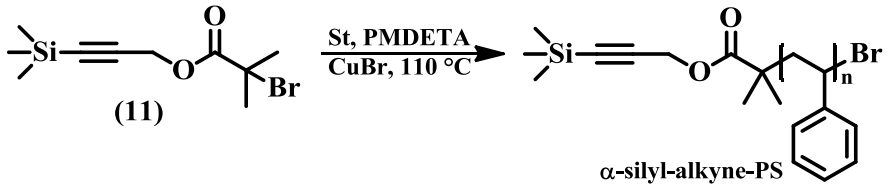

(4.20)

All polymerization conditions and results of the linear precursors used in the synthesis of multiarm star polymer, multiarm star block and multiarm star mixed-block copolymers were tabulated in Table 4.5.

DP_n of α-silyl-alkyne-PS was calculated to be 61.5 by comparing integration areas of signal at 7.5-6.5 (Ar*H* of PS) to that of (CH_3)$_3$Si- (α-end group of PS) at 0.17 ppm (Figure 4.21). Consequently, $M_{n,NMR}$ of α-silyl-alkyne-PS was calculated to be $M_{n,NMR}$= 61.5 X 104.1 + 278 (MW of **11**) = 6680 g/mol.

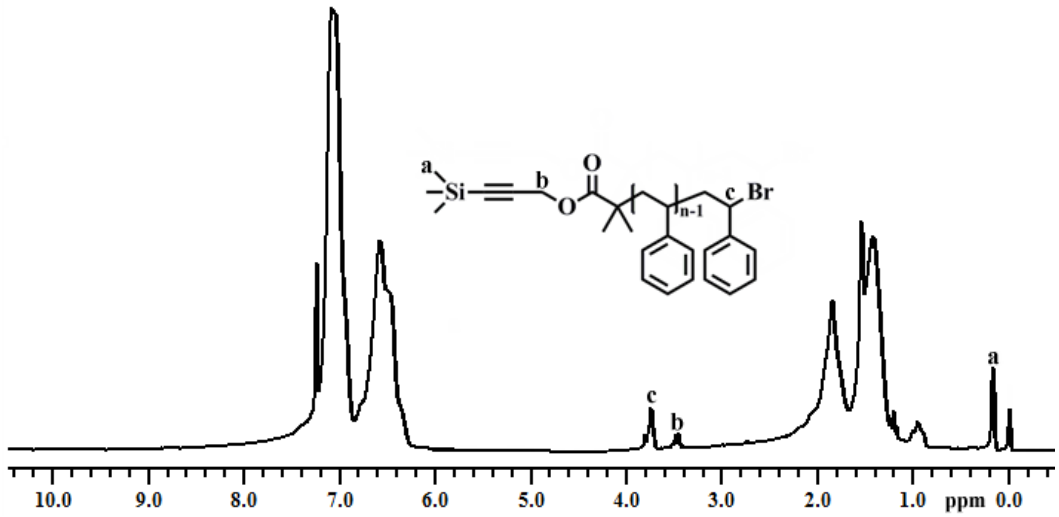

Figure 4.21 : ^{1}H NMR spectrum of α-silyl-alkyne-PS in $CDCl_3$.

On the other hand, the outer precursor of multiarm star block and multiarm star mixed-block copolymers, P*t*BA-N_3 was prepared in two steps (Scheme 4.21). First P*t*BA-Br was efficiently synthesized by ATRP of *t*BA using ethyl 2-bromoisobutyrate as initiator. DP_n and $M_{n,NMR}$ was calculated to be 33.5 and 4500 g/mol, respectively via an integration area ratio of CH_2OC=O and C*H*Br end groups at 4.1 ppm to that of C*H* on the P*t*BA backbone at 2.2 ppm. The results from NMR and GPC displayed that a successful living polymerization reaction occurred (Table 4.5). As a second step, the terminal Br functionality of linear P*t*BA-Br was then facilely converted to the azide moiety by reacting with NaN_3 in DMF at 50 ^{o}C in order to give P*t*BA-N_3.

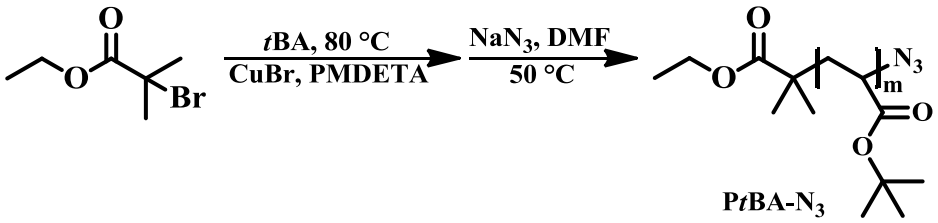

(4.21)

Azidation was clearly evidenced from ^{1}H NMR spectrum of P*t*BA-N_3 that a new signal corresponding to -C*H*N_3 at 3.7-3.6 ppm emerged (Figure 4.22). Moreover, it should be noted that azidation reaction did not resulted in a discrepancy in both $M_{n,NMR}$ and $M_{n,GPC}$ of P*t*BA.

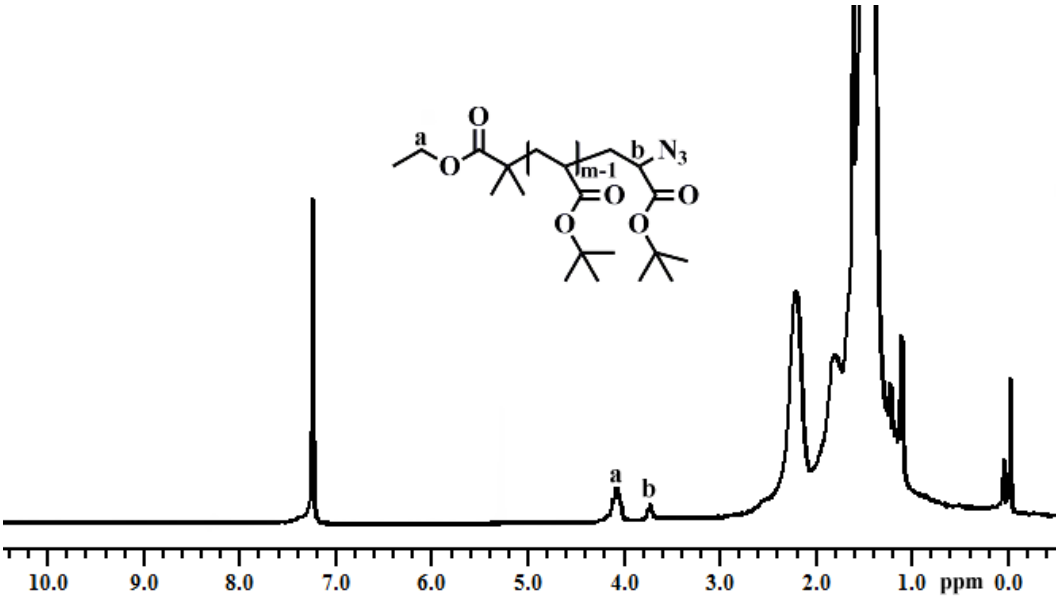

Figure 4.22 : ^{1}H NMR spectrum of P*t*BA-N_3 in $CDCl_3$.

Starting from PEG-OH, two esterification reaction steps are needed to produce PEG-N_3. First, PEG-COOH was achieved with a reaction of PEG-OH and succinic anhydride catalyzed by Et_3N/DMAP in CH_2Cl_2 (Scheme 4.22).

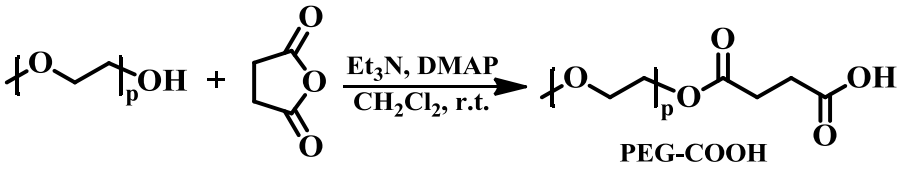

(4.22)

Meanwhile, a similar procedure as described before was applied to the synthesis of 2-azidoethanol (**12**). 2-azidoethanol (**12**) was obtained quantitatively via simple substitution reaction using bromo ethanol and NaN_3 in the presence of acetone/water mixture (Scheme 4.23).

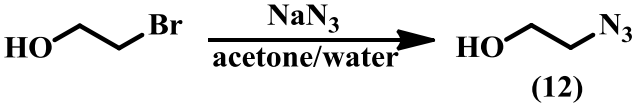

(4.23)

It was observed from ^{1}H NMR spectrum of **12**, a signal related to methylene protons next to Br atom at 4.52 ppm completely disappeared and a new peak linked to -N_3 was observed at 3.44 ppm. Additionaly, FT-IR spectrum of **12** revealed the presence of absorbance peak at 2100 cm^{-1}, which is characteristic of the terminal azide group. Second, esterification reaction between PEG-COOH and 2-azido ethanol afforded the synthesis of PEG-N_3 (Scheme 4.24).

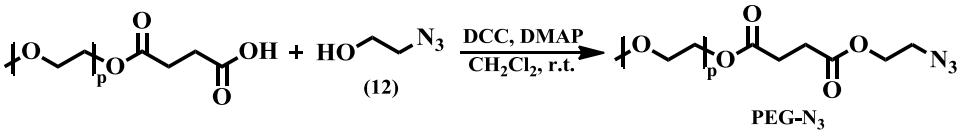

(4.24)

^{1}H NMR analysis confirmed the azido group introduction to the structure, displaying new signals corresponding to -CH_2N$_3$ appeared at 3.55-3.45 ppm (Figure 4.23). DP_n was calculated to be 10 from a ratio of terminal protons of PEG backbone (C=OCH_2CH_2C=O) (δ 2.67) to that of OCH_2CH_2O backbone (δ 3.70-3.55). $M_{n,NMR}$ was consequently determined to be 620 using an equation $M_{n,NMR}$ = 10 X 44 + MW of 2-azidoethanol and succinic anhydride.

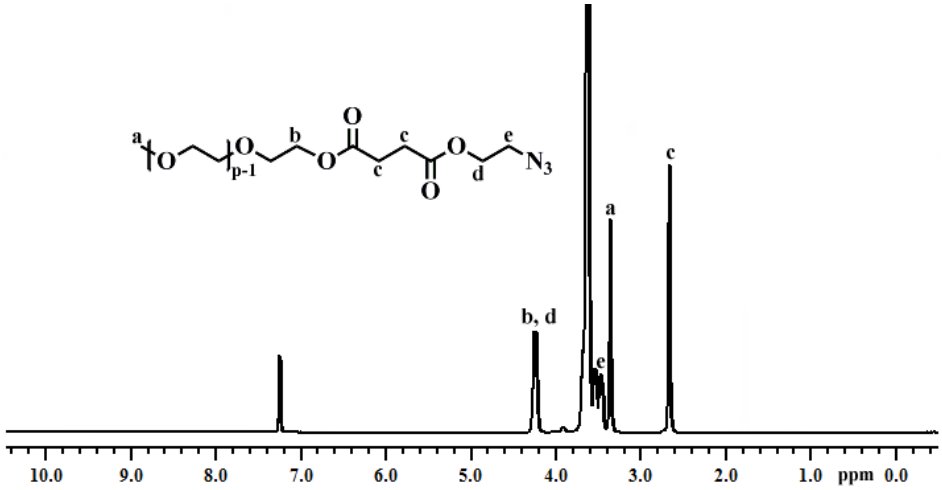

Figure 4.23 : ^{1}H NMR spectrum of PEG-N$_3$ in CDCl$_3$.

Table 4.5 : The conditions and results of linear polymers used in the synthesis of multiarm star polymer, multiarm star block and multiarm star mixed-block copolymers.

Polymer	Time (min)	Conv.[d] (%)	$M_{n,GPC}$[e] (g/mol)	M_w/M_n[e]	$M_{n,theo}$ (g/mol)	$M_{n,NMR}$ (g/mol)
α-silyl-alkyne-PS[a]	45	30	6800	1.07	6530[f]	6680
P*t*BA-N$_3$[b]	30	30	4050	1.10	4000[f]	4500
PEG-N$_3$[c]	-	-	480	1.05	720[g]	620

[a] $[M]_0$:$[I]_0$:[CuBr]:[PMDETA] = 200:1:1:1; polymerization was carried out at 110 °C.
[b] $[M]_0$:$[I]_0$:[CuBr]:[PMDETA] = 100:1:1:1; polymerization was carried out at 80 °C. *t*BA / EC = 10 (w/w). Then NaN_3 in DMF stirred at room temperature for overnight.
[c] Obtained by an esterification reaction between compound PEG-OH (550) and **12**.
[d] Determined by gravimetrically.
[e] Determined by using GPC in THF at 30 ºC relative to PS standards.
[f] $M_{n,theo}$ = ($[M]_0/[I]_0$) X conversion % X MW of monomer + MW of initiator.
[g] $M_{n,theo}$ = M_n of PEG-OH (550) + MW of **12**.

Thereafter, α-silyl-alkyne-PS was used as a macroinitiator DVB as cross-linker in ATRP condition at 110 ºC to give (α-silyl-alkyne-PS)$_n$-polyDVB multiarm star homopolymer (Scheme 4.25).

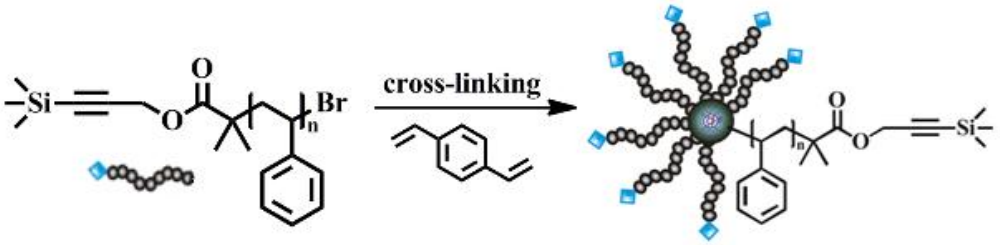

(4.25)

The progress of polymerization was followed by GC and GPC while taking samples at time intervals. We observed a peak originating from the α-silyl-alkyne-PS arms during the course of reaction process, where the peak gradually shifts toward higher molecular weight region and becomes monomodal as the polymerization proceeds, indicating that the molecular weight distribution becomes narrower. After 9 h, the reaction was stopped at 85% conversion and the reaction mixture was easily purified by two dissolution-precipitation cycles (THF-methanol/diethyl ether) to remove unreacted linear α-silyl-alkyne-PS. The relevant chromatograms and the purified multiarm star polymer are overlaid in Figure 4.24.

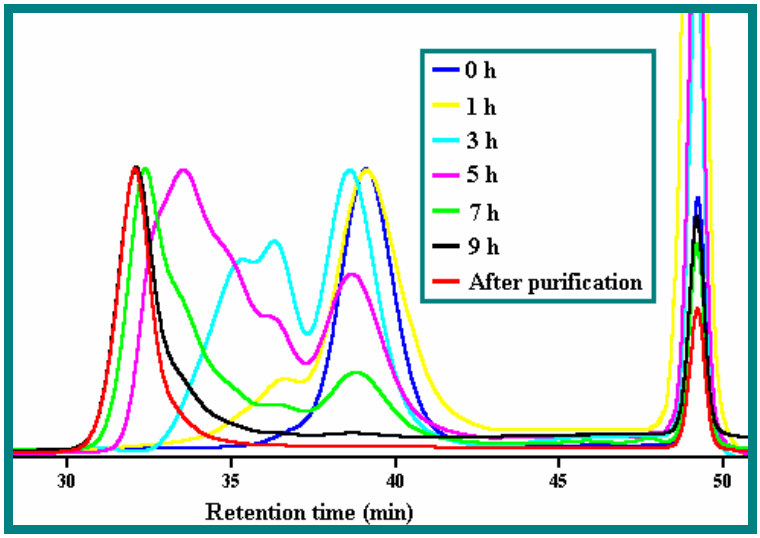

Figure 4.24 : Evolution of GPC traces of (α-silyl-alkyne-PS)$_n$-polyDVB multiarm star polymer using RI detector in THF at 30 ^{o}C ([DVB]$_0$/15 = [α-silyl-alkyne-PS]$_0$ = [CuBr]$_0$ = [PMDETA]$_0$ = 0.023 M in anisole at 110 ºC).

A monomodal GPC trace and narrow molecular weight distribution for (α-silyl-alkyne-PS)$_n$-polyDVB multiarm star polymer were detected. Later on, (α-silyl-

alkyne-PS)$_n$-polyDVB multiarm star polymer was then efficiently deprotected using TBAF in order to give corresponding (Alkyne-PS)$_n$-polyDVB. Figure 4.25 compares the ^{1}H NMR spectra recorded before and after deprotection. The disappearance of the signal at δ 0.17 corresponding to (C*H*$_3$)$_3$Si- confirmed the structure of (alkyne-PS)$_n$-polyDVB multiarm star polymer.

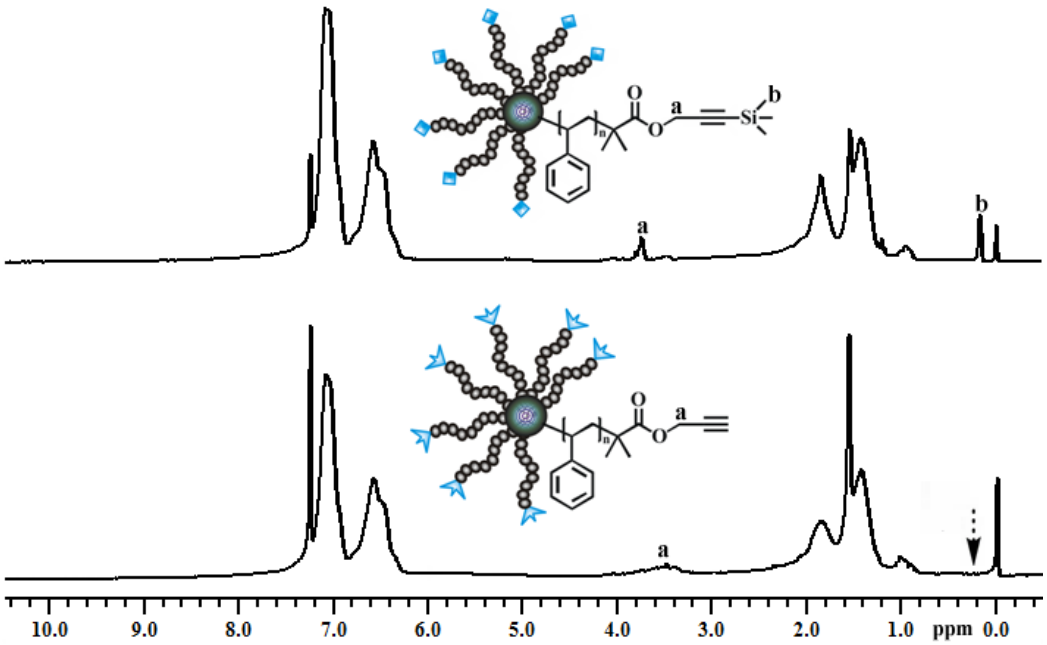

Figure 4.25 : Comparison of the ^{1}H NMR spectra of a) (α-silyl-alkyne-PS)$_n$-polyDVB multiarm star polymer and b) (alkyne-PS)$_n$-polyDVB multiarm star polymer in $CDCl_3$.

Additionally, TD-GPC measurement of (α-silyl-alkyne-PS)$_n$-polyDVB and (Alkyne-PS)$_n$-polyDVB multiarm star polymers were carried out. The molecular weight values (M_w, and M_p) of (Alkyne-PS)$_n$-polyDVB star polymer were obtained using TD-GPC instrument given in Table 4.6. As mentioned above, TD-GPC instrument provides more advanced and accurate technique to measure the absolute molecular weight of star polymers. Although, d*n*/dc value of linear PS is available, an attempt has been made to clarify the effect of cross-linked DVB core on the d*n*/dc value of multi arm PS star polymer. Therefore, the d*n*/dc of (Alkyne-PS)$_n$-polyDVB was measured by TD-GPC instrument and found to be 0.185 mL/g in THF at 35 ^{o}C, which is equal to that of linear PS. The weight average arm number (f) of multiarm (Alkyne-PS)$_n$-polyDVB star polymer was calculated using the following equation based on the absolute molecular weights (M_w) of multiarm star polymer.

$$f = \frac{\mathrm{W}F_{\mathrm{arm}} \times M_{\mathrm{w,star}}}{M_{\mathrm{w,arm}}} = \frac{M_{\mathrm{w,star}}}{M_{\mathrm{w,arm}} + M_{\mathrm{DVB}} \times conv_{\mathrm{DVB}} \times [\mathrm{DVB}]/[\alpha\text{-silyl-alkyne-PS}]} \quad \textbf{(Eq. 4.2)}$$

Where $\mathrm{W}F_{\mathrm{arm}}$ is the weight fraction of PS arm in the star polymer, $M_{\mathrm{w,star}}$ and $M_{\mathrm{w,arm}}$ are the absolute molecular weights of the (Alkyne-PS)$_n$-polyDVB star and the α-silyl-alkyne-PS arm, respectively obtained from TD-GPC instrument introducing the predetermined d*n*/dc value of PS to OmniSEC software, M_{DVB} is the molecular weight of DVB, [DVB]/[α-silyl-alkyne-PS] is a feed molar ratio of the DVB to α-silyl-alkyne-PS before cross-linking polymerization. The conversion of DVB ($conv_{\mathrm{DVB}}$) was determined by GC. Thus, the *f* of multiarm (Alkyne-PS)$_n$-polyDVB star polymer was calculated to be 27 and listed in Table 4.6. It is generally accepted that the intrinsic viscosity comparison of star polymer and its linear counterpart provides the most convenient method to elucidate the structure of star polymers, where g*'* is the contraction factor as given in Eq. 4.3.

$$g' = [\eta]_{\mathrm{star}} / [\eta]_{\mathrm{linear}} \quad (M = \text{constant}) \quad \textbf{(Eq. 4.3)}$$

Where $[\eta]_{\mathrm{star}}$ and $[\eta]_{\mathrm{linear}}$ are the intrinsic viscosities of star polymer and the linear polymer with the same molecular weight and the composition, respectively [248]. It is also shown that in regular (equal arm length) star polymers, *g'* is related with the number of arms, *f* as follows:

$$\log g' = 0.36 - 0.8 \log f \quad \textbf{(Eq. 4.4)}$$

Mark-Houwink-Sakurada (MHS) parameters K and *a* for linear PS were determined to be 1.44×10^{-4} dL/g and 0.707, respectively in THF at 35 ^{o}C using a series of linear narrow PS standards by TD-GPC. Then, using these parameters $[\eta]_{\mathrm{linear}}$ was calculated to be 0.955 dL/g for a specified molecular weight (M_{w} = 250750) of linear PS. Moreover, the $[\eta]_{\mathrm{star}}$ of (Alkyne-PS)$_n$-polyDVB star polymer was measured to be 0.162 dL/g by the viscometer detector in TD-GPC. The number of arms, *f* was calculated to be 26 using Eqs. 4.3-4 and in close agreement with that obtained from Eq. 4.2. Absolute molecular weight (M_{w}), M_{p}, $M_{\mathrm{w}}/M_{\mathrm{n}}$ and hydrodynamic radius (R_{h}) for (Alkyne-PS)$_n$-polyDVB multiarm star polymer are given in Table 4.6.

Table 4.6 : GPC characterization of multiarm star polymer, multiarm star block and multiarm star mixed-block copolymers.

Polymers	GPC				TD-GPC						
	M_n (g/mol)	M_w (g/mol)	M_p[b] (g/mol)	M_w/M_n	M_w (g/mol)	M_p[b] (g/mol)	M_w/M_n	$[\eta]$ (dL/g)	R_h (nm)	d*n*/dc (mL/g)	f[d]
(Alkyne-PS)$_n$-polyDVB[a]	73700	87500	84500	1.18	250750	223400	1.18	0.162	8.45	0.185	27(26)[e]
(P*t*BA)$_m$-(PS)$_n$-polyDVB	45000	48100	50800	1.07	383700	325700	1.18	0.159	9.69	0.135[c]	-
(P*EG*)$_k$-(PS)$_n$-polyDVB	86700	110500	102900	1.27	269100	222300	1.04	0.151	8.59	0.179[c]	-
(P*EG*)$_k$-(P*t*BA)$_m$-(PS)$_n$-polyDVB	64000	70800	71400	1.11	359400	318400	1.07	0.208	10.21	0.143[c]	-

[a]$[DVB]_0/15 = [\alpha\text{-silyl-alkyne-PS}]_0 = [CuBr]_0 = [PMDETA]_0 = 0.023$ M in anisole at 110 °C. Then deprotection with TBAF at room temperature.
[b]Molecular weight at peak apex.
[c]Calculated according to eq. 4.1.
[d]Calculated according to eq. 4.2.
[e]Calculated according to eqs. 4.3 and 4.4.

Next, (P*t*BA)$_m$-(PS)$_n$-polyDVB multiarm star block copolymer was achieved via a click reaction of linear P*t*BA-N_3 precursor with (Alkyne-PS)$_n$-polyDVB multiarm star polymer in the presence of CuBr/PMDETA in DMF at room temperature for 24 h (Scheme 4.26). In this case, an excess of linear precursors (1.3 equiv.) was employed with respect to that of multiarm star polymer. The unreacted linear precursors were easily removed from the reaction medium due to their solubility in methanol. After purification, the obtained multiarm star block copolymers were characterized by ^{1}H NMR, TD-GPC and GPC.

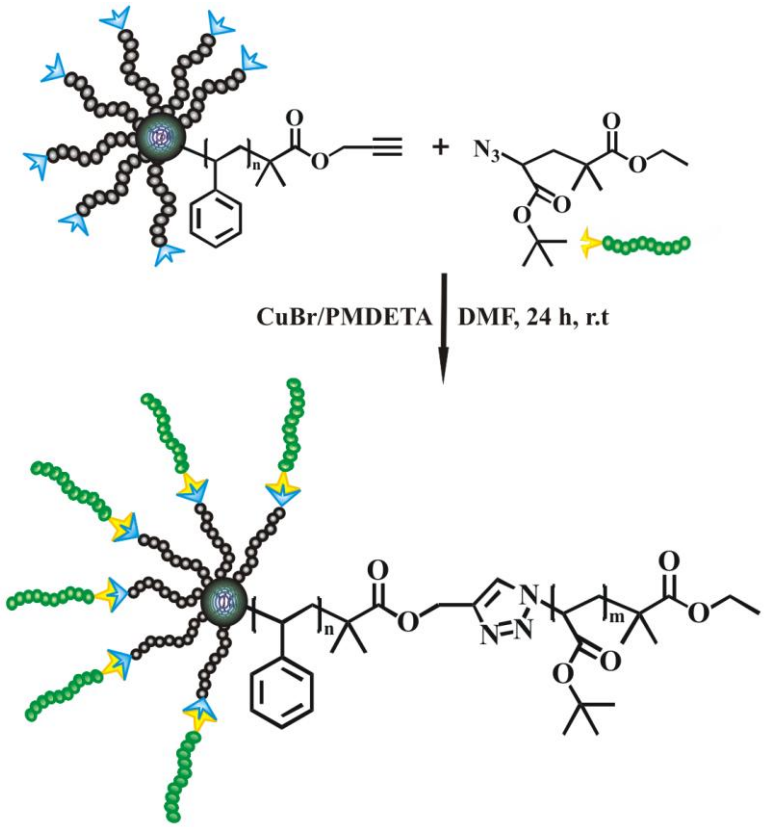

(4.26)

From ^{1}H NMR spectrum of (P*t*BA)$_m$-(PS)$_n$-polyDVB multiarm star block copolymer, characteristic signals at 2.2 and 1.4 ppm related with C*H* and C(CH_3)$_3$ of P*t*BA, respectively along with signals of PS block confirmed a successful azide-alkyne click reaction (Figure 4. 26).

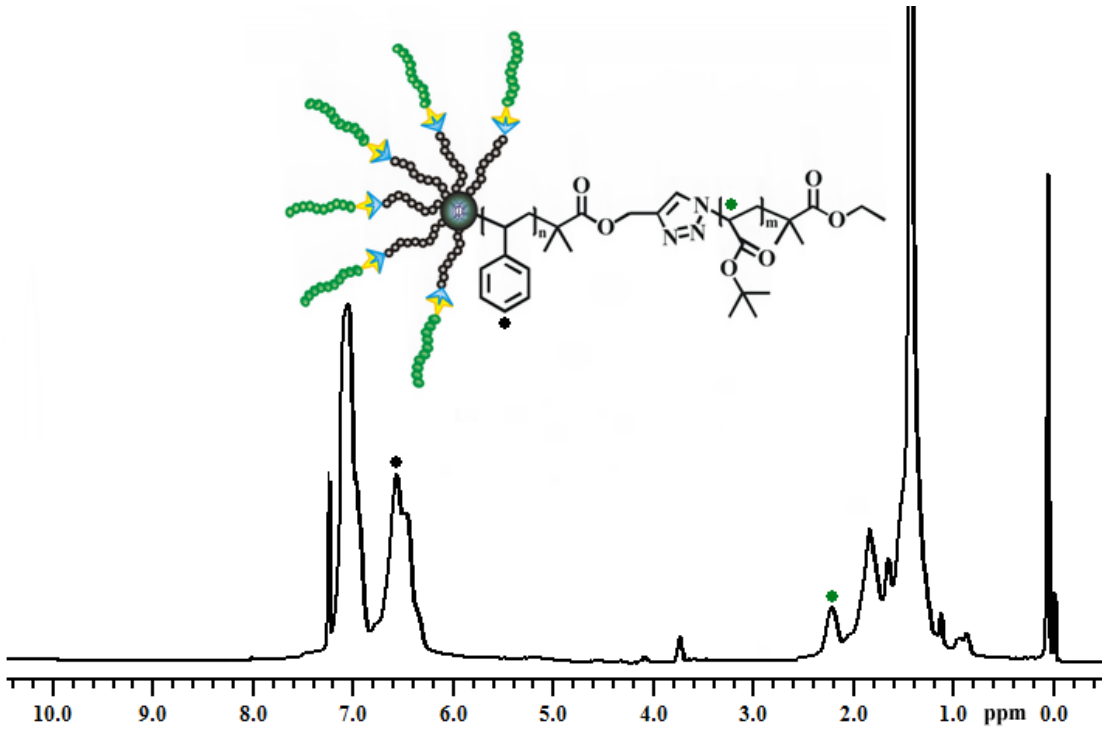

Figure 4.26 : ^{1}H NMR spectrum of (P*t*BA)$_m$-(PS)$_n$-polyDVB multiarm star block copolymer in $CDCl_3$.

Using weight fractions of PS (0.64) and P*t*BA (0.36) blocks derived from ^{1}H NMR, d*n*/dc of corresponding star block copolymer is calculated to be 0.135 mL/g by using an equation 4.1 assuming that the d*n*/dc of linear PS and P*t*BA precursors is 0.185 and 0.049 mL/g, respectively. Thus, the obtained d*n*/dc is then introduced into the Omni-Sec software of TD-GPC for the calculation of M_w and R_h of the multiarm star block copolymer (Table 4.6).

A GPC trace of (P*t*BA)$_m$-(PS)$_n$-polyDVB multiarm star block copolymer displayed a shift to lower retention time region compared to that of the precursor (PS)$_n$-polyDVB, indicating that the former had higher hydrodynamic volume than that of the precursor (Figure 4.27). Remarkably, it is noted that a trace for P*t*BA-N_3 was not detected.

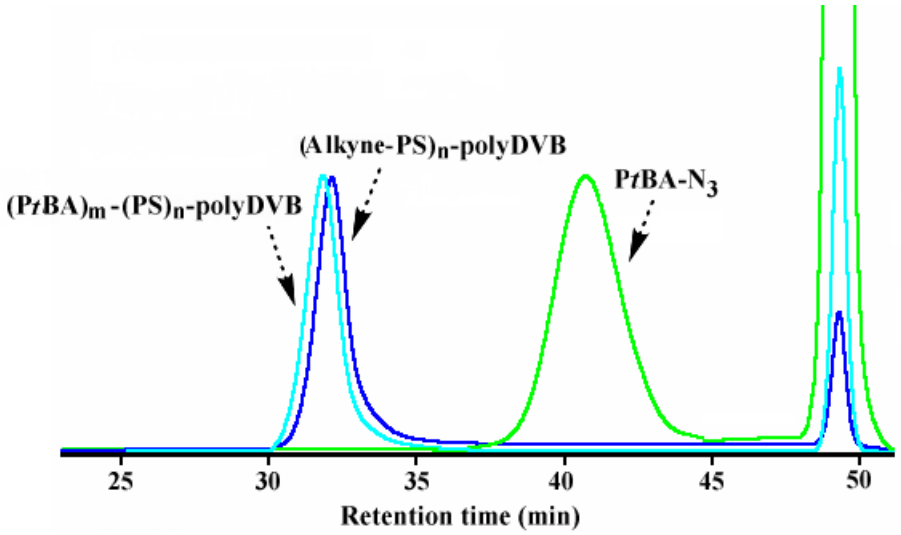

Figure 4.27 : GPC traces of (Alkyne-PS)$_n$-polyDVB multiarm star, (P*t*BA)$_m$-(PS)$_n$-polyDVB multiarm star block copolymer and linear P*t*BA-N$_3$ precursor using RI detector in THF at 30 ^oC.

As a second example, (PEG)$_k$-(PS)$_n$-polyDVB multiarm star block copolymer was achieved in a similar way via the CuAAC reaction of linear PEG-N$_3$ precursor with (alkyne-PS)$_n$-polyDVB multiarm star polymer in the presence of CuBr/PMDETA in DMF at room temperature for 24 h (Scheme 4.27).

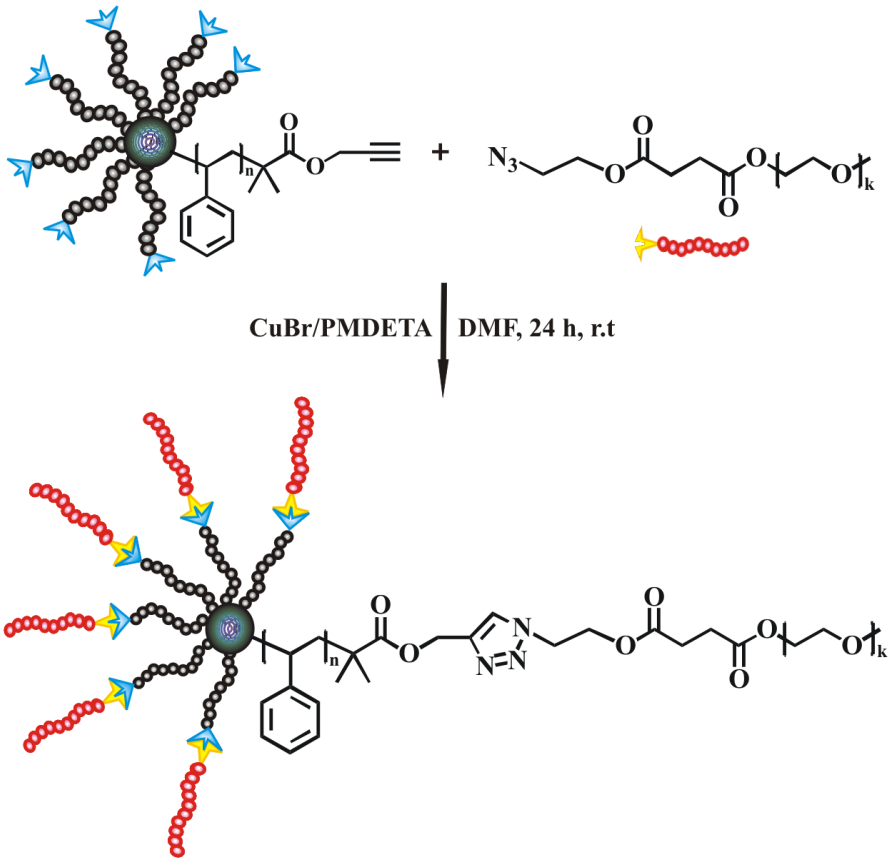

(4.27)

$(PEG)_k$-$(PS)_n$-polyDVB multiarm star block copolymer was analyzed by ^1H NMR and GPC measurements. ^1H NMR spectrum showed characteristic resonances of Ar*H* at 7.5-6.5 and CH_2CH_2O at 3.6 ppm for PS and PEG, respectively (Fgure 4.28). Again, weight fractions for the PS and PEG blocks were determined to be 0.95 and 0.05, respectively from NMR.

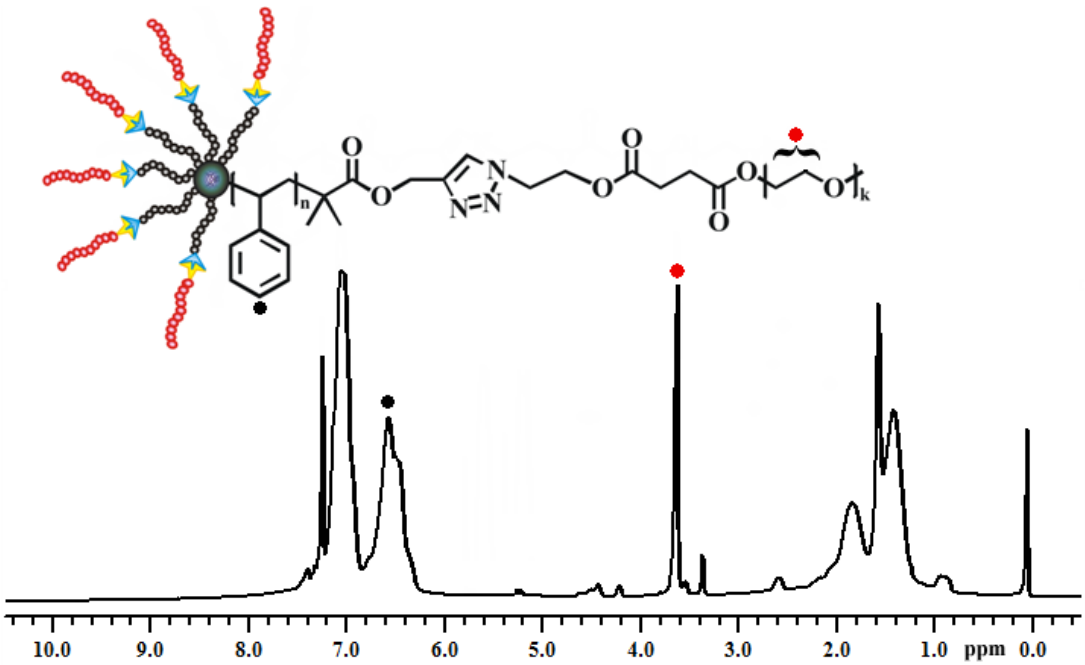

Figure 4.28 : ^1H NMR spectrum of $(PEG)_k$-$(PS)_n$-polyDVB multiarm star block copolymer in $CDCl_3$.

Using these weight fractions, d*n*/dc = 0.179 mL/g of star block copolymer was subsequently calculated depending on an assumption that the d*n*/dc of PS and PEG was 0.185 and 0.078 mL/g, respectively. Similarly, M_w, M_p, M_w/M_n and R_h were obtained from TD-GPC along with [η] introducing the above d*n*/dc into the Omni-Sec software (Table 4.6).

GPC analysis of $(PEG)_k$-$(PS)_n$-polyDVB multiarm star block copolymer showed a monomodal trace, however, which shifted to higher retention time with respect to that of $(Alkyne\text{-}PS)_n$-polyDVB multiarm star polymer (Figure. 4.29). This may be due to that adsorption of the PEG segment with stationary phase caused a shift to lower molecular weight region. Moreover, from Table 4.6, it is deduced that R_h of multiarm star block copolymer is slightly higher than that of $(Alkyne\text{-}PS)_n$-polyDVB multiarm star polymer, indicating that GPC trace shift is not the result of a decrease in the hydrodynamic volume.

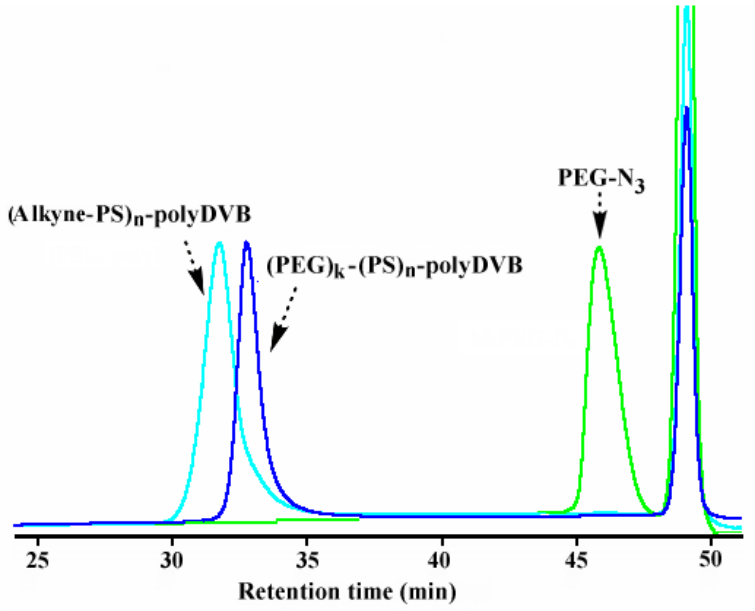

Figure 4.29 : GPC traces of (Alkyne-PS)$_n$-polyDVB multiarm star, (PEG)$_k$-(PS)$_n$-polyDVB multiarm star block copolymer and linear PEG-N_3 precursor using RI detector in THF at 30 ^oC.

As a third sample, (PEG)$_k$-(P*t*BA)$_m$-(PS)$_n$-polyDVB multiarm star mixed-block copolymer was simply prepared from a azide-alkyne click reaction of (Alkyne-PS)$_n$-polyDVB multiarm star polymer with linear precursors, P*t*BA-N_3 and PEG-N_3, concurrently in the CuBr/PMDETA in DMF at room temperature for 24 h. A 1.2 equiv. of linear precursors to that of (Alkyne-PS)$_n$-polyDVB multiarm star polymer was used in the reaction. Similarly, unreacted linear precursors were easily removed from the reaction medium. The resulting multiarm star mixed-block copolymer is characterized by ^{1}H NMR, GPC and TD-GPC. Characteristic signals for PS, PEG and P*t*BA segments are detected at 7.5-6.5 (Ar*H*), 3.6 (CH_2CH_2O-) and 2.2 ppm (C*H*), respectively from ^{1}H NMR spectrum (Figure 4.30).

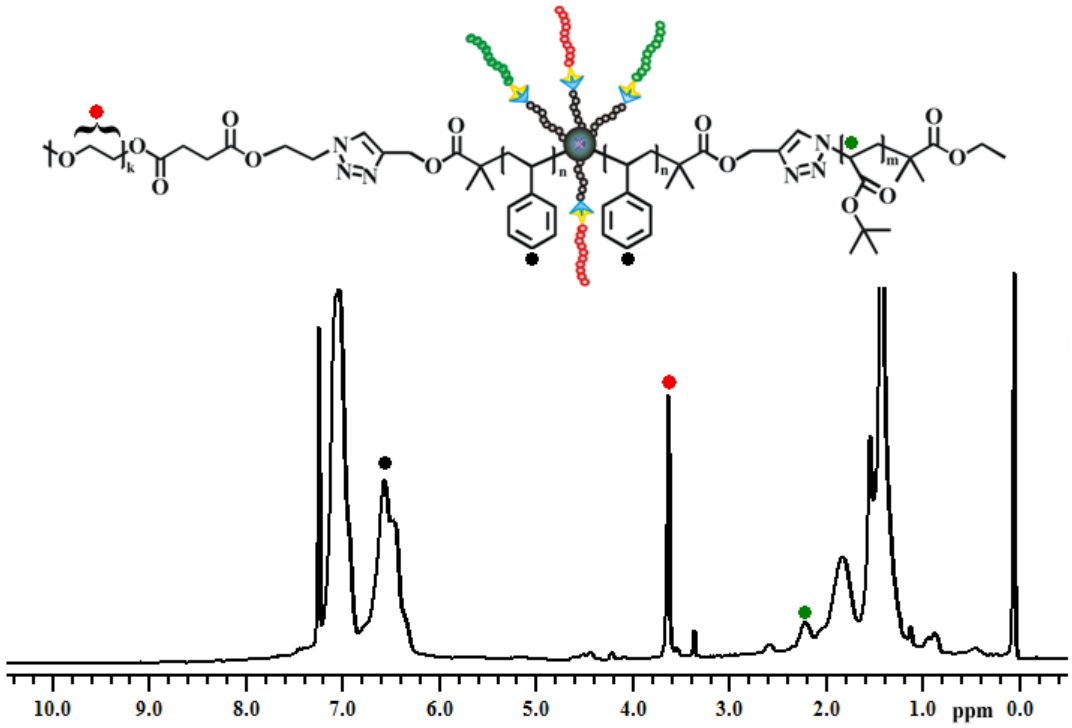

Figure 4.30 : ^{1}H NMR spectrum of $(PEG)_k$-(P*t*BA)$_m$-$(PS)_n$-polyDVB multiarm star mixed-block copolymer in $CDCl_3$.

Additionally, d*n*/dc = 0.143 mL/g of the target multiarm star mixed-block copolymer is calculated by using the weight fractions and d*n*/dc values of individual segments. The weight fractions for PS, P*t*BA and PEG segments from ^{1}H NMR were found to be 0.70, 0.27 and 0.03, respectively. After introduction of this d*n*/dc to the software, molecular weight data and R_h were obtained together with [η] for $(PEG)_k$-(P*t*BA)$_m$-$(PS)_n$-polyDVB multiarm star mixed-block copolymer (Table 4.6).

GPC trace of multiarm star mixed-block copolymer displayed a shift to higher retention time with respect to that of $(PS)_n$-polyDVB multiarm star polymer (Figure 4.31). Once more, an aforementioned explanation for the GPC analysis of $(PEG)_k$-$(PS)_n$-polyDVB may be given for that of $(PEG)_k$-(P*t*BA)$_m$-$(PS)_n$-polyDVB multiarm star mixed- block copolymer.

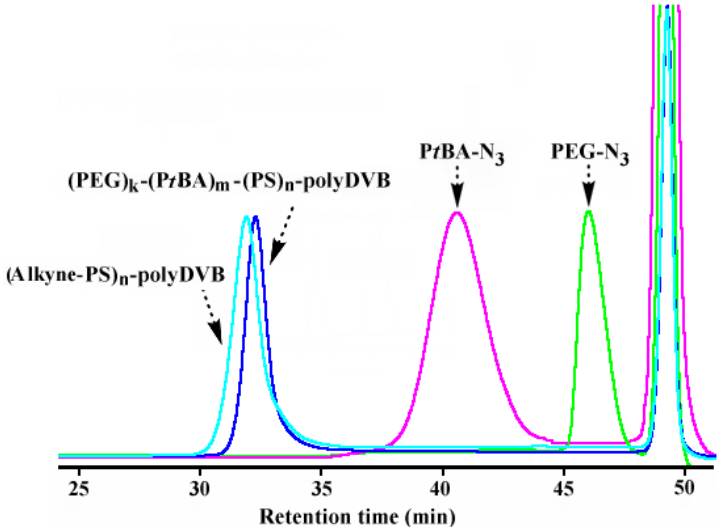

Figure 4.31 : GPC traces of (Alkyne-PS)$_n$-polyDVB multiarm star, (PEG)$_k$-(P*t*BA)$_m$-(PS)$_n$-polyDVB multiarm star mixed-block copolymer and linear P*t*BA-N_3 and PEG-N_3 precursors using RI detector in THF at 30 ^oC.

In general from Table 4.6, it can be inferred that the absolute molecular weights and R_h values of multiarm star polymers ascend from multiarm star to multiarm star mixed-block copolymer and all polymers have narrow molecular weight distribution. The size and the morphology of multiarm star polymers were further characterized by DLS and AFM, respectively. The AFM investigations of the spin coated dilute solutions (c ~ 10^{-3} mg/mL) on silicon wafers showed the individual multiarm star molecules. The AFM height image Figure 4.32a and the corresponding phase image Figure 4.32b show the general view of (PS)$_n$-polyDVB multi arm polymer in a 2 μm x 2 μm area on the silicon substrate. The objects seen can be separated into three groups depending on their height: (i) aggregates larger than 20 nm in height (Figure 4.32b lower inset), (ii) circular objects having height ~ 6-10 nm (Fig. 4.32b upper inset), and (iii) circular ring objects having height ~ 1-2 nm (Fig. 4.32c-4.32d).

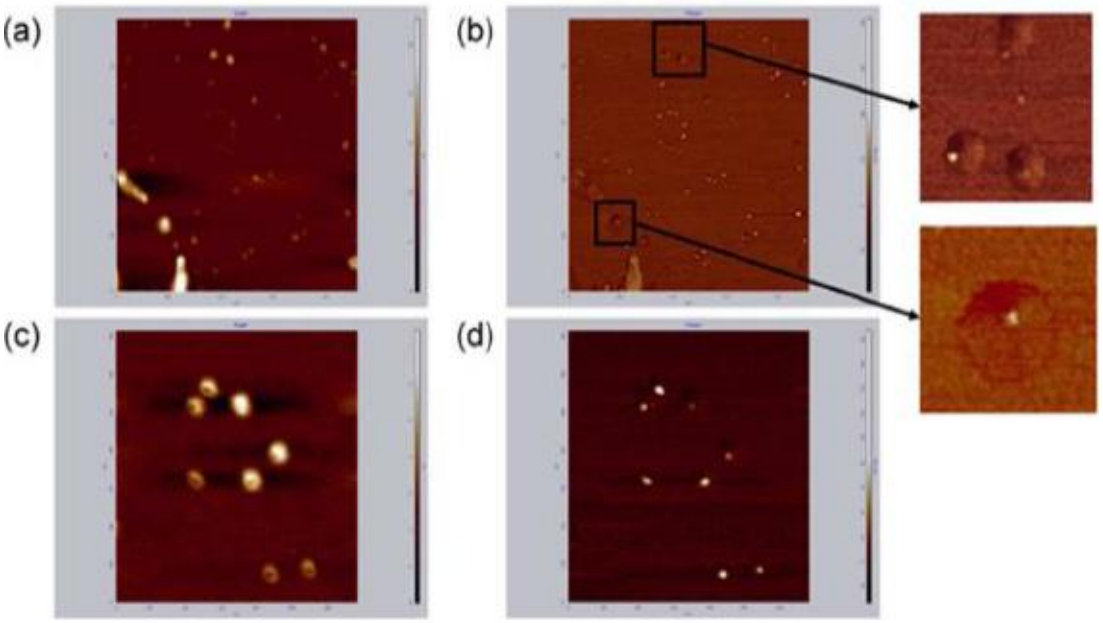

Figure 4.32 : AFM height image (a) and the phase image (b) showing the general view of the spin coated dilute solutions of $(PS)_n$-polyDVB multi arm polymer in a 2 μm x 2 μm area on the silicon substrate. The areas inside the drawn squares in (b) were magnified as insets. The height (c) and the phase images (d) of the individual molecules are seen in detail in 0.7 μm x 0.7 μm scans.

We attribute the observed circular rings (Fig. 4.32c-4.32d) to the individual multiarm star molecules. The observed lateral dimensions of these molecules were between 23-27 nm which corresponds to a real size of 14-17 nm after deconvolution of the finite size of the AFM tip (assumed to be 10 nm). The hydrodynamic diameter of the $(PS)_n$-polyDVB multi arm polymers in toluene was measured to be 16.0 ± 3.1 nm by DLS (Figure 4.33a) which compares quite well to the sizes determined by AFM. The ring shape in height images (Fig. 4.32c) is due to flattening of the molecules by the substrate which results in a slight 0.5-1.0 nm decrease in height on top of the central core of the molecules exposing the polyDVB region. These polyDVB rich regions showed a clear bright contrast in the phase image indicating the relative hardness of the central core compared to the PS arms surrounding it. In the case of larger aggregates (group (i)) and circular objects of height ~ 6-10 nm (group (ii)), these polyDVB rich regions were not all noticeable in the height images, but a clear bright phase could be seen in the phase images (insets of Fig 4.32b). The lateral dimensions of ~ 6-10 nm high circular objects were ~ 70 nm, much larger than twice the expected length of PS arms and the measured hydrodynamic diameter of 16 nm. We attribute these circular objects (group (ii), Fig. 4.32b upper inset) and the larger

objects (group (i), Fig. 4.32b lower inset) to the aggregates containing more than one multiarm star molecule. Aggregates of several 18-arm polybutadiene (PB) star molecules have previously been observed on mica surfaces and the number of associated star molecules within the aggregates was reported to increase with the amount of molecules on the surface [249]. For star polymers having less than ~32 arms [249] the interaction and the interpenetration of the arms of different molecules lead to such aggregation. In the case of (Alkyne-PS)$_n$-polyDVB, the interaction of the alkyne end groups may be an additional source for aggregation.

The hydrodynamic sizes of the four multiarm star polymers were determined by DLS. Figure 4.33 shows the DLS size histograms.

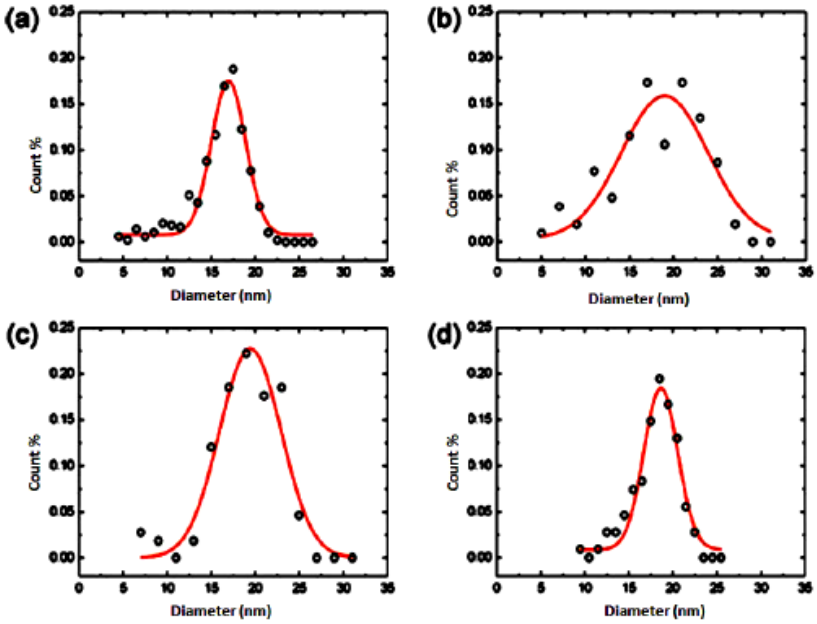

Figure 4.33 : DLS size histograms. The solid lines are the Gaussian fits to the data. (a) (Alkyne-PS)$_n$-polyDVB in toluene. (b) (P*t*BA)$_m$-(PS)$_n$-polyDVB in CH_2Cl_2. (c) (PEG)$_k$-(PS)$_n$-polyDVB in CH_2Cl_2. (d) (PEG)$_k$-(P*t*BA)$_m$-(PS)$_n$-polyDVB in CH_2Cl_2.

The average hydrodynamic diameter of (Alkyne-PS)$_n$-polyDVB multiarm star polymer was measured to be 16.0 ± 3.1 nm in toluene. The hydrodynamic diameter of other three polymers; (P*t*BA)$_m$-(PS)$_n$-polyDVB, (PEG)$_k$-(PS)$_n$-polyDVB and (PEG)$_k$-(P*t*BA)$_m$-(PS)$_n$-polyDVB, were all measured in CH_2Cl_2 and found to be 18.1 ± 4.9 nm, 18.9 ± 3.7 nm and 18.0 ± 2.5 nm, respectively. These sizes compares well to those determined by TD-GPC (Table 4.6) which ranges between 17-20 nm. The average hydrodynamic diameter was ~2-3 nm larger for (P*t*BA)$_m$-(PS)$_n$-polyDVB, (PEG)$_k$-(PS)$_n$-polyDVB and (PEG)$_k$-(P*t*BA)$_m$-(PS)$_n$-polyDVB confirming the

successful addition of (P*t*BA-N_3) and (PEG-N_3) to (alkyne-PS)$_n$-polyDVB via click reaction.

The individual molecules of (P*t*BA)$_m$-(PS)$_n$-polyDVB, (PEG)$_k$-(PS)$_n$-polyDVB and (PEG)$_k$-(P*t*BA)$_m$-(PS)$_n$-polyDVB multi arm polymers were also clearly observed in the AFM images of spin coated dilute solutions on silicon substrates (Figure 4.34).

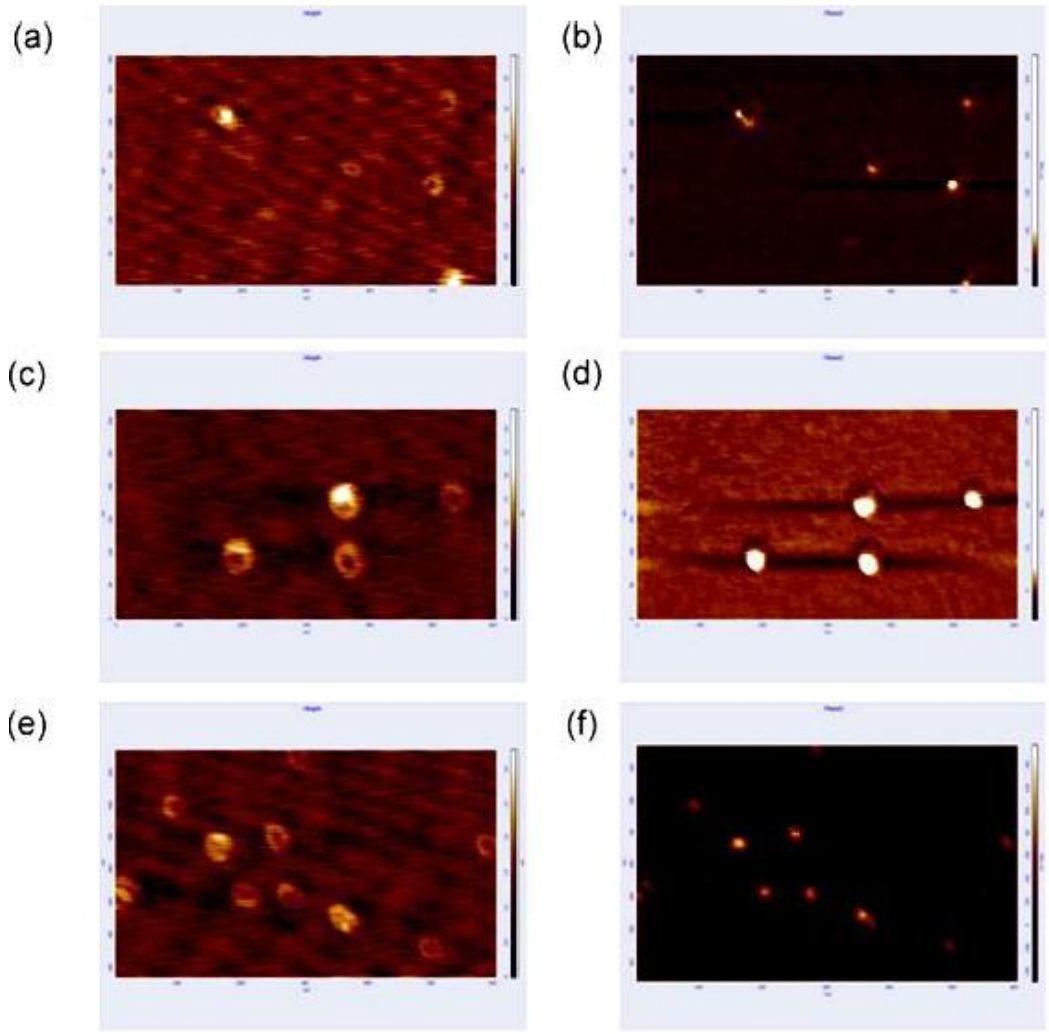

Figure 4.34 : 0.6 µm x 0.3 µm AFM height (a,c,e) and phase (b,d,f) images of multi blockcopolymer arm star polymers on silicon substrates: (a-b) (P*t*BA)$_m$-(PS)$_n$-polyDVB. (c-d) (PEG)$_k$-(PS)$_n$-polyDVB. (e-f) (PEG)$_k$-(P*t*BA)$_m$-(PS)$_n$-polyDVB.

The molecules showed circular ring shapes having a height of ~1-2 nm, and lateral size of ~25 nm similar to (Alkyne-PS)$_n$-polyDVB molecules (Fig.4.33-4.33d). It was not possible to detect differences of 2-3 nm in lateral size compared to that of (Alkyne-PS)$_n$-polyDVB as determined by DLS. Similar to (Alkyne-PS)$_n$-polyDVB, aggregates containing more than one molecule were also observed in larger area scans.

4.4 Synthesis of Multi-miktoarm Star Block Copolymers via Sequential CuAAC and Diels-Alder Click Reactions

As a new synthetic route, sequential double click reactions involving CuAAC and Diels–Alder for the preparation of multi-miktoarm star block copolymers were employed by using the arm-first approach. Multiarm star PS with both alkyne and anthracene moieties at the periphery, (Alkyne-PS)$_m$–polyDVB–(PS-Anth)$_m$, was simply obtained via ATRP of DVB concurrently initiated with linear α-silyl alkyne-PS and Anth-PS macroinitiators. It is followed by sequential CuAAC and Diels–Alder click reactions with P*t*BA–N_3 and MI-PMMA, respectively, resulting in the formation of target multi-miktoarm star block copolymer (P*t*BA)$_m$–(PS)$_n$–polyDVB–(PS)$_n$–(PMMA)$_k$ (Scheme 4.28).

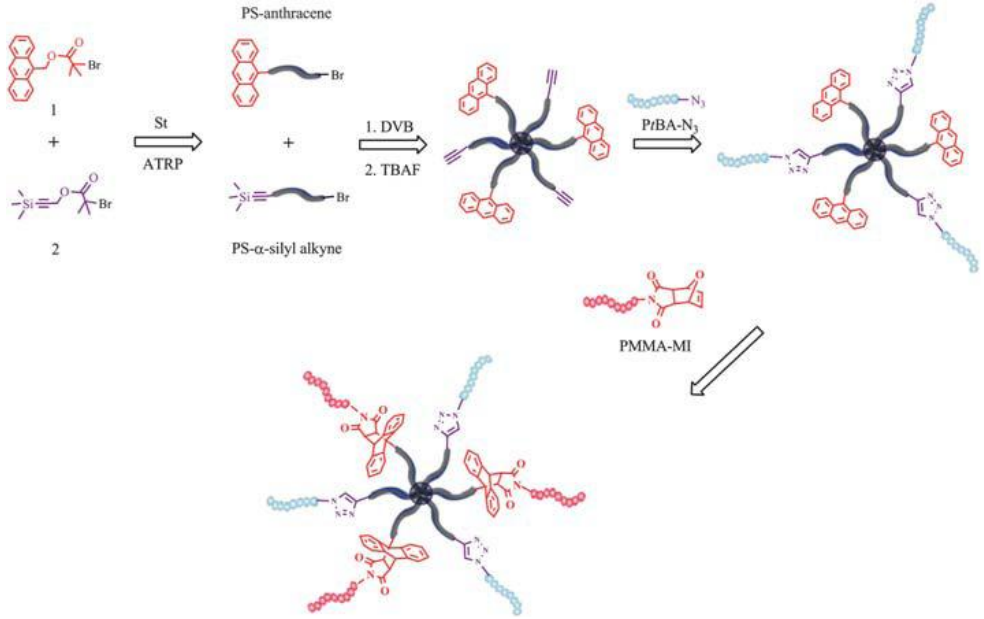

(4.28)

For the preparation of (Alkyne-PS)$_m$–polyDVB–(PS-Anth)$_m$ multiarm star polymer bearing alkyne and anthracene functionalities at the periphery, initially a mixture of linear α-silyl-alkyne-PS and Anth-PS was obtained via one-pot ATRP of St concurrently initiated by using **9** and **11**. From the ^{1}H NMR spectrum, the α-anthracene and α-silyl protected alkyne moieties of linear PS were found to be 47 and 53 mol%, respectively according to a ratio of integrated areas of anthracene Ar*H* (δ 8.5–7.4) and –Si(C*H*$_3$)$_3$ (δ 0.16) (Figure 4.35). Moreover this ratio was consistent with an equimolar feed ratio of **9** to **11** in the ATRP of St.

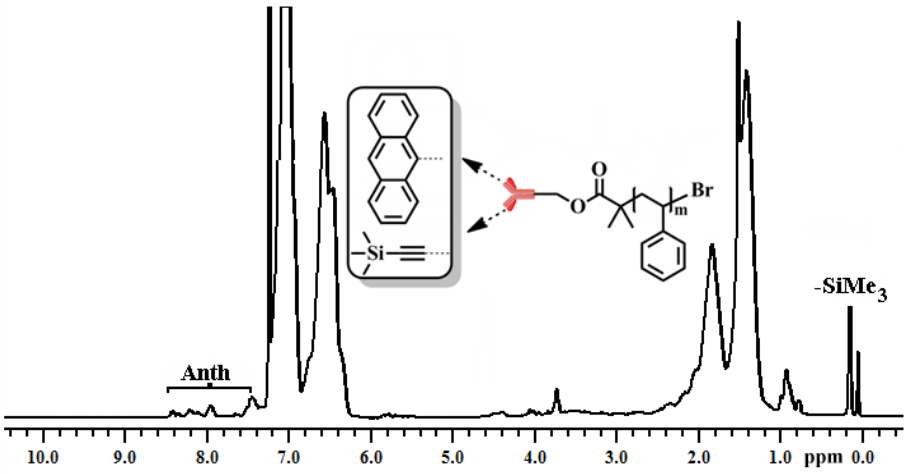

Figure 4.35 : ^{1}H NMR spectrum of mixture of linear α-silyl alkyne-PS and Anth-PS in $CDCl_3$.

$M_{n,GPC}$ and M_w/M_n were determined by conventional GPC and fit well with those of NMR and theoretical number-average molecular weight (Table 4.7). On the other hand, the outer precursors of multi-miktoarm star block copolymers, P*t*BA-N_3 and MI-PMMA were synthesized similiar procedures as described above. All polymerization conditions and results of the linear precursors used in the synthesis of multi-miktoarm star block copolymers were presented in Table 4.7.

Table 4.7 : The conditions and results of linear polymers used in the synthesis of multi-miktoarm star block copolymers

Polymer	Ini	Time (min)	Conv.[d] (%)	$M_{n,GPC}$[e] (g/mol)	M_w/M_n[e]	$M_{n,theo}$[f] (g/mol)	$M_{n,NMR}$ (g/mol)
α-silyl-alkyne-PS + Anth-PS[a]	**9+11**	40	23	5400	1.10	5100	6050
P*t*BA-N_3[b]	EiBr	30	25	3800	1.10	3350	5100
MI-PMMA[c]	**3**	210	56	3900	1.17	2800	3000

[a] $[M]_0:[I]_0:[CuBr]:[PMDETA]$ = 200:1:1:1; polymerization was carried out at 110 °C.
[b] $[M]_0:[I]_0:[CuBr]:[PMDETA]$ = 100:1:1:1; polymerization was carried out at 80 °C. *t*BA / EC = 10 (w/w). Then NaN_3 in DMF stirred at 50 °C for overnight.
[c] $[M]_0:[I]_0:[CuCl]:[PMDETA]$ = 50:1:1:1; polymerization was carried out at 40 °C. MMA/toluene = 1/1 (v/v).
[d] Determined by gravimetrically.
[e] Determined by using GPC in THF at 30 ºC relative to PS standards.
[f] $M_{n,theo} = ([M]_0/[I]_0)$ X conversion % X MW of monomer + MW of initiator.

In the following, a mixture of Anth-PS and α-silyl-alkyne PS was subsequently used as macroinitiator in ATRP of DVB catalyzed by PMDETA/CuBr at 110 ºC for the preparation of (α-silyl alkyne-PS)$_m$–polyDVB–(PS-Anth)$_m$ multiarm star polymer bearing both alkyne and anthracene at the periphery.

The star formation was monitored by GC and GPC via taking samples at specified time intervals and stopped after 12 h at 94% of DVB conversion. The (α-silyl alkyne-PS)$_m$–polyDVB–(PS-Anth)$_m$ multiarm star polymer was purified by dissolution/precipitation in THF/MeOH–ether, respectively.

The absolute molecular weight (M_w) of the multiarm star polymer (α-silyl-alkyne-PS)$_m$–polyDVB–(PS-Anth)$_m$ was measured using TD-GPC and the number of arms (*f*) per molecule of the multiarm star polymer was calculated to be 31 using the equation 4.2.

Again, the ^{1}H NMR analysis of the multiarm star polymer revealed that star polymer contains 46 and 54 mol% of anthracene and silyl-alkyne moieties at the periphery, respectively, using similar NMR assignments to those given above for a mixture of linear α-silyl-alkyne-PS and Anth-PS (Figure 4.36 (a)). It should be noted that the number of arms per star molecule containing silyl-alkyne and anthracene moieties is determined to be 17 and 14, respectively.

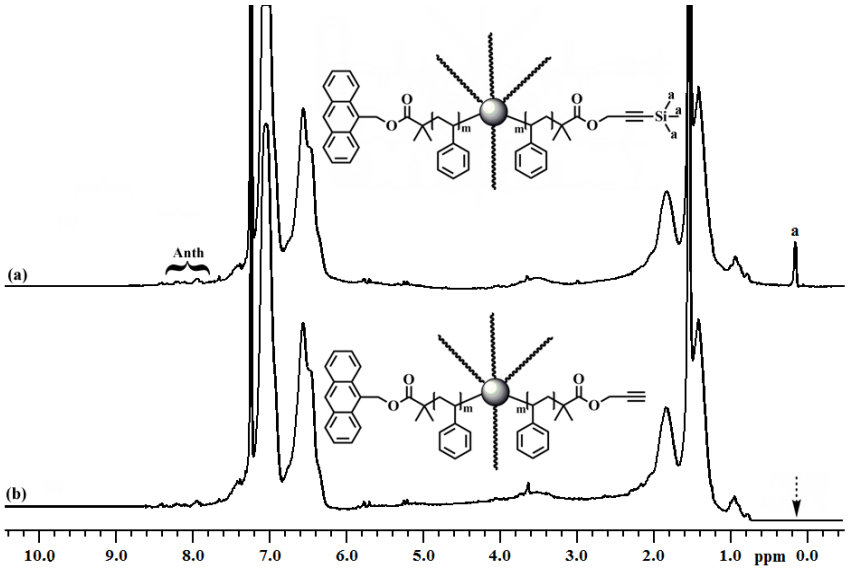

Figure 4.36 : ^{1}H NMR spectra of (α-silyl-alkyne-PS)$_m$–polyDVB–(PS-Anth)$_m$ multiarm star polymer (a) and (Alkyne-PS)$_m$–polyDVB–(PS-Anth)$_m$ multiarm star polymer (b) in $CDCl_3$.

Next, silyl groups at the periphery were deprotected by reacting with TBAF at room temperature for 2 h. The complete disappearance of the signal at δ 0.16 corresponding to $(CH_3)_3Si$- confirmed the structure of $(Alkyne\text{-}PS)_m$–polyDVB–$(PS\text{-}Anth)_m$ multiarm star polymer (Figure 4.36 (b)).

After deprotection, $(Alkyne\text{-}PS)_m$–polyDVB–$(PS\text{-}Anth)_m$ multiarm star polymer was reacted with well-defined linear P*t*BA–N_3 CuBr/PMDETA in DMF at room temperature to obtain $(PtBA)_n$–$(PS)_m$–polyDVB–$(PS\text{-}Anth)_m$ multi-miktoarm star block copolymer. A molar ratio of P*t*BA–N_3 to the star molecule was adjusted to be 20 slightly exceeding the number of arms bearing alkyne at the periphery. Unreacted linear P*t*BA–N_3 was simply removed from the reaction mixture by precipitation in methanol/diethyl ether.

NMR analysis showed that P*t*BA (δ 2.2) precursor had successfully been incorporated into the multiarm star polymer. (Figure 4.37)

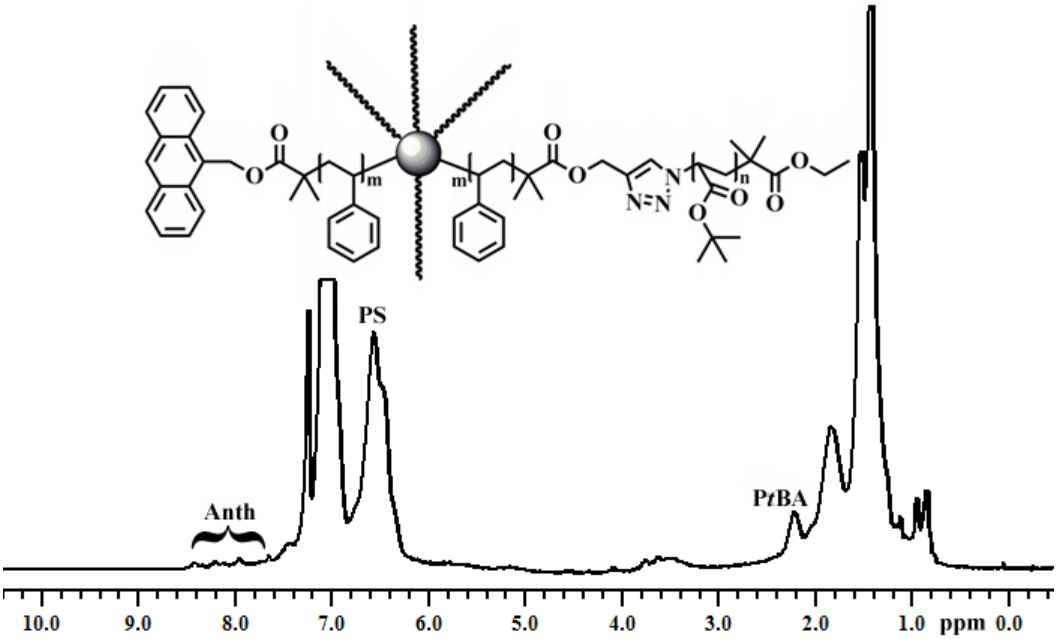

Figure 4.37 : ^1H NMR spectrum of $(PtBA)_n$–$(PS)_m$–polyDVB–$(PS\text{-}Anth)_m$ multi-miktoarm star block copolymer in $CDCl_3$.

The d*n*/dc value for the $(PtBA)_n$–$(PS)_m$–polyDVB–$(PS\text{-}Anth)_m$ multi-miktoarm star block copolymer was determined to be 0.146 mL g^{-1} using an equation 4.1, which correlates linearly with weight fractions of PS and P*t*BA segments (w_{PS} = 0.715 and w_{PtBA} = 0.285) and d*n*/dc of the linear precursors. For this calculation, DP_n of the PS segment in the $(PtBA)_n$–$(PS)_m$–polyDVB–$(PS\text{-}Anth)_m$ star polymer and the d*n*/d*c*

value for the linear P*t*BA were assumed to be 55 and 0.049 mL g^{-1}, respectively. After introducing d*n*/dc = 0.146 to the software of TD-GPC, molecular weight data and R_h were obtained together with [η] for $(PtBA)_n$–$(PS)_m$–polyDVB–$(PS\text{-}Anth)_m$ star polymer were obtained. (Table 4.8).

Monomodal GPC trace and clear shift with respect to the precursors were observed indicating the successful CuAAC click reaction, and thus the formation of the multi-miktoarm star block copolymer (Figure 4. 38).

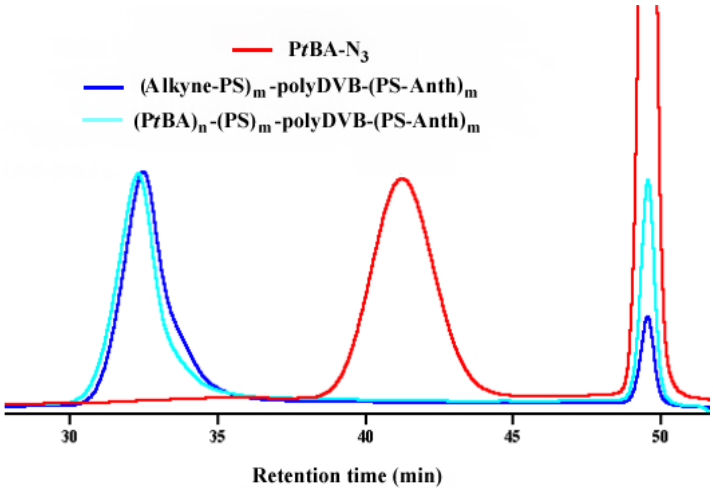

Figure 4.38 : GPC traces of $(PtBA)_n$-$(PS)_m$-polyDVB-$(PS\text{-}Anth)_m$, $(Alkyne\text{-}PS)_m$-polyDVB-$(PS\text{-}Anth)_m$ multiarm star polymer and linear P*t*BA-N_3 precursors using RI detector in THF at 30 ^oC.

After that, Diels–Alder click reaction strategy was applied to the preparation of $(PtBA)_n$–$(PS)_m$–polyDVB–$(PS)_m$–$(PMMA)_k$ by simply reacting anthracene groups at the periphery of $(PtBA)_n$–$(PS)_m$–polyDVB–$(PS\text{-}Anth)_m$ with linear MI-PMMA precursor. The Diels–Alder click reaction was performed in the presence of 1.4-fold molar excess of MI-PMMA per arm of the star molecule bearing anthracene at the periphery. The formation of target multi-miktoarm star block copolymer is followed over time by UV spectroscopy upon the disappearance of the signal of the anthryl group at 366 nm (Figure 4.39). By using UV data, Diels–Alder click reaction efficiency was found to be over 95%.

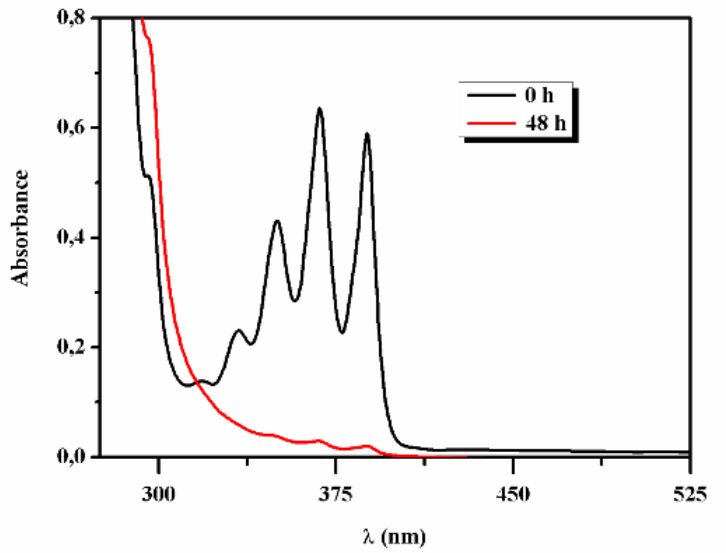

Figure 4.39 : UV spectra of multiarm anthracene end-functionalized $(PtBA)_n$-$(PS)_m$-polyDVB-$(PS\text{-}Anth)_m$ star polymer during the synthesis of multiarm $(PtBA)_n$-$(PS)_m$-polyDVB-$(PS)_m$-$(PMMA)_k$ star block copolymer (C_0= 3.32 X 10^{-6} mol/L in CH_2Cl_2).

The reaction was stopped after 48 h and the remaining solid was purified by a two times dissolution–precipitation cycle in THF–MeOH. NMR analysis showed that PMMA block (δ 3.58) was incorporated into the star polymer (Figure 4.40). The d*n*/d*c* value for $(PtBA)_n$-$(PS)_m$-polyDVB-$(PS)_m$-$(PMMA)_k$ is calculated to be 0.137 mL/g using the equation 4.1, which correlates linearly with weight fractions of PS, P*t*BA and PMMA segments in the star (w_{PS} = 0.63, w_{PtBA} = 0.25, and w_{PMMA} = 0.12), and d*n*/dc values of linear precursors.

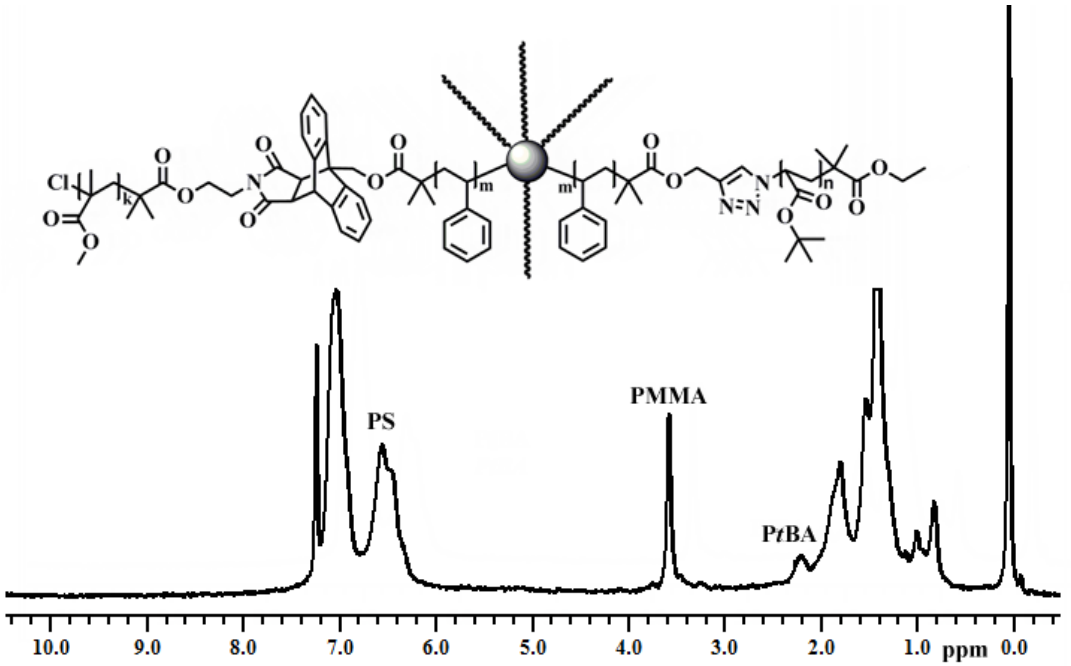

Figure 4.40 : ^{1}H NMR spectrum of (P*t*BA)$_n$–(PS)$_m$–poly-DVB–(PS)$_m$–(PMMA)$_k$ in $CDCl_3$.

For this calculation it is assumed that the DP_ns of PS and P*t*BA were 55 and 18, respectively, and the d*n*/dc value for the linear PMMA was 0.076 mL g^{-1}. Next, after introducing the d*n*/dc = 0.137 into the OmniSec, $M_{w,TD\text{-}GPC}$, R_h and [η] for (P*t*BA)$_n$–(PS)$_m$–poly-DVB–(PS)$_m$–(PMMA)$_k$ were calculated and are listed in Table 4.8.

As can be deduced from Table 4.8, all star polymers have a narrow polydispersity index and a gradual increase in R_h and $M_{w,TD\text{-}GPC}$ values of star polymers confirmed a successful sequential incorporation of blocks into the star. It is also noted that $M_{w,theo}$ = 385000 of (P*t*BA)$_n$–(PS)$_m$–poly-DVB–(PS)$_m$–(PMMA)$_k$ is fairly consistent with that of $M_{w,TD\text{-}GPC}$ = 407000.

From Figure 4.41, it can be seen that a monomodal GPC trace of (P*t*BA)$_n$–(PS)$_m$–poly-DVB–(PS)$_m$–(PMMA)$_k$ displayed a slight shift to a lower retention time with respect to that of (P*t*BA)$_n$–(PS)$_m$–polyDVB–(PS-Anth)$_m$ indicating an incorporation of PMMA segment into the star.

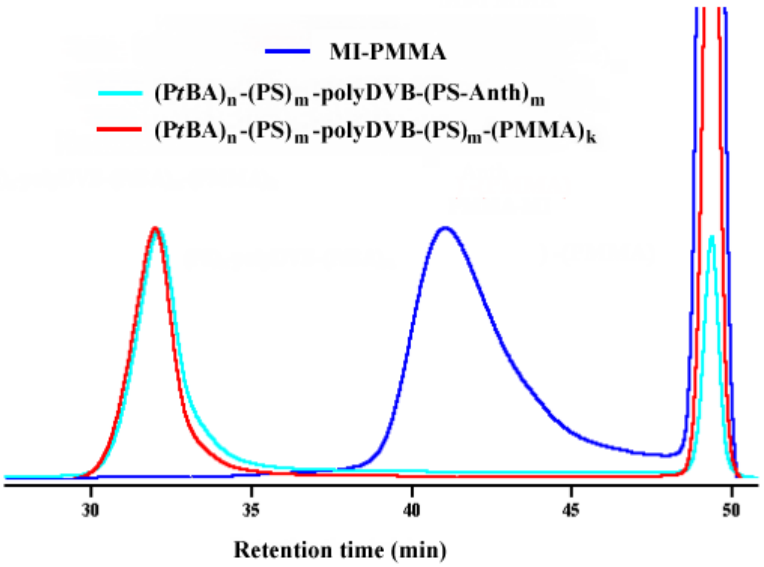

Figure 4.41 : GPC traces of (P*t*BA)$_n$-(PS)$_m$-polyDVB-(PS)$_m$-(PMMA)$_k$, (P*t*BA)$_n$-(PS)$_m$-polyDVB-(PS-Anth)$_m$, multiarm star polymer and linear MI-PMMA precursors using RI detector in THF at 30 ^{o}C.

Additionally, d*n*/dc values for all multi-miktoarm star block copolymers were calculated experimentally from a slope of RI area-concentration (g/mL) linear plot containing at least four different polymer concentrations. The calculation is based on an assumption that truly size-exclusion mechanism is operative in the columns of GPC. This experimental d*n*/d*c* values were subsequently introduced to the TD-GPC to give their corresponding $M_{w,TD\text{-}GPC}$, [η] and R_h of the analyzed multi-miktoarm star block copolymers (Table 4.8).

Table 4.8 : TD-GPC characterization of multiarm star and multi-miktoarm star block copolymers

Polymers	TD-GPC[a]						
	M_w/M_n	M_w (g/mol)	$M_{w,theo}$ (g/mol)	$[\eta]$ (dL/g)	R_h (nm)	dn/dc (mL/g)	f[f]
(Alkyne-PS)$_m$-polyDVB-(PS-Anth)$_m$[b]	(1.26)	(250000)	250000	(0.155)	8.28	(0.185)	31 (27)[g]
(P*t*BA)$_n$-(PS)$_m$-polyDVB-(PS-Anth)$_m$	1.25 (1.26)	355000 (350000)	321000[c]	0.142 (0.150)	9.03 (9.13)	0.146[e] (0.151)	- -
(P*t*BA)$_n$-(PS)$_m$-polyDVB-(PS)$_m$-(PMMA)$_k$	1.30 (1.31)	407000 (414000)	385000[d]	0.177 (0.171)	10.1 (10.0)	0.137[e] (0.133)	- -

[a]Data in parentheses are obtained from TD-GPC by using experimental dn/dc values.
[b][DVB]$_0$/15 = [PS-Br]$_0$ = [CuBr]$_0$ = [PMDETA]$_0$= 0.023 M in anisole at 110 °C. Then deprotection with TBAF at room temperature.
[c]$M_{w,theo}$ = M_w of (Alkyne-PS)$_m$-polyDVB-(PS-Anth)$_m$ + 17 X $M_{w,GPC}$ of linear P*t*BA-N$_3$.
[d]$M_{w,theo}$= $M_{w,theo}$ of (P*t*BA)$_n$-(PS)$_m$-polyDVB-(PS-Anth)$_m$ + 14 X $M_{w,GPC}$ of linear MI-PMMA).
[e]Calculated according to eq. 4.1.
[f] Calculated according to eq. 4.2.
[g] Calculated according to eqs. 4.3 and 4.4.

5. CONCLUSIONS

The objective of this thesis is to design and the synthesis of different macromolecular arhitectures with highly efficient click reactions, which have been recently shown to be modular tools for polymer synthesis. In particular two versatile click reactions, namely the CuAAC and Diels-Alder reaction, which have been intensively studied in our groups were employed to obtain graft and star copolymers via a variety of controlled polymerization methods.

In first study, the PS backbone was prepared successfully containing various amounts of antryl and azide pendant groups. Using the CuAAC and Diels-Alder click reactions in one-pot, two samples of PS-*g*-(PMMA-PEG) hetero graft copolymers were achieved with low polydispersity indices (1.15–1.17). A high click reaction efficiency of 94 and 90% for both hetero-graft copolymers was obtained from ^{1}H NMR measurement. Thus, it proved that double click reactions using a one-pot technique were versatile and simple strategy for the preparation of well-defined hetero-graft copolymer.

The second strategy consists of the synthesis of 3-arm star block copolymers, (PS-*b*-PMMA)$_3$ and (PS-*b*-PEG)$_3$ by using double click reactions (CuAAC and Diels-Alder) in a one-pot process. The deconvoluted GPC traces of the observed 3-arm star block copolymers displayed highly efficient double click reactions over 82% of yield. Moreover, the molecular weights of the observed 3-arm starblock copolymers measured by TD-GPC were found to have $M_{n,TD\text{-}GPC}$ = 23200 and 24300 g/mol and M_w/M_n = 1.06. Hence, it was demonstrated that the preparation of 3-arm star block copolymers via a combination of two click reactions in one-pot technique was successful.

The synthesis of multiarm star block and mixed-block copolymers by combination of CuAAC reaction with arm-first approach was the third strategy of this thesis. After cross-linking reaction, the average number of arms of multiarm (Alkyne-PS)$_n$-polyDVB star polymer was found to be ca 27 using two different calculation methods. This result enabled a proof for the well-defined structure and low degree of

heterogeneity of the multiarm star polymer. All star polymers were characterized by NMR, GPC, TD-GPC, AFM, and DLS. From TD-GPC, R_h values of all star polymers were calculated to be in the range of 8.4–10.2 nm. Moreover, star molecules were imaged on silicon substrates by AFM and had a diameter of ~16–18 nm in consistent with DLS measurements.

Following this study, a new efficient approach to prepare well-defined multi-miktoarm star block copolymers through a combination of 'arm-first' method with sequential double click reactions involving CuACC and Diels–Alder was presented. A mixture of anthracene and alkyne functional PS macroinitiators was first prepared by employing double ATRP initiators concurrently bearing proper functionalities. Then multiarm star PS with both alkyne and anthracene moieties at the periphery, $(\text{Alkyne-PS})_m$–polyDVB–$(\text{PS-Anth})_m$, was obtained by ATRP of DVB with the α-silyl-alkyne-PS-Br and Anth-PS-Br as macroinitiators. Equimolar concentrations of the ATRP initiators resulted in 17 and 14 arms out of a 31-arm star polymer bearing alkyne and anthracene, respectively. Next, linear P*t*BA and PMMA blocks were easily introduced into that 31-arm star polymer, $(\text{Alkyne-PS})_m$-polyDVB-$(\text{PS-Anth})_m$, via sequential double click reactions in order to give well-defined multi-miktoarm star block copolymers, $(\text{P}t\text{BA})_n$-$(\text{PS})_m$-polyDVB-$(\text{PS-Anth})_m$ and $(\text{P}t\text{BA})_n$-$(\text{PS})_m$-polyDVB-$(\text{PS})_m$-$(\text{PMMA})_k$, with narrow molecular weight distribution and higher molecular weights up to 400000 g/mol. Absolute molecular weight ($M_{w,\text{TD-GPC}}$), polydispersity index, R_h and [η] for all multiarm star polymers were measured by TD-GPC based on both calculated and experimental d*n*/d*c* values and $M_{w,\text{TD-GPC}}$ values were found to be reliable with $M_{w,\text{theo}}$ calculated from a sum of molecular weights of the core and the individual arms.

It is noteworthy to say that click chemistry is a versatile and efficient route for the preparation of well-defined macromolecules. Ultimately, their widespread acceptance and exploitation in polymer synthesis is justified by their seemingly unlimited potential to create a wide range of macromolecules with various architectures.

REFERENCES

[1] **Szwarc M., L.M., and Milkovich R.,** 1956. Polymerization Initiated by Electron Transfer to Monomer. A New Method of Formation of Block Polymers*, J. Am. Chem. Soc.*, **78,** 2656-2657.

[2] **Szwarc, M.**, 1956: Living Polymers*, Nature*, **178,** 1168-1169.

[3] **Miyamoto, M., Sawamoto, M., and Higashimura, T.,** 1984. Living Polymerization of Isobutyl Vinyl Ether with the Hydrogen Iodide Iodine Initiating System*, Macromolecules*, **17,** 265-268.

[4] **Webster, O.W.**, 1991. Living Polymerization Methods*, Science*, **251,** 887-893.

[5] **Webster, O.W., Hertler, W.R., Sogah, D.Y., Farnham, W.B., and Rajanbabu, T.V.**, 1983. Group-Transfer Polymerization .1. A New Concept for Addition Polymerization with Organo-Silicon Initiators*, J. Am. Chem. Soc.*, **105,** 5706-5708.

[6] **Gorman, C.B., Ginsburg, E.J., and Grubbs, R.H.**, 1993. Soluble, Highly Conjugated Derivatives of Polyacetylene from the Ring-Opening Metathesis Polymerization of Monosubstituted Cyclooctatetraenes - Synthesis and the Relationship between Polymer Structure and Physical-Properties*, J. Am. Chem. Soc.*, **115,** 1397-1409.

[7] **Matyjaszewski, K. and Davis, T.P.,** 2002. *Handbook of Radical Polymerization;* Wiley :Hoboken: NJ.

[8] **Johnson, C.H.J., Moad, G., Solomon, D.H., Spurling, T.H., and Vearing, D.J.**, 1990: The Application of Supercomputers in Modeling Chemical-Reaction Kinetics - Kinetic Simulation of Quasi-Living Radical Polymerization*, Aust. J. Chem.*, **43,** 1215-1230.

[9] **Matyjaszewski, K.**, 1995. Introduction to Living Polymerization, Living and/or Controlled Polymerization*, J. Phys. Org. Chem.*, **8,** 197-207.

[10] **Percec, V. and Tirrell, D.A.**, 2000. Living or Controlled?*, J. Polym. Sci., Part A: Polym. Chem.*, **38,** 1705-1705.

[11] **Georges, M.K., Veregin, R.P.N., Kazmaier, P.M., and Hamer, G.K.,** 1993. Narrow Molecular-Weight Resins by a Free-Radical Polymerization Process*, Macromolecules*, **26,** 2987-2988.

[12] **Hawker, C.J., Bosman, A.W., and Harth, E.,** 2001. New Polymer Synthesis by Nitroxide Mediated Living Radical Polymerizations*, Chem. Rev.*, **101,** 3661-3688.

[13] **Wang, J.S. and Matyjaszewski, K.**, 1995. Controlled Living Radical Polymerization - Atom-Transfer Radical Polymerization in the Presence of Transition-Metal Complexes*, J. Am. Chem. Soc.*, **117,** 5614-5615.

[14] **Kato, M., Kamigaito, M., Sawamoto, M., and Higashimura, T.,** 1995. Polymerization of Methyl-Methacrylate with the Carbon-tetrachloride dichlorotris(triphenylphosphine)Ruthenium(II) Methylaluminum Bis(2,6-di-tert-butylphenoxide) Initiating System - Possibility of Living Radical Polymerization*, Macromolecules*, **28,** 1721-1723.

[15] **Xia, J.H., Gaynor, S.G., and Matyjaszewski, K.**, 1998. Controlled/"Living" Radical Polymerization. Atom Transfer Radical Polymerization of Acrylates at Ambient Temperature*, Macromolecules*, **31,** 5958-5959.

[16] **Kamigaito, M., Ando, T., and Sawamoto, M.**, 2001. Metal-Catalyzed Living Radical Polymerization*, Chem. Rev.*, **101,** 3689-3745.

[17] **Matyjaszewski, K. and Xia, J.H.**, 2001. Atom Transfer Radical Polymerization*, Chem. Rev.*, **101,** 2921-2990.

[18] **Rizzardo, E., Chiefari, J., Mayadunne, R., Moad, G., and Thang, S.**, 2001. Tailored Polymer Architectures by Reversible Addition-Fragmentation Chain Transfer*, Macromolecular Symposia*, **174,** 209-212.

[19] **Chiefari, J., Chong, Y.K., Ercole, F., Krstina, J., Jeffery, J., Le, T.P.T., Mayadunne, R.T.A., Meijs, G.F., Moad, C.L., Moad, G., Rizzardo, E., and Thang, S.H.**, 1998. Living Free-Radical Polymerization by Reversible Addition-Fragmentation Chain Transfer: The RAFT Process*, Macromolecules*, **31,** 5559-5562.

[20] **Moad, G., Chiefari, J., Chong, Y.K., Krstina, J., Mayadunne, R.T.A., Postma, A., Rizzardo, E., and Thang, S.H.**, 2000. Living Free Radical Polymerization with Reversible Addition-Fragmentation Chain Transfer (the Life of Raft)*, Polym. Int.*, **49,** 993-1001.

[21] **Kolb, H.C., Finn, M.G., and Sharpless, K.B.**, 2001. Click Chemistry: Diverse Chemical Function from a Few Good Reactions*, Angew. Chem. Int. Ed.*, **40,** 2004-2021.

[22] **Matyjaszewski, K. and Gaynor, S.G.,** 2000. *In Applied Polymer Science*, p. 929, ed., C.D. Craver and C.E. Carraher., Oxford: Pergamon Press..

[23] **Hawker, C.J.**, 1996. Advances in 'Living' Free-Radical Polymerization: Architectural and Structural Control*, Trends in Polymer Science*, **4,** 183-188.

[24] **Sawamoto, M. and Kamigaito, M.**, 1996. Living Radical Polymerization Based on Transition Metal Complexes*, Trends in Polymer Science*, **4,** 371-377.

[25] **Fischer, H.**, 2001. The Persistent Radical Effect: A Principle for Selective Radical Reactions and Living Radical Polymerizations*, Chem. Rev.*, **101,** 3581-3610.

[26] **Otsu, T. and Yoshida, M.**, 1982. Role of Initiator-Transfer Agent-Terminator (Iniferter) in Radical Polymerizations - Polymer Design by Organic Disulfides as Iniferters*, Makromolekulare Chemie-Rapid Communications*, **3,** 127-132.

[27] **Barner-Kowollik, C., Davis, T.P., Heuts, J.P.A., Stenzel, M.H., Vana, P., and Whittaker, M.**, 2003. Rafting Down Under: Tales of Missing Radicals, Fancy Architectures, and Mysterious Holes*, J. Polym. Sci., Part A: Polym. Chem.*, **41,** 365-375.

[28] **Moad, G., Rizzardo, E., and Solomon, D.H.**, 1982. Selectivity of the Reaction of Free-Radicals with Styrene, *Macromolecules*, **15,** 909-914.

[29] **Druliner, J.D.**, 1991. Living Radical Polymerization Involving Oxygen-Centered Species Attached to Propagating Chain Ends, *Macromolecules*, **24,** 6079-6082.

[30] **De Leon-Saenz, E., Morales, G., Guerrero-Santos, R., and Gnanou, Y.**, 2000. New Insights into the Mechanism of 1,2-Bis(trimethylsilyloxy)-tetraphenylethane-Induced Free Radical Polymerization: Application to the Synthesis of Block and Graft Copolymers, *Macromol. Chem. Phys.*, **201,** 74-83.

[31] **Yamada, B., Nobukane, Y., and Miura, Y.**, 1998. Radical Polymerization of Styrene Mediated by 1,3,5-Triphenylverdazyl, *Polym. Bull.*, **41,** 539-544.

[32] **Steenbock, M., Klapper, M., and Mullen, K.**, 1998. Triazolinyl Radicals - New Additives for Controlled Radical Polymerization, *Macromol. Chem. Phys.*, **199,** 763-769.

[33] **Puts, R.D. and Sogah, D.Y.**, 1996. Control of Living Free-Radical Polymerization by a New Chiral Nitroxide and Implications for the Polymerization Mechanism, *Macromolecules*, **29,** 3323-3325.

[34] **Grimaldi, S., Finet, J.P., Le Moigne, F., Zeghdaoui, A., Tordo, P., Benoit, D., Fontanille, M., and Gnanou, Y.**, 2000. Acyclic Beta-Phosphonylated Nitroxides: A New Series of Counter-Radicals for "Living"/Controlled Free Radical Polymerization, *Macromolecules*, **33,** 1141-1147.

[35] **Benoit, D., Grimaldi, S., Robin, S., Finet, J.P., Tordo, P., and Gnanou, Y.**, 2000. Kinetics and Mechanism of Controlled Free-Radical Polymerization of Styrene and *n*-Butyl acrylate in the Presence of an Acyclic Beta-Phosphonylated Nitroxide, *J. Am. Chem. Soc.*, **122,** 5929-5939.

[36] **Benoit, D., Chaplinski, V., Braslau, R., and Hawker, C.J.**, 1999. Development of a Universal Alkoxyamine for "Living" Free Radical Polymerizations, *J. Am. Chem. Soc.*, **121,** 3904-3920.

[37] **Hawker, C.J., Barclay, G.G., and Dao, J.L.**, 1996. Radical Crossover in Nitroxide Mediated "Living" Free Radical Polymerizations, *J. Am. Chem. Soc.*, **118,** 11467-11471.

[38] **Veregin, R.P.N., Georges, M.K., Kazmaier, P.M., and Hamer, G.K.**, 1993. Free-Radical Polymerizations for Narrow Polydispersity Resins - Electron-Spin-Resonance Studies of the Kinetics and Mechanism, *Macromolecules*, **26,** 5316-5320.

[39] **Veregin, R.P.N., Georges, M.K., Hamer, G.K., and Kazmaier, P.M.**, 1995: Mechanism of Living Free-Radical Polymerizations with Narrow Polydispersity - Electron-Spin-Resonance and Kinetic-Studies, *Macromolecules*, **28,** 4391-4398.

[40] **Skene, W.G., Scaiano, J.C., Listigovers, N.A., Kazmaier, P.M., and Georges, M.K.**, 2000. Rate Constants for the Trapping of Various Carbon-Centered Radicals by Nitroxides: Unimolecular Initiators for Living Free Radical Polymerization, *Macromolecules*, **33,** 5065-5072.

[41] **Wang, J.S. and Matyjaszewski, K.**, 1995. Controlled Living Radical Polymerization - Halogen Atom-Transfer Radical Polymerization Promoted by a Cu(I)Cu(II) Redox Process*, Macromolecules*, **28,** 7901-7910.

[42] **Percec, V. and Barboiu, B.**, 1995. Living Radical Polymerization of Styrene Initiated by Arenesulfonyl Chlorides and Cu-I(Bpy)(N)Cl*, Macromolecules*, **28,** 7970-7972.

[43] **Goto, A. and Fukuda, T.**, 1999. Determination of the Activation Rate Constants of Alkyl Halide Initiators for Atom Transfer Radical Polymerization*, Macromol. Rapid Commun.*, **20,** 633-636.

[44] **Matyjaszewski, K.**, 1997. Mechanistic and Synthetic Aspects of Atom Transfer Radical Polymerization*, Journal of Macromolecular Science-Pure and Applied Chemistry*, **A34,** 1785-1801.

[45] **Patten, T.E. and Matyjaszewski, K.**, 1999. Copper(I)-Catalyzed Atom Transfer Radical Polymerization*, Acc. Chem. Res.*, **32,** 895-903.

[46] **Sonmez, H.B. and Bicak, N.**, 2002: Quaternization of Poly(4-vinyl pyridine) Beads with 2-Chloroacetamide for Selective Mercury Extraction*, Reactive & Functional Polymers*, **51,** 55-60.

[47] **Tunca, U., Hizal, G., Acar, M.H., Tasdelen, M.A., Yagci, Y., and Mishra, M.K.,** *Controlled/Living Radical Polymerization*, in *Handbook of Vinyl Polymers*, Y. Yagci and M.K. Mishra, Editors. 2009, CRC Press Taylor & Francis Group,: New York. p. 256-281.

[48] **Davis, K., Omalley, J., Paik, H.J., and Matyjaszewski, K.**, 1997. Effect of the Counteranion in Atom Transfer Radical Polymerization Using Alkyl (Pseudo) Halide Initiators*, Abstr. Pap. Am. Chem. Soc.*, **213,** 320-POLY.

[49] **Nishimura, M., Kamigaito, M., and Sawamoto, M.**, 1999. Living-Radical Polymerization of Styrene with Transition-Metal Dithiocarbamate/AIBN Systems: Halogen-Free Living Processes*, Abstr. Pap. Am. Chem. Soc.*, **218,** 521-POLY.

[50] **Singha, N.K. and Klumperman, B.**, 2000. Atom-Transfer Radical Polymerization of Methyl Methacrylate (MMA) Using Cuscn as the Catalyst*, Macromol. Rapid Commun.*, **21,** 1116-1120.

[51] **Matyjaszewski, K., Wang, J.L., Grimaud, T., and Shipp, D.A.**, 1998. Controlled/"Living" Atom Transfer Radical Polymerization of Methyl Methacrylate Using Various Initiation Systems*, Macromolecules*, **31,** 1527-1534.

[52] **Kotani, Y., Kamigaito, M., and Sawamoto, M.**, 1999. Re(V)-Mediated Living Radical Polymerization of Styrene: Reo2i(Pph3)(2)/R-I Initiating Systems*, Macromolecules*, **32,** 2420-2424.

[53] **Kato, M., Kamigaito, M., Sawamoto, M., and Higashimura, T.**, 1995. Polymerization of Methyl-Methacrylate with the Carbon-Tetrachloride Dichloride Dichlorotris(Triphenylphosphine)Ruthenium (II) Methylaliminum bis (2,6-di-ter-butylphenoxide) Initiating System Possibility of Living Radical Polymerization*, Macromolecules*, **28,** 1721-1723.

[54] **Simal, F., Demonceau, A., and Noels, A.F.**, 1999. Highly Efficient Ruthenium-Based Catalytic Systems for the Controlled Free-Radical Polymerization of Vinyl Monomers*, Angew. Chem. Int. Ed.*, **38,** 538-540.

[55] **Percec, V., Barboiu, B., Neumann, A., Ronda, J.C., and Zhao, M.Y.**, 1996. Metal-Catalyzed "Living" Radical Polymerization of Styrene Initiated with Arenesulfonyl Chlorides. From Heterogeneous to Homogeneous Catalysis*, Macromolecules*, **29,** 3665-3668.

[56] **Tang, H.D., Radosz, M., and Shen, Y.Q.**, 2009. Atom Transfer Radical Polymerization and Copolymerization of Vinyl Acetate Catalyzed by Copper Halide/Terpyridine*, AlChE J.*, **55,** 737-746.

[57] **Matyjaszewski, K., Wei, M.L., Xia, J.H., and McDermott, N.E.**, 1997. Controlled/"Living" Radical Polymerization of Styrene and Methyl Methacrylate Catalyzed by Iron Complexes*, Macromolecules*, **30,** 8161-8164.

[58] **Ando, T., Kamigaito, M., and Sawamoto, M.**, 1997. Iron(II) Chloride Complex for Living Radical Polymerization of Methyl Methacrylate*, Macromolecules*, **30,** 4507-4510.

[59] **O'Reilly, R.K., Gibson, V.C., White, A.J.P., and Williams, D.J.**, 2004. Five-Coordinate Iron(II) Complexes Bearing Tridentate Nitrogen Donor Ligands as Catalysts for Atom Transfer Radical Polymerisation*, Polyhedron*, **23,** 2921-2928.

[60] **Teodorescu, M., Gaynor, S.G., and Matyjaszewski, K.**, 2000. Halide Anions as Ligands in Iron-Mediated Atom Transfer Radical Polymerization*, Macromolecules*, **33,** 2335-2339.

[61] **Uchiike, C., Ouchi, M., Ando, T., Kamigaito, M., and Sawamoto, M.**, 2008. Evolution of Iron Catalysts for Effective Living Radical Polymerization: P-N Chelate Ligand for Enhancement of Catalytic Performances*, J. Polym. Sci., Part A: Polym. Chem.*, **46,** 6819-6827.

[62] **Granel, C., Dubois, P., Jerome, R., and Teyssie, P.**, 1996. Controlled Radical Polymerization of Methacrylic Monomers in the Presence of a Bis(ortho-chelated) Arylnickel(II) Complex and Different Activated Alkyl Halides*, Macromolecules*, **29,** 8576-8582.

[63] **Uegaki, H., Kotani, Y., Kamigaito, M., and Sawamoto, M.**, 1997. Nickel-Mediated Living Radical Polymerization of Methyl Methacrylate*, Macromolecules*, **30,** 2249-2253.

[64] **Riva, R., Schmeits, S., Jerome, C., Jerome, R., and Lecomte, P.**, 2007. Combination of Ring-Opening Polymerization and "Click Chemistry": Toward Functionalization and Grafting of Poly(epsilon-caprolactone)*, Macromolecules*, **40,** 796-803.

[65] **Woodworth, B.E., Metzner, Z., and Matyjaszewski, K.**, 1998. Copper Triflate as a Catalyst in Atom Transfer Radical Polymerization of Styrene and Methyl Acrylate*, Macromolecules*, **31,** 7999-8004.

[66] **Haddleton, D.M., Jasieczek, C.B., Hannon, M.J., and Shooter, A.J.**, 1997. Atom Transfer Radical Polymerization of Methyl Methacrylate Initiated by Alkyl Bromide and 2-Pyridinecarbaldehyde Imine Copper(I) Complexes*, Macromolecules*, **30,** 2190-2193.

[67] **Matyjaszewski, K., Patten, T.E., and Xia, J.H.**, 1997. Controlled/"Living" Radical Polymerization. Kinetics of the Homogeneous Atom Transfer Radical Polymerization*, J. Am. Chem. Soc.*, **119,** 674-680.

[68] **Matyjaszewski, K., Nakagawa, Y., and Jasieczek, C.B.**, 1998. Polymerization of *n*-Butyl Acrylate by Atom Transfer Radical Polymerization. Remarkable Effect of Ethylene Carbonate and Other Solvents*, Macromolecules*, **31,** 1535-1541.

[69] **Odian, G.,** 1991. In *Principles of Polymerization*, John Wiley & Sons: New York.

[70] **Hawker, C.J. and Hedrick, J.L.**, 1995. Accurate Control of Chain-Ends by a Novel Living Free-Radical Polymerization Process*, Macromolecules*, **28,** 2993-2995.

[71] **Gromada, J. and Matyjaszewski, K.**, 2001. Simultaneous Reverse and Normal Initiation in Atom Transfer Radical Polymerization*, Macromolecules*, **34,** 7664-7671.

[72] **Matyjaszewski, K., Jakubowski, W., Min, K., Tang, W., Huang, J.Y., Braunecker, W.A., and Tsarevsky, N.V.**, 2006. Diminishing Catalyst Concentration in Atom Transfer Radical Polymerization with Reducing Agents*, Proc. Natl. Acad. Sci. U.S.A.*, **103,** 15309-15314.

[73] **Mueller, L. and Matyjaszewski, K.**, 2010. Reducing Copper Concentration in Polymers Prepared via Atom Transfer Radical Polymerization*, Macromol. React. Eng.*, **4,** 180-185.

[74] **Pintauer, T. and Matyjaszewski, K.**, 2008. Atom Transfer Radical Addition and Polymerization Reactions Catalyzed by ppm Amounts of Copper Complexes*, Chem. Soc. Rev.*, **37,** 1087-1097.

[75] **Plichta, A., Li, W.W., and Matyjaszewski, K.**, 2009. ICAR ATRP of Styrene and Methyl Methacrylate with Ru(Cp*)Cl(Pph3)(2)*, Macromolecules*, **42,** 2330-2332.

[76] **Jakubowski, W., Min, K., and Matyjaszewski, K.**, 2006. Activators Regenerated by Electron Transfer for Atom Transfer Radical Polymerization of Styrene*, Macromolecules*, **39,** 39-45.

[77] **Tanaka, K. and Matyjaszewski, K.**, 2007. Controlled Copolymerization of *n*-Butyl Acrylate with Nonpolar 1-Alkenes Using Activators Regenerated by Electron Transfer for Atom-Transfer Radical Polymerization*, Macromolecules*, **40,** 5255-5260.

[78] **Jakubowski, W. and Matyjaszewski, K.**, 2005. Activator Generated by Electron Transfer for Atom Transfer Radical Polymerization*, Macromolecules*, **38,** 4139-4146.

[79] **Min, K., Gao, H.F., and Matyjaszewski, K.**, 2005. Preparation of Homopolymers and Block Copolymers in Miniemulsion by ATRP Using Activators Generated by Electron Transfer (AGET)*, J. Am. Chem. Soc.*, **127,** 3825-3830.

[80] **Min, K., Jakubowski, W., and Matyjaszewski, K.**, 2006. AGET ATRP in the Presence of Air in Miniemulsion and in Bulk*, Macromol. Rapid Commun.*, **27,** 594-598.

[81] **Percec, V., Guliashvili, T., Ladislaw, J.S., Wistrand, A., Stjerndahl, A., Sienkowska, M.J., Monteiro, M.J., and Sahoo, S.**, 2006. Ultrafast Synthesis of Ultrahigh Molar Mass Polymers by Metal-Catalyzed Living Radical Polymerization of Acrylates, Methacrylates, and Vinyl Chloride Mediated by Set at 25 Degrees C*, J. Am. Chem. Soc.*, **128,** 14156-14165.

[82] **Rosen, B.M. and Percec, V.**, 2008. Implications of Monomer and Initiator Structure on the Dissociative Electron-Transfer Step of SET-LRP*, Journal of Polymer Science Part a-Polymer Chemistry*, **46,** 5663-5697.

[83] **Rosen, B.M., Jiang, X., Wilson, C.J., Nguyen, N.H., Monteiro, M.J., and Percec, V.**, 2009. The Disproportionation of Cu(I)X Mediated by Ligand and Solvent into Cu(0) and Cu(II)X-2 and Its Implications for Set-Lrp*, J. Polym. Sci., Part A: Polym. Chem.*, **47,** 5606-5628.

[84] **Rosen, B.M. and Percec, V.**, 2009. Single-Electron Transfer and Single-Electron Transfer Degenerative Chain Transfer Living Radical Polymerization*, Chem. Rev.*, **109,** 5069-5119.

[85] **Nguyen, N.H. and Percec, V.**, 2010. Dramatic Acceleration of SET-LRP of Methyl Acrylate During Catalysis with Activated Cu(0) Wire*, J. Polym. Sci., Part A: Polym. Chem.*, **48,** 5109-5119.

[86] **Oh, J.K., Perineau, F., Charleux, B., and Matyjaszewski, K.**, 2009. AGET ATRP in Water and Inverse Miniemulsion: A Facile Route for Preparation of High-Molecular-Weight Biocompatible Brush-Like Polymers*, J. Polym. Sci., Part A: Polym. Chem.*, **47,** 1771-1781.

[87] **Min, K., Gao, H.F., and Matyjaszewski, K.**, 2007. Use of Ascorbic Acid as Reducing Agent for Synthesis of Well-Defined Polymers by ARGET ATRP*, Macromolecules*, **40,** 1789-1791.

[88] **Gnanou, Y. and Hizal, G.**, 2004. Effect of Phenol and Derivatives on Atom Transfer Radical Polymerization in the Presence of Air*, J. Polym. Sci., Part A: Polym. Chem.*, **42,** 351-359.

[89] **Mert, H., Tunca, U., and Hizal, G.**, 2006. Thiophenol Derivatives as a Reducing Agent for in Situ Generation of Cu(I) Species via Electron Transfer Reaction in Copper-Catalyzed Living/Controlled Radical Polymerization of Styrene*, J. Polym. Sci., Part A: Polym. Chem.*, **44,** 5923-5932.

[90] **Dag, A., Mert, H., Dervaux, B., Du Prez, F.E., Tunca, U., and Hizal, G.**, 2007. Fructose as a Reducing Agent for in Situ Generation of Cu(I) Species via an Electron-Transfer Reaction in Copper-Catalyzed Living/Controlled Radical Polymerization of Styrene*, Des. Monomers Polym.*, **10,** 425-438.

[91] **Barner-Kowollik, C.,** 2008. *Handbook of Raft Polymerization*, Weinheim: Wiley-VCH.

[92] **Moad, G., Rizzardo, E., and Thang, S.H.**, 2006. Living Radical Polymerization by the RAFT Process - A First Update*, Aust. J. Chem.*, **59,** 669-692.

[93] **Moad, G., Rizzardo, E., and Thang, S.H.**, 2009. Living Radical Polymerization by the RAFT Process - A Second Update*, Aust. J. Chem.*, **62,** 1402-1472.

[94] **Moad, G., Rizzardo, E., and Thang, S.H.**, 2008. Toward Living Radical Polymerization*, Acc. Chem. Res.*, **41,** 1133-1142.

[95] **Alberti, A., Benaglia, M., Laus, M., Macciantelli, D., and Sparnacci, K.**, 2003. Direct ESR Detection of Free Radicals in the RAFT Polymerization of Styrene*, Macromolecules*, **36,** 736-740.

[96] **Convertine, A.J., Ayres, N., Scales, C.W., Lowe, A.B., and McCormick, C.L.**, 2004. Facile, Controlled, Room-Temperature RAFT Polymerization of N-Isopropylacrylamide*, Biomacromolecules*, **5,** 1177-1180.

[97] **Quinn, J.F., Rizzardo, E., and Davis, T.P.**, 2001. Ambient Temperature Reversible Addition-Fragmentation Chain Transfer Polymerisation*, Chem. Commun.*, 1044-1045.

[98] **Quinn, J.F., Barner, L., Barner-Kowollik, C., Rizzardo, E., and Davis, T.P.**, 2002. Reversible Addition-Fragmentation Chain Transfer Polymerization Initiated with Ultraviolet Radiation*, Macromolecules*, **35,** 7620-7627.

[99] **Bai, R.K., You, Y.Z., and Pan, C.Y.**, 2001. Co-60 Gamma-Irradiation-Initiated "Living" Free-Radical Polymerization in the Presence of Dibenzyl Trithiocarbonate*, Macromol. Rapid Commun.*, **22,** 315-319.

[100] **Barner, L., Quinn, J.F., Barner-Kowollik, C., Vana, P., and Davis, T.P.**, 2003. Reversible Addition-Fragmentation Chain Transfer Polymerization Initiated with Gamma-Radiation at Ambient Temperature: An Overview*, Eur. Polym. J.*, **39,** 449-459.

[101] **Huisgen, R.**, 1963. 1.3-Dipolare Cycloadditionen - Ruckschau Und Ausblick*, Angew. Chem. Int. Ed.*, **75,** 604-637.

[102] **Tornoe, C.W., Christensen, C., and Meldal, M.**, 2002. Peptidotriazoles on Solid Phase: 1,2,3 -Triazoles by Regiospecific Copper(I)-Catalyzed 1,3-Dipolar Cycloadditions of Terminal Alkynes to Azides*, J. Org. Chem.*, **67,** 3057-3064.

[103] **Gothelf, K.V. and Jorgensen, K.A.**, 1998. Asymmetric 1,3-Dipolar Cycloaddition Reactions*, Chem. Rev.*, **98,** 863-909.

[104] **Appukkuttan, P., Dehaen, W., Fokin, V.V., and Van der Eycken, E.**, 2004. A Microwave-Assisted Click Chemistry Synthesis of 1,4-Disubstituted 1,2,3-Triazoles via a Copper(I)-Catalyzed Three-Component Reaction*, Org. Lett.*, **6,** 4223-4225.

[105] **Rostovtsev, V.V., Green, L.G., Fokin, V.V., and Sharpless, K.B.**, 2002. A Stepwise Huisgen Cycloaddition Process: Copper(I)-Catalyzed Regioselective "Ligation" of Azides and Terminal Alkynes*, Angew. Chem. Int. Ed.*, **41,** 2596-2599.

[106] **Rodionov, V.O., Fokin, V.V., and Finn, M.G.**, 2005. Mechanism of the Ligand-Free Cu-I-Catalyzed Azide-Alkyne Cycloaddition Reaction*, Angew. Chem. Int. Ed.*, **44,** 2210-2215.

[107] **Punna, S., Kuzelka, J., Wang, Q., and Finn, M.G.**, 2005. Head-to-Tail Peptide Cyclodimerization by Copper-Catalyzed Azide-Alkyne Cycloaddition*, Angew. Chem. Int. Ed.*, **44,** 2215-2220.

[108] **Molteni, G. and Ponti, A.**, 2003. Arylazide Cycloaddition to Methyl Propiolate: Dft-Based Quantitative Prediction of Regioselectivity, *Chemistry-A European Journal*, **9,** 2770-2774.

[109] **Himo, F., Lovell, T., Hilgraf, R., Rostovtsev, V.V., Noodleman, L., Sharpless, K.B., and Fokin, V.V.**, 2005. Copper(I)-Catalyzed Synthesis of Azoles. Dft Study Predicts Unprecedented Reactivity and Intermediates, *J. Am. Chem. Soc.*, **127,** 210-216.

[110] **Bock, V.D., Hiemstra, H., and van Maarseveen, J.H.**, 2006. Cu-I-Catalyzed Alkyne-Azide "Click" Cycloadditions from a Mechanistic and Synthetic Perspective, *Eur. J. Org. Chem.*, 51-68.

[111] **Straub, B.F.**, 2007. Mu-Acetylide and Mu-Alkenylidene Ligands in "Click" Triazole Syntheses, *Chem. Commun.*, 3868-3870.

[112] **Meng, J.C., Fokin, V.V., and Finn, M.G.**, 2005. Kinetic Resolution by Copper-Catalyzed Azide-Alkyne Cycloaddition, *Tetrahedron Lett.*, **46,** 4543-4546.

[113] **Wu, P., Feldman, A.K., Nugent, A.K., Hawker, C.J., Scheel, A., Voit, B., Pyun, J., Frechet, J.M.J., Sharpless, K.B., and Fokin, V.V.**, 2004. Efficiency and Fidelity in a Click-Chemistry Route to Triazole Dendrimers by the Copper(I)-Catalyzed Ligation of Azides and Alkynes, *Angew. Chem. Int. Ed.*, **43,** 3928-3932.

[114] **Diels, O.a.A., K.**, 1928. Synthesen in Der Hydroaromatischen Reihe, Justus Liebig's Annalen Der Chemie, *460*, 98-122.

[115] **Fringuelli, F.a.T., A.**, 1990. Dienes in the Diels-Alder Reaction, *Jhon Wiley: New York*.

[116] **Stein, K.A.a.G.**, 1937. *Angew. Chem. Int. Ed.*, **50,** 510-519.

[117] **Alder, K., and Vogt, W.** , 1951. *Liebigs Ann. Chem.*, **571,** 137-152.

[118] **Alder, K., and Schumacher, M.**, 1951. *Liebigs Ann. Chem.*, **571,** 87-107.

[119] **Alder, K., and Schumacher, M.**, 1951. *Liebigs Ann. Chem.*, **571,** 108-122.

[120] **Fleming, I.**, 1976. Frontier Orbitals Organic Chemical Reactions, Chapter 4, p. 114-142, Jhon Wiley: New York

[121] **Woodward, R.B.a.H., R.**, 1965. Stereochemistry of Electrocyclic Reactions, *J. Am. Chem. Soc.*, **87,** 395-397.

[122] **Woodward, R.B.a.H., R.**, 1970. The Conservation of Orbital Symmetry, *Weinheim/Bergstr.: Verlag Chemie*.

[123] **Birney, D.M. and Houk, K.N.**, 1990. Transition Structures of the Lewis Acid-Catalyzed Diels-Alder Reaction of Butadiene with Acrolein - the Origins of Selectivity, *J. Am. Chem. Soc.*, **112,** 4127-4133.

[124] **Fringuelli, F. and Taticchi, A.,** 2002. *The Diels Alder Reaction: Selected Practical Methods*. Chichester; New York: Wiley.

[125] **Pindur, U., Lutz, G., and Otto, C.**, 1993. Acceleration and Selectivity Enhancement of Diels-Alder Reactions by Special and Catalytic Methods, *Chem. Rev.*, **93,** 741-761.

[126] **Houk, K.N.a.S., R.W.**, 1973. Lewis Acid Catalysis of Diels-Alder Reactions*, J. Am. Chem. Soc.*, **95,** 4094-4096.

[127] **Fleming**, 1990. Orbitals and Organic Chemical Reactions:*, Wiley: New York*, .

[128] **Paquette, L.**, 1984. *Synthesis: Morrison, J.D., Ed.; Accademic Press: Orlando*, **3,** 455.

[129] **Sauer, J.a.K., J.**, 1966. *Tetrahedron Lett.*, 731-736.

[130] **Sauer, J.**, 1967. *Angew. Chem. Int. Ed.*, **6,** 16.

[131] **Sauer, J. and Sustmann, R.**, 1980. Mechanistic Aspects of Diels-Alder Reactions - A Critical Survey*, Angew. Chem. Int. Ed.*, **19,** 779-807.

[132] **Cativiela, C., Garcia, J.I., Mayoral, J.A., and Salvatella, L.**, 1996. Modelling of Solvent Effects on the Diels-Alder Reaction*, Chem. Soc. Rev.*, **25,** 209-&.

[133] **Kumar, A.**, 2001. Salt Effects on Diels-Alder Reaction Kinetics*, Chem. Rev.*, **101,** 1-19.

[134] **Durmaz, H., Colakoclu, B., Tunca, U., and Hizal, G.**, 2006. Preparation of Block Copolymers Via Diels Alder Reaction of Maleimide- and Anthracene-End Functionalized Polymers*, J. Polym. Sci., Part A: Polym. Chem.*, **44,** 1667-1675.

[135] **Durmaz, H., Dag, A., Altintas, O., Erdogan, T., Hizal, G., and Tunca, U.**, 2007. One-Pot Synthesis of Abc Type Triblock Copolymers via in Situ Click [3+2] and Diels-Alder [4+2] Reactions*, Macromolecules*, **40,** 191-198.

[136] **Dag, A., Durmaz, H., Hizal, G., and Tunca, U.**, 2008. Preparation of 3-Arm Star Polymers (A(3)) via Diels-Alder Click Reaction*, J. Polym. Sci., Part A: Polym. Chem.*, **46,** 302-313.

[137] **Kose, M.M., Yesilbag, G., and Sanyal, A.**, 2008. Segment Block Dendrimers via Diels-Alder Cycloaddition*, Org. Lett.*, **10,** 2353-2356.

[138] **Tonga, M., Cengiz, N., Kose, M.M., Dede, T., and Sanyal, A.**, 2010. Dendronized Polymers via Diels-Alder "Click" Reaction*, J. Polym. Sci., Part A: Polym. Chem.*, **48,** 410-416.

[139] **Vieyres, A., Lam, T., Gillet, R., Franc, G., Castonguay, A., and Kakkar, A.**, 2010. Combined Cu-I-Catalysed Alkyne-Azide Cycloaddition and Furan-Maleimide Diels-Alder "Click" Chemistry Approach to Thermoresponsive Dendrimers*, Chem. Commun.*, **46,** 1875-1877.

[140] **Franc, G. and Kakkar, A.K.**, 2010. "Click" Methodologies: Efficient, Simple and Greener Routes to Design Dendrimers*, Chem. Soc. Rev.*, **39,** 1536-1544.

[141] **Gacal, B., Durmaz, H., Tasdelen, M.A., Hizal, G., Tunca, U., Yagci, Y., and Demirel, A.L.**, 2006. Anthracene-Maleimide-Based Diels-Alder "Click Chemistry" as a Novel Route to Graft Copolymers*, Macromolecules*, **39,** 5330-5336.

[142] **Durmaz, H., Dag, A., Cerit, N., Sirkecioglu, O., Hizal, G., and Tunca, U.**, 2010. Graft Copolymers via ROMP and Diels-Alder Click Reaction Strategy*, J. Polym. Sci., Part A: Polym. Chem.*, **48,** 5982-5991.

[143] **Dag, A., Sahin, H., Durmaz, H., Hizal, G., and Tunca, U.**, 2011. Block-Brush Copolymers Via Romp and Sequential Double Click Reaction Strategy*, J. Polym. Sci., Part A: Polym. Chem.*, **49,** 886-892.

[144] **Dondoni, A.**, 2008. The Emergence of Thiol-Ene Coupling as a Click Process for Materials and Bioorganic Chemistry*, Angew. Chem. Int. Ed.*, **47,** 8995-8997.

[145] **Hoyle, C.E. and Bowman, C.N.**, 2010. Thiol-Ene Click Chemistry*, Angew. Chem. Int. Ed.*, **49,** 1540-1573.

[146] **Morgan, C.R., Magnotta, F., and Ketley, A.D.**, 1977. Thiol-Ene Photo-Curable Polymers*, J. Polym. Sci., Part A: Polym. Chem.*, **15,** 627-645.

[147] **Griesbau.K**, 1970. Problems and Possibilities of Free-Radical Addition of Thiols to Unsaturated Compounds*, Angew. Chem. Int. Ed.*, **9,** 273-&.

[148] **Mather, B.D., Viswanathan, K., Miller, K.M., and Long, T.E.**, 2006. Michael Addition Reactions in Macromolecular Design for Emerging Technologies*, Prog. Polym. Sci.*, **31,** 487-531.

[149] **Chan, J.W., Yu, B., Hoyle, C.E., and Lowe, A.B.**, 2008. Convergent Synthesis of 3-Arm Star Polymers from RAFT-Prepared Poly(*N*,*N*-diethylacrylamide) Via a Thiol-Ene Click Reaction*, Chem. Commun.*, 4959-4961.

[150] **Killops, K.L., Campos, L.M., and Hawker, C.J.**, 2008. Robust, Efficient, and Orthogonal Synthesis of Dendrimers Via Thiol-Ene "Click" Chemistry*, J. Am. Chem. Soc.*, **130,** 5062-+.

[151] **Campos, L.M., Killops, K.L., Sakai, R., Paulusse, J.M.J., Damiron, D., Drockenmuller, E., Messmore, B.W., and Hawker, C.J.**, 2008. Development of Thermal and Photochemical Strategies for Thiol-Ene Click Polymer Functionalization*, Macromolecules*, **41,** 7063-7070.

[152] **Pounder, R.J., Stanford, M.J., Brooks, P., Richards, S.P., and Dove, A.P.**, 2008. Metal Free Thiol-Maleimide 'Click' Reaction as a Mild Functionalisation Strategy for Degradable Polymers*, Chem. Commun.*, 5158-5160.

[153] **Boyer, C., Granville, A., Davis, T.P., and Bulmus, V.**, 2009. Modification of RAFT-Polymers Via Thiol-Ene Reactions: A General Route to Functional Polymers and New Architectures*, J. Polym. Sci., Part A: Polym. Chem.*, **47,** 3773-3794.

[154] **Lowe, A.B.**, 2010. Thiol-Ene "Click" Reactions and Recent Applications in Polymer and Materials Synthesis*, Polym. Chem.*, **1,** 17-36.

[155] **Kade, M.J., Burke, D.J., and Hawker, C.J.**, 2010. The Power of Thiol-Ene Chemistry*, J. Polym. Sci., Part A: Polym. Chem.*, **48,** 743-750.

[156] **Takaki, M., Asami, R., and Kuwata, Y.**, 1979. Preparation of Well-Defined Polymers by Polymer-Coupling Reaction .6. Side Reactions in the Grafting Reaction of Living Polystyrene with Polymers Having Pendant Benzylic Halides*, Macromolecules*, **12,** 378-382.

[157] **Gauthier, M. and Moller, M.**, 1991. Uniform Highly Branched Polymers by Anionic Grafting - Arborescent Graft Polymers*, Macromolecules*, **24,** 4548-4553.

[158] **Ryu, S.W. and Hirao, A.**, 2000. Anionic Synthesis of Well-Defined Poly(m-halomethylstyrene)s and Branched Polymers via Graft-onto Methodology*, Macromolecules*, **33,** 4765-4771.

[159] **Xenidou, M. and Hadjichristidis, N.**, 1998. Synthesis of Model Multigraft Copolymers of Butadiene with Randomly Placed Single and Double Polystyrene Branches*, Macromolecules*, **31,** 5690-5694.

[160] **Rahlwes, D., Roovers, J.E.L., and Bywater, S.**, 1977. Synthesis and Characterization of Poly(styrene-*g*-isoprene) Copolymers*, Macromolecules*, **10,** 604-609.

[161] **Roovers, J.**, 1979. Synthesis and Dilute-Solution Characterization of Comb Polystyrenes*, Polymer*, **20,** 843-849.

[162] **Cameron, G.G. and Qureshi, M.Y.**, 1981. Grafting of Polybutadiene Functionalized with Chlorosilane Groups*, Makromolekulare Chemie-Rapid Communications*, **2,** 287-291.

[163] **Fu, Q., Lin, W.C., and Huang, J.L.**, 2008. A New Strategy for Preparation of Graft Copolymers Via "Graft onto" by Atom Transfer Nitroxide Radical Coupling Chemistry: Preparation of Poly(4-glycidyloxy-2,2,6,6-tetramethylpiperidine-1-oxyl-co-ethylene oxide)-graft-Polystyrene and Poly(*tert*-Butyl Acrylate)*, Macromolecules*, **41,** 2381-2387.

[164] **Gao, H.F. and Matyjaszewski, K.**, 2007. Synthesis of Molecular Brushes by "Grafting onto" Method: Combination of ATRP and Click Reactions*, J. Am. Chem. Soc.*, **129,** 6633-6639.

[165] **Tsarevsky, N.V., Bencherif, S.A., and Matyjaszewski, K.**, 2007. Graft Copolymers by a Combination of ATRP and Two Different Consecutive Click Reactions*, Macromolecules*, **40,** 4439-4445.

[166] **Quemener, D., Le Hellaye, M., Bissett, C., Davis, T.P., Barner-Kowollik, C., and Stenzel, M.H.**, 2008. Graft Block Copolymers of Propargyl Methacrylate and Vinyl Acetate via a Combination of RAFT/Madix and Click Chemistry: Reaction Analysis*, J. Polym. Sci., Part A: Polym. Chem.*, **46,** 155-173.

[167] **S. Cesana, A.K., M. A. Baur, and J. Auernheimer, O.N.**, 2007. Polymer-Bound Thiol Groups on Poly(2-oxazoline)s*, Macromol. Rapid Commun.*, **28,** 608–615.

[168] **Ruokolainen, J., Torkkeli, M., Serimaa, R., Komanschek, E., tenBrinke, G., and Ikkala, O.**, 1997. Order-Disorder Transition in Comblike Block Copolymers Obtained by Hydrogen Bonding between Homopolymers and End-Functionalized Oligomers: Poly(4-vinylpyridine)-pentadecylphenol*, Macromolecules*, **30,** 2002-2007.

[169] **Ruokolainen, J., Tanner, J., Ikkala, O., ten Brinke, G., and Thomas, E.L.**, 1998. Direct Imaging of Self-Organized Comb Copolymer-Like Systems Obtained by Hydrogen Bonding: Poly(4-Vinylpyridine)-4-Nonadecylphenol*, Macromolecules*, **31,** 3532-3536.

[170] **Orfanou, K., Topouza, D., Sakellariou, G., and Pispas, S.**, 2003. Graftlike Interpolymer Complexes from Poly(2-vinylpyridine) and End-Sulfonic Acid Polystyrene and Polyisoprene: Intermediates to Noncovalently Bonded Block Copolymer-Like Micelles*, J. Polym. Sci., Part A: Polym. Chem.*, **41,** 2454-2461.

[171] **Bazuin, C.G. and Tork, A.**, 1995. Generation of Liquid Crystalline Polymeric Materials from Non Liquid Crystalline Components via Ionic Complexation*, Macromolecules*, **28,** 8877-8880.

[172] **Ikkala, O., Ruokolainen, J., Tenbrinke, G., Torkkeli, M., and Serimaa, R.**, 1995. Mesomorphic State of Poly(Vinylpyridine)-Dodecylbenzenesulfonic Acid Complexes in Bulk and in Xylene Solution*, Macromolecules*, **28,** 7088-7094.

[173] **Antonietti, M., Conrad, J., and Thunemann, A.**, 1994. Polyelectrolyte-Surfactant Complexes - A New-Type of Solid, Mesomorphous Material*, Macromolecules*, **27,** 6007-6011.

[174] **Schubert, U.S. and Hofmeier, H.**, 2002. Metallo-Supramolecular Graft Copolymers: A Novel Approach toward Polymer-Analogous Reactions*, Macromol. Rapid Commun.*, **23,** 561-566.

[175] **Falk, J.C., Schlott, R.J., and Hoeg, D.F.**, 1973. Anionic Graft Copolymers .1. Vinylaromatic Grafts on Polydienes*, Journal of Macromolecular Science-Chemistry*, **A 7,** 1647-1662.

[176] **Hadjichristidis, N. and Roovers, J.**, 1978. Conformation of Poly(isoprene-*g*-styrene) in Dilute-Solution*, J. Polym. Sci., Part B: Polym. Phys*, **16,** 851-858.

[177] **Beers, K.L., Gaynor, S.G., Matyjaszewski, K., Sheiko, S.S., and Moller, M.**, 1998. The Synthesis of Densely Grafted Copolymers by Atom Transfer Radical Polymerization*, Macromolecules*, **31,** 9413-9415.

[178] **Grubbs, R.B., Hawker, C.J., Dao, J., and Frechet, J.M.J.**, 1997. A Tandem Approach to Graft and Dendritic Graft Copolymers Based on "Living" Free Radical Polymerizations*, Angew. Chem. Int. Ed.*, **36,** 270-272.

[179] **Inceoglu, S., Hizal, G., and Tunca, U.**, 2004. Synthesis of Styrene-Methyl Methacrylate Graft and Block-Graft Copolymers via Combination of Atom Transfer Radical Polymerization and Stable Free Radical Polymerization*, Des. Monomers Polym.*, **7,** 203-214.

[180] **Borner, H.G., Beers, K., Matyjaszewski, K., Sheiko, S.S., and Moller, M.**, 2001. Synthesis of Molecular Brushes with Block Copolymer Side Chains Using Atom Transfer Radical Polymerization*, Macromolecules*, **34,** 4375-4383.

[181] **Lee, H.I., Matyjaszewski, K., Yu-Su, S., and Sheiko, S.S.**, 2008. Hetero-Grafted Block Brushes with PCL and PBA Side Chains*, Macromolecules*, **41,** 6073-6080.

[182] **Cheng, G.L., Boker, A., Zhang, M.F., Krausch, G., and Muller, A.H.E.**, 2001. Amphiphilic Cylindrical Core-Shell Brushes via a "Grafting from" Process Using ATRP*, Macromolecules*, **34,** 6883-6888.

[183] **Min, K., Yu, S., Lee, H.I., Mueller, L., Sheiko, S.S., and Matyjaszewski, K.**, 2007. High Yield Synthesis of Molecular Brushes via ATRP in Miniemulsion, *Macromolecules*, **40,** 6557-6563.

[184] **Yamada, K., Miyazaki, M., Ohno, K., Fukuda, T., and Minoda, M.**, 1999. Atom Transfer Radical Polymerization of Poly(vinyl ether) Macromonomers, *Macromolecules*, **32,** 290-293.

[185] **Christodoulou, S., Iatrou, H., Lohse, D.J., and Hadjichristidis, N.**, 2005. Anionic Copolymerization of Styrenic-Tipped Macromonomers: A Route to Novel Triblock-Comb Copolymers of Styrene and Isoprene, *J. Polym. Sci., Part A: Polym. Chem.*, **43,** 4030-4039.

[186] **Xia, Y., Kornfield, J.A., and Grubbs, R.H.**, 2009. Efficient Synthesis of Narrowly Dispersed Brush Polymers via Living Ring-Opening Metathesis Polymerization of Macromonomers, *Macromolecules*, **42,** 3761-3766.

[187] **Hadjichristidis, N., Iatrou, H., Pitsikalis, M., and Mays, J.**, 2006. Macromolecular Architectures by Living and Controlled/Living Polymerizations, *Prog. Polym. Sci.*, **31,** 1068-1132.

[188] **Gnanou, Y. and Taton, D.**, 2001. Stars and Dendrimer-Like Architectures by the Divergent Method Using Controlled Radical Polymerization, *Macromolecular Symposia*, **174,** 333-341.

[189] **Tsitsilianis, C., Lutz, P., Graff, S., Lamps, J.P., and Rempp, P.**, 1991. Core-1st Synthesis of Star Polymers with Potentially Ionogenic Branches, *Macromolecules*, **24,** 5897-5902.

[190] **Lutz, P. and Rempp, P.**, 1988. New Developments in Star Polymer Synthesis - Star-Shaped Polystyrenes and Star-Block Copolymers, *Makromolekulare Chemie-Macromolecular Chemistry and Physics*, **189,** 1051-1060.

[191] **Quirk, R.P. and Tsai, Y.S.**, 1998. Trifunctional Organolithium Initiator Based on 1,3,5-Tris(1-phenylethenyl)benzene. Synthesis of Functionalized, Three-Armed, Star-Branched Polystyrenes, *Macromolecules*, **31,** 8016-8025.

[192] **Shohi, H., Sawamoto, M., and Higashimura, T.**, 1991. Tri-Armed Star Polymers by Living Cationic Polymerization .1. Trifunctional Initiators for Living Polymerization of Isobutyl Vinyl Ether, *Macromolecules*, **24,** 4926-4931.

[193] **Matyjaszewski, K.**, 2003. The Synthesis of Functional Star Copolymers as an Illustration of the Importance of Controlling Polymer Structures in the Design of New Materials, *Polym. Int.*, **52,** 1559-1565.

[194] **Matyjaszewski, K., Miller, P.J., Fossum, E., and Nakagawa, Y.**, 1998. Synthesis of Block, Graft and Star Polymers from Inorganic Macroinitiators, *Appl. Organomet. Chem.*, **12,** 667-673.

[195] **Angot, S., Murthy, K.S., Taton, D., and Gnanou, Y.**, 1998. Atom Transfer Radical Polymerization of Styrene Using a Novel Octafunctional Initiator: Synthesis of Well-Defined Polystyrene Stars, *Macromolecules*, **31,** 7218-7225.

[196] **Heise, A., Nguyen, C., Malek, R., Hedrick, J.L., Frank, C.W., and Miller, R.D.**, 2000. Starlike Polymeric Architectures by Atom Transfer Radical Polymerization: Templates for the Production of Low Dielectric Constant Thin Films, *Macromolecules*, **33,** 2346-2354.

[197] **Matyjaszewski, K., Miller, P.J., Pyun, J., Kickelbick, G., and Diamanti, S.**, 1999. Synthesis and Characterization of Star Polymers with Varying Arm Number, Length, and Composition from Organic and Hybrid Inorganic/Organic Multifunctional Initiators, *Macromolecules*, **32,** 6526-6535.

[198] **Costa, R.O.R., Vasconcelos, W.L., Tamaki, R., and Laine, R.M.**, 2001. Organic/Inorganic Nanocomposite Star Polymers Via Atom Transfer Radical Polymerization of Methyl Methacrylate Using Octafunctional Silsesquioxane Cores, *Macromolecules*, **34,** 5398-5407.

[199] **Narrainen, A.P., Pascual, S., and Haddleton, D.M.**, 2002. Amphiphilic Diblock, Triblock, and Star Block Copolymers by Living Radical Polymerization: Synthesis and Aggregation Behavior, *J. Polym. Sci., Part A: Polym. Chem.*, **40,** 439-450.

[200] **Hawker, C.J.**, 1995. Architectural Control in Living Free-Radical Polymerizations - Preparation of Star and Graft Polymers, *Angew. Chem. Int. Ed.*, **34,** 1456-1459.

[201] **Erdogan, T., Ozyurek, Z., Hizal, G., and Tunca, U.**, 2004. Facile Synthesis of AB2)-Type Miktoarm Star Polymers through the Combination of Atom Transfer Radical Polymerization and Ring-Opening Polymerization, *J. Polym. Sci., Part A: Polym. Chem.*, **42,** 2313-2320.

[202] **Tunca, U., Ozyurek, Z., Erdogan, T., and Hizal, G.**, 2004. Novel Miktofunctional Initiator for the Preparation of an ABC-Type Miktoarm Star Polymer via a Combination of Controlled Polymerization Techniques, *J. Polym. Sci., Part A: Polym. Chem.*, **42,** 4228-4236.

[203] **Celik, C., Hizal, G., and Tunca, U.**, 2003. Synthesis of Miktoarm Star and Miktoarm Star Block Copolymers via a Combination of Atom Transfer Radical Polymerization and Stable Free-Radical Polymerization, *J. Polym. Sci., Part A: Polym. Chem.*, **41,** 2542-2548.

[204] **Erdogan, T., Gungor, E., Durmaz, H., Hizal, G., and Tunca, U.**, 2006. Photoresponsive Poly(methyl methacrylate)(2)-(Polystyrene)(2) Miktoarm Star Copolymer Containing an Azobenzene Moiety at the Core, *J. Polym. Sci., Part A: Polym. Chem.*, **44,** 1396-1403.

[205] **Zilliox J-G, R.P., Parrod J.**, 1968. *J Polym Sci Part C*, **22,** 145-156.

[206] **Kanaoka, S., Sawamoto, M., and Higashimura, T.**, 1991. Star-Shaped Polymers by Living Cationic Polymerization .1. Synthesis of Star-Shaped Polymers of Alkyl Vinyl Ethers, *Macromolecules*, **24,** 2309-2313.

[207] **Xia, J.H., Zhang, X., and Matyjaszewski, K.**, 1999. Synthesis of Star-Shaped Polystyrene by Atom Transfer Radical Polymerization Using an "Arm First" Approach, *Macromolecules*, **32,** 4482-4484.

[208] **Zhang, X., Xia, J.H., and Matyjaszewski, K.**, 2000. End-Functional Poly(*tert*-butyl acrylate) Star Polymers by Controlled Radical Polymerization*, Macromolecules*, **33,** 2340-2345.

[209] **Baek, K.Y., Kamigaito, M., and Sawamoto, M.**, 2001. Star-Shaped Polymers by Metal-Catalyzed Living Radical Polymerization. 1. Design of Ru(II)-Based Systems and Divinyl Linking Agents*, Macromolecules*, **34,** 215-221.

[210] **Baek, K.Y., Kamigaito, M., and Sawamoto, M.**, 2001. Core-Functionalized Star Polymers by Transition Metal-Catalyzed Living Radical Polymerization. 1. Synthesis and Characterization of Star Polymers with PMMA Arms and Amide Cores*, Macromolecules*, **34,** 7629-7635.

[211] **Baek, K.Y., Kamigaito, M., and Sawamoto, M.**, 2002. Star-Shaped Polymers by Ru(II)-Catalyzed Living Radical Polymerization. Ii. Effective Reaction Conditions and Characterization by Multi-Angle Laser Light Scattering/Size Exclusion Chromatography and Small-Angle X-Ray Scattering*, J. Polym. Sci., Part A: Polym. Chem.*, **40,** 2245-2255.

[212] **Gao, H.F. and Matyjaszewski, K.**, 2006. Structural Control in ATRP Synthesis of Star Polymers Using the Arm-First Method*, Macromolecules*, **39,** 3154-3160.

[213] **Dag, A., Durmaz, H., Tunca, U., and Hizal, G.**, 2009. Multiarm Star Block Copolymers Via Diels-Alder Click Reaction*, J. Polym. Sci., Part A: Polym. Chem.*, **47,** 178-187.

[214] **Durmaz, H., Dag, A., Gursoy, D., Demirel, A.L., Hizal, G., and Tunca, U.**, 2010. Multiarm Star Triblock Terpolymers Via Sequential Double Click Reactions*, J. Polym. Sci., Part A: Polym. Chem.*, **48,** 1557-1564.

[215] **Gao, H. and Matyjaszewski, K.**, 2007: Arm-First Method as a Simple and General Method for Synthesis of Miktoarm Star Copolymers*, J. Am. Chem. Soc.*, **129,** 11828-11834.

[216] **Abrol, S., Kambouris, P.A., Looney, M.G., and Solomon, D.H.**, 1997. Studies on Microgels. 3. Synthesis Using Living Free Radical Polymerization*, Macromol. Rapid Commun.*, **18,** 755-760.

[217] **Tsoukatos, T., Pispas, S., and Hadjichristidis, N.**, 2001. Star-Branched Polystyrenes by Nitroxide Living Free-Radical Polymerization*, J. Polym. Sci., Part A: Polym. Chem.*, **39,** 320-325.

[218] **Narumi, A., Satoh, T., Kaga, H., and Kakuchi, T.**, 2002. Glycoconjugated Polymer. 3. Synthesis and Amphiphilic Property of Core-Glycoconjugated Star-Shaped Polystyrene*, Macromolecules*, **35,** 699-705.

[219] **Narumi, A., Yamane, S., Miura, Y., Kaga, H., Satoh, T., and Kakuchi, T.**, 2005. Star-Shaped Polystyrenes with Glycoconjugated Periphery and Interior: Synthesis and Entrapment of Hydrophilic Molecule*, J. Polym. Sci., Part A: Polym. Chem.*, **43,** 4373-4381.

[220] **Bosman, A.W., Vestberg, R., Heumann, A., Frechet, J.M.J., and Hawker, C.J.**, 2003. A Modular Approach toward Functionalized Three-Dimensional Macromolecules: From Synthetic Concepts to Practical Applications*, J. Am. Chem. Soc.*, **125,** 715-728.

[221] **Bosman, A.W., Heumann, A., Klaerner, G., Benoit, D., Frechet, J.M.J., and Hawker, C.J.**, 2001. High-Throughput Synthesis of Nanoscale Materials: Structural Optimization of Functionalized One-Step Star Polymers, *J. Am. Chem. Soc.*, **123,** 6461-6462.

[222] **Moad, G., Mayadunne, R.T.A., Rizzardo, E., Skidmore, M., and Thang, S.H.**, 2003. Synthesis of Novel Architectures by Radical Polymerization with Reversible Addition Fragmentation Chain Transfer (RAFT Polymerization), *Macromolecular Symposia*, **192,** 1-12.

[223] **Lord, H.T., Quinn, J.F., Angus, S.D., Whittaker, M.R., Stenzel, M.H., and Davis, T.P.**, 2003. Microgel Stars Via Reversible Addition Fragmentation Chain Transfer (RAFT) Polymerisation - A Facile Route to Macroporous Membranes, Honeycomb Patterned Thin Films and Inverse Opal Substrates, *J. Mater. Chem.*, **13,** 2819-2824.

[224] **Morton M, H.T., Gadkary SD, Bueche F.**, 1962. Preparation and Properties of Monodisperse Branched Polystyrene, *J Polymer Science*, **57,** 471-482.

[225] **Orofino T, W.F.**, 1963. Dilute Solution Properties of Branched Polymers, Polystyrene Trifunctional Star Molecules, *J Phys Chem* **67,** 566-575.

[226] **R., M.**, 1974. Organized Structures in Amorphous Styrene/Cis- 1,4-Isoprene Block Copolymers: Low Angle X-Ray Scattering and Electron Microscopy, *Polymer*, **15,** 137-145.

[227] **Roovers, J., Zhou, L.L., Toporowski, P.M., Vanderzwan, M., Iatrou, H., and Hadjichristidis, N.**, 1993 Regular Star Polymers with 64 and 128 Arms - Models for Polymeric Micelles, *Macromolecules*, **26,** 4324-4331.

[228] **Zhou, L.L. and Roovers, J.**, 1993. Synthesis of Novel Carbosilane Dendritic Macromolecules, *Macromolecules*, **26,** 963-968.

[229] **Pennisi, R.W. and Fetters, L.J.**, 1988. Preparation of Asymmetric 3-Arm Polybutadiene and Polystyrene Stars, *Macromolecules*, **21,** 1094-1099.

[230] **Mays, J.W.**, 1990. Synthesis of Simple Graft Poly(Isoprene-*g*-Styrene) by Anionic-Polymerization, *Polym. Bull.*, **23,** 247-250.

[231] **Iatrou, H. and Hadjichristidis, N.**, 1992. Synthesis of a Model 3-Miktoarm Star Terpolymer, *Macromolecules*, **25,** 4649-4651.

[232] **Gao, H.F. and Matyjaszewski, K.**, 2006. Synthesis of Star Polymers by a Combination of ATRP and the "Click" Coupling Method, *Macromolecules*, **39,** 4960-4965.

[233] **Altintas, O., Hizal, G., and Tunca, U.**, 2006. ABC-Type Hetero-Arm Star Terpolymers through "Click" Chemistry, *J. Polym. Sci., Part A: Polym. Chem.*, **44,** 5699-5707.

[234] **Altintas, O., Yankul, B., Hizal, G., and Tunca, U.**, 2007. One-Pot Preparation of 3-Miktoarm Star Terpolyrmers Via Click 3+2 Reaction, *J. Polym. Sci., Part A: Polym. Chem.*, **45,** 3588-3598.

[235] **Durmaz, H., Karatas, F., Tunca, U., and Hizal, G.**, 2006. Preparation of ABC Miktoarm Star Terpolymer Containing Poly(ethylene glycol), Polystyrene, and Poly(*tert*-butylacrylate) Arms by Combining Diels-Alder Reaction, Atom Transfer Radical, and Stable Free Radical Polymerization Routes*, J. Polym. Sci., Part A: Polym. Chem.*, **44,** 499-509.

[236] **Dag, A., Durmaz, H., Sirkecioglu, O., Hizal, G., and Tunca, U.**, 2009. Three-Arm Star Ring Opening Metathesis Polymers via Alkyne-Azide Click Reaction*, J. Polym. Sci., Part A: Polym. Chem.*, **47,** 2344-2351.

[237] **Gozgen, A., Dag, A., Durmaz, H., Sirkecioglu, O., Hizal, G., and Tunca, U.**, 2009. ROMP-NMP-ATRP Combination for the Preparation of 3-Miktoarm Star Terpolymer via Click Chemistry*, J. Polym. Sci., Part A: Polym. Chem.*, **47,** 497-504.

[238] **Altintas, O., Hizal, G., and Tunca, U.**, 2009. Synthesis of an ABCD 4-Miktoarm Star Quaterpolymer through a Diels-Alder Click Reaction*, Des. Monomers Polym.*, **12,** 83-98.

[239] **Gungor, E., Durmaz, H., Hizal, G., and Tunca, U.**, 2008. H-Shaped (ABCDE Type) Quintopolymer via Click Reaction [3+2] Strategy*, J. Polym. Sci., Part A: Polym. Chem.*, **46,** 4459-4468.

[240] **Gungor, E., Hizal, G., and Tunca, U.**, 2009. One-Pot Double Click Reactions for the Preparation of H-Shaped ABCDE-Type Quintopolyrner*, J. Polym. Sci., Part A: Polym. Chem.*, **47,** 3409-3418.

[241] **Gungor, E., Cote, G., Erdogan, T., Durmaz, H., Demirel, A.L., Hizal, G., and Tunca, U.**, 2007. Heteroarm H-Shaped Terpolymers through Click Reaction*, J. Polym. Sci., Part A: Polym. Chem.*, **45,** 1055-1065.

[242] **Mantovani, G., Lecolley, F., Tao, L., Haddleton, D.M., Clerx, J., Cornelissen, J., and Velonia, K.**, 2005. Design and Synthesis of N-Maleimido-Functionalized Hydrophilic Polymers via Copper-Mediated Living Radical Polymerization: A Suitable Alternative to Pegylation Chemistry*, J. Am. Chem. Soc.*, **127,** 2966-2973.

[243] **Altintas, O., Yankul, B., Hizal, G., and Tunca, U.**, 2006. A(3)-Type Star Polymers Via Click Chemistry*, J. Polym. Sci., Part A: Polym. Chem.*, **44,** 6458-6465.

[244] **Lei, X.G. and Porco, J.A.**, 2004. Synthesis of a Polymer-Supported Anthracene and Its Application as a Dienophile Scavenger*, Org. Lett.*, **6,** 795-798.

[245] **Chen, F., Cheng, Z.P., Zhu, J., Zhang, W., and Zhu, X.L.**, 2008. Synthesis of Poly(Vinyl Acetate) with Fluorescence via a Combination of RAFT/Madix and "Click" Chemistry*, Eur. Polym. J.*, **44,** 1789-1795.

[246] **Erdogan, M., Hizal, G., Tunca, U., Hayrabetyan, D., and Pekcan, O.**, 2002. Molecular Weight Effect on Swelling of Polymer Gels in Homopolymer Solutions: A Fluorescence Study*, Polymer*, **43,** 1925-1931.

[247] **Opsteen, J.A. and van Hest, J.C.M.**, 2005. Modular Synthesis of Block Copolymers via Cycloaddition of Terminal Azide and Alkyne Functionalized Polymers*, Chem. Commun.*, 57-59.

[248] **Grest, G.S., Fetters, L.J., Huang, J.S., and Richter, D.**, 1996. Star Polymers: Experiment, Theory, and Simulation*, Advances in Chemical Physics, Vol Xciv*, **94,** 67-163.

[249] **Glynos, E., Chremos, A., Petekidis, G., Camp, P.J., and Koutsos, V.**, 2007. Polymer-Like to Soft Colloid-Like Behavior of Regular Star Polymers Adsorbed on Surfaces*, Macromolecules*, **40,** 6947-6958.

CURRICULUM VITAE

Candidate's full name: Aydan DAĞ

Place and date of birth: İstanbul, 12/03/1980

Permanent Address: 5 Telsiz Mah. 103-A Sok. No:30/11, 34760 Zeytinburnu/Istanbul, Turkey

Universities and Colleges attended:

2006-2011 *Philosophy of Doctorate* (Polymer Science and Technology) Istanbul Technical University, Istanbul, Turkey.

2004-2006 *Master of Science* (Polymer Science and Technology), Istanbul Technical University, Istanbul, Turkey

1999–2003 *Bachelor of Science* (Chemistry), Trakya University, Istanbul, Turkey

1994-1998 Pertevniyal Super Highschool, İstanbul, Turkey

Projects:

2007- 2009 Istanbul Technical University- TÜBİTAK Project (107T438) Surface Modification of Carbon Nanotube *via* 1,3-Dipolar Cycloaddition (Click) and Diels-Alder (DA) Chemistry

2005-2007 Istanbul Technical University- TÜBİTAK Project (105T225) Diels-Alder Chemistry in Macromolecular Engineering

Publications:

- Various Brush Polymers Through ROMP and Nitroxide Radical Coupling Reaction, N. Cerit, N. Cakir, **A. Dag,** O. Sirkecioglu, H. Durmaz, G.Hizal, U. Tunca, J. Polym Sci, Part A Poly. Chem. Ed, 49, 2850-2858 (**2011**).
- Sequential double polymer click reactions for the preparation of regular graft copolymers, H. Durmaz, **A. Dag**, G. Hizal, U. Tunca, J. Polym Sci, Part A Poly. Chem. Ed, 49, 1195–1200 (**2011**).
- Block-brush copolymers via ROMP and sequential double click reaction strategy, **A. Dag**, H. Sahin, H. Durmaz, G. Hizal, U. Tunca, J. Polym Sci, Part A Poly. Chem. Ed, 49, 886-892 (**2011**).
- Graft copolymers via ROMP and Diels–Alder click reaction strategy, H. Durmaz, **A. Dag**, N. Cerit, O. Sirkecioglu, G. Hizal, U. Tunca, J. Polym Sci, Part A Poly. Chem. Ed, 48, 5982-5991 (**2010**).

- Cyclic Homo and Block Copolymers Through Sequential Double Click Reactions, H. Durmaz, **A. Dag**, G. Hizal, U. Tunca, *J. Polym Sci, Part A Poly. Chem. Ed.*, 48, 5083-5091 (**2010**).
- Multiarm Star polymers with peripheral dendritic PMMA arms through Diels-Alder click reaction, H. Durmaz, **A. Dag**, C. Onen, O. Gok, A. Sanyal G. Hizal, U. Tunca, *J. Polym Sci, Part A Poly. Chem. Ed.*, 48, 4842-4846 (**2010**).
- An Easy Way to the Preparation of Multi-miktoarm Star Block Copolymers *via* Sequential Double Click Reactions, **A. Dag**, H. Durmaz, V. Kirmizi, G. Hizal, U. Tunca *Polym. Chem*.,1, 621-623 (**2010**).
- Multiarm Star Triblock Terpolymers via Sequential Double Click Reactions, H. Durmaz, **A. Dag**, D. Gursoy, A. Levent Demirel, G. Hizal, U. Tunca, *J. Polym Sci, Part A Poly. Chem. Ed.*, 48, 1557-1564 (**2010**).
- Multiarm Star Block and Multiarm Star Mixed-Block Copoplymers via Azide-Alkyne Click Reaction, H. Durmaz, **A. Dag**, E. Erdogan, A. Levent Demirel, G. Hizal, U. Tunca, *J. Polym Sci, Part A Poly. Chem. Ed.*, 48, 99-108 (**2010**).
- 3-Arm Star Ring Opening Metathesis Polymers via Alkyne-Azide Click Reaction, **A. Dag**, H. Durmaz, O. Sirkecioglu, G. Hizal, U. Tunca, *J. Polym Sci, Part A Poly. Chem. Ed.*, 47, 2344-2351 (**2009**).
- ROMP-NMP-ATRP Combination for the Preparation of 3-Miktoarm Star Terpolymer via Click Chemistry, A. Gozgen, **A. Dag**, H. Durmaz, O. Sirkecioglu, G. Hizal, U. Tunca, *J. Polym Sci, Part A Poly. Chem. Ed.*, 47, 497-504 (**2009**).
- Multiarm Star Block Copolymers via Diels-Alder Click Reaction, **A. Dag**, H. Durmaz, G. Hizal, U. Tunca, *J. Polym Sci, Part A Poly. Chem. Ed.*, 47, 178-187 (**2009**).
- One-Pot Synthesis of Star-Block Copolymers Using Double Click Reactions, H. Durmaz, **A. Dag**, A. Hizal, G. Hizal, U. Tunca, *J. Polym Sci, Part A Poly. Chem. Ed.*, 46, 7091-7100 (**2008**).
- Hetero Graft Copolymers via Double Click Reactions Using One-Pot Technique, **A. Dag**, H. Durmaz, E. Demir, G. Hizal, U. Tunca, *J. Polym Sci, Part A Poly. Chem. Ed.*, 46, 6969-6977 (**2008**).
- Preparation of 3-Arm Star Polymers (A 3) via Diels-Alder Click Reaction, **A. Dag**, H. Durmaz, G. Hizal, U. Tunca, *J. Polym Sci, Part A Poly. Chem. Ed.*, 46, 302-313 (**2008**).
- One-Pot Synthesis of ABC Type Triblock Copolymers via *In Situ* Click [3+2] and Diels-Alder [4+2] Reactions, H. Durmaz, **A. Dag**, O. Altintas, T. Erdogan, G. Hizal**,** U. Tunca, *Macromolecules*, 40, 191-198 (**2007**).
- Fructose as a Reducing Agent for in situ Generation of Cu(I) Species via an Electron-Transfer Reaction in Copper-Catalyzed Living/Controlled Radical Polymerization of Styrene, **A. Dag**, H. Mert, B. Dervaux, F. E. Du Prez, U. Tunca, G. Hizal, *Designed Mon.& Polym*, 10, 425–438, (**2007**).